Université du Québec
Institut National de la Recherche Scientifique
Institut Armand Frappier

INVESTIGATING THE STRUCTURE-FUNCTION-FLEXIBILITY RELATIONSHIP OF CHITIN- AND XYLAN-DEGRADING ENZYMES

Par

Nhung Nguyen-Thi

Thèse présentée pour l'obtention du grade
de Philosophiae doctor (Ph.D.) en biologie

Jury d'évaluation

Président du jury et examinateur interne	David Chatenet INRS-Institut Armand-Frappier
Examinateur externe	Denis Groleau Université de Sherbrooke
Examinateur externe	Steve Bourgault Université du Québec à Montréal
Directeur de recherche	Nicolas Doucet INRS-Institut Armand-Frappier

ACKNOWLEDGEMENTS

Completing my PhD has been a long journey that has required a lot of energy and effort. I could not have succeeded without the tremendous help and guidance from my professor, Nicolas Doucet. He has inspired me during the course of the research and has given me a lot of knowledge, particularly of new techniques like NMR - an interesting approach in protein science. I would like to deeply thank you for your great direction and continuous encouragement during more than 4 years of my study here. You have been a great mentor to me. I will remember all the enjoyable moments when working with you, during which I always received priceless advice and knowledge with good-humor. I thank you again for being your student to get the scholarships and chances to participate in national and international conferences.

I would also like to express my gratitude to my previous director, Professor Claude Dupont, who gave me this wonderful chance to study at INRS. You are the first person who trained me in techniques in protein science, which were completely new to me when I started my study at INRS. I wish you good health and all the best of luck during your retirement. I am also very thankful to my professor at VAST (Vietnam Academy of Science and Technology), Tong Kim Thuan, who recommended the program to me and encouraged me throughout my study at INRS. I would also like to thank my committee members, Dr. David Chatenet, Dr. Denis Groleau, and Dr. Steve Bourgault for serving as my committee members. Your corrections, comments and suggestions are of remarkable help for completing my thesis.

I would like to thank my lab-mate, Donald Gagne, for his help, especially in the NMR experiments and analyses. You gave me a lot of useful advice and invaluable constructive criticism during my research. You always took responsibility in the lab and helped me with a lot of enthusiasm and kindness. I will remember all the friendships we have developed during the time I spent at INRS. I would also like to express my gratitude to Anastasia Nikolakakis for her help in correcting my writing. I would especially like to thank Roger Dubuc who supported me a lot. I will remember forever the cheerful and warm times when working with you. I will never forget Raymonde Jette for her help and encouragement during the beginning of my studies at INRS. I would also like to thank Julie Payet for her kindness in helping me with biomolecular techniques. And many thanks to all my lab-mates who worked and shared

with me every day in the lab in a friendly atmosphere. I also want to thank Sameer Al-Abdul-Wahid and Tara Sprules from the Québec/Eastern Canada High Field NMR Facility (McGill) and Michael Osborne from IRIC-Institut de Recherche en Immunovirologie et Cancérologie (Université de Montréal) for their excellent assistance in the NMR experiments. Without you guys, I would not have the amazing data for my thesis.

I would like to take this opportunity to thank Mrs. Vu Thi Bich, Professor Sinh Le Quoc, Professor Alain Fournier and others from VAST and INRS. I am sincerely grateful to them for building and operating the Co-operation Program in Doctoral Training between VAST and INRS, which gave me the excellent chance and wonderful time to study at INRS. This was an invaluable help for my career. I would also like to thank the leaders of Institute of New Technology, Institute of Military Science and Technology, Group 871 for facilitating my study process and to sincerely thank the Vietnamese Ministry of Education and Training and INRS for the financial assistance.

I also want to give my thanks to my friends – especially Mai, Nhung, My, and Oanh – who have been always beside me, helped me, and shared with me thousands of happy, glad, funny, sad, and stressful moments not only in life but also in science during my time in Canada. Love you all.

Finally, special thanks and love to my beloved husband and little girls for your support, sacrifice and care for me from the other side of the earth. Words cannot express how grateful I am to you. I also want to thank my parents who always care, encourage and worry for me in all my life. I am also very grateful to my parents-in-law who supported me from abroad during my studies and took care of my little girl with love and protection during my absence. I would like to send my gratitude to my mother-in-law who is now blessing my family and me from the sky. I would also like to underline the support and help from my brother-in-law, sisters-in-law, my brothers, and to most deeply thank Ms Loan for taking care of my daughter during my absence.

RÉSUMÉ

La dégradation enzymatique de la biomasse est un procédé biotechnologique de pointe visant la production de petites molécules hautement pertinente en synthèse organique. Ce processus a été largement étudié en raison de ses avantages en chimie verte, en plus de son application potentielle dans de nombreux domaines de la vie. Malgré l'accumulation des connaissances au niveau des principes qui régissent la dégradation enzymatique de la biomasse, les objectifs fondamentaux et industriels de cette technologie demeurent encore sommaires. La découverte d'enzymes efficaces et adaptées aux domaines biotechnologiques demeure un défi majeur en raison des problèmes de pureté des produits synthétisés, des faibles rendements de production enzymatique et du coût élevé des processus industriels provenant de la complexité de la biomasse de départ. Conséquemment, nous visons principalement à découvrir et à caractériser des glycoside hydrolases hautement actives et adaptées à de nombreuses applications industrielles.

Une β-N-acétylhexosaminidase (*Sc*HEX) et une chitinase (ChiC) de *Streptomyces coelicolor* A3(2) possédant des activités élevées envers les chitooligomères et les chitines cristallines ont été exprimées et caractérisées avec succès. En collaboration avec un groupe de l'Université York (York, Royaume-Uni), les structures cristallines de *Sc*HEX native et du mutant *Sc*HEX-E314Q ont été résolues afin de comprendre le mécanisme catalytique d'hydrolyse des chitooligosaccharides. En utilisant un mélange de divers surnageants composés de *Sc*HEX et ChiC dans un essai en présence de chitine cristalline comme substrat, le produit final GlcNAc a été obtenu avec une pureté de 95% après 8 heures d'incubation, promettant un moyen efficace pour la production industrielle de GlcNAc pur.

La flexibilité atomique chez les enzymes se révèle d'une importance cruciale dans la conversion enzymatique de polysaccharides. Il a été démontré que les mouvements moléculaires de protéines à différentes échelles de temps peuvent être impliqués dans la régulation de l'activité enzymatique, en jouant notamment un rôle essentiel dans le contrôle de la relation entre la structure et la fonction chez plusieurs systèmes enzymatiques. Pour étudier la dynamique interne et dans le but de déterminer si cette dynamique doit être considérée dans le génie enzymatique des glycoside hydrolases, des expériences de RMN ont été réalisées

avec XlnB2 et XlnB2-E87A de *Streptomyces lividans* 66 en l'absence et en présence de ligands (xylobiose et xylopentaose). Les résultats de cristallographie révèlent que XlnB2 possède une structure conservée appelée "β-*jelly-roll*", ressemblant à l'architecture de la main droite. Nos données RMN montrent que, sous forme libre, les mouvements à l'échelle de temps de la catalyse enzymatique sont principalement regroupés sur la face de la cavité catalytique. Lors de la liaison aux ligands, l'échange conformationnel émerge sur les deux faces de la cavité catalytique et dans le motif de la boucle "*thumb loop*", ce qui suggère un mouvement global de fermeture. D'autres résultats indiquent que l'implication des résidus de la boucle et de la cavité catalytique demeurent similaires suite à la liaison avec de courtes et longues chaînes de glucides. Ces résultats fournissent une preuve expérimentale directe validant le mécanisme d'ouverture et de fermeture précédemment prédit par des structures cristallines et des simulations de dynamique moléculaire effectuées sur des xylanases homologues. En bref, cette étude permet de mieux comprendre la dynamique à l'échelle atomique de XlnB2, démontrant une relation directe entre la fonction et la dynamique de l'enzyme.

Les résultats recueillis dans cette thèse permettent de mieux comprendre comment les glycoside hydrolases dégradent la biomasse. D'autres études seront nécessaires pour maximiser leur activité enzymatique et leur efficacité catalytique, ainsi que pour obtenir des informations supplémentaires visant l'amélioration par ingénierie enzymatique de biocatalyseurs efficaces dans de multiples applications industrielles.

SUMMARY

The enzymatic degradation of biomass is an advanced biotechnological method for the production of small molecules of organic synthesis relevance. This process has been extensively studied because of its benefits in green chemistry and its potential application in many fields of life. Although much knowledge about the principles that govern the enzymatic breakdown of biomass has been gathered, fundamental and industrial goals remain unachieved. Finding efficient enzymes adapted to applied biotechnology disciplines remains a challenge due to product purity issues, yields of enzymatic production, and high costs of degrading processes due to biomass recalcitrance. As a result, we are interested in finding and characterizing highly active glycoside hydrolases aimed at numerous industrial applications.

A β-*N*-acetylhexosaminidase (*Sc*HEX) and a chitinase (ChiC) from *Streptomyces coelicolor* A3(2) with high activity toward chitooligomers and crystalline chitins were successfully expressed and characterized. In collaboration with a group at the University of York (York, UK), crystal structures of the native *Sc*HEX and of the mutant *Sc*HEX-E314Q have been resolved in order to understand the catalytic mechanism of chitooligosaccharide hydrolysis. Using a mixture of supernatants from *Sc*HEX and ChiC in an assay with crystalline chitin as substrate, GlcNAc was produced as a final product with yield of 90% after 8h of incubation, promising efficient applicability for the industrial production of pure GlcNAc.

Enzyme flexibility was found to play an important role in enzymatic conversion of polysaccharides. It has been shown that internal protein motions on various timescales can be involved in regulating enzyme activity, playing a critical role in controlling the relationship between structure and function in several enzyme systems. To study internal dynamics and to investigate whether they should be considered in glycoside hydrolase engineering, NMR experiments were carried out with XlnB2 and XlnB2-E87A from *Streptomyces lividans* 66 in the absence and presence of ligands (xylobiose and xylopentaose). Crystallographic results reveal that XlnB2 conserves a β-jelly-roll scaffold, with a right-hand architecture. Our NMR data show that in the free XlnB2 form, catalytic time-scale motions primarily cluster on one face of the catalytic cleft. Upon ligand binding, conformational exchange emerges on both faces of the catalytic cleft and in the thumb-loop motif, suggesting a global clamping

movement. Other results indicate very similar involvement of residues located on the thumb loop and active-site cleft upon binding with short- and long-chain carbohydrates. These results provide direct experimental evidence to validate the previously postulated open-closed mechanism predicted by crystal structures and molecular dynamics simulations performed on xylanase homologues. In short, this study provides further insight into the atomic-scale dynamics of XlnB2, indicating a relationship between function and the dynamics of the enzyme.

The results collected in this thesis provide a better understanding of the glycoside hydrolase enzymes in biomass degradation. Further studies are required to optimize their enzymatic activity and catalytic efficiency, as well as to gain additional information for the proper engineering of improved biocatalysts used in several industrial applications.

TABLE OF CONTENTS

LIST OF TABLES

LIST OF FIGURES

Chapter 1

Chapter 2

Chapter 3

ABBREVIATIONS

Å	Ångström (10^{-10} meter)
ANM	Anisotrophic network model
^{13}C	Carbon-13
CAZY	Carbohydrate-active enzymes
CBM	Carbohydrate-binding module
CBP	Chitin-binding protein
CBP21	Chitin-binding protein family 21
CDH	Cellobiose dehydrogenase
ChtB	Chitin-binding domain
CPMG	NMR relaxation-compensated Carr-Purcell-Meiboom-Gill
DP	Degree of polymerization
δ	Chemical shift
Δδ	Chemical shift variation
ε	Extinction coefficient
EC	Enzyme Commission
g	gravity
GH	Glycoside hydrolase
GH3	Glycoside hydrolase family 3
GH11	Glycoside hydrolase family 11
GH20	Glycoside hydrolase family 20
GH84	Glycoside hydrolase family 84
GalNAc	*N*-Acetylgalactosamine
GlcNAc	*N*-Acetyl-β-glucosamine
HEX	β-*N*-Acetylhexosaminidases
HSQC	Heteronuclear Single Quantum Coherence
HPLC	High Pressure Liquid Chromatography
ITC	Isothermal titration calorimetry
k_{cat}	Catalytic constant
K_M	Michaelis–Menten Constant
kb	Kilobases
K_d	Dissociation constant
kDa	Kilo Dalton

MD	Molecular dynamics
MeGA	4-*O*-methyl-α-D-glucuronic acid
MW	Molecular weight
MWCO	Molecular weight cut off
m/z	Mass/charge (mass-to-charge ratio)
mM	Millimolar
μs	Microsecond (10^{-6} s)
ms	Millisecond (10^{-3} s)
^{15}N	Nitrogen-15
nm	Nanometer
NOE	Nuclear Overhauser Effect
ns	Nanosecond (10^{-9} s)
NA	Not available
NMR	Nuclear Magnetic Resonance
PCR	Polymerase chain reaction
PDB	Protein Data Bank
PM	Peritrophic membranes
*p*NP-	*para*-nitrophenyl-
ps	Picosecond (10^{-12} s)
R_1	Longitudinal relaxation rate
R_2	Transverse relaxation rate
R_{ex}	Conformational exchange parameter (motions μs-ms)
RMSD	Root Mean Square Deviation
rpm	Revolutions per minute
SDS-PAGE	Sodium dodecyl sulphate polyacrylamide gel electrophoresis
*Sp*Hex	β-*N*-Acetylhexosaminidase from *Streptomyces plicatus*
Temp.	Temperature
UV	Ultraviolet
v/v	Volume/volume
V_{max}	Maximum rate of conversion of an enzyme-catalyzed reaction
Xln	Xylanase
w/v	weight/volume

CHAPTER 1. INTRODUCTION

Introduction

Polysaccharides, such as chitin and xylan—two of the most abundant biomass polymers of the biosphere—serve as major carbon and energy sources for many bacterial species. In general, growth on these carbohydrate polymers is associated with the secretion of an enzymatic system that breaks down the polymer chains to release monomers, which are in turn easily utilized as carbon and energy sources. It is hoped that biomass can be used as an inexhaustible and renewable energy source *via* enzymatic hydrolysis in fuel production, in the food industry, and in medical treatments. As a result, these enzymes have become promising biocatalysts for the industrial breakdown of biomass compounds.

Nowadays, using biocatalysts in organic synthesis or for biomass degradation is considered as a strategy for green chemistry — a global target in order to prevent global warming. Benefits of green chemistry could be obtained from the use of biomass and biocatalysts in manufacturing processes and of renewable carbon in final products (*1*). Indeed, billions of tons of biomass derived from many sources, such as fungi, insects or plants, are accumulated annually in nature. The processes making use of the biomass reduce the cost of production processes and decrease biomass accumulation. The enzymatic processes using biocatalysts are considered as an approach for sustainable development owing to their potential in decreasing waste emissions, pollution, or negative effects on the environment and human health. The products of biomass degradation that can be used as renewable energy sources are incorporated into the nitrogen and carbon cycle. For instance, xylose produced from xylan degradation can be applied to biofuel production, whose products can be used in transportation – a process that generates CO_2 which is incorporated into the carbon cycle on earth. Therefore, the processes using biomass and biocatalysts are advantageous in green chemistry and continue to grow in order to be used on a large scale in the future. In particular, enzymatic degradation of chitin and xylan using biocatalysts meets one of the principles of green chemistry.

Chitinolytic enzymes take part in the degradation of chitin, whose abundance renders it an important polymer that should be made use of in the future. In this degradation, the complete conversion of chitin involves the synergistic action of two hydrolyzing enzymes—

β-*N*-acetylhexosaminidase (HEX) and chitinase—generating the end product *N*-acetyl-D-glucosamine (GlcNAc), a monosaccharide with great value in medical and cosmetic applications (*2*). Other derivatives of the degradation, which are chitosan and chitooligosaccharides, can be used in many applications such as antimicrobial, antitumor, anti-cholesterol activities, wastewater treatment, drug delivery, or wound healing (*3*). Due to the widespread and valuable applications of products of the process, attempts have been made to find efficient enzymes as well as to modify the enzymes in order to adapt to such applications. However, to this day, these objectives remain a challenge due to product purity issues, yields of enzymatic production and high costs of degradation processes due to biomass recalcitrance. Due to the above restraints, the processes require many conversion and separation steps, causing higher costs and energy demands and waste emissions. Consequently, improving the efficiency of known enzymes, finding new and more active enzymes, and creating optimized enzyme mixtures can be solutions in order to break the barrier for large-scale production of the target products (*4*).

With regards to GlcNAc production, despite the strong demand due to its potential use as a non-toxic supplement to protect the bone surfaces of the friction joint (*5, 6*), to treat inflammatory bowel disease (including Crohn's disease) (*7, 8*) and to use in dermatological and cosmetic applications (*2*), large-scale GlcNAc production faces many problems. Typically, GlcNAc is produced by hydrolysis of chitin using hydrochloric acid (15-36% HCl, 40-80^{o}C) (*2*), which is extremely energy demanding, costly and polluting—an issue that is being avoided in green biochemistry nowadays. The products somehow cannot be considered as a safe supplement due to chemical processes or modifications. In fact, the chemical methods carried out under these extreme conditions have many drawbacks including instability of products. Enzymatic hydrolysis does not show these negative effects on the sugar product. Therefore, enzymatic processes for GlcNAc production using more efficient and environmentally friendly methods are being developed. Indeed, the enzymatic production of GlcNAc by endochitinases (EC 3.2.1.14), exochitinases (EC 3.2.1.52) and *N*-acetylhexosaminidases (HEX) (EC 3.2.1.96) yielded about 80 g/L/h of GlcNAc with no environmental release (*9*). However, the final product is contaminated with chitobiose [$(GlcNAc)_2$] and other derivatives whose removal is necessary to obtain a pure product for commercial demand. Other enzymatic process for GlcNAc productions are limited in

productivity and time-cost consideration. Hence, finding efficient enzymes that can overcome these issues and which have appropriate properties for large-scale or industrial-scale production is crucial.

Other enzymes seen as promising biocatalysts for the industrial breakdown of biomass are xylanases. They are glycoside hydrolases that cleave internal β-1,4-xylosidic bonds in heteroxylan, a major hemicellulose fraction of plant cell walls. These glycosidases are of widespread importance in biofuel, food and non-food biotechnological applications, bioconversion of hemicellulosic biomass to fermentable sugars and platform molecules. The enzymes are particularly important in bioethanol production. In fact, bioethanol is produced from starch sources or other food plants (the first generation of biofuels) that are considered unsustainable since it affects food security. The production of the first generation of bioethanol is also limited because of inconsistent supply sources due to the dependence on weather and agriculture (*10*). Therefore, the second generation of bioethanol produced from abundant xylan and cellulose is one of the most popular biofuel technologies nowadays. Moreover, other breakdown products of xylan degradation have been used in many diverse fields, such as pulp and paper production and the textile industry. Because of high industrial demands for environmentally friendly and cost-effective biomass technologies, the principles that govern the enzymatic breakdown of xylan are of particular interest. Because of the highly complex nature of heteroxylans as well as the diversity in biochemical properties of xylanases, efficient use of the enzymes requires a molecular insight into the structure-function relationship of their catalytic mechanisms to improve their efficiency. Moreover, proteins are naturally dynamic and are thought to depend on flexibility to perform their function. Therefore, understanding the mechanism that regulates enzyme activity and the relationship between structure, function and motion is a serious option for engineering improved biocatalysts.

Xylanases form a group of highly homologous biocatalysts displaying a conserved β-jelly-roll structure. A number of three-dimensional structures demonstrated that xylanases adopt different mechanisms and architectures in the substrate-binding cleft, whereby xylanases bind and hydrolyze structurally different heteroxylans and xylo-oligosaccharides. Evidence from kinetics, mutagenesis, crystal structures and molecular dynamic simulations in

the presence and absence of ligands have proposed the existence of a “thumb-loop” motion and an “open-closed” movement of the active site which may play a major role in substrate binding, catalysis, inhibition, and stability of the proteins (*11*). The hypothesis was obtained from inappropriate methods such as crystallography or molecular dynamic simulations – methods which give a rigid image of protein motion or information on a timescale that is not relevant to enzymatic catalysis, respectively. The hypothesis is neither in agreement with other results suggesting the immobility of the active site or the thumb motif. As a result, further information about protein dynamics in xylanases is required for understanding the structure-function-motion relationship in biomass degradation.

In enzymatic degradation of biomass, the ability of enzymes to disrupt crystalline polysaccharides contributes to enzyme efficiency in the process. However, in xylan degradation, the study of this process faces difficulties due to the variety and recalcitrance in the structure of xylan, as well as difficulties in detecting and determining substrate and product molecules in the reactions. Insights on how enzymes access and disrupt structural polysaccharides were obtained from studies on enzymatic conversion of chitin (*12*). The lesson learned from chitin conversion could be useful for bioethanol production including the importance of accessible accessory proteins and the processive mechanism, which could improve enzyme efficiency and substrate accessibility, respectively. Some hallmarks for the processivity have been identified including protein flexibility (*13*). These findings suggest new approaches for the design and development of enzyme technology in degradation of recalcitrant biomass. This thesis includes studies on chitinases and xylanases, and could bring more information to the field.

In the biomass structure, both chitin and xylan contain β-1,4-glycosidic bonds, which link GlcNAc and xylose residues, respectively. The chitinases and xylanases that catalyze the cleavage of the linkages belong to different glycoside hydrolase (GH) families. Because of the same ability to cleave the β-1,4-glycosidic bonds of the polymers with long saccharide chains, all of the GH families utilize a general acid/base catalytic mechanism and may share a similar active-site architecture with multiple subsites to fit polysaccharide chains. Therefore, the commonality in the structural, functional and motional properties of these enzymes may provide more understanding of the polymer cleavage mechanism.

In general, the principles that govern the enzymatic breakdown of these polymers remain elusive, while great fundamental and industrial goals could be achieved from their understanding. As a result, we are interested in characterizing highly active glycoside hydrolases aimed at numerous industrial applications. *Streptomyces* are known to degrade cellulose, chitin and xylan polymers. To develop highly efficient biocatalysts and to get a better insight into their structure-function-flexibility relationship, we aim at characterizing β-*N*-acetylhexosaminidase (*Sc*HEX), and chitinase (ChiC) from *Streptomyces coelicolor* A3(2) and at studying enzyme flexibility in xylanase B2 (XlnB2) from *Streptomyces lividans* 66. In addition to providing a better understanding of the glycoside hydrolase enzymes, we expect this project to offer additional information for engineering improved biocatalysts.

1.1 Polysaccharides and their degradation

1.1.1 Biomass, polysaccharides

Biomass is a biological material derived from living organisms, mostly plants, and some from other kingdoms such as fungi, yeast, insects or animals (Biomass Energy Center.: Biomassenergycentre.org.uk). Apart from providing food and feed, biomass plays a crucial role for energy supplies that are utilized for cooking, heating, power and transportation. In fact, biomass is the most attractive and the largest source of renewable energy, which accounts for 14% of the total energy demand on the world (*14*). Every year, more than 130 billion tons of biomass are produced in nature (*15*), making biomass an inexhaustible source of energy. Moreover, biomass was employed throughout recorded history to extract valuable products such as medicinal drugs, supplements, flavors and fragrances (*2, 14*).

Biomass is carbon-based and mainly composed of carbohydrate polymers (cellulose, hemicellulose, chitin), and aromatic polymers (lignin). Carbohydrates, with the general formula $C_m(H_2O)_n$ and known as saccharides, are involved in a variety of biological processes. Monosaccharides are the simplest forms of carbohydrates. They consist of one carbohydrate molecule (e.g., glucose). They serve as the main source of energy for metabolism and are used in biosynthesis or bioconversion. Polysaccharides usually contain more than 20 monosaccharides linked together. They also serve as the main source and storage form of energy or exist as structural components. Polysaccharides vary in the type of monosaccharide unit, type of linkage, degree of branching and degree of polymerization. Some polysaccharides, such as cellulose, hemicellulose, and chitin, are crystalline networks of polymer chains held together by strong hydrogen bonds, thus, forming insoluble and highly rigid structures (*2, 14*).

1.1.2 Chitin, degradation of chitin, and GlcNAc production

1.1.2.1. Chitin, chitooligosaccharides

Chitin is a long-chain biopolymer of *N*-acetylglucosamine (GlcNAc) units linked together by β-(1, 4) bonds. This linear biopolymer is of variable length and the GlcNAc units

are rotated 180° relative to each other, making this functional and structural unit a disaccharide (Figure 1.1) (*16*). It is one of the most abundant natural polymers in the world, and is found in the main component of the cell walls of fungi, the exoskeletons of arthropods such as crustaceans (*e.g*. crabs, lobsters and shrimps) and insects, the radulas of mollusks and the beaks of cephalopods (*17*). Chitin may be compared to the polysaccharide cellulose and has also been proven useful in numerous manufacturing processes including food, chemical, pharmaceutical, medical, and industrial (*18*). Chitin, like cellulose, is insoluble in most solvent systems since its regular hydrogen bonding network requires solvents, which either induce inter-chain repulsions or disturb intermolecular hydrogen bonding for dissolution. The annual accumulation of chitin in nature is estimated to be 100 billion tons, making chitin an unlimited source of material for the production of GlcNAc and its derivatives (*17-20*).

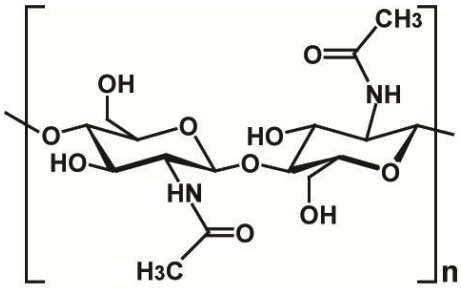

Figure 1.1. Repetitive unit of chitin. Figure adapted from reference (*17*).

The molecular configuration of a single chitin chain includes 6 amino-sugar residues per turn. In nature, the orientation of this single crystalline chain defines three allomorphs: α-, β- and γ-chitin (*21, 22*). The most abundant and stable form is the α-chitin in which one polymer chain is antiparallel to the other, while in the β-chitin form the chains are oriented in a parallel fashion with reducing ends pointing in the same direction (*23*). The least common form of chitin, γ-chitin, is a mixture of parallel and antiparallel chain packing. α-Chitin is found in insect cuticles, crustacean shells, and cell walls of fungi, while β-chitin is mainly found in squid pen and in some algae. γ-Chitin was described in the PM matrix and insect cocoons. The different packing patterns of the chitin polymorphs confer their different physicochemical properties. α-Chitin, having the most tightly packed crystalline structure, is insoluble in water, whereas β-chitin and γ-chitin being less tightly packed are structurally more flexible and more soluble in water (*17, 24*).

Chitooligosaccharides **(**GlcNAc)$_n$ (n=2-20) are water soluble chitin polymers of 2-acetylamino-2-deoxy-D-glucose monomers with a molecular formula: $(C_6H_{11}O_4N)_n$.

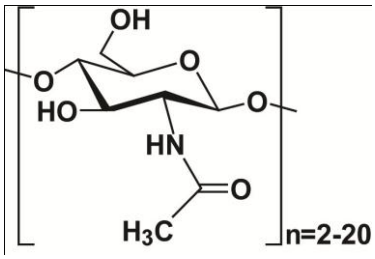

Figure 1.2. The chemical formula of a chitooligosaccharide.

The chitomonomer (GlcNAc) and chitooligosaccharides are produced from chitin or chitosan by chemical or enzymatic decomposition methods. With their excellent physiological activity and function, they are widely used in medicine, health food, agriculture, and cosmetic chemistry. GlcNAc has been proposed as a treatment for autoimmune diseases. Chitooligosaccharide derivatives have diverse applications in wastewater treatment, drug delivery, and wound healing. Specifically, its chitosan derivatives are known to have antimicrobial, antitumor, and anti-cholesterol activities (*3*).

1.1.2.2. Chitin degradation

Chitin degradation is an important process for recycling carbon and nitrogen in the biosphere. Chitin is degraded by enzymes that catalyze the hydrolysis of *N*-linked acetyl groups from GlcNAc residues or break down 1,4-glycosidic bonds (Figure 1.3). The first type of hydrolysis is deacetylation, which is an effective way to make the polymer soluble (*25*). Deacetylation is a process that weakens or breaks the inter- or intra-molecular bonds in the compact structure by deacetylases (EC 3.5.1.41, belonging to the carbohydrate esterase family 4). This process can partially deacetylate chitin to 35%, which renders chitin soluble in dilute acids due to protonation of the amino group of GlcNAc. The product, chitosan, is further degraded by chitosanases (EC3.2.1.132, belonging to the glycoside hydrolase families 5, 7, 8, 46, 75 and 80), which cleave the β-1,4-glycosidic bonds to produce oligomers of GlcNAc or GlcN (glucosamine) (*12*). In the industry, chitosan is made by treating chitin under alkaline conditions at high temperatures (*26*).

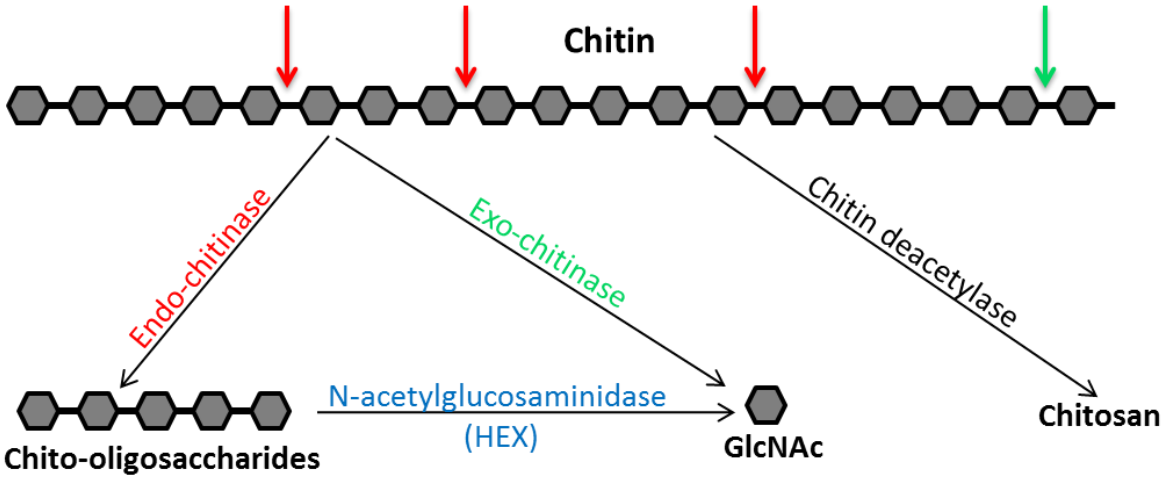

Figure 1.3. Enzymatic degradation of chitin. The red (green) arrows correspond to endo-cleavages (exo-cleavage) catalyzed by endo-chitinase (exo-chitinase).

The second type of chitin hydrolysis is deglycosylation, in which chitin is degraded through the breakdown of 1,4-glycosidic bonds by chitinolytic enzymes (*27*). This chitinolytic system is comprised of endo- and exo-acting chitinases, working in synergy for the complete degradation of chitin. They include chitinases (EC 3.2.1.14, belonging to the glycoside hydrolase families 18 and 19) which degrade chitin to produce chitooligomers and $(GlcNAc)_2$, which is further hydrolyzed to monomers by *N*-acetyhexosaminidases (HEX) (EC 3.2.1.29, belonging to the glycoside hydrolase family 20). For commercial GlcNAc or chitooligosaccharides, chitin is hydrolysed using high concentrations of HCl or NaOH.

Due to the recalcitrant nature of the chitin polymer, it is energetically demanding for chitin-degrading enzymes to access the insoluble substrate (*28*, *29*). Recently, lytic polysaccharide monooxygenases (LPMOs), which cleave glycosidic linkages on the crystalline surface of chitin by an oxidative mechanism, have been found. These enzymes create an entry point for hydrolytic chitinases, helping to increase substrate accessibility towards chitinases, thereby ensuring effective hydrolysis of chitin (*30, 31*).

In nature, chitin microfibrils are normally associated with proteins (arthropods) or glucans (fungi), therefore, chitin hydrolysis often requires accompanying protease or glucanase activities. In some chitin-forming organisms, such as filamentous fungi and yeast, chitin degradation is a fundamental physiological process for growth and development.

Fungal chitinases are responsible for the normal growth of chitin-containing fungi, including morphogenesis (hyphal growth and branching, sporulation, spore germination), autolysis, nutrition, and mycoparasitism (*32-35*). They control cell wall lysis and regulate their reconstitution in hypha expansion and cell bursting prevention (*36, 37*). They assist nutrient release in the saprophytic and mycoparasitic growth phases and may be involved in insect pathogenesis and phytopathogenesis (*38*). In *Coccidioides* spp., the complex morphologic changes during the spherule-endospore phase require the biosynthesis and degradation of cell wall structural components such as chitin, glucan or maman. This process needs the participation of chitin synthase, chitinase, β-glucosidase, and HEX (*39-41*). In insects, chitin is a structural part of the cuticle and peritropic membranes, where it is degraded by chitinolytic HEX in the turnover of chitin exoskeleton during metamorphosis (*38, 42, 43*). In some insects, such as mosquitoes, these enzymes are also important in the formation and in the degradation of the peritrophic matrix, which is formed in the midgut of adult females feeding on blood. Chitin is not only a nutritional source for chitinolytic micro-organisms but also for invertebrate and vertebrate organisms. Some insectivorous plants or mycopathogens can use chitinolytic systems to access insect prey or to penetrate fungal cell walls (*17*). In other plants, induction of chitinase is one of the defense mechanisms that plants use to react to attacks by phytopathogens and arthropod pests.

In general, chitin degradation occurs widely in many organisms. The synergic action of chitinolytic enzymes as well as other proteins such as chitosanases, glucanases or LPMOs is required for complete degradation of chitin in nature. In many industrial applications, in order to produce chitosan, chitooligomers or GlcNAc, chitin is usually hydrolyzed under extreme conditions using chemicals, which is not the most efficient and environmental-friendly method.

1.1.2.3. GlcNAc production

GlcNAc is the monomeric unit that constitutes the chitin polymer. It is a basic component of hyaluronic acid located in the extracellular matrix and of keratia sulfate on the cell surface. In mammals, it plays a role as building block of biomacromolecules such as glycoproteins, proteoglycans, glycosaminoglycans, and other connective tissue building

blocks (*2*). It also exists in human milk in the free form at concentrations of 600-1500 mg/mL. It is also present in growth factors and hormones, such as follicle-stimulating hormone (FSH), luteinizing hormone (LH), thyroid-stimulation hormone (TSH) and human chorionic gonadotropin (hCG) hormone. GlcNAc is also a component of chondroitin, which is abundant in connective tissues, particularly in blood vessels, bone and cartilage. In fact, GlcNAc and sulfated GlcNAc can be isolated from heparin or keratan sulfate, which are distributed in the cornea, cartilage and bone and usually act as an anticoagulant and a cushion in joints to absorb mechanical shock, respectively (*44, 45*). Besides, GlcNAc plays a role in plant organogenesis and invertebrate embryogenesis. Due to its versatile functions and non-toxic properties, GlcNAc can be used as a potentially therapeutic element in the treatment of many diseases as well as in economic feed-stocks. It has been used among others as a supplement to protect bone surfaces of the friction joint (*5, 6*) and to treat inflammatory bowel disease (including Crohn's disease) (*7, 8*). It emerges as a novel candidate for drug development, cosmetic, and other significant applications (*17-20*).

Every year, billions of tons of chitin are accumulated in nature, making chitin an unlimited source of material for the production of GlcNAc. Because of extreme insolubility, large-scale production of GlcNAc from this resource is rarely applied and is mainly based on chemical hydrolysis methods, which use concentrated HCl at high temperatures (15-36%, at 40-80°C) (*46, 47*). This process causes many problems, such as acidic wastes, low product yield, high cost of energy and product separation (*2*). On the other hand, enzymatic processes have gained efficiency, and environmentally-friendly performances but issues of final product purity and low productivity remain (*46, 48-53*). Biotransformation and a new method using glucose as a substrate can also be applied to produce GlcNAc. However, these two methods show some limitations due to time-cost or high technique issues (*2*). Production of GlcNAc using chitin as substrate is schemed in Figure 1.4.

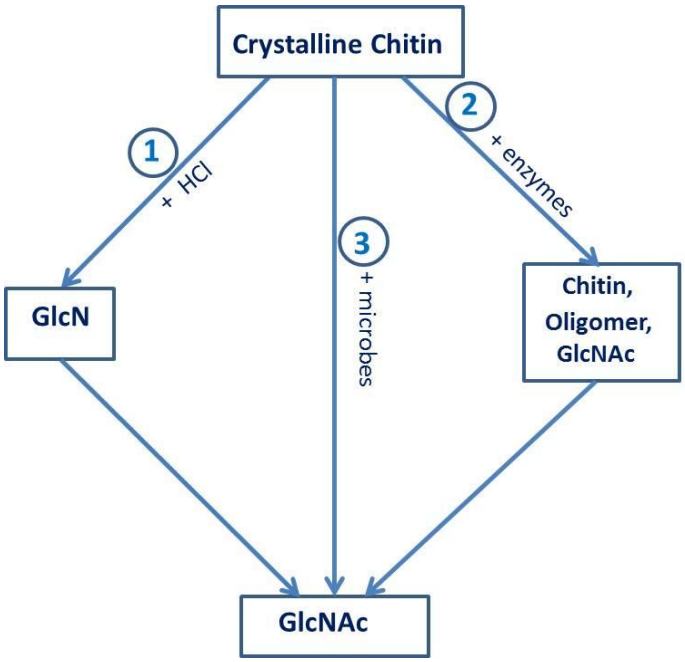

Figure 1.4. Production of GlcNAc using chitin as substrate. (1) Chemical method. (2) Enzymatic method. (3) Biotransformation method. Figure modified from reference (*2*)**.**

Via chemical methods, crude chitin is degraded by a strong acid, such as HCl, at strict exact temperature and concentration to sufficiently degrade chitin but to prevent destroying GlcNAc. In this procedure, GlcNAc can be obtained up to 6.42 g/L per hour. In another procedure, chitin is dissolved in concentrated HCl and heated in boiling water for 3 h to remove the acetyl group of the GlcNAc units. An *N*-acetylation reaction with acetic anhydride or pyridine must then be executed to produce GlcNAc. After a series of purification procedures, this process can generate an overall yield of 43% or 70% GlcNAc, respectively. Despite acceptable economic yields, these chemical procedures create a product which is not considered a natural material due to its chemical modification (*54*). Moreover, by-products, such as *O*-acetylated products or tributylamine, and large quantities of chemical waste resulting from the processes are the main drawbacks for this chemical approach.

The enzymatic hydrolysis of chitin that can produce GlcNAc under mild conditions can overcome the drawbacks of the chemical approach. The collective use of chitinolytic enzymes including endochitinases, exochitinases and *N*-acetylglucosaminidases can produce GlcNAc from chitin. Many crude enzymes isolated from *Penicillium monoverticillium* CFR, *Aspergillus flavus* CFR 10, *Fusarium oxysporum* CFR, *Trichoderma viride*, *Aspergillus niger*,

Aeromonas sp. PTCC, and *Aeromonium* have been found to degrade chitin and to efficiently produce GlcNAc (*2, 51, 53, 54*). The main problem of enzymatic methods is the production and reuse of the enzymes as well as time-cost of the processes. For industrial applications, a large amount of pure enzymes is required. However, enzymes in organisms are present at low concentrations, thus the production and purification of a large amount of a pure enzyme is expensive. Several inexpensive, commercial enzymes such as those derived from *Aeromonas hydrophila* H2330 or crude chitinases from *Bacillus licheniformis* SK-1, or *Serratia marcescens* QM B1466 (*2, 48, 49*) can be easily obtained but then require a long process for GlcNAc production.

Using whole microbes in a fermentation system with chitin as substrate is another way to produce GlcNAc. Li *et al*. (2005) isolated chitinases from *Aeromonas caviae* DYU-BT4 and after optimizing the fermentation process, about 7.8 g/L of GlcNAc were produced using 2% colloidal chitin as substrate. Another microbe, *Chitinibacter tainanensis*, isolated from a soil sample in Southern Taiwan, was utilized to produce GlcNAc. This organism produced the sugar with a yield of 75% (98%) when using α-chitin (β-chitin) as substrate. After concentration and crystallization, the purity of the product was determined to be greater than 99%. This process seems to be very effective but unfortunately the microbes are killed and cannot be reused (*2, 55*).

Finally, GlcNAc can be produced through genetic modification of microorganisms using glucose as a substrate. This method makes use of metabolic pathways for GlcN and GlcNAc synthesis in microorganisms. A genetically engineered *E. coli* strain has been developed in which some enzymes taking part in GlcNAc synthesis are overexpressed, such as GlcN-6-P acetyltransferase, GlcN-6-P synthase and GlcN-1-P acetyltransferase. In this process, about 120 g/L of GlcNAc was produced after 60 h of fermentation. This process is the most efficient process by far (*2*).

1.1.3 Xylan and degradation of xylan

Xylan, a major component of hemicellulose, is a highly complex polysaccharide that is found in plant cell walls and some algae. In some higher plants and agricultural wastes, xylan constitutes from 20-40% of the dry weight of the plant biomass (*56, 57*). Xylan is a

heteropolymer consisting of a repeating β-1,4-linked xylose (a pentose sugar) backbone branched with acetyl, arabinofuranosyl, and 4-O-methyl glucuronyl groups (*58*). Xylan, derived from different plants, has the same backbone structure but different substitutions in its branches. The proportion of those substitutions is based on the source of the plant tissue. Xylan can be classified into homoxylans, arabinoxylans, glucuronoxylans, and arabinoglucuronoxylans. Homoxylans, which consist of a chain of β-1,4- and β-1,3-linked xylose units, are mainly found in cell walls of red seaweeds. Arabinoxylans, consisting of xyloses with arabinose residues branched at the O-2 or O-3 position, are principal components of plant cell walls, especially in cereal grains. Glucuronoxylans, with 4-O-methyl-α-D-glucuronic acid (MeGA) residues linked at the O-2 xylose backbone, are mainly found in hardwoods, herbs, and woody plants. Finally, arabinoglucuronoxylans are typically found in grass lignocelluloses and have arabinofuranosyl and acetyl side chains linked to the xylose backbone (*10*).

The chemical formula of xylan and its enzymatic breakdown mechanism are displayed in Figure 1.5 and 1.6.

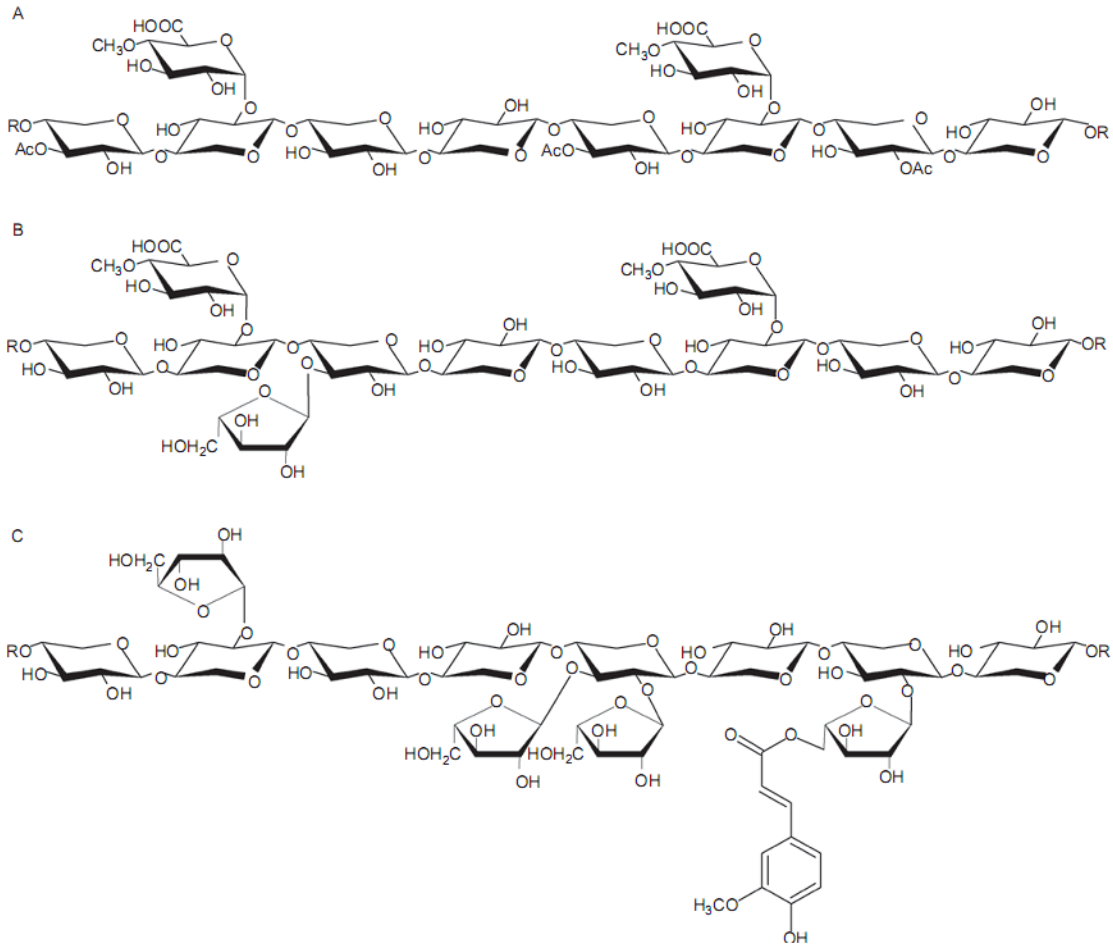

Figure 1.5. Structure of xylan from different sources. A, Glucuronoxylan from hardwoods. **B**, Arabino-methylglucuronoxylan from softwoods. **C**, Arabinoxylan from cereals. Figure taken from reference (*59*).

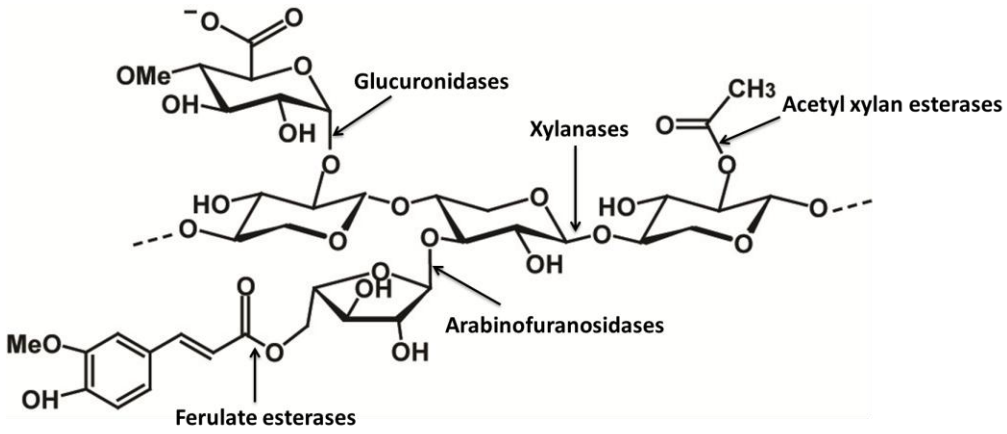

Figure 1.6. Enzymatic breakdown of xylan. Figure reproduced from reference (*60*).

Xylan, together with cellulose, plays an important role in ruminant animal and insect nutrition, where it can be converted by microorganisms. Heteroxylans and homoxylans in plants also have important functions in many cereal-based food and feed biotechnology processes (*11*). In plant biomass degradation, complete hydrolysis of the two major components, cellulose and xylan, releases glucose, xylose, and arabinose, which can then be fermented or bioconverted to biofuels (*10*). Furthermore, other hydrolysis products including acetate, propionate, lactate, or succinate are essential feedstock for the chemical and pharmaceutical industries (*61*). As a result, xylanases that cleave the internal xylan backbone to modify its physicochemical properties have been used for many applications in the industry. One attractive application is the use of hemicellulase and endoxylanase enzymes to eliminate xylan from wood pulp in the manufacture of dissolved pulp (*62*). Also, cellulase-free xylanases were applied in pulping and bleaching processes, in which the use of chlorine (Cl_2) and chlorine dioxide (ClO_2) for biobleaching can be reduced (*56*). In fact, xylanases hydrolyze reprecipitated xylan to remove it from the surface of the cellulose fibers after pulping (*56*) due to improvement of permeability of the pulp fibers to bleaching chemicals. Xylanases also help to improve the chemical extraction of lignin from pulp. The use of xylanases instead of chemicals in pulp bleaching reduces the level of toxic chlorine compounds released into the environment. Many xylanases have shown high stability and activity under severe conditions that are applicable and economical in the pulp industry. For instance, xylanases from *Actinomadura* sp. FC7, *Nonomuraea* lexuosa (*63, 64*) and other xylanases from fungi and actinomycetes, which have high temperature and pH stability, have been widely employed in paper and pulp industries.

Despite the rather high level of industrial applications, a larger use of xylanase for different applications in biomass conversion is still difficult to obtain. The major obstacle is the lack of detailed knowledge of the xylan structure, which is diverse due to many linkages of different substitutions within the complex of the heteropolymer. As a result, it is difficult to design enzyme cocktails for efficient hydrolysis of the polymer. It is also unclear as to how individual sugar components in the polymer are chemically linked within the plant cell wall. Also, the complicated structure of the plant cell wall responsible for its recalcitrance is another limitation for bioconversion of plant polymers. Finally, due to different targets, it is appropriate to have suitable, adapted, specific and affordable enzymes for these various biotechnological processes.

Therefore, acquiring a better understanding of this type of enzyme helps improving biotechnological methods to hydrolyze polysaccharides, thus providing a fully renewable resource of molecules from biomass.

1.2 Enzymes in enzymatic degradation of polysaccharides

1.2.1 Carbohydrate-active enzymes

Carbohydrates play a role as central metabolites in energy storage and biosynthesis or bioconversion. Carbohydrates are also present in the form of glycoproteins, glycolipids and polysaccharides, which play fundamental roles in cell physiology and development of microbes, plants and animals. The enzymes that catalyze the breakdown, biosynthesis or modification of oligosaccharides, polysaccharides and glycoconjugates, comprise a group of enzymes named 'carbohydrate-active enzymes' (CAZymes) (*65*). This enzyme group acts on the most structurally diverse substrates in nature. According to the carbohydrate-active enzyme database (CAZy; www.cazy.com), CAZymes are classified into families which reflect homology in amino acid sequence, protein structure and catalytic mechanism. Based on the type of catalysis, they have been grouped into 5 classes: Glycoside Hydrolases (GH), Glycosyl Transferases (GT), Polysaccharide Lyases (PL), Carbohydrate Esterases (CE), and Auxiliary Activities (AA) (*66*) (Figure 1.7). A sixth class of proteins in CAZymes are the carbohydrate-binding modules (CBM), which are non-catalytic but help the enzyme to bind the substrate (*67*). Due to the recalcitrance of polysaccharides, many CAZymes face the problem of binding to the substrate, disrupting its crystalline surface, and directing a single polysaccharide-chain into the catalytic site (*12*). Therefore, synergistic action of several enzymes belonging to different classes is necessary for full degradation. For example, deacetylases (belonging to CE4) can disrupt the crystalline surface of chitin by deacetylating (*22, 68*), LPMOs (belonging to AA9 or AA10) can make a 'scratch' on the biomass surface to produce an entry point for GHs (*30, 31*), or CMBs promote binding of GHs to the substrate, disrupting the plant cell wall structure to make it more accessible or sometimes to help by directing the chain into the active site (*59, 69*). To this date (April 2015), 133 families of GHs,

97 families of GTs, 23 families of PLs, 16 families of CEs, 13 families of AAs and 71 families of CBMs are listed in the database.

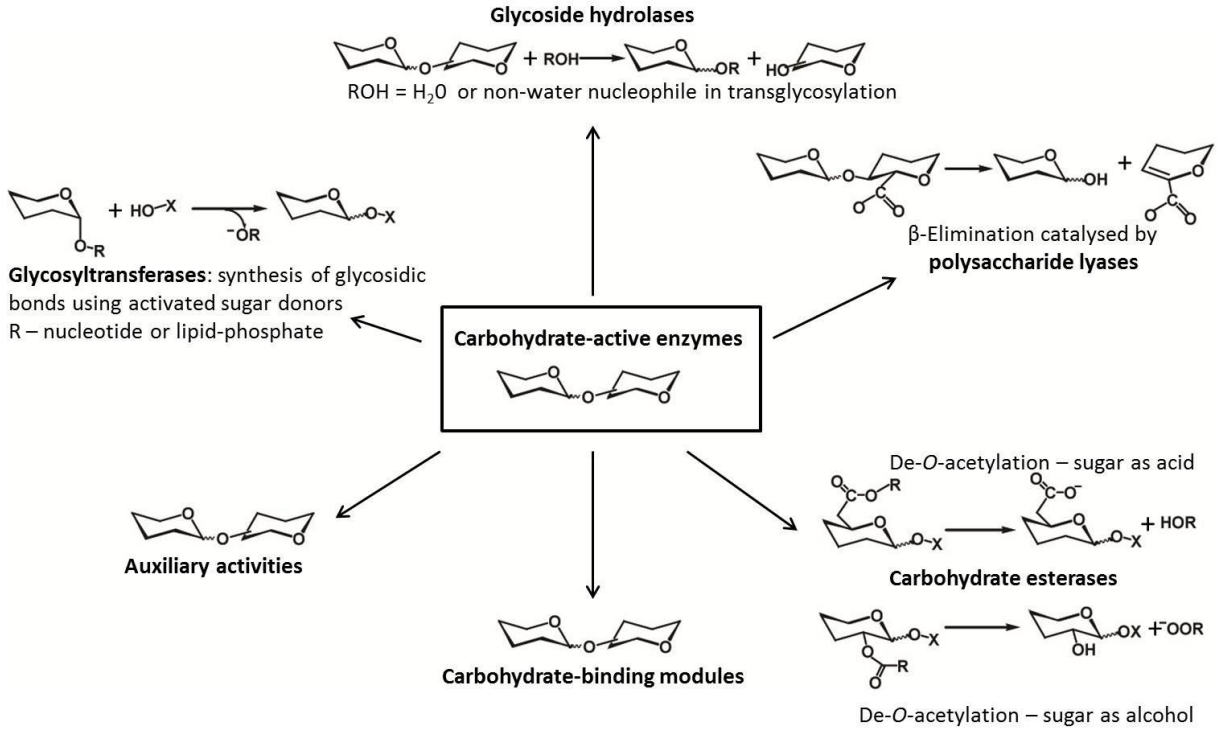

Figure 1.7. Carbohydrate-active enzymes. Figure modified from reference (*66*)**.**

1.2.2 Glycoside hydrolases

1.2.2.1. General properties

Among the carbohydrate-active enzymes, glycoside hydrolases (hereafter glycosidases or GHs) are the best-characterized enzymes that are active on disaccharides, oligosaccharides and polysaccharides. The glycosidases are enzymes that enzymatically catalyze the hydrolysis of the glycosidic bond between two or more carbohydrates or between a carbohydrate and a non-carbohydrate moiety (*70*). The GH enzymes play not only a fundamental role in enzymatic catalysis but also in diverse biological processes. Therefore, glycosidases are widely used in the hydrolysis of biomass as well as in human physiology and disease treatment.

For nomenclature, these GH enzymes are classified into a number of families based on amino acid sequence similarity. To this date (April 2015), the Carbohydrate-Active Enzymes database (**CAZy**) provides a list of 133 glycoside hydrolase families. This classification reflects the homology in structural features and the evolutionary relationships among these enzymes.

1.2.2.2. Structure of glycoside hydrolases

Regarding structure, some of GH families are grouped into "clans", which describe the conserved folding architecture of the proteins. For example, clan GH-A is comprised of 19 families that share the same TIM-barrel fold. Clan GH-B includes the proteins from the GH7 and GH16 families with a β-jelly roll fold in the tertiary structure, etc. (*65*). Based on substrate specificity and catalytic mechanisms, glycosidases have different active site conformations. Because of the physicochemical resistance of tightly packed linear glycan polysaccharides, such as cellulose and chitin, many GHs that break carbohydrate chains are found to possess a deep cleft or tunnel active site architecture (Figure 1.8) (*30*). In most cases, this active site shape is effective for enzymes which adopt processive mechanisms in polysaccharide degradation. In processive GHs, the deep cleft or tunnel in the active site is usually paved with aromatic residues that are important and ensure packing, binding and sliding of the polymer through the active site (*16, 71-73*). These aromatic residues bind to carbohydrate substrates by hydrogen bonding and stacking, which are the dominant interactions in carbohydrate-protein complexes (*13, 69*). However, non-processive GH enzymes show active sites with a more open cleft or pocket with fewer aromatic residues.

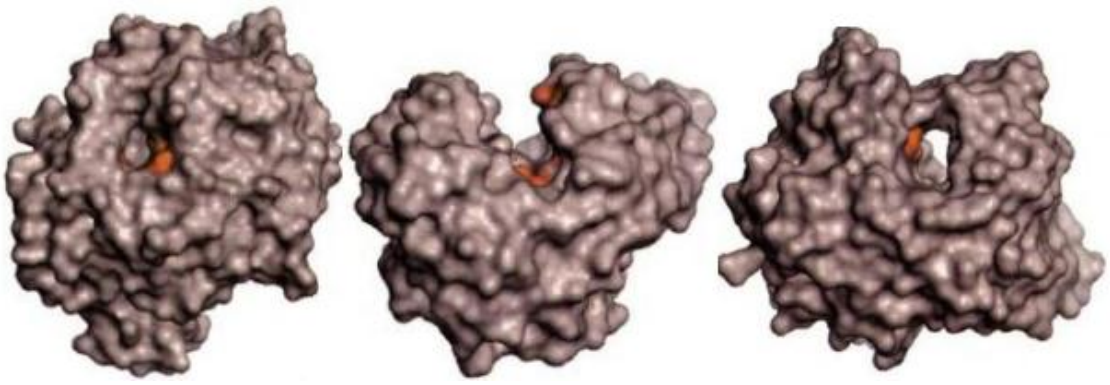

Figure 1.8. Active-site shapes in GH enzymes: left, pocket (glucoamylase from *Aspergillus awamori*, PDB entry 1GLM); middle, cleft (endoglucanase E2 from *Thermobifida fusca*, PDB entry 1TML); right, tunnel (cellobiohydrolase II from *Trichoderma reesei*, PDB entry 3CBH). The catalytic residues are colored in red. Figure adapted from reference (*74*)**.**

1.2.2.3. Mode of action

GH enzymes can be classified as exo- and endo-enzymes (Figure 1.9), which refers to the ability of a glycoside hydrolase to cleave a substrate in the middle or at the end of a chain (mostly but not always the non-reducing end). For example, *Sc*HEX in this research thesis is an exo-acting enzyme, whereas ChiC and XlnB2 are endo-acting enzymes.

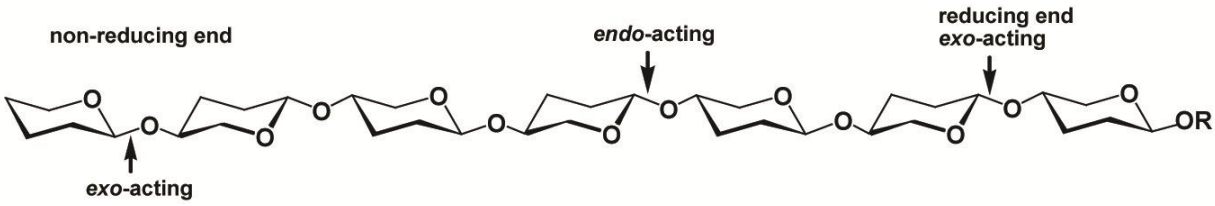

Figure 1.9. Endo-, exo-acting cleavage mechanism type. Figure reproduced from reference (*65*)**.**

The two standard mechanisms of glycosidic bond cleavage are inversion or retention of the configuration of the anomeric carbon, as originally outlined by Koshland in 1953 (*66*) (Figure 1.10). In these mechanisms, the cleavage of the glycosidic bond is catalyzed by two amino acid residues: a general acid/base residue and a nucleophilic one. Depending on the spatial position of these catalytic residues, hydrolysis occurs *via* overall retention (the initial configuration of the scissile bond is retained by the newly generated reducing end) or overall

inversion of the anomeric configuration (*65*). Moreover, in recent years, several interesting modified mechanisms have been discovered such as substrate assistance, alternative nucleophile, or one fundamentally different mechanism catalyzed by an NADH cofactor. In this thesis, only the two standard and the substrate-assisted mechanisms are described.

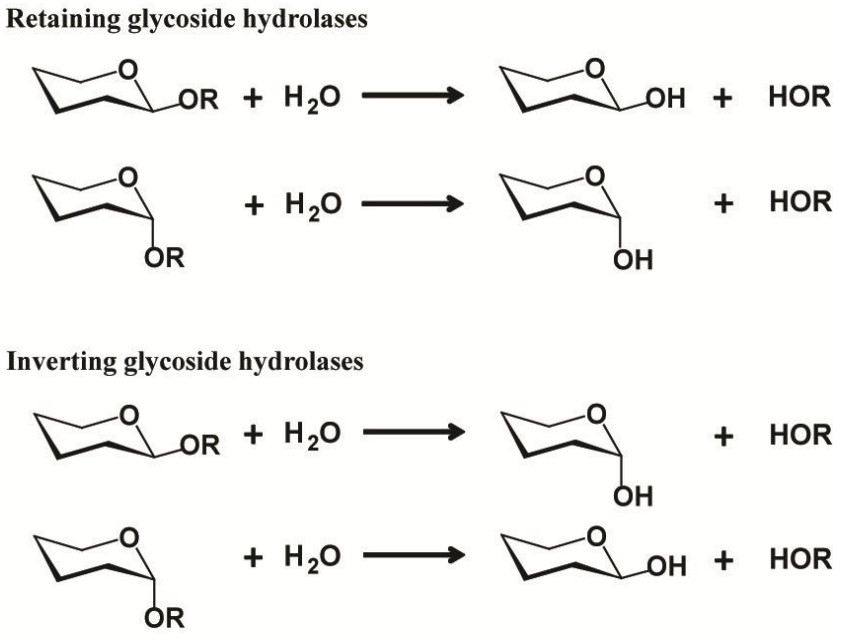

Figure 1.10. Retaining, inverting mechanism types with GH enzymes. Figure reproduced from reference (*65*)

The inverting mechanism is a one step, single-displacement mechanism involving oxocarbenium ion-like transition states (Figure 1.11). The reaction typically occurs with general acid and general base assistance from two amino acid's side chains (normally glutamic or aspartic acid) that are typically located 6-11 Å apart. After hydrolysis, the anomeric configuration of the glycoside is inverted (*74*).

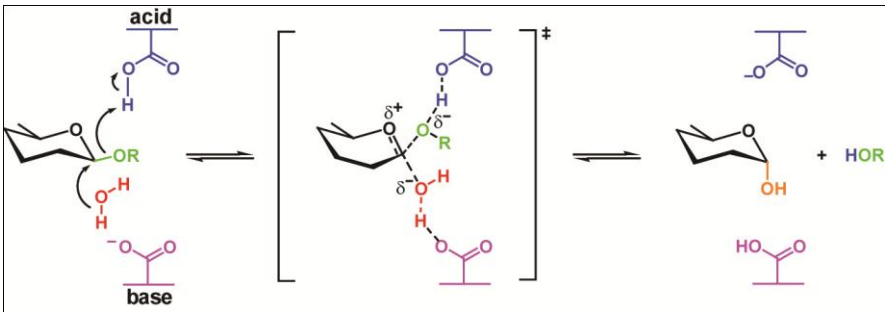

Figure 1.11. Inverting mechanism with GH enzymes. Figure reproduced from reference (*65*) **.**

The retaining mechanism is a two-step, double-displacement mechanism involving a covalent glycosyl-enzyme intermediate (Figure 1.12). Each step passes through an oxocarbenium ion-like transition state. Similarly to the inversion mechanism, the reaction occurs with acid/base and nucleophilic assistance provided by two amino acid's side chains, typically glutamate or aspartate, located 5.5 Å apart. In the first step or glycosylation step, the nucleophilic residue attacks the anomeric centre to displace the aglycon and form a glycosyl-enzyme intermediate, meanwhile the acid catalyst protonates the glycosidic oxygen as the bond is being cleaved. In the second step or deglycosylation step, the base catalyst abstracts protons from the water molecule as it attacks, hydrolyzing the glycosyl intermediate, and finally generating a glycon product with net retention of the configuration.

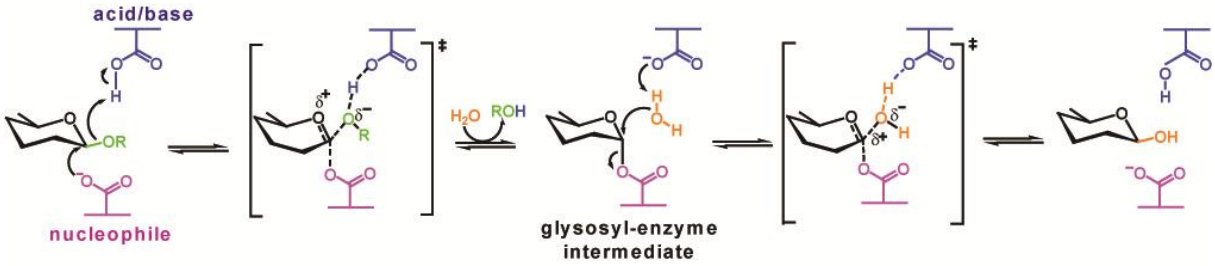

Figure 1.12. Retaning mechanism with GH enzymes (for a β-glycosidase). Adapted from reference (*65*)**.**

One of the modified mechanisms is the substrate-assisted mechanism with neighboring group participation of the substrate (Figure 1.13). Many polysaccharides contain an *N*-acetyl (acetamido) or *N*-glycosyl group at the 2-position of the pyranoside ring. GH families 18, 20, 25, 56, 84, and 85 have no catalytic nucleophile, instead they utilize the 2-acetamido group to act as an intra-molecular nucleophile. The participation of the 2-acetamido group leads to formation of an oxazoline (or more specifically an oxazolinium ion) intermediate, which is stabilized by another conserved residue. In the next step, a general acid/base accepts a proton from the substituent, then the oxazoline ring is attacked by a water molecule at the anomeric center to form a hemiacetal product (*38*, *75*, *76*). Not all enzymes that cleave substrates possessing a 2-acetamido group adopt the substrate-assisted mechanism. For instance, GH3 and GH22 enzymes utilize a classical retaining mechanism and hexosaminidases of the GH19 family utilize an inverting mechanism. The research presented in this thesis focuses on three enzymes: chitinase, *N*-acetylhexosaminidase, and xylanase that are all GH enzymes. Chitinase ChiC from *S. coelicolor* A3(2) is a GH18 family member,

meanwhile *N*-acetylhexosaminidase *Sc*HEX, also from *S. coelicolor* A3(2), belongs to the GH20 family, and xylanase XlnB2 from *S. lividans* belongs to the GH11 family. Among them, ChiC and *Sc*HEX adopt the substrate-assisted mechanism, and XlnB2 shows a retaining mechanism.

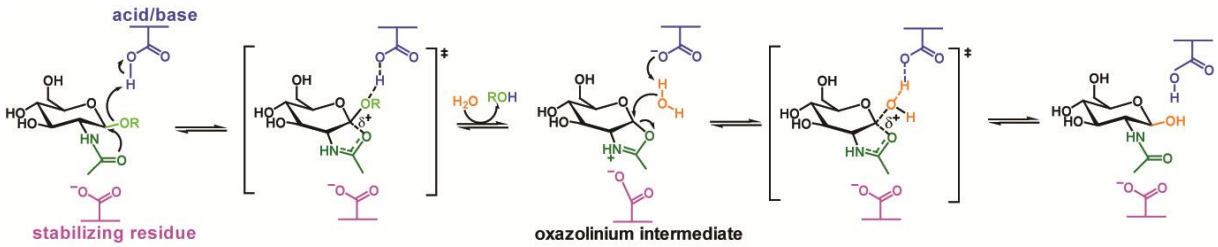

Figure 1.13. **Substrate-assisted mechanism utilized by GH enzymes**. Figure adapted from reference (*38*).

The subsite theory developed by Hiromi *et al.* (*77, 78*) and by Allen, Thoma and co-workers (*79, 80*) recommends a nomenclature in which the binding surface of the protein is divided into several subsites and represents the point of cleavage. Davies *et al.* proposed that GHs have five or more subsites, labeling −3, −2, −1, and +1, +2, etc., which accommodate a long substrate inside the active site. This nomenclature indicates that the subsites interact with glycosyl residues from the non-reducing end to the reducing end of the substrate. The cleavage takes place at the point between the -1 and +1 subsites, indicating whether the non-reducing or reducing end is being enzymatically attacked (Figure 1.14) (*81*).

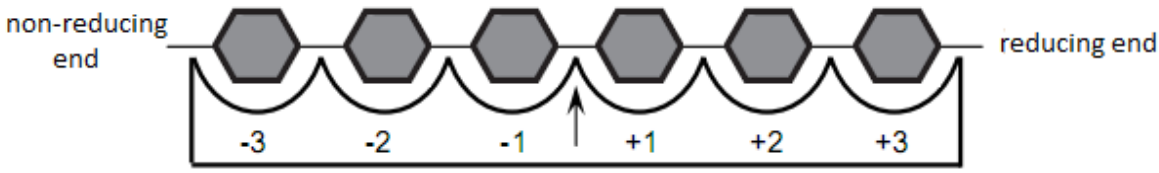

Figure 1.14. Subsites nomenclature in GH enzymes. Subsites -3 to +3 from the non-reducing end to the reducing end. The arrow indicates the site of cleavage**.** Figure adapted from reference (*81*) **.**

Regarding structure, the cleft or tunnel topology of active sites in GHs allows these enzymes to release the product while remaining firmly bound to the polysaccharide chain by several subsites, thereby, creating the conditions for processivity. Figure 1.15 illustrates the processive mechanism, which is often found in GH enzymes. When a product is released, the enzyme keeps binding to the substrate through several subsites. The empty

subsites or other factors, such as loop movement, assist the chain in sliding along the active site for the next hydrolysis to occur (*81*).

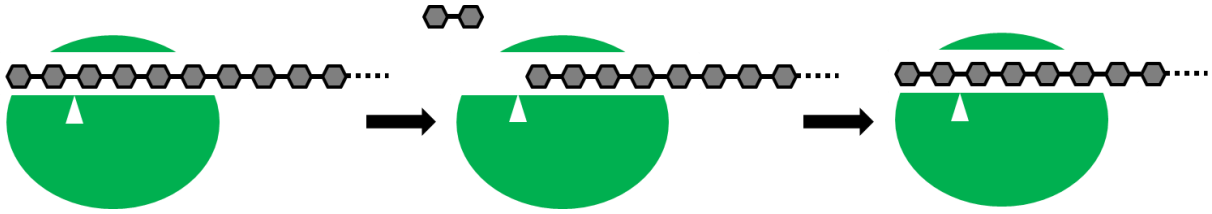

Figure 1.15. The processive mechanism of GH enzymes. Once a dimer product is released (shown as two linked hexagons), the enzyme remains bound to the polysaccharide chain, the « lid » closing the active site. The chain keeps threading along the active site by two sugar units until the next hydrolysis occurs. Figure reproduced from reference (*81*).

1.3 Chitinolytic enzymes

Chitinolytic enzymes, which hydrolyze the β(1,4) linkage of chitin, are key enzymes in the natural processing of this material. Based on their hydrolytic functions, chitinolytic enzymes are classified into endochitinases (E.C. 3.2.1.14), exochitinases (E.C. 3.2.1.29), and *N*-acetylglucosaminidases (HEX) (EC 3.2.1.30) (*24*). The first group randomly cleaves the chitin polymer to yield soluble, low molecular weight oligomers, such as chitotetraose and chitopentaose. The second group catalyzes the progressive release of chitobiose from the non-reducing or the reducing end of the polymer chain. The last category releases *N*-acetylglucosamine monomers from chito-oligomers and chitobiose, which are produced by the endochitinases and exochitinases, respectively. It was reported that complete degradation of chitin requires chitinase and HEX acting in a concerted fashion (*33, 35*). In this degradation, chitinase degrades chitin into chitooligomers, which are then hydrolyzed by HEX to release GlcNAc (*82, 83*). The oligomers of the degradation process seem to be promising candidates for biomedical applications. For example, they can be used in antimicrobial, anticancer, wound-healing, antitumor, or antioxidant effectuations (*84*).

Based on their primary structure, endo- and exo-chitinases are grouped into two GH families: GH18 and GH19 (*85-87*). Meanwhile, HEXs that hydrolyze chitooligomers belong

to the GH20 family. GH18 and GH19 family members, both of which contain enzymes of the endo- or exo-type hydrolytic mechanism, display no sequence homology as well as unrelated three-dimensional structures. GH18 enzymes retain the typical $(\alpha/\beta)_8$ protein fold in the catalytic domain (Figure 1.16), whereas GH19 enzymes present a relatively high α-helical content as well as several core structural elements similar to those of chitosanases and lysozymes (*88-90*). Due to the differences in sequence and structure, members of the two families display distinguishing catalytic mechanisms. Chitinases from family GH19 employ a single displacement cleavage mechanism, yielding a reducing end product with inverted configuration relative to the hydrolyzed bond (*91*). Meanwhile, GH18 members catalyze chitin hydrolysis through a double displacement cleavage mechanism in which the initial configuration of the scissile bond is retained by the newly generated reducing end (*74*). In more detail, GH18 members hydrolyze chitin through a substrate-assisted mechanism with participation of the adjacent pyranose acetamido group of the chitin substrate (*92*).

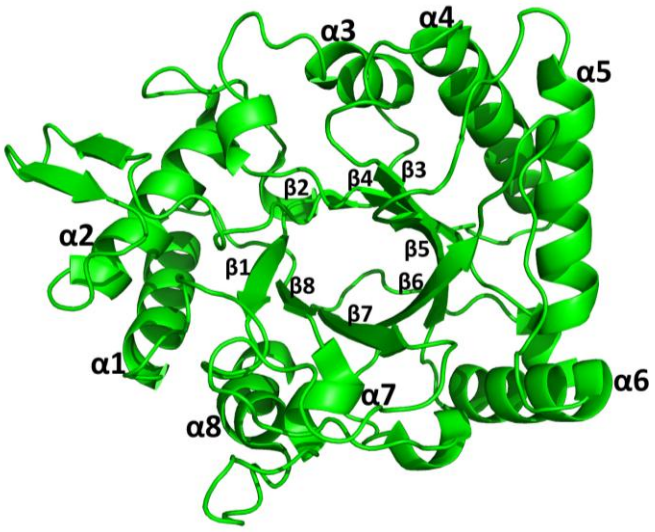

Figure 1.16. A typical $(\alpha/\beta)_8$ protein fold in GH18 enzymes. An example from *Serratia marcescens* Chitinase C (*13*), PDB entry 4AXN. The α-helices and β-strands composing $(\alpha/\beta)_8$ barrel are labeled α1–8, β1-8, respectively. Figure was generated using PyMOL.

The third group of chitinolytic enzymes, HEX, belongs to the GH20 family. HEXs are exo-type glycoside hydrolases that catalyze the cleavage of GlcNAc and β-*N*-acetylgalactosamine (GalNAc) residues from the non-reducing end in *N*-acetylhexosaminides. The enzymes have been studied since the 1970s when Matsushima and coworkers reported for

the first time the characteristics of a HEX from crude commercial preparations of Takadiastase (*38*). Since then, HEXs have been intensively studied due to their very broad range of functions and because they are universally distributed among most types of living organisms. Chitinolytic HEXs exist in bacteria, fungi, and insects. In chitinolytic bacteria, HEXs are required for the complete degradation of chitin and they also take part in chitinase inducer formation (*93, 94*). In biofilm-forming bacteria, HEXs called Dispersin B detach cells from biofilm colonies, spreading the biofilm to other surfaces (*95-97*). Fungal HEXs are responsible for the normal growth of chitin-containing fungi, including morphogenesis (hyphal growth and branching, sporulation, spore germination), autolysis, nutrition, and mycoparasitism (*32-35*). They control cell wall lysis and regulate their reconstitution in hypha expansion and cell bursting prevention (*36, 37*). HEXs assist nutrient release in the saprophytic and mycoparasitic growth phases and may be involved in insect pathogenesis and phytopathogenesis (*38*). In *Coccidioides* spp., the complex morphologic changes during the spherule-endospore phase require biosynthesis and degradation of cell wall structural components such as chitin, glucan or maman. This process requires the participation of chitin synthase, chitinase, β-glucosidase, and HEX (*39-41*). HEXs isolated from insects have recently attracted a lot of attention because they may potentially be targeted for developing pesticides and bactericides. In insects, chitin is a structural part of the cuticle and peritropic membranes, where it is degraded by chitinolytic HEXs in the turnover of the chitin exoskeleton during metamorphosis (*38, 42, 43*).

1.3.1 Chitinase GH18

Different organisms produce chitinases for different purposes based on their own physiology. Therefore, chitinases GH18 perform their fundamental function in chitin hydrolysis and other diverse physiological functions in different species. In yeast, such as *Saccharomyces cerevisiae*, they are required for cell separation during growth (*98*). For fungi, they are important for cell wall degradation and modification, *e.g.* spore germination, tip growth, branching of hyphae, spore differentiation, autolysis and mycoparasitism (*98*). In bacteria, GH18 members play a role in processing and digestion of GlcNAc-containing macromolecules, which form their nutrient source (*84*). In insects, GH18 chitinases promote growth and take part in cuticle turnover and mobilization and in nutrient digestion (*84, 98*).

Chitinases GH18 from plants appear to play a defensive role against pathogenic or pestiferous organisms. Furthermore, they are found to be involved in gene duplication, diversification, and to promote growth in mammals (*98*).

1.3.1.1. Biochemical properties

The molecular mass of most GH18 enzymes is in the range of 20-80 kDa. They are found to be active over a wide range of pH and temperature. The optimal working pH values of many GH18 chitinases, for example, chitinases from *Streptomyces violasceusniger* MTCC 3959 (*50*), *Stenotrophomonas maltophilia* C3 (*84*) and those from *Ralstonia* sp. A-471 (*99*), *Bacillus cereus* (*100*), and *Aeromonas* sp. GJ-18 (*101*), are in the slightly acidic range of 4.5-6. On the contrary, other chitinases active within a wide range of pH values include *Streptomyces violasceusniger* MTCC 3959, which retains activity between pH 3–10 (*50*), and ChiA from *Serratia marcescens*, active between pH 4–11 (*102*). Besides, other GH18 members show different optimal pH working conditions, such as the chitinases from *Microbispora* sp. V2 (pH 3) (*103*), *Bacillus* sp. Hu1 (pH 6.5) (*46*), *Bacillus circulans* No.4.1 (pH 8) (*104*), and *Bacillus* sp. BG-11 (pH 8.5) (*105*). Meanwhile, the optimal working temperature of a number of GH18 chitinases is 50-60^{o}C (*68*), such as ChiA, ChiB, ChiC from *Serratia marcescens* (*102*), BG-11 from *Bacillus* sp. (*105*), chitinases from *Bacillus* sp. Hu1 (*46*).

In addition to such wide ranges of optimal pH, GH18 chitinases also show a broad range of working temperature conditions. Many of them show an optimal temperature below 50^{o}C, such as ChiA, ChiB, ChiC from *Serratia marcescens* (*102*), chitinase from *Bacillus* sp. Hu1 (*46*), BG-11 from *Bacillus* sp. (*105*), and Chit62 from *Serratia marcescens* B4A (*106*). On the other hand, many others show a broad spectrum of optimal temperatures, for example, endochitinase from *Streptomyces violaceusniger* and the thermostable chitinase from *Streptomyces thermoviolaceus* OPC-520 have optimal temperatures of 28^{o}C and ~80^{o}C, respectively (*84*).

1.3.1.2. Substrate specificity

GH18 chitinases, which are diverse in their sequence (*107*), are known to degrade both soluble and insoluble chitin, chitosan with degrees of acetylation even as low as 13%, and

peptidoglycan (http://www.cazypedia.org/index.php/Glycoside_Hydrolase_Family_18). The GH18 family contains non-processive endo-type enzymes and processive enzymes with both endo- and exo-binding modes. With respect to polysaccharide degradation, the processive enzymes keep detached single-polymer chains through the active site cleft, then, bind and successfully cleave the substrate without dissociation until every possible hydrolyzed linkage in a sequence has been cleaved (*71, 74, 108-110*). In this mode, the substrate keeps binding to the active site cleft after successful cleavage and slides along for the next hydrolysis step to occur. The substrate can bind to the active site in an endo- (binding at internal positions) or in an exo-fashion (binding at the end of the sugar chain).

1.3.1.3. Structure and catalytic mechanism

The biochemical properties of GH18 enzymes are evolutionarily diverse with multi-domains in structure but their catalytic domain retains the TIM protein fold. Generally, the structure of GH18 members presents various combinations of signal peptides, catalytic domains, chitin-binding domains (ChtB) and serine/threonine-rich linkers (*98*). While several complete bi-modular chitanase structures have been resolved, compared to other multi-modular chitinases, only the structure of the isolated catalytic domain is available (*65*). The catalytic domain is composed of eight (α/β) motifs with oligosaccharide-binding active sites. ChtBs show their critical role in effectively breaking down crystalline chitin by increasing substrate accessibility and facilitating hydrolysis of the insoluble substrate via aromatic residues (*98, 104, 111*). The catalytic domain and ChtB are usually connected by an S/T-rich linker, which can be glycosylated to protect the chitinase from proteolysis (*98, 112*).

These enzymes catalyze chitin hydrolysis through a double displacement mechanism with retention of the anomeric configuration (*74*). GH18 enzymes also retain the conserved catalytic motif DXDXE (*113, 114*) and hydrolyze chitin through neighboring group participation (*92*). As mentioned in the above section, the enzyme adopts this mechanism and provides a general acid residue to protonate the leaving group, enabling its departure with the substrate carbonyl oxygen playing a role as a nucleophile to form an oxazolinium intermediate. Such anchimeric assistance was confirmed by studies on the well-known GH18

inhibitor allosamidine, a pseudo-trisaccharide that mimics the oxazolinium intermediate of chitin cleavage (*113*, *115*).

One of the typical properties of enzymes acting on polysaccharides is their substrate-binding clefts lined with aromatic residues. The processive GH18 chitinases' active site cavities are packed with some conserved Trp or Tyr residues, whose hydrophobic properties play a crucial role in processivity (*29*). In fact, GH18 chitinases have been thoroughly investigated to get insight into the processive mechanism and its importance for biomass conversion efficiency (*12*, *116*).

1.3.2 β-*N*-Acetylhexosaminidase GH20

1.3.2.1. Biochemical properties

Until now, the GH20 family has been the most numerous and most characterized group of carbohydrate-active enzymes because of their diverse distribution, varied structure as well as their valuable applications in industry. Table 1.1 shows biochemical properties of some GH20 representatives.

Table 1.1 Biochemical properties of several GH20 enzymes.

Enzyme ***(Reference)***	***Organism***	**MW (kDa)**	**pH stability**	**Optimal pH/Temp.(^{o}C)**	**K_m* (mM)**	**V_{max}* (μmol.min^{-1}.mg^{-1})**
Hex 1 (*117*)	*Paenibacillus sp.*	98	NA	6/NA	0.117/NA	212/NA
Hex 2 (*117*)	*Paenibacillus sp.*	105	NA	6/NA	0.119/NA	150/NA
Hex (*118*)	*Sotalia fluviatilis*	10	NA	5.0/60^{o}C	2.72/NA	9.5 x 10^{-6} /NA
*Sp*Hex (*119*)	*Streptomyces plicatus*	55	NA	3/NA	0.14/NA	53.2 $\pm$ 2.1 /NA
Hex (*120*)	*Aspergillus nidulans*	190	5-9	5.0/ 50^{o}C	0.581/0.589	10/2
Hex (*121*)	*Paecilomyces persicinu*	95	2-10	4.6/35-37^{o}C	0.625/0.322	220/115
Hex (*122*)	*Bipolaris sorokiniana*	120	4-10	4.5/55^{o}C	0.081/1.24	NA
Hex (*123*)	*Trichoderma harzianum*	150	3-9	4.0-5.5/50^{o}C	0.24/NA	NA
Hex(*124*)	*Aspergillus niger*	149	3.5-7.5	3.9-4.6/NA	NA	NA

K_m*, V_{max}*: towards *p*NP-GlcNAc / *p*NP- GalNAc

NA: not available

1.3.2.2. Structure and catalytic mechanism

The GH20 family has been thoroughly studied with respect to structure, mechanism, substrate specificity, and biosynthetic potential. The GH20 family possesses numerous representatives whose crystal structures have been resolved, with 12 structures of 28 members resolved within three families (*38*, *65*). All of them present a highly conserved fold, which is the $(\beta/\alpha)_8$-barrel (TIM-barrel) architecture in the catalytic domain. They reveal a consensus sequence motif His/Asn-Xaa-Gly-Ala/Cys/Gly/Met-Asp-Glu-Ala/Ile/Leu/Val, where the Glu residue acts as the general acid/base in the catalytic mechanism of these enzymes. The difference between the bacterial, fungal or human GH20 Hex structures is found mainly in their subunit constitution. In bacteria, they are monomeric while in humans they are dimeric with two active sites; and in fungi, they consist of catalytic units bound to propeptides (*38*). The first HEX crystal structure resolved was that from *Serratia marcescens* in its free form and as a complex with chitobiose (*125*). Then, in order to gain some insight into the mechanism of action of the GH20 family, the HEX from *Streptomyces plicatus* was crystallized as a complex with many compounds. The structure of the *S. plicatus* HEX (*Sp*Hex) is shown in Figure 1.17.

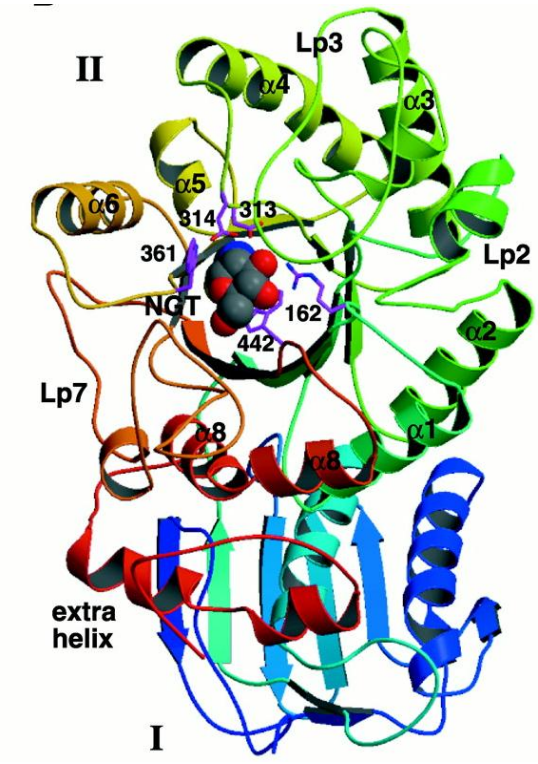

Figure 1.17. Ribbon diagram of *Sp*Hex in complex with NAG-thiazoline (*NGT*). Coloring proceeds from *blue* (N-terminus) to *red* (C-terminus). The α-helices of the (β/α) barrel composing domain II are labelled α1–8. Active site residues are numbered and shown in *magenta*. NGT bound inside the active site of *Sp*Hex. Figure adapted from reference (*119*).

Apart from their structure, the GH20 family is also the most studied group in regards to their mechanism of action, which is known as substrate-assisted catalysis (or as neighbouring group participation mechanism). In this mechanism, the carbonyl oxygen of the 2-acetamido substrate moiety acts as a nucleophile, yielding a bicyclic oxazoline intermediate, which is stabilized by a conserved Asp residue. In the next step, a highly conserved catalytic residue Glu, acting as general acid/base, accepts a proton from the substituent. Finally, the oxazoline ring is attacked by a water molecule at the anomeric center to form a hemiacetal product (Figure 1.13) (*38, 75, 76*).

1.3.2.3. Substrate specificity

Although the members of the GH20 family share a common catalytic domain with conserved active site residues, they demonstrate specificity toward diverse substrates. This family is known to have the ability to cleave a broad spectrum of substrates, including substrates containing β(1,6), β(1,4), β(1,3), or β(1,2) glycosidic bonds, branched compounds such as glycoproteins, glycolipids, or sulfated glycoconjugates or substrates modified at the C2, C4 or C6 position of the pyranose ring (*95, 119, 126-129*).

Several studies on *Aggregatibacter actinomycetemcomitants* DispersinB, whose substrate specificity towards the β(1,6)- linkage was elucidated, have revealed that the low sequence identity between the DispersinB and other GH20 members results in a difference within their loop conformations associated with substrate specificity (*95-97, 130*). In terms of structure, the same subsite -1 residues appear in the active site of all GH20 enzymes, while the amino acid residues in subsites +1, +2 and +3 vary with the substrate specificity of the enzymes (*95, 126*). Particularly, in DispersinB, the lack of one Trp residue (Trp685 in human HEX, Trp408 in *S. plicatus* HEX), which interacts with the +1 subsite moiety via a hydrophobic stacking interaction with β(1,4)-linked saccharides (*97, 131*), is consistent with a conformational change due to a curved β(1,6)-linked oligosaccharide (*95, 126*). It was further confirmed that the aromatic amino acids Trp237, Tyr187 and Tyr278 of DispersinB play a role in the substrate specificity (*132*).

Chitinolytic HEXs grouped within the GH20 family take part in the degradation of chitin, the linear polymer of β(1,4)-linked GlcNAc. These enzymes are present in bacteria

(such as *Streptomyces plicatus, Vibrio furnissii* or *Alterromonas* sp.), fungi (such as *Aspergillus oryzae, Penicillium oxalicum*) and insects (such as *Ostrinia furnacalis*), and have been extensively studied as potential targets for developing pesticides and bactericides. Liu *et al*. (*133*) found that the chitinolytic HEX structure is distinguished from other HEX in that it adopts a substrate specificity towards the β(1,4)-linkage. The representative chitinolytic HEX, *Of*Hex 1 (from *Ostrinia furnacalis*) and *Sm*CHB (from *Serratia marcescens*), possess a deep substrate-binding pocket with subsite -1 and +1 in the active site that enable them to tightly bind long- and linear-chains of the substrate. Moreover, this pocket is comprised of the conserved Val327 and Trp490 (number in *Of*Hex 1) residues, which are proven to be very important for binding long chitooligomers (*133*).

Another study has reported that a GH20 HEX from *Paenibacillus* sp. TS12 is capable of degrading Gb4Cer, a glycosphingolipid, which contains a β(1,3) glycoside linkage. This HEX shares no common feature in the C-terminal region of its sequence and has a disulfide bond at a different position in its structure when compared with the chitinolytic *Sp*Hex from *Streptomyces plicatus*. These differences may play a role in substrate recognition (*117*).

Recently, Jiang *et al.* (2011) (*129*) reported on a GH20 HEX - StrH from *Streptococcus pneumonia* R6 which can remove the β(1,2)-linked β-*N*-acetylglucosamine from host defense molecules. This enzyme harbors two loops at the entrance of the substrate binding pocket, which are distinct from other GH20 members. Structural and mutagenesis studies of this enzyme revealed two key residues, Trp443 and Tyr482 at subsite +1, which reside on the two loops and are crucial for the β(1,2) substrate specificity.

It has been shown that the substrate specificity of human HEX differs from that of its chitinolytic counterparts due to differences between their active site structures. The active pocket of chitinolytic HEX is deep, whereas that of human HEX is shallow and possesses only subsite -1, which can bind branched *N*-glycan or branched substrates such as glycolipids and glycoprotein G_{M2} and G_{A2} gangliosides. The substrate specificity towards branched substrates was also found in HEX from fungi, insects, and plants. *Bombyx mori* HEX and *Spodoptera frugiperda* HEX isolated from insects, display activity towards *N*-glycans (*42,*

43). Similarly, the enzymes from plants, such as those from *D. melanogaster*, and *S. frugiperda* carry out post-translational modifications of *N*-glycans (*134, 135*).

Applying HEXs as biosynthetic tools *in vitro* provided information on the fact that HEXs can catalyze transglycosylation or reverse hydrolysis reactions using structurally modified substrates. Husakova *et al*. (*136*) reported on the ability of HEX to use a substrate acetylated at the C6 position in a transglycosylation reaction. Later, many reports described synthetic methods catalyzed by HEX using modified substrates at the C6 position, such as an aldehyde or a sulfate substitution (*137, 138*). The versatile transglycosylation potential of fungal HEXs is further demonstrated by various C2 alterations such as acyl length and substituting hydroxyls as substrates, which were catalyzed by HEXs from *Talaromyces flavus*, *Aspergillus oryzae,* and *Penicillium oxalicum (136, 139)*. The substrate flexibility of HEXs is also demonstrated in the reaction using 4-deoxy sugars (lack of -OH group at C4) or alternative aglycons at C1 (azide, or nitro-2-pyridyl group) (*38*).

In general, even though GH20 enzymes share a common catalytic domain structure and utilize the substrate-assisted catalytic mechanism, they display a broad specificity towards many substrates, which are different in their type of glycosidic linkage (either β(1,2)-, β(1,3)-, β(1,4)-, or β(1,6)-linked), linear or branched substrates, and substrates modified at the C1, C2, C4 or C6 positions.

1.3.3 Chitinolytic machinery of *Streptomyces coelicolor* A3(2)

Streptomycetes are well known for their ability to exploit the different nutrient sources available in the soil and are thus considered as the main decomposers of soil chitin (*140*). Since chitin is insoluble and is an unusual polysaccharide containing nitrogen, complex extracellular systems are needed for utilizing chitin as a carbon and a nitrogen source (*141*). The genome of the *Streptomyces* representative species, *S. coelicolor* A3(2), was sequenced in 2002 by Bentley and co-workers (*62*). The *S. coelicolor* genome showed a wide diversity in chitinase coding genes, potentially enabling them to hydrolyze the natural diversity of chitin types. The chromosome of *S. coelicolor* encodes nine genes for family GH18 (*chiA, B, C, D, E, H, sco1444, sco2799, sco7263*), 2 genes for family GH19 (*chiF* and *chiG*) and 11 putative HEX members (*107, 142*).

1.4 Xylanases

1.4.1. Xylanases

Due to the structural diversity of xylan, there are limited enzymatic strategies for microoganisms to hydrolyze this complex heteropolymer. However, efforts have been made to understand the structural basis for substrate specificity of a number of xylanolytic enzymes belonging to different GH families. Xylan depolymerization requires a mixture of different GH enzymes, including endo-1,4-β-xylanases (EC 3.2.1.8), β-D-xylosidases (EC 3.2.1.37), α-L-arabinofuranosidases (EC 3.2.1.55), α-glucuronidases (EC 3.2.1.139), acetyl xylan esterases (EC 3.1.1.72), and ferulic/coumaric acid esterases (EC 3.1.1.73) (Figure 1.6). Among them, endo-1,4-β-xylanases, which cleave the β-1,4-glycosidic linkage between xylose residues in the backbone of xylans, is one of the crucial enzymes required for complete degradation of the polymer. They are classified into GH families 5, 8, 10, 11, 16, 26, 30, 43, and 62 based on amino acid sequences, tertiary structure, and catalytic mechanisms (*67*). True β-(1,4)-acting xylanases are included in families 5, 8, 10, 11, and 30 with different structures and substrate specificities. GH5, GH10 and GH30 enzymes display the same $(\beta/\alpha)_8$-fold but differently hydrolyze arabinoxylan, glucuronosyl-xylan, and heteroxylan, respectively. GH8 xylanases have an $(\alpha/\alpha)_6$ architecture and can cleave many types of heteroxylan, including aryl-cellobiosides that is close to GH10 substrate specificity. Finally, GH11 members, which are the smallest xylanases with a β-jelly-roll structure, are highly specific and increasingly interesting as efficient tools and green catalysts for biotechnological applications (*11, 59*).

1.4.2. Xylanase GH11

1.4.2.1. Biochemical properties

GH11s are true endo-β-1,4-xylanases that catalyze the cleavage of β-1,4-xylosidic bonds of substrates. Due to potentially wide applications in industry and in order to find more adapted, specific and affordable enzymes that are suitable for biotechnological processes, numerous GH11 members have been thoroughly characterized. They are found to be diverse in enzyme activity, pH and thermo stability despite high structural and sequence similarities. They are divided into acidic and alkaline xylanases based on their optimal pH, which varies

considerably from 2 to 11 (*143-145*). GH11s with pI<5.0 are considered acidic xylanases, which is in contrast to alkaline members with pI>5.0. Several studies have demonstrated that the pI value is strongly correlated with the type of residue adjacent to the acid/base catalyst at position 46 (when not mentioned, xylanase residue numbers derive from *Streptomyces lividans* XlnB2). Xylanases possess a pI<5.0 if the residue is Asp, and in contrast, a pI>5.0 if the residue is Asn (*143-148*). One example that can be listed is the two xylanases XYNI and XYNII from *H. jecorina* having two different pH_{opt} values (3–4 and 5–5.5 respectively). Beside the diversity in pH_{opt}, GH11s also show variation in thermostability and thermoactivity. GH11 members display optimal temperatures ranging from 35°C to 85°C, corresponding to mesophilic, thermophilic and even hyperthermophilic enzymes (*11*). Table 1.2 shows biochemical properties of some GH11 representatives.

Table 1.2 Biochemical properties of several GH11 representatives.

Enzyme	Organism	pI	pH_{opt}	T_{opt}	V_{max} (UI/mg)	K_m (mg/mL)
Xyn11A (*149*)	*Chaetomium thermophilum*	NA	5.0-7.0	80 °C	NA	NA
XynA (*150*)	*Clostridium stercorarium F-9*	4.5	7.0	75 °C	2800	1.9
X22 (*151*)	*Aspergillus nidulans*	NA	6.0	62 °C	NA	4.2
Xylanase (*152*)	*Paecilomyces varioti*	3.9	5.5-7.0	65 °C	NA	2.5
XYN XynA (*153*)	*Bacillus subtilis*	8.9	NA	55 °C	NA	NA
Tx-xyl (*11*)	*Thermobacillus xylanilyticus*	7.7	6.0	75 °C	NA	1.6
TfxA (*154*)	*Thermomonospora fusca*	10.0	7.0	75 °C	600	1.1
XlnC (*155*)	*Streptomyces lividans*	> 10.2	6.0	57 °C	3000	4.1
XlnB (*156*)	*Streptomyces lividans*	8.5	6.5	55 °C	1.96 mmol/mg	3.71

UI - µmol/min.

1.4.2.2. Substrate specificity

GH11 xylanases are specific to heteroxylans but their specificity depends on the type of these polymers. Heteroxylans have xylose-based backbones with typical substitution at O2 or O3 by arabinose, galactose, xylose, ferulic and glucuronic acids. The substitutions are different depending on plant source and the tissue localization. Indeed, GH11 xylanases prefer linear xylans and preferably cleave in unsubstituted regions of the backbone since they cannot hydrolyse xylosidic bonds at the non-reducing end next to branched xylose. As a result, heteroxylans with high degrees of substitution are not fully hydrolyzed by GH11s. This observation reflects the relation of substrate specificity to the relative narrow cleft of GH11, in comparison, for example, to that of GH10s, which are widely opened and larger. GH10s have broader substrate specificity towards highly substituted xylan, such as branched arabinoxylans, β-(1,3)-linked xylans and short cello-oligosaccharides (*11, 59*).

The major unsubstituted products released from hydrolysis of these substrates by GH11s are xylobiose and xylotriose. This family shows no detectable activity towards these products, but has only a very low activity on xylotetraose and increasing activity on oligomers with a degree of polymeration from DP5 to DP9 (*59, 157, 158*). With respect to glucuronoxylan, GH11 enzymes can cleave the polymer to generate xylotetraose with MeGA bound at the second xylose from the non-reducing end as the major substituted product. Meanwhile, hydrolysis of arabinoxylan yields xylotriose with O3-linked arabinose on the central xylose (*59, 157, 159*).

1.4.2.3. Structure and catalytic mechanism

The typical point in GH11 architecture is the overall conserved structure of the β-jelly roll domain, which presents a closed right-handed architecture and a long, deep active site cleft covered by a “thumb-loop”. The catalytic domain is comprised of one α-helix, and two β-sheets A and B that mimic the fingers and the palm, while the thumb is formed from the loops between B7 and B8. The thumb backbones are highly homologous in size with a typical length of 11 residues. The disulfide bridge between the “cord” (the loop joining β-strand B6-B9) and β-strand B8 or between the α-helix and the β-strand B9 can be found in several GH11 members (*147, 148, 152, 160*). The catalytic cleft of GH11 xylanases is deep, narrow, and

long, which fully accommodates the long xylan polymer (*11*). The shape of the active site also reflects their typical substrate specificity as well as enzyme specificity, showing affinity towards unsubstituted xylose units (*157*). The majority of GH11 xylanases contain at least five subsites from -2 to +3, in which the glycone subsites (−1, −2) are marked from the scissile bond towards the non-reducing end and the aglycone subsites (+1, +2, +3) heading away from the scissile bond towards the reducing end of the bound substrate (*11*) (Figure 1.18). This active site includes mainly aromatic residues and a few polar residues that belong to β-strands B2, B3, B4 on one side and to β-strand B8 and the thumb on the other side.

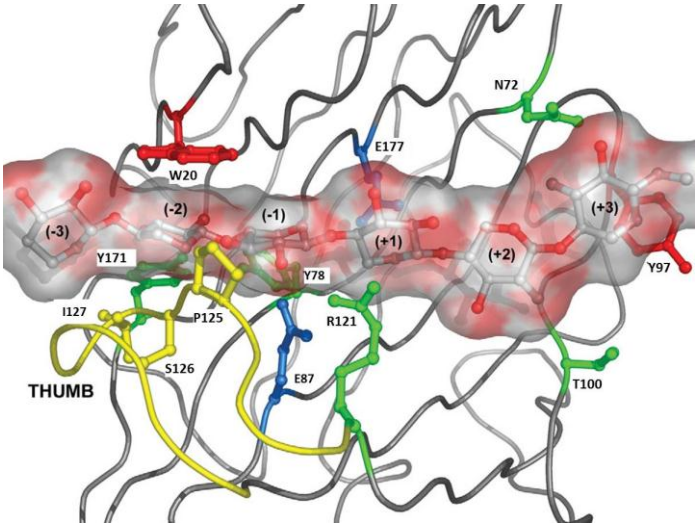

Figure 1.18. Xylohexaose modeled into six subsites in the active cleft of Tx-Xyl (from *Thermobacillus xylanilyticus*). Catalytic residues are in blue, aromatic residues in red, hydrogen-bonded residues in green. Figure is adapted from reference (*167*).

The conserved Pro residue of the thumb loop together with the conserved aromatic residues (Trp and/or Tyr) of the β-strand B2 form an environment to pack the substrate during binding and catalysis (*11*). Among aromatic residues, many are highly conserved (Trp20, Tyr74, Tyr78, Trp80, Tyr89, Tyr 171, Tyr 179) and show their role in substrate binding. The catalytic residues (Glu87 and Glu177) are the best conserved with 96% and 100% conserved in sequence and in three dimensional structure, respectively. The residue at position 48, which is mainly occupied by Val, is a structure related residue together with the catalytic residues forming a catalytic dyad. Residues at position 18 and 46 are also conserved polar residues. The residues Arg121 and Gln135 are also conserved and pave the catalytic cleft. Overall, the GH11 structure is highly conserved both in sequence and in space; especially the catalytic and

substrate binding cleft is highly maintained within the family and supports the endo-acting mode of action towards the long polymeric substrate (*11*). Figure 1.19 illustrates the spatial conservation of residues paving the catalytic cleft in GH11 enzymes.

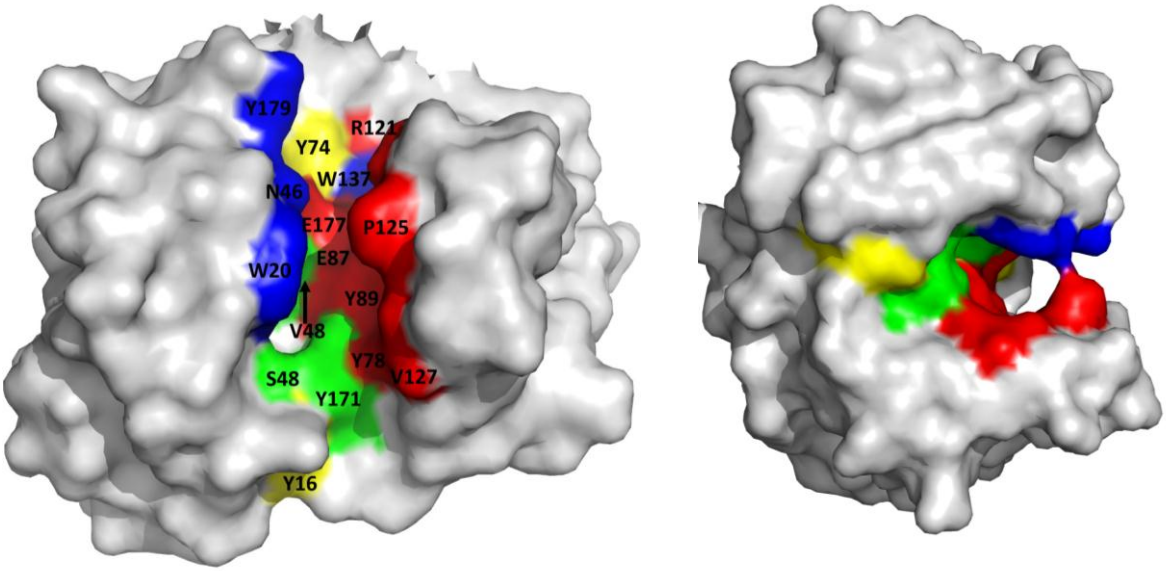

Figure 1.19. Residues paving the catalytic cleft of GH11 enzymes (example from *S. lividans* XlnB2). Left, front view. Right, side-view. Figure was produced by PyMOL. Adapted from reference (*11*)

Regarding the catalytic mechanisms, GH11 xylanases are retaining enzymes that adopt a double-displacement catalytic mechanism with the existence of a covalent glycosyl-enzyme intermediate (Figure 1.12). In the glycosylation step, the acid/base residue plays the role of a Lewis-acid to protonate the substrate, while the nucleophile residue stimulates a leaving group departure. This step forms a glycosyl-enzyme intermediate after going through an oxocarbenium-ion-like transition state. In the second step (deglycosylation), the base catalyst deprotonates the water molecule, creating a nuleophile attack on the carbonyl carbon of the intermediate. At this step, the xylose moiety is generated, retaining the β-configuration as the substrate (*11*).

1.4.2.4. Dynamic property

Proteins are not rigid but represent flexible ensembles with a close link between structure, dynamics, and catalysis (*161*). Understanding this flexibility is essential to learn how proteins perform their functions. Due to this importance, movement in GH11 has also

been demonstrated from several GH11 models through crystal structures, molecular dynamic simulations and a few data from NMR experiments (*153, 162-166*). Evidence from mutagenesis, crystal structure and molecular dynamic simulations has proposed the existence of a "thumb-loop" motion, which may play a major role in substrate binding and/or catalysis (*153, 166-169*). Deletion mutagenesis produced a thumbless variant of Tx-Xyl from *Thermobacillus xylanilyticus* that was almost catalytically inactive. Re-positioning of the thumb of the same protein through the deletion of the linker residues T120 and T132, which connect the thumb to the main enzyme scaffold, significantly reduced enzyme activity. In another experiment, site-saturation mutagenesis on the conserved sequence at the tip of the thumb Pro-Ser-Ile, making a new triplet Pro-Gly-Cys, increases enzyme turnover by 20% (*167*). A similar work on Xyl-11 from *P. griseofulvum* xylanase (PgXynB) led to an increase in catalytic efficiency (*168*). This change at the tip was proposed to account for improving flexibility of the thumb, hence, promoting enzyme activity.

It has also been suggested that there is an open/closed propensity of the active site to follow the catalytic process with three different conformations: Bind → Close → Loose → Bind (*11, 153, 163*). This propensity is accompanied with motion of the thumb along the conformational changes of the active site during catalysis. The precise position of the thumb is supposed to determine the width of the catalytic cavity and the ligand binding event is accompanied by altered thumb positioning (*164, 170*). The thumb of the XYN from *Bacillus circulans* is able to move and thus regulates the width of the active site cleft, suggesting an open-close conformation (*170*). The three-dimensional structures of XYNII from *Trichoderma reesei* complexed with three different epoxyalkyl xylosides (4,5-epoxypentyl β-D-xyloside, 3,4-epoxybutyl β-D-xyloside, and 2,3-epoxypropyl β-D-xyloside) suggested that the thumb moved at least 2.6 Å and partially closed the active site in the presence of the ligands (*164*). The authors proposed that all these structural changes may be coupled together and are induced by binding of the ligands. Another structural evidence for the potential flexibility of the thumb was discovered in the xylanase from *B. subtilis* (*169*), where the presence of a specific mutation allowed to observe the thumb in its open conformation with a large space (more than 15 Å) for the open-close motion of the thumb. It was also suggested that similar conformational variations may exist in other GH11 xylanases (*11*).

Despite the evidence of a correlation between backbone and side-chain ps-ns motions and crystalline conformers (i.e the ps-ns motions observed in solution occur also in the crystalline state) (*171*), all other information about protein motions obtained from mutagenesis or crystal pack is still a "snapshot" picture, thus, it is still difficult to infer protein dynamics in catalysis. In order to overcome the limitations of protein dynamic studies, molecular dynamic simulations (MD) were applied and their accuracy is demonstrated in a wide variety of chemical problems. By MD, Vieira *et al*. predicted that BCX demonstrates an open-close motion of the thumb that depends on the presence of the substrate (*166*). In another MD work on the *endo*-1,4-xylanase II from *Trichoderma reesei*, Muilu *et al.* also confirmed a similar type of active site opening and closing upon xylose binding that was predicted by its crystal structure (*163*). Nevertheless, in these studies, the simulations were on a very short time scale (800-1000 ps), during which the conformational changes of side-chains may occur, but not catalytic events. Overall, despite high structural and sequence homology, the dynamic properties of GH11 members have not been sufficiently characterized to conclude on their functional importance.

1.4.2.5. Applications of GH11s

Many heteroxylans and homoxylans have high water holding capacity and show potential for generating viscous solutions by extracting water. Therefore, xylanases that can cleave the internal xylan backbone have an important function in many cereal-based food and feed biotechnologies as well as in other applications such as: fiber biotechnology, pulp and paper industry, biofuel production, soap technology, and plant defense. Moreover, they can be used as molecular tools for *in situ* plant cell wall investigations, which is important in biomass conversion and biorefinery approaches (*10, 11, 172*).

In food biotechnology, xylanase mixtures from several families can be used to promote bread quality by increasing shelf life and volume of the bread, improving the crumb structure and reducing the stickiness of the dough (*173, 174*). GH11s can also increase wheat flour separation into starch and gluten by hydrolyzing unextractable arabinoheteroxylans, which leads to an increase viscosity (*175*). Xylanases from *Sclerotinia sclerotiorum* help in juice clarification by releasing oligo- and mono-saccharides, and concomitantly decreasing the

level of insoluble materials up to 27% (*176*). For bread products, the potential of *B. subtilis* GH11 for production of prebiotics was earlier demonstrated on barley and wheat flours (*11*).

In feed technology, xylanases from *Trichoderma viride* improved the digestibility of crude fiber by 60% and concomitantly increased the body weight of broiler chicken (*11*). In ruminant breeding, GH11s help to increase the assimilation of feeds, therefore, they have been used as animal feed inoculums or additives, mostly as enzyme cocktails (*11*). Moreover, in the last decade, xylanases have been employed for the production of xylooligosaccharides as prebiotics in the food and feed sectors (*59*). The use of xylooligosaccharides as prebiotics is due to their capacity for enriching bifidobacteria levels in the cecum, feces, and short-chain fatty acid biomarkers (*11*).

In the fiber and paper industry, robust enzymes, notably GH11, can reduce the amount of chlorine and chlorine dioxide used for biobleaching the wood pulp. The bleaching process is generally performed under high temperatures; therefore, thermostable GH11s are extremely suitable for this process. The GH11s with low MW can easily penetrate into the inner part of the cell wall, resulting in an improved deletion of lignin from the wood pulp (*177*). In the fiber industry, GH11s are used for flax fiber separation of core cells leading to separation of the fiber bundles from the non fiber parts (*11*).

One of the most important applications of GH11s is their use in biofuel production. Lignocellulosic biomass conversion produces a mixture of glucose, xylose and arabinose, which can be further fermented to produce bio-ethanol as second generation biofuel (*10*, *11*, *178*). In this production, xylanases can break down the structure of the lignocellulosic matrix and depolymerize the polymers into sugars, which are subsequently fermented into ethanol, generally by yeast strains. The ethanol, then, needs to be separated and purified to meet fuel specifications. Corn residues, sugarcane bagasse and grasses are potential sources of biofuels, due to their high yield, minimal requirement for nutrient and water input, and the fact that they can be grown in locations which would not compete with current food crops (*10*). Because of this unlimited source, it is valuable to replace fossil fuels by biofuels that may have a positive impact on global climate change and minimize the decrease of fossil fuel.

In order to produce an optimized enzymatic cocktail of xylanases for the abovementioned applications, it will be valuable to gain insight at the molecular level of the GH11 structure-function-flexibility relationship.

1.4.3 Xylanase B from *Streptomyces lividans* 66

S. lividans has been shown to secrete a number of enzymes involved in the degradation of lignocellulosic biomass, which is mainly comprised of cellulose and xylan. Among the proteins, three xylanase, A, B, and C, were purified and characterized, showing good activity towards soluble, insoluble xylan and oligoxylose (*155, 156, 179*).

The nucleotide sequence of xylanase B (XlnB) from *Streptomyces lividans* 66 was first reported by Vats-Mehta *et al.(180).* Then, the cloned and expressed protein was purified and characterized from cultures of *S. lividans* 66. The purified enzyme has a molecular mass of 34 kDa and a pI of 8.4. Using enzyme kinetic assays with xylan, it was observed that the optimal activity was at 55^{o}C and pH 6.5, with kinetic parameters of K_m=3.71 mg/ml, V_{max}=1.96 mmol/mg (*156*). The results also pointed out that the enzyme is stable at 30^{o}C, whereas above 37^{o}C the stability decreased gradually. The hydrolysis activity of XlnB was determined by using insoluble oat spelts xylan and soluble larchwood xylan. The results showed that the enzyme preferentially degrades the long, insoluble xylan and could be classified as an endoxylanase (*156*).

In the culture medium of *S. lividans* 66, two forms of XlnB are secreted, namely XlnB1 and XlnB2. XlnB1 is composed of two discrete structural and functional units, an N-terminal catalytic domain and a C-terminal xylan-binding domain, whereas XlnB2 contains the catalytic domain only. Both forms have the same specific activity on xylan (*181*). As mentioned above, with GH11 family, there exist hypotheses about an open-closed movement during catalysis as well as the movement of the thumb involved in substrate binding, catalytic reaction and product release. In this thesis, XlnB2 with a molecular weight of 22 kDa that is ideally suited for NMR experiments is used as a model to study the dynamic motions of the glycoside hydrolase GH11; in particular, to elucidate the abovementioned hypotheses.

1.5 Streptomyces

Streptomyces belong to the *Actinomycetes* group, *Actinobacteria* class, *Actinobacteridae* subclass, *Actinomycetales* order, *Streptomycineae* suborder, *Streptomycetaceae* family, and *Streptomyces* genus. From the first useful antibiotic Streptomycin, which is effective against tuberculosis, isolated from *S. griseus* in 1943, the *Streptomyces* genus is well-known for its ability to synthesize an amazing variety of active compounds, including antibiotics, fungicides, cytostatics, modulators of the immune response, and effectors of plant growth (*182*).

Streptomyces are high GC Gram-positive bacteria (according to NCBI taxonomy) (*183*). *Streptomyces* are well-known for biomass degradation, such as cellulose, chitin, and xylan degradation, because of their exceptionally large number of secreted hydrolytic enzymes. The ability to secrete large quantities of enzymes helps the bacteria to hydrolyze complex organic materials, therefore, allowing for their survival in the environment. *Streptomycetes* are well known for their ability to exploit the different nutrient sources available in the soil and are thus considered the main decomposers of soil chitin (*140*). Since chitin is an unusual and insoluble polysaccharide containing nitrogen, complex extracellular systems are needed for utilizing chitin as a carbon and a nitrogen source (*141*). The genome of the sequenced *Streptomyces* representative species, *S. coelicolor* A3(2), shows a wide diversity in chitinase genes, potentially enabling them to hydrolyze the natural diversity of chitin types (*62*). The chromosome of *S. coelicolor* encodes nine genes of the GH18 family (*chiA, B, C, D, E, H, sco1444, sco2799, sco7263*), 2 genes for family GH19 (*chiF* and *chiG*) and 11 putative HEX members (*107, 142*). Many other *Streptomycetes* species also contain known chitinases (*184*). Gene duplication of a common ancestor would explain this wide diversity of chitinases among *Streptomycetes*. In addition to the expression of many chitinase genes, *Streptomycetes* possess many other chitin-degrading enzymes such as chitosanases and putative lysozymes (*185-187*). These chitinases harbour unique properties in terms of thermostability and activity in wide pH ranges which make them suitable for industrial applications (*84*). Certain species, such as *S. lividans*, even possess a carbohydrate esterase that has a broad enough specificity to be able to transform chitin into its chitosan counterpart. Many *Streptomycetes* can degrade soluble carboxymethyl cellulose by secreted enzymes. *Streptomyces* spp. also produce a xylanase,

another commercially important enzyme, which is used in many applications, such as in the treatment of rice straw pulp to improve the pulp bleach ability or in biofuel production (*56*).

1.6 Structure-function-flexibility relationship

In cells, proteins have diverse biological functions ranging from DNA replication, transportation, enzymatic catalysis, or they can serve as storage components, etc. (*188*). It is known that protein function is defined from its structure, which is encoded from the primary sequence. Only when a protein folds into its unique and proper shape, or conformation, it is able to function efficiently (*189*). Many structural properties can contribute to protein function. For example, in membrane proteins, the hydrophobic regions of the protein interact favorably with the hydrophobic lipids in the membrane, forming a stable membrane structure. Protein folding allows amino acids that may be distant in the primary sequence to interact with each other. In enzymes, an active site formed from several catalytic amino acids binds specifically to the substrate and catalyzes the enzymatic reaction. Any change in this active site leads to changes in the chemical interactions between the amino acids and, thus, enzyme activity (*188*).

Although static structures are known for many proteins, and protein function was thought to depend on its fixed three-dimensional structure (for example, enzymes have fixed shapes that perfectly fit to specific substrates, as described in the Fischer's 'lock-and-key' model), the function of a protein is governed ultimately by dynamic character (*161*). The clearest illustration for the protein flexibility taking into account its function is regulatory proteins, which can change their conformations in order to interact with multiple targets (*190*). Some proteins can also be dynamic in terms of their quaternary structure when functioning. A typical case for this dynamic type is hemoglobin, which can change its conformation during oxygen binding (*191*). Hemoglobin includes 2 α single chains and 2 β single chains but each α subunit interacts with specific a β subunit; this means that hemoglobin is a dimer of αβ dimers. The tertiary structure of each subunit changes when it is bound to oxygen. However, only when oxygen has bound to at least one monomer in each αβ dimer, the quaternary structure of hemoglobin changes from an inactive state into the active

state in order to carry out its function. This is an excellent example of how protein structure and dynamics relate to physiological function.

In enzymatic catalysis, it is now clear from structural insights that proteins show some transitional state conformations during catalytic reactions and that different proteins use different pathways (*70*). It is also known that flexibility is required for proteins to achieve their essential conformation for assembly processes. In the process, conformational fluctuations are evidently shown to enhance binding of substrates, to correctly position catalytic groups, to trap reaction intermediates, to release products, and to promote the rate-limiting step of enzyme turnover (*192*). Historically, flexibility of proteins in catalysis was first introduced in the "induced-fit" theory of Koshland (*193*). In this model, the conformational changes of proteins upon ligand binding are a result of the binding interactions driving the protein towards a new conformation that is more complementary to its ligand. Recently, the mechanism of ligand binding coupled to conformational changes has been described as two limiting cases: the ''induced fit'' and the ''conformational selection'' mechanism (Figure 1.20) (*194-196*) . In both cases, it is postulated that all protein conformations pre-exist. In the induced fit mechanism, the ligand binds to the predominant free conformation followed by a conformational change in the protein to give the preferred ligand-bound conformation. Meanwhile, in the ''conformational selection" mechanism, the ligand selects the most favored conformation that is present only in small amounts, eventually undergoing a population shift of conformation, redistributing the conformational states. In this mechanism, the binding interaction does not 'induce' a conformational change, therefore, in many cases, enzymes at every step select their proper conformation optimized for substrate binding, chemical reaction, and product release.

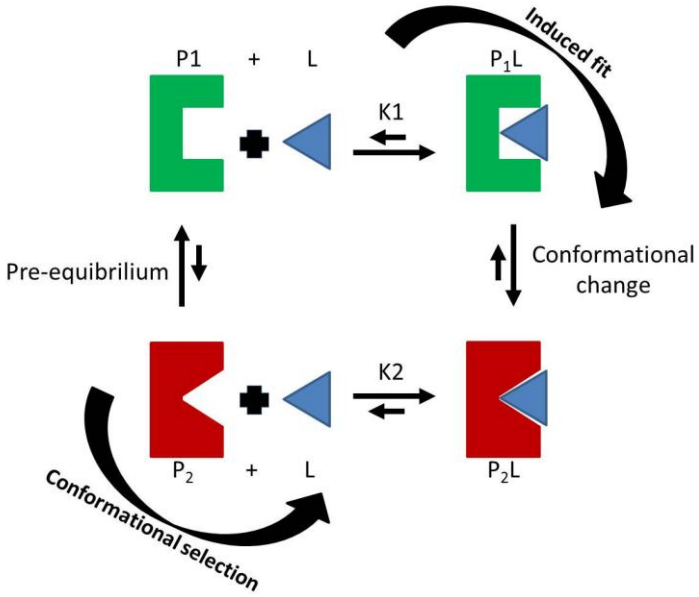

Figure 1.20. General mechanism for ligand binding coupled to conformational change. In induced fit, the predominant free conformation (green, P1) interact with ligand (L) induced a conformational change from P_1L to P_2L. In conformational selection, the binding competent conformation (red, P2) is pre-existing in solution before the addition of ligand. Figure reproduced from reference (*195*)

Moreover, within a protein family, dynamics in a certain family seem to be conserved among structural and functional homologs catalyzing similar enzymatic reactions (*197*, *198*). In many other cases, proteins are dynamic in evolution; evolutionary changes in protein sequence and structure are often closely related to local or global protein flexibility (*199*). Other evidence suggests that structurally conserved proteins may not share the same dynamic properties and that dynamics are encoded from the primary sequence (*200*). Due to the different behavior of dynamics relating sequence and structure, getting insight into the structure-function-dynamic relationship is necessary for engineering improved biocatalysts. In particular, investigation on protein dynamic motion is important to get a full live picture of protein action in substrate binding, catalysis, or product release, thus, uncovering how proteins perform their functions and how these are determined by their structures and flexibility.

1.7 NMR approach and protein dynamics at the atomic level

As mentioned above, to perform their function, protein structures constantly fluctuate between different conformational states along the catalytic pathway. Biologists attempt to understand how proteins function by watching proteins in motion.

In proteins, bond vector fluctuations, rotations and vibrations of side-chains are found on the fast ps-ns time scale. Structural domains, loops and other secondary structural elements move slower on a ns-ms time scale. Dynamics of buried groups and motions associated with catalysis and ligand binding occur in μs to seconds, meanwhile folding and allosterism range from μs to minutes and hours. Currently, X-ray crystallography and NMR spectroscopy are the only techniques which allow the determination of the three-dimensional structure of proteins at atomic resolution. Crystallography clearly proves the existence of transition state conformations of proteins but provides neither transition state poise nor the dynamics along the pathways (*70*). Even though the B-factor parameter could roughly estimate the flexibility of residues in protein crystals, there is no clear definition of a dynamic timescale (only room-temperature X-ray crystallography can give a description of a timescale that is not always obtained for most proteins) (*171*). Like crystallography, NMR is a technique that allows the determination of protein structure, but it has the advantage of providing information about the internal dynamics of proteins at the atomic level and over a wide range of timescales (*161, 201*). Another advantage of the NMR method is that it can be carried out in solution, which simulates proteins in their natural environment. Therefore, NMR is a powerful technique to determine the structures of small proteins even as they tumble, twist and turn in solution. In fact, NMR relaxation R_1, R_2, NOE (Nuclear Overhauser enhancement) experiments allow the determination of the amplitudes of bond vector fluctuations on ps-ns timescales (*171*). NMR relaxation-compensated Carr-Purcell-Meiboom-Gill (CPMG) experiments can probe the conformational or chemical exchange on μs-ms timescale (*202*). Nuclear Overhauser enhancement technique can even detect concerted motion of proteins by reflecting on through-space spin-spin coupling between NMR-active nuclei (*203*). So far, solution NMR spectroscopy has been used in atomic resolution studies of sparsely populated, transiently formed protein conformations that exchange with the native state, protein folding and misfolding, ligand binding, and molecular recognition (*204*). In general, NMR appears to be

the most advanced method in relating the importance of dynamics to biomolecular function (Figure 1.21).

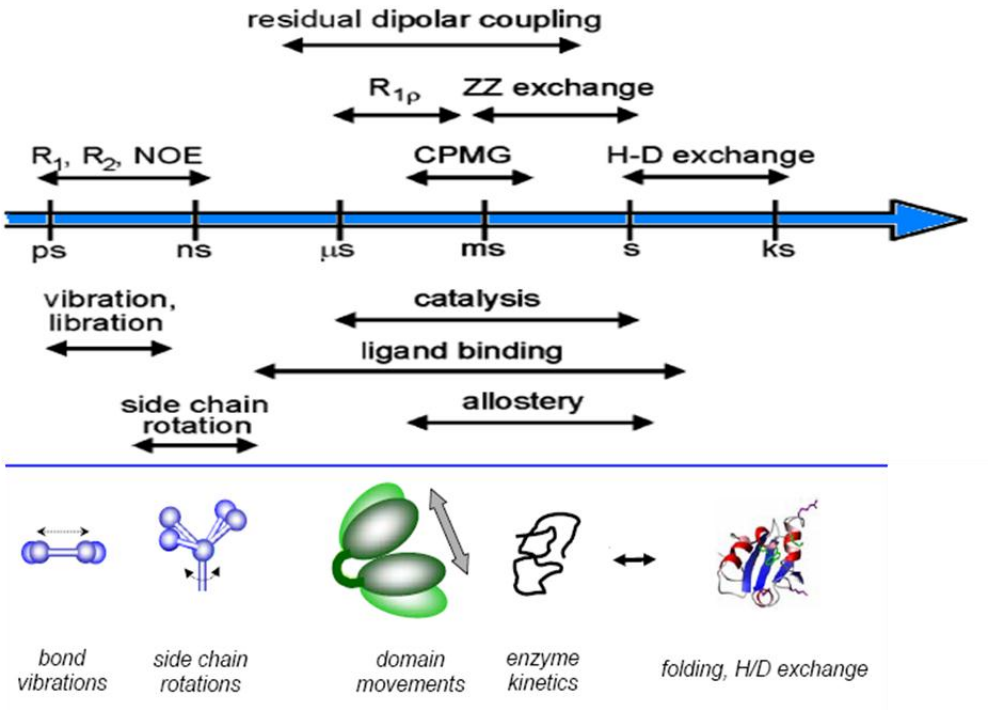

Figure 1.21. **Solution NMR techniques cover the complete range of dynamic events in enzymes**. Figure adapted from reference (*205*).

1.8 Objectives

As mentioned above, due to their unlimited supply and renewable nature, chitin and xylan have been utilized in many applications, such as in production of fermentable sugars and platform molecules. Finding efficient enzyme cocktails for the large-scale production and also for the solving of remaining problems, such as product purity, output, high production costs, or wastes derived from the process is still challenging. Therefore, we are focusing on finding, characterizing and applying highly active enzymes that are able to efficiently hydrolyze the biomass and also meet the abovementioned demands.

Moreover, understanding the principles that govern the enzymatic breakdown could provide great advances in the application of the enzymes for industrial goals. Since both chitin

and xylan contain β-1,4-glycosidic bonds, linking GlcNAc and xylose units, respectively, chitinases and xylanases that catalyze this hydrolytic reaction belong to different GH families. Because they share the same ability to cleave the β-1,4-glycosidic bonds of polymers with long saccharide chains, they utilize a general acid/base catalytic mechanism and share a similar active site architecture with multiple subsites to fit polysaccharide chains. Moreover, proteins are naturally dynamic and are thought to depend on flexibility to perform their function. As a result, we are interested in understanding the link between structure, function and motility properties in these enzymes, therefore providing a better understanding of the catalytic reaction involved in polymer cleavage and offering new means to control or inhibit their molecular function.

To develop highly efficient biocatalysts and to get a better insight on their structure-function-flexibility relationship, we focused on the characterization of β-*N*-acetylhexosaminidases, chitinases and xylanases from the soil organisms *Streptomyces coelicolor* A3(2) and *Streptomyces lividans*. The project involves the following objectives:

General objective

Investigating the structure-function-flexibility relationship of enzymes acting on chitin and xylan polymers to develop biocatalysts of industrial importance.

Specific objectives

(1) Cloning, expression and purification of the highly active β-*N*-acetylhexosaminidase (*Sc*HEX), chitinase C (ChiC) and xylanase B (XlnB2) from *S. coelicolor* and *S. lividans.*

(2) Characterizing the chitinolytic potential of β-*N*-acetylhexosaminidase (*Sc*HEX) and chitinase C (ChiC) in GlcNAc production.

(3) Investigating the structure-function-flexibility relationship of XlnB2 to help decipher its reaction mechanism.

CHAPTER 2. CHITINOLYTIC POTENTIAL OF β-*N*-ACETYLHEXOSAMINIDASE AND CHITINASE C FROM *STREPTOMYCES COELICOLOR* A3(2) IN *N*-ACETYLGLUCOSAMINE PRODUCTION

2.1. Context of chapter 2

GlcNAc is a monomeric sugar that is in high demand due to its great value in medical, supplemental, and cosmetic applications. The development of a method for fast and large-scale production of GlcNAc from chitin is urgently needed for industrial applications. GlcNAc and its derivative oligosaccharides are typically obtained by hydrolysis of chitin using HCl. This approach is extremely energy demanding and polluting. The production costs are still prohibitive, causing inefficient in performance. Biotransformation and biosynthesis using glucose as substrate can also be used to produce GlcNAc with high efficiency, however, they expose some limitations due to product purity, time-cost or highly demanding technology (*2, 9*). Meanwhile, the enzymatic degradation of chitin is much more efficient, economic, and environmentally friendly. Nevertheless, the remaining problem of the enzymatic method is product purity and productivity. Indeed, the final product is often GlcNAc contaminated with chitobiose [$(GlcNAc)_2$] and other chitooligomers, whose elimination is essential but challenging. Besides, because chitin is resistant to degradation, it requires not only hours but days to efficiently degrade chitin enzymatically. In order to ensure a pure final product and improve the yield of GlcNAc production, we are focusing on characterizing highly active chitinolytic enzymes (ChiC and *Sc*HEX) from *S. coelicolor* A3(2). The recipe in which the enzymes combine in a cocktail to powerfully hydrolyze raw chitin for GlcNAc release with high purity, high yield, low cost and environmentally-friendly methods was also tested. Moreover, in order to gain a better insight into the catalytic mechanism of the enzymes, we also resolved the crystal structure of *Sc*HEX in the absence and presence of ligand.

This chapter consists of two articles: The first one is focusing on the characterization of *Sc*HEX from *Streptomyces coelicolor* A3(2). By sequence alignment, it was observed that *Sc*HEX belongs to GH family 20, whose members have a substrate specificity towards polysaccharides containing β(1,2), β(1,3), β(1,4), or β(1,6) glycosidic linkages. Therefore, the purpose of the work was to understand substrate specificity in order to find out which type of linkage the enzyme cleaves, and which is the best substrate for the most efficient hydrolysis. For that purpose, we performed experiments on chitin polymers with different degrees of polymerization, from short oligomers [$(GlcNAc)_{n=2-6}$] to long polysaccharides, such as colloidal chitin, crab shell chitin, etc. The reaction conditions (pH, temperature, buffer, etc.)

were optimized and the specific activity as well as the catalytic efficiency of the enzyme for each substrate were also calculated. Besides, the crystal structure of *Sc*HEX in the presence and absence of ligands has been resolved in order to gain a better insight into the catalytic mechanisms as well as the inhibition profiles.

Results from the first paper have shown that *Sc*HEX displays significant activity towards chitooligomers but has no ability to cleave long chitin. Hence, it was necessary to find an enzyme that is able to convert chitin, and/or could act in tandem with *Sc*HEX to fully degrade the fibril. The second article is to characterize ChiC from *S. coelicolor* A3(2), an enzyme which could satisfy the requirement of finding an enzyme possessing chitin hydrolytic activity. The enzyme could degrade chitin to generate chitooligomers, which would then be digested by *Sc*HEX and subsequently cleaved into GlcNAc. The best combination of ChiC and *Sc*HEX in an assay for the highest efficient GlcNAc production was finally established.

2.2. Presentation of article 1 - "Structure and activity of the *Streptomyces coelicolor* A3(2) β-*N*-acetylhexosaminidase provides further insight into GH20 family catalysis and inhibition"

The scientific article entitled "Structure and activity of the *Streptomyces coelicolor* A3(2) β-*N*-acetylhexosaminidase provides further insight into GH20 family catalysis and inhibition" was published in the journal Biochemistry (pubs.acs.org/biochemistry; impact factor of 3.194 as of October 2014) on February 21, 2014 (Issue 11, Volume 53, DOI: 10.1021/bi401697j). The formatted version by the publisher is in PDF format and the published online version is presented in this document.

2.2.1. Contribution of authors

Results presented in this article were obtained principally by the student and by Wendy A. Offen. The student planned and performed the cloning, gene expression, protein purification, lyophilization and enzymatic characterization. The crystallographic experiments were done by Wendy A. Offen and the structural analyses were done by the student, Nicolas Doucet and Gideon J. Davies. The article was written by the student, Nicolas Doucet and

Gideon J. Davies. François Shareck verified the portion of the experiment and manuscript related to cloning.

2.2.2. Résumé

Les β-*N*-acétylhexosaminidases (HEX) sont des glycosidases qui catalysent l'hydrolyse d'une liaison glycosidique de *N*-acétyl-β-D-galacto-hexosaminides. Ces enzymes sont importantes dans la physiologie humaine et sont des candidates pour la production biocatalytique d'hydrates de carbone et de glycomimétiques. Dans cette étude, la structure tridimensionnelle du type sauvage et d'un mutant catalytiquement déficient (E302Q) de la bactérie *Streptomyces coelicolor* A3(2) (*Sc*HEX) ont été résolus dans leurs formes libres et en présence du ligand 6-acétamido-6-désoxy-castanospermine (6-Ac-Cas). De plus, nous avons été en mesure de capturer l'oxazoline, un intermédiaire de réaction, au site actif du mutant E302Q. Nous avons observé des changements structuraux dans la boucle 3, ce qui laisse suggérer qu'il pourrait y avoir une hétérogénéité entre les résidus clés du site actif chez les membres de la famille des GH20. L'activité catalytique d'acétylhexosaminidase a été étudiée en présence de substrats chitooligomères et *p*NP-acétyle et *N*-acétyle gluco- et galacto-hexosaminides. Les résultats cinétiques confirment la préférence de l'enzyme pour les substrats possédant une liaison glycosidique β(1-4), alors que les profiles HPLC supportent l'hypothèse d'un mécanisme d'exoglycosidase, où l'enzyme clive les sucres à l'extrémité non réductrice des substrats. *Sc*HEX possède une activité significative envers les chitooligosaccharides de différents niveaux de polymérisation. L'hydrolyse finale produit du GlcNAc pur sans sous-produits dérivés, un résultat prometteur pour la production enzymatique de ce composé à forte valeur ajoutée. Par ailleurs, des essais de thermostabilité et d'activation suggèrent des conditions efficaces applicables à la production enzymatique de GlcNAc à partir de chitooligomères.

2.2.3. Article 1

BIOCHEMISTRY
including biophysical chemistry & molecular biology

Article

pubs.acs.org/biochemistry

Structure and Activity of the *Streptomyces coelicolor* A3(2) *β*-*N*-Acetylhexosaminidase Provides Further Insight into GH20 Family Catalysis and Inhibition

Nhung Nguyen Thi,[†,‡,§,⊥,∥] Wendy A. Offen,[○] François Shareck,[†] Gideon J. Davies,[○] and Nicolas Doucet*[,†,‡,§]

[†]INRS-Institut Armand-Frappier, Université du Québec, 531 Boul. des Prairies, Laval, Québec H7V 1B7, Canada

[‡]PROTEO, the Québec Network for Research on Protein Function, Structure, and Engineering, 1045 Avenue de la Médecine, Université Laval, Québec, Québec G1V 0A6, Canada

[§]GRASP, the Groupe de Recherche Axé sur la Structure des Protéines, 3649 Promenade Sir William Osler, McGill University, Montréal, Québec H3G 0B1, Canada

[⊥]Military Institute of Science and Technology, 17 Hoang Sam, Hanoi, Vietnam

[∥]Vietnam Academy of Science and Technology, 18 Hoang Quoc Viet, Hanoi, Vietnam

[○]Structural Biology Laboratory, Department of Chemistry, University of York, York YO10 5DD, United Kingdom

Supporting Information

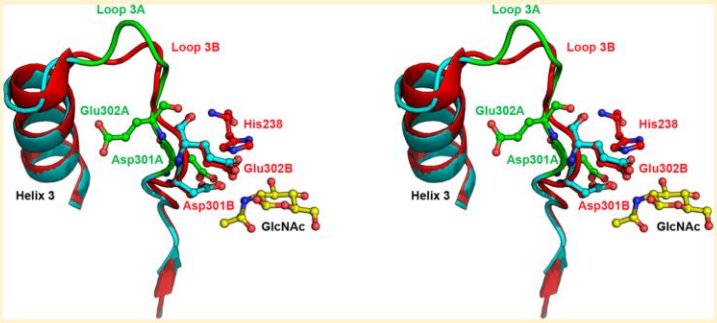

ABSTRACT: *β*-*N*-acetylhexosaminidases (HEX) are glycosidases that catalyze the glycosidic linkage hydrolysis of *gluco*- and *galacto*-configured *N*-acetyl-*β*-D-hexosaminides. These enzymes are important in human physiology and are candidates for the biocatalytic production of carbohydrates and glycomimetics. In this study, the three-dimensional structure of the wild-type and catalytically impaired E302Q HEX variant from the soil bacterium *Streptomyces coelicolor* A3(2) (*Sc*HEX) were solved in ligand-free forms and in the presence of 6-acetamido-6-deoxy-castanospermine (6-Ac-Cas). The E302Q variant was also trapped as an intermediate with oxazoline bound to the active center. Crystallographic evidence highlights structural variations in the loop 3 environment, suggesting conformational heterogeneity for important active-site residues of this GH20 family member. The enzyme was investigated for its *β*-*N*-acetylhexosaminidase activity toward chitooligomers and *p*NP-acetyl *gluco*- and *galacto*-configured *N*-acetyl hexosaminides. Kinetic analyses confirm the *β*(1−4) glycosidic linkage substrate preference, and HPLC profiles support an exoglycosidase mechanism, where the enzyme cleaves sugars from the nonreducing end of substrates. *Sc*HEX possesses significant activity toward chitooligosaccharides of varying degrees of polymerization, and the final hydrolytic reaction yielded pure GlcNAc without any byproduct, promising high applicability for the enzymatic production of this highly valued chemical. Thermostability and activation assays further suggest efficient conditions applicable to the enzymatic production of GlcNAc from chitooligomers.

β-*N*-acetylhexosaminidases (HEX, E.C. 3.2.1.52) are glycosidases that hydrolyze the glycosidic linkage of both *gluco*- and *galacto*-configurations of *N*-acetyl-*β*-D-hexosaminides, which are found in oligosaccharides, glycoproteins, glycolipids, and glycosaminoglycans. HEX members have been extensively studied due to their physiological and functional roles in bacteria, fungi, insects, plants, and mammals.[1] These enzymes have also attracted considerable attention due to their importance in human diseases; defects in human lysosomal HEX causes neurodegenerative Tay-Sachs and Sandhoff

Received: December 23, 2013
Revised: February 19, 2014
Published: February 21, 2014

dx.doi.org/10.1021/bi401697j | *Biochemistry* 2014, 53, 1789−1800

Scheme 1. Proposed Catalytic Mechanism of *Sc*HEX (Based on Ref 1, See Text for Details)

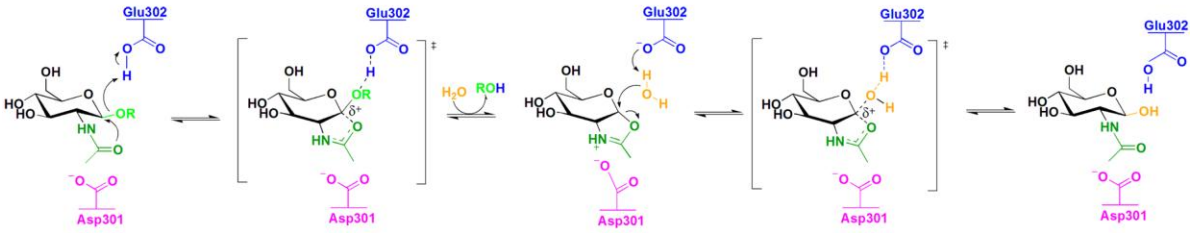

diseases.[2] Additionally, they have been used as a means to control fungal and insect pests, in addition to being efficient tools for a number of biotechnological applications.[1] Based on amino acid sequence similarity, the Carbohydrate-Active Enzyme Database (CAZy, http://cazy.org/) classifies HEX members into four distinct families: GH3, GH20, GH84, and GH85. The GH20 family has been thoroughly characterized with respect to substrate specificity, structure, catalytic mechanism, and biosynthetic potential.[1] GH20 members have the ability to cleave a broad range of substrates, including $\beta(1-4)$, $\beta(1-3)$, $\beta(1-2)$, and/or $\beta(1-6)$ glycosidic linkages, as well as branched compounds such as glycoproteins, glycolipids, or sulfated glycoconjugates.[3−8] To date, a number of GH20 crystal structures have been resolved, including bacterial, insect, and human enzymes.[1,9] The catalytic domain of all members presents a highly similar $(\beta/\alpha)_8$-barrel (TIM-barrel) architecture, with structural differences lying mainly in subunit organization.[1]

The catalytic mechanism of GH20 enzymes has also been extensively investigated. The enzymes use a double-displacement retaining mechanism with neighboring group participation (Scheme 1).[1] In the first part of the reaction, the carbonyl oxygen of the terminal 2-acetamido substrate moiety acts as a nucleophile, yielding a bicyclic oxazoline (or oxazolinium ion as shown in Scheme 1) intermediate, aided by a conserved aspartate residue (D301 in *Sc*HEX), and with protonic assistance to leaving group departure provided by a conserved acid/base (E302 in *Sc*HEX). In the second step, the catalytic base activates the incoming nucleophile (water, or another sugar in the case of transglycosylation reactions) to form the reaction product.[1,10,11]

GH20 enzymes have been used for the synthesis of carbohydrates and glycomimetics in a number of biotechnological applications. In particular, they can hydrolyze chitooligomers generated from the chitin degradation process to produce *N*-acetyl-D-glucosamine (GlcNAc), a monosaccharide with significant added value in the medical and cosmetic fields.[12] In recent years, enzymatic processes have gained efficiency at replacing harsh and environmentally damaging chemical processes for the industrial production of GlcNAc.[13] However, several issues remain with this production method, which are mainly caused by product purity and productivity.[14,15] There is therefore impetus for investigating diverse HEX enzymes that may result in more efficient production of GlcNAc.

The *Streptomyces* species are well-known chitinolytic organisms. *Streptomyces coelicolor* A3(2) is a Gram-positive bacterium that produces many different hydrolases, including chitinases and *N*-acetylhexosaminidases.[16,17] The sequenced genome of *S. coelicolor* A3(2) reveals 13 putative chitinases and 11 putative HEX members.[18] It is known that HEX and chitinases act in a concerted fashion to degrade chitin fully.[19,20] Previous genetic studies have revealed that, in the presence of colloidal chitin and/or $(GlcNAc)_2$, *S. coelicolor* A3(2) secretes chitinases to degrade chitin into chitooligomers, which are subsequently hydrolyzed by HEX to produce GlcNAc in vivo.[21,22] To date, numerous studies have focused on the importance of *S. coelicolor* A3(2) chitinases,[16,17,23−25] but less attention has been paid to the *N*-acetylhexosaminidase activity. The goal of the present study was to clarify the chitinolytic system of *S. coelicolor* A3(2) by providing detailed structural, kinetics, and stability characterization of the *β*-*N*-acetylhexosaminidase activity from *S. coelicolor* A(3)2. Here, we report the cloning and expression of the *S. coelicolor* A3(2) SCC105.17c *hex* gene and the kinetic and structural characterization of the resulting protein. *Sc*HEX possesses significant activity toward chitooligosaccharides of varying degrees of polymerization, and the final hydrolytic reaction yielded pure GlcNAc without any byproduct, promising high applicability for the enzymatic production of GlcNAc. Additional factors such as enzyme preincubation with small saccharides also proved efficient in activating enzyme efficiency.

EXPERIMENTAL PROCEDURES

Reagents. All reagents used were of the highest commercial purity available. Restriction enzymes and DNA-modifying enzymes were purchased from New England Biolabs and Roche Diagnostics. Chitooligosaccharides $[(GlcNAc)_n; n = 1-6]$ were purchased from V-Laboratories. *p*NP-*N*-acetylgalactosamine was purchased from Gold Biotechnology. 4-Nitrophenyl *N*-*N*′-diacetylchitobioside $[(GlcNAc)_2$-*p*NP], 4-nitrophenyl *N*-acetyl glucosaminide [(GlcNAc)-*p*NP], *p*NP-pyranosides, and practical-grade crab shell chitin were purchased from Sigma-Aldrich. Cell wall peptidoglycan from the Gram-positive *Bacillus subtilis* and *Streptomyces sp.* were also purchased from Sigma-Aldrich. Glycol chitin-80 (80% acetylated) was prepared as previously described.[26] Chitosan-24 (24% acetylated) was obtained from HaloSource. 6-Acetamido-6-deoxy-castanospermine (6-Ac-Cas) was purchased from GlycoSyn, Industrial Research Limited, New Zealand and di-*N*-acetyl-chitobiose $(GlcNAc)_2$ from Seikagaku Biobusiness, Japan. The strain *S. lividans* IAF 10-164 [*msiK*$^-$] was used for all protein expressions.[27]

Cloning of *Sc*HEX. All molecular biology procedures and DNA manipulations in *S. lividans* were performed according to standard published methods.[28] The gene encoding for the *β*-*N*-acetylhexosaminidase from *Streptomyces coelicolor* A3(2) (SCC105.17c) was amplified by PCR using the following DNA primers: 5′-AAAGCATGCGACCTCATCGACGGCACCACAGAA-3′ (forward), coding for the ATG start codon within a *Sph*I restriction site (underlined), and 5′-TTTGAGCTCTCAGGTCCAGGGCACCTG-3′ (reverse),

Table 1. Data Collection, Refinement, and Structure Quality Statistics for *Sc*HEX and Complexes

	*Sc*HEX	*Sc*HEX-6-Ac-Cas	E314Q-*Sc*HEX-NGO
resolution of data (outer shell), Å	52.24−1.85 (1.95−1.85)	48.95−2.0 (2.10−2.0)	41.35−1.80 (1.90−1.80)
space group	$P2_12_12_1$	$P2_12_12_1$	$P2_12_12_1$
unit cell params	a = 72.7 Å	a = 72.8 Å	a = 58.2 Å
	b = 128.9 Å	b = 129.2 Å	b = 64.5 Å
	c = 150.3 Å	c = 149.9 Å	c = 143.7 Å
	$\alpha = \beta = \gamma = 90°$	$\alpha = \beta = \gamma = 90°$	$\alpha = \beta = \gamma = 90°$
R merge[a] (outer shell)	0.064 (0.56)	0.17 (0.53)	0.10 (0.51)
mean I/sI (outer shell)	16.8 (3.3)	8.8 (3.2)	12.2 (3.5)
completeness (outer shell), %	99.9 (99.9)	99.4 (98.6)	100.0 (100.0)
multiplicity (outer shell)	6.1 (6.2)	5.6 (5.7)	7.1 (7.3)
no. unique reflns	120 786	95 616	50 954
R_{cryst}	0.17	0.16	0.18
R_{free}	0.20	0.18	0.21
no. protein atoms	7870	7847	3903
no. ligand atoms	0	32 (6-Ac-Cas)	14 (NGO)
no. solvent waters	904	1150	456
no. EDO[b] atoms	88	136	44
Rmsd for bonds (Å)	0.019	0.019	0.019
Rmsd for angles (°)	1.883	1.854	1.814
rmsd chiral volume (Å^3)	0.149	0.137	0.145
average protein B factor (Å^2)	27	11	19
average main chain B factor (Å^2)	26	10	18
average side chain B factor (Å^2)	28	11	20
average B factor for ligand/EDO (ligand only) (Å^2)	43	22 (9)	28 (18)
average solvent B factor (Å^2)	39	24	29
PDB entry	4C7D	4C7F	4C7G

[a] $R_{merge} = \Sigma_{hkl}\Sigma_i\backslash Ihkli - \langle I_{hkl}\rangle/\Sigma_{hkl}\Sigma_i\backslash I_{hkli}$. [b] EDO is ethylene glycol.

coding for a TGA stop codon and a *Sac*I restriction site (underlined). The *Sac*I−*Sph*I-digested PCR product was ligated into the 5.3 kb *Sac*I−*Sph*I-digested pC109 plasmid, which carries a thiostrepton resistance marker. The resulting construct was used to transform *Streptomyces lividans* 10-164 protoplasts and plated on R5 medium without antibiotic for 16 h at 34 °C, at which point agar plates were flooded with thiostrepton solution and further incubated 3−4 days at 34 °C. The 6.9 kbp plasmid was isolated, and positive clones were confirmed by DNA sequencing. The E302Q mutation was introduced by overlap extension PCR[29] using the following DNA primers: 5′-AAAGCATGCCGCTACCTGCACATCGGCGGCGAC-CAGGCGCACTCCACGCCGCAGGCC-3′ (forward) and 5′-TTTGAGCTCGGCCTGCGGCGTGGAGTGCG-GACCGTCGCCGCCGATGTGCAGGTAGCGGC-3′ (reverse).

Gene Expression and Protein Purification. Expression of the *Sc*Hex gene was performed in *S. lividans* 10-164 using slight modifications of previously published methods.[28] Strains were cultivated in 500 mL Erlenmeyer flasks for 72 h at 34 °C with agitation (250 rpm) in M14 medium supplemented with 1% xylose (w/v) as the sole carbon source. Mycelium was removed by centrifugation, and the supernatant was filtered through a 0.2 μm Whatman nylon membrane (GE Healthcare). The protein solution was concentrated by ultrafiltration and dialyzed against 10 mM citric buffer, pH 4.5 prior to loading onto a Protein-Pak HR CM-8 AP-1 column (Waters) pre-equilibrated with 10 mM citric buffer, pH 4.5. *Sc*HEX was eluted with a linear gradient of 10 mM citric buffer, pH 4.5 containing 1 M NaCl, and protein elution was monitored at 280 nm. Fractions containing *Sc*HEX were pooled after analysis by SDS-PAGE, and mass spectrometry was used to assess purity. Total protein concentration was determined using a Bio-Rad Protein Assay (Bio-Rad).

Mass Spectrometry. SDS-PAGE protein bands were excised and destained with water/sodium bicarbonate buffer and acetonitrile. Before in-gel digestion with trypsin, proteins were reduced by DTT and alkylated with iodoacetamide. The tryptic peptides were eluted and then separated on an Agilent Nanopump using a trap column (ZORBAX 300 SB-C18) and a reverse-phase column (ZORBAX 300 SB-C18, 150 mm × 75 μm, 3.5 μm particle size) (Agilent). Mass spectra were obtained using a Q-trap mass spectrometer (Applied Biosystems/MDS SCIEX instruments) equipped with a nanoelectrospray ionization source. Accumulation of MS-MS data was performed with the Analyst Software, version 1.4 (Applied Biosystems/MDS SCIEX). MASCOT (Matrix Science) was used for database searching.

Crystallization, Data Collection, and Structure Solution. Freeze-dried protein was solubilized in 10 mM CHES buffer, pH 9.5, and crystallized using the hanging drop method, with the drop containing *Sc*HEX at 5 mg/mL in a ratio of 2.5: 1 with well solution (0.1 M HEPES pH 7.3, 8% (w/v) PEG 6000). The crystal was fished via a cryoprotectant, which comprised the well solution supplemented with 25% (v/v) ethylene glycol, into liquid nitrogen. Data were collected at beamline IO3, Diamond, to 1.85 Å, at 100 K. Structure solution used the CCP4 suite of programs.[30] The structure was solved by Molecular Replacement with PHASER,[31] using PDB entry 1HP4 as a model (94% sequence identity).[10] The model was improved by iterative cycles of manual building in COOT,[32] followed by refinement with REFMAC.[33]

For the complex with 6-acetamido-6-deoxy-castanospermine (6-Ac-Cas), a crystal which had grown after 4 weeks in a

hanging drop, comprising protein at approximately 7 mg/mL in 50 mM HEPES pH 7.5, 0.2 M NaCl, 20 mM CHES pH 9.3, mixed 1:1 with well solution consisting of 0.1 M BIS-TRIS pH 6.5, 4% (w/v) PEG 6000, 5% DMSO, was soaked with a speck of solid 6-Ac-Cas introduced around the crystal with a needle. Following soaking for approximately 40 min, the crystal was fished via cryoprotectant (as above). Data were collected at beamline IO2, Diamond, to 2 Å resolution, although the crystal was of poor quality reflected by a relatively high R_{merge}. The structure was refined using the (isomorphous) wild-type structure as the starting model, using REFMAC and COOT.

A crystal of the site-directed mutant E302Q, initially in complex with the disaccharide di-*N*-acetyl-chitobiose $(GlcNAc)_2$, was crystallized at 5 mg/mL in 10 mM CHES pH 9.5, mixed 1:0.8 with well solution comprising 0.1 M HEPES pH 7.0, 4% (w/v) PEG 6000. A small amount of solid $(GlcNAc)_2$ powder was added to the protein drop, and the crystal was fished after 5 days via 6% (w/v) PEG 6000, 0.1 M HEPES pH 7.0, 25% (v/v) ethylene glycol also supplemented with 20 mM $(GlcNAc)_2$. Data were collected at beamline IO4 Diamond, to 1.8 Å resolution. The structure was solved using PHASER, with the wild-type structure as the search model and refined as above. Upon structure solution it became immediately apparent that the ligand bound was the trapped intermediate GlcNAc (NAG)−oxazoline (NGO) rather than the intact substrate (see below). Data collection and structure refinement statistics are given in Table 1.

β-*N*-Acetylhexosaminidase Activity. β-*N*-acetylhexosaminidase activity against *p*-nitrophenyl β-*N*-acetylhexosaminides and *p*-nitrophenyl pyranosides was determined by continuous spectrophotometric assays by measuring the release of *p*-nitrophenol at 405 nm on a Cary 300 Bio spectrophotometer (Agilent) equipped with a circulating heating water bath (Lauda). Reactions were carried out at 55 °C for 10 min in 50 mM phosphate buffer containing 150 mM NaCl (pH 5.5). Activity was expressed in IU/mg of protein (1 IU = 1 μmole of *p*-nitrophenol released per minute). Determination of *Sc*HEX enzyme activity toward chitooligosaccharides was performed by an isocratic HPLC method in the same buffer conditions. Aliquots (100 μL) were taken at various time intervals and mixed with 100 μL of 0.4 M H_2SO_4 to quench the reaction. Samples (100 μL) were subsequently injected on an Aminex HPX-87H Ion Exclusion Column (7.8 mm × 30 cm) (Bio-Rad), and elution was performed in isocratic mode with a mobile phase of 5 mM H_2SO_4 at a flow rate of 0.5 mL/min (45 °C). Identification of molecular species was performed by comparison with the retention time of known standards, and product concentrations were calculated from HPLC peak areas. Activity was expressed in IU/mg of protein (1 IU = 1 μmole of GlcNAc released per minute). The growth supernatant of a pC109-transformed *S. lividans* 10-164 subjected to the same gene expression protocol was used as a mock control for all enzyme assays.

Substrate Specificity. Substrate specificity of the purified *Sc*HEX was determined using chromogenic compounds *p*NP-GlcNAc, *p*NP-GalNAc, and *p*NP-pyranosides, in addition to natural chitins and chitooligosaccharides of varying degrees of polymerization $[(GlcNAc)_n;\ n = 1-6]$. To investigate the activity toward long chain chitins, enzyme assays were carried out in the aforementioned buffer using either 2.5 mg/mL of 80% glycol chitin, 40% glycol chitin, 24% chitosan, chitin crabshell, colloidal chitin or 1 mg/mL peptidoglycan from *Streptomyces sp*. or *Bacillus subtilis*. To initiate the reaction, the purified enzyme was added to a final concentration of 10 μg/mL. Reactions were performed for 24 h with aliquots taken after 18h and 24h of incubation at 55 °C. Products were detected at 210 nm by an isocratic HPLC ion exclusion method using an Aminex HPX-42A column (7.8 mm × 30 cm) (Bio-Rad). Elution was performed with H_2O as the mobile phase at a flow rate of 0.5 mL/min (45 °C). In all cases, control assays were also performed with water and a mock supernatant.

Optimal pH, Temperature, and Stability. Optimal temperature for *Sc*HEX was determined in 50 mM phosphate buffer containing 150 mM NaCl with chitooligosaccharides $[(GlcNAc)_n;\ n = 1-6]$ as substrates. Enzyme assays were performed for 10 min at 25, 30, 37, 40, 45, 50, 55, 60, 65, and 70 °C. The optimal pH for chitooligosaccharide hydrolysis was determined at 55 °C by performing the same enzyme assays in 50 mM citric buffer with 150 mM NaCl (pH 3, 3.5, 4, 4.5), 50 mM phosphate buffer with 150 mM NaCl (pH 5, 5.5, 6, 6.5, 7), and 50 mM Tris-HCl buffer with 150 mM NaCl (pH 8). Reactions were carried out for 10 min, and enzyme activity was calculated as mentioned above. The pH stability and thermal stability of *Sc*HEX were estimated by incubating enzyme solutions (100 μL, 200 μg/mL) at different pHs (1h and 3 months at 4 °C) and temperatures (15 min) prior to initiating enzyme reaction with *p*NP-GlcNAc, as described above. Activity was compared to a control, which was performed with pure enzyme kept in water at 4 °C.

Michaelis−Menten Kinetics. The kinetic parameters k_{cat} and K_M were determined at 55 °C and optimal pH in 50 mM phosphate buffer, 150 mM NaCl for chitooligosaccharide substrates $[(GlcNAc)_n;\ n = 1-6]$. Enzyme assays were initiated by the addition of 0.5 μg/mL *Sc*HEX with substrate concentrations ranging from 0.25 to 3 mM. *Sc*HEX activity was calculated as μmoles of GlcNAc released per minute per milligram of enzyme, and kinetic parameters k_{cat}, K_M and k_{cat}/K_M were calculated by a nonlinear regression fit to the Michaelis−Menten equation using GraphPad Prism 5.

Carbohydrate Activation/Inhibition. The effect of potential activators and inhibitors on β-*N*-acetylhexosaminidase activity was examined by preincubating enzyme solutions (100 μL, 200 μg/mL) with 3 mM of the following carbohydrates for 15 min prior to reaction initiation: mannose, fructose, arabinose, glucuronic acid, sucrose, galactose, glucose, xylose, lactose, and GlcNAc. Enzyme assays were carried out with *p*NP-GlcNAc as described above, and sugars were prepared in the same reaction buffer. Activities were compared to a control of pure *Sc*HEX performed under the same reaction conditions but preincubated in the absence of any sugar.

RESULTS AND DISCUSSION

ScHEX Expression, Purification, and Structural Analysis. *Sc*HEX was produced from a culture of *S. lividans* grown in M14 minimal medium containing xylose as the sole source of carbon. Under these conditions, *Sc*HEX was overproduced with an expression yield of 700−800 mg/L after 72 h incubation. The *S. lividans* expression system allows extracellular secretion of *Sc*HEX with an extremely low background of contaminant proteins, yielding an enzyme purity of 95% directly from the growth supernatant. Ion-exchange chromatography was nevertheless employed to purify enzymes to homogeneity, and mass spectrometry was employed to confirm the identity and sequence integrity of the produced enzyme. To rule out the possibility of a contaminant GH activity, the strain *S. lividans* 10-164 with empty plasmid pC109 was cultured to test the

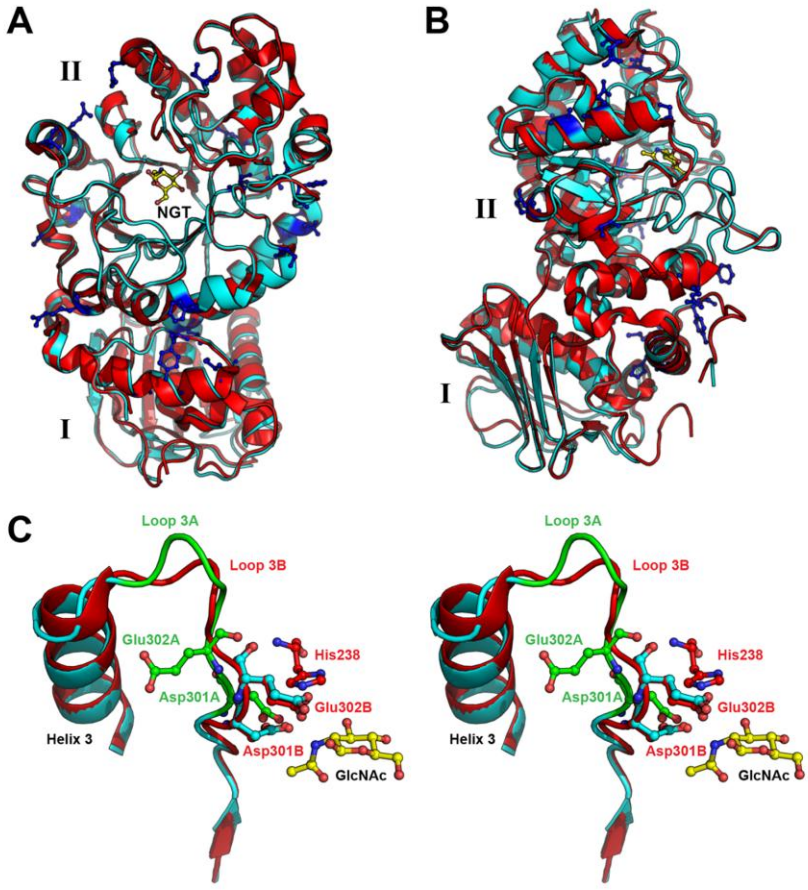

Figure 1. Structural comparison between *Sp*HEX and *Sc*HEX. (A) Front-view overlay of wild-type *Sp*HEX (PDB entry 1HP5, red) with wild-type *Sc*HEX (PDB entry 4C7D, cyan). The position of the active site is defined by the presence of NAG−thiazoline bound within the *Sp*HEX binding pocket (NGT, yellow). The β/α topology domain I and $(\beta/\alpha)_8$ barrel domain II are identified by roman numerals. Residues of the $(\beta/\alpha)_8$ barrel comprising catalytic domain II that differ in sequence between *Sp*HEX and *Sc*HEX are shown in ball-and-stick representation in *Sc*HEX (blue). (B) Side-view of the complex (90° counter clockwise rotation about the *y*-axis relative to (A)). (C) Stereo view of *Sp*HEX (PDB entry 1M01, red) and *Sc*HEX (cyan/green) showing two alternate conformations adopted by loop 3 in *Sc*HEX. Positions of the modeled loop 3 conformations A (0.7 occupancy) and B (0.3 occupancy) are shown in green and red, respectively. The loop 3B conformation corresponds to the active orientation of catalytic residues Asp301B and Glu302B (cyan in *Sc*HEX and red in *Sp*HEX), which are ideally positioned to hydrogen bond with glycans in the active-site pocket. Residues Asp301A and Glu302A in conformation A are shown in green. The *N*-acetylglucosamine (GlcNAc) product complexed to *Sp*HEX is shown in yellow. This figure was drawn with MacPyMOL 1.3.

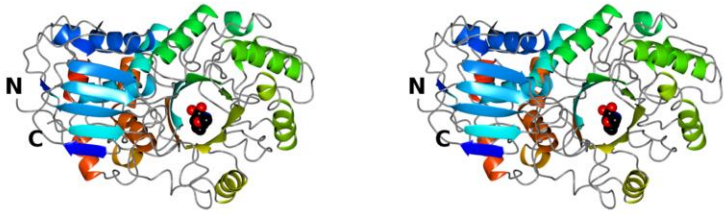

Figure 2. Stereo view of a ribbon diagram of *Sc*HEX. The enzyme is color-ramped from the N-terminus (blue) to C-terminus (red), showing the position of 6-Ac-Cas as a CPK model. This figure was drawn with CCP4*mg*.[52]

growth supernatant for acetylhexosaminidase activity against $(GlcNAc)_2$ and $(GlcNAc)_6$. Results showed no activity toward these substrates, ruling out the possibility of a contaminant HEX activity in the cell extract of the expression host.

Amino acid sequence alignment of *Sc*HEX with other GH20 family members exhibits 99%, 94%, 77%, 60%, 43%, and 27% sequence identity with *S. lividans*, *S. plicatus*, *S. avermitilis*, *Saccharopolyspora erythraea*, *Paenibacillus sp.*, and *Homo sapiens* (HEXB), respectively (Figure S1). Like other members of the family, *Sc*HEX retains the highly conserved active site motif His/Asn-X_{aa}-Gly-Ala/Cys/Gly/Met-Asp-Glu-Ala/Ile/Leu/Val, in which a glutamate residue (E302 in *Sc*HEX) acts as the

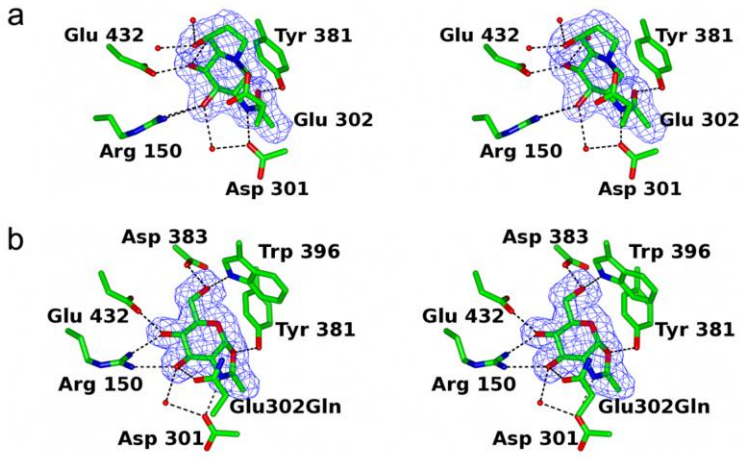

Figure 3. Stereo views (divergent "wall-eyed" stereo) of the *Sc*HEX 6-Ac-Cas and E302Q *Sc*HEX NAG−oxazoline active-site complexes. F_o-F_c omit electron density maps (with phases calculated *prior* to any modeling or refinement of any ligand) of each complex are shown in blue, contoured at 3.0 σ. (A) *Sc*HEX 6-Ac-Cas complex (molecule A). (B) E302Q *Sc*HEX NAG−oxazoline complex. Hydrogen bonds ≤3.2 Å are shown as dashed lines. This figure was drawn with CCP4*mg*.

general acid/base in the catalytic mechanism.[34] The closest HEX homologue for which a crystal structure was previously solved is the GH20 β-*N*-acetylhexosaminidase from *S. plicatus* (*Sp*HEX), an enzyme displaying 94% sequence identity with *Sc*HEX.[10] As expected, this high similarity between the two enzymes results in very similar three-dimensional structures, discussed below. This is in agreement with the fact that the catalytic domains of *Sp*HEX and *Sc*HEX only differ at 21 out of 355 residue positions. None of these replacements occur at positions in or near the active site cavity and/or involved in catalysis (Figure S1, Figure 1A,B), confirming that both enzymes rely on the same catalytic mechanism and display similar substrate specificities.

Structure of *Sc*HEX, and Complexes *Sc*HEX-6-Acetamido-6-deoxy-castanospermine and E302Q *Sc*HEX-NAG−oxazoline. The structure of *Sc*GH20 has a very similar two domain architecture to that of *Sp*HEX, with an N-terminal domain (up to Arg138) consisting predominantly of a solvent-exposed seven-stranded β-sheet, sequestering two α-helices against the C-terminal domain, which comprises a $(\beta/\alpha)_8$ barrel with an additional α-helix near the C terminus occupying the groove between the two domains (Figure 2).[10] The barrel motif is irregular, in that helix 7 is replaced by a loop, helix 5 is very short, and there are 2 additional loops at the C-termini of β-strands 2 and 3. There are two molecules in the asymmetric unit for the native structure, and the complex with 6-Ac-Cas, designated A and B in the PDB entries, and one for that of the mutant E302Q soaked with $(GlcNAc)_2$, which has NAG−oxazoline in the active site.

In molecule A of the native structure, residues 299−308 on loop 3 follow a different pathway to the equivalent residues in both complex structures (Figure 1C). In molecule B, the same region has two alternate conformations, A and B, with partial occupancies of 0.7 and 0.3, respectively. Conformation A is the same as that observed for molecule A, and loop conformation B is equivalent to that observed in both ligand-bound structures and the structure of *Sp*HEX bound to GlcNAc (PDB entry 1M01).[11] The main difference is in the orientations of the side chains of Asp301, Glu302 (both catalytic residues) and Ala303. In conformation B, and both complexes, the side chains of residue 302 are hydrogen bonded to NE2 of His238, but in the native structure, molecule A and conformation A of region 299−308 on molecule B, the side chain of Glu302 points away from, and cannot hydrogen bond to the histidine. This alternate ligand-bound conformation facilitates the formation of hydrogen bonding interactions. In the 6-Ac-Cas structure, OD2 of Asp301 is hydrogen bonded to the nitrogen of the ligand acetamido group (2.8 Å), and OE2 of Glu302 is 2.8 Å from the castanospermine nitrogen atom (Figure 3A). In the complex with NAG−oxazoline, the loop is positioned in such a way that there are hydrogen bonds between OD2 of Asp301 and the nitrogen atom of NAG−oxazoline (2.9 Å), and between OE1 of Gln302 and O3 of NAG−oxazoline (2.8 Å) (Figure 3B). For molecule B of the native structure, the alternate loop conformations differ in some main chain hydrogen bonding interactions, for example the carbonyl O of Asp301B loop in conformation A is hydrogen bonded to the main chain N of Gly237B, whereas in loop B it is hydrogen bonded to that of Ala303B (not shown).

In an attempt to trap a Michaelis complex, the crystal structure of the acid/base variant E302Q was determined in complex with di-*N*-acetyl-chitobiose. In contrast to what was expected, the structure clearly revealed electron density for a trapped intermediate oxazoline in the −1 subsite. In trapping of oxazolines on related GH84 enzymes, He and colleagues[35] used active center variants in conjunction with highly activated substrates; here serendipitously the intermediate has accumulated without the requirement for an activated substrate. As expected, the NAG−oxazoline and active site residues occupy very similar positions to those in the complex of the inhibitor *N*-acetylglucosamine−thiazoline (NAG−thiazoline) with *Sp*HEX (PDB entry 1HP5).

The trapped oxazoline complex, along with the complex with 6-Ac-Cas informs a complete description of the interaction in the −1 subsite. Both ligand sugars are close to a $^4C_1$ conformation. The acetamido group is anchored by hydrogen bonding interactions between its nitrogen atom and OD2 of Asp301, and oxygen and OH of Tyr381 (Figure 3, Scheme 2). The structure of GlcNAc bound to *Sp*HEX exhibits a similar pattern of bonding between the equivalent N and O atoms of

Scheme 2. Schematic Diagram of the Interactions between *Sc*HEX and the Intermediate Oxazoline Trapped on the E302Q Variant[a]

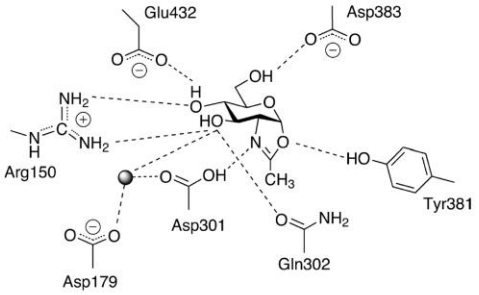

[a]Hydrogen bonding distances ≤3.2 Å are indicated by dashed lines. The water molecule is shown as a shaded sphere.

the ligand and residues Asp313 and Tyr393.[11] Four tryptophan residues, 332, 349, 396 and 430, provide a hydrophobic environment that protects the oxazolinium ion intermediate from solvolysis (Figure 4). The positive charge on the nitrogen of the acetamido group in the NAG−oxazoline complex is likely stabilized by Asp301, which is itself within hydrogen bonding distance of Asp234, and therefore probably deprotonated. The oxygen atom O3 of NAG−oxazoline is 2.8 Å from OE1 of the mutated residue Gln302, and in the 6-Ac-Cas complex N1 of the castanospermine group is hydrogen bonded to OE2 of Glu302 (2.8 Å). Further residues interact, via hydrogen bonding interactions with their side chains, to hold the sugar moiety of both ligands in place as follows: Asp179 (OD2 via a water molecule to O4 of 6-Ac-Cas and O3 of NAG−oxazoline), Arg150 (both terminal guanidinium N atoms with O4 of 6-Ac-Cas, and one each to O3 and O4 NAG−oxazoline), Glu432 (OE2 to O2 of 6-Ac-Cas and O4 of NAG−oxazoline) and Asp383 and Trp396 (OD2 and NE1 respectively *via* a water molecule to O2 of 6-Ac-Cas, directly to O6 of NAG−oxazoline) (Figure 3, Scheme 2). In addition, a water molecule, which is hydrogen bonded to both OD2 Asp301 and OD2 Asp179, forms a hydrogen bond to O4 6-Ac-Cas and to O3 NAG−oxazoline in their respective complexes (3.0 Å in each case).

In the *Sp*HEX NAG−thiazoline complex, a glycerol molecule occupies subsite +1 and forms a hydrogen bond with OE2 Glu314 (2.7 Å). There is an equivalent ethylene glycol molecule in the E302Q *Sc*HEX NAG−oxazoline structure, which lies 2.7 Å from the side chain of Gln302. The wild-type structure also has an ethylene glycol molecule (at half occupancy) in a different orientation, but with a hydroxyl group in a position equivalent to the hydroxyl binding to Gln302 in the NAG−oxazoline structure, and a second ethylene glycol with hydroxyl groups occupying similar positions to NAG−oxazoline O6 and O4.

Enzyme Specificity. Glycoside hydrolases are classified into 130 families based on their amino acid sequence similarities.[36−38] Although members of the GH20 family share a common catalytic domain with conserved active site residues—confirmed by the detailed description of the structure above—they nevertheless show a wide variety of substrate specificities. Overall, GH20 enzymes have the ability to cleave $\beta(1-2)$, $\beta(1-3)$, $\beta(1-4)$, $\beta(1-6)$ glycosidic linkages from oligosaccharides, glycoproteins, glycolipids, and glycosaminoglycans.[8,39−41] The GH20 family also relies on a substrate-assisted mechanism wherein the 2-acetamido group of the substrate is indispensable for catalysis (Scheme 1).[1,10,11,42] To determine the substrate specificity of *Sc*HEX and to confirm its anchimeric mode of action, we tested chromogenic and natural substrates with 2-acetamido groups such as *p*NP-GlcNAc, *p*NP-GalNAc, chitooligosaccharides, and long chain chitins. As expected, the enzyme showed significant activity toward *p*NP-GlcNAc, *p*NP-GalNAc, and chitooligosaccharides (Table 2). The highest specific activity (666 ± 11 IU/mg) was observed with *p*NP-GlcNAc as substrate, which is 2.9-fold higher than that observed with the homologous *p*NP-GalNAc (230 ± 4 IU/mg). This result confirms the D-*gluco* configuration substrate preference of *Sc*HEX, in agreement with the 1.5 to 4 GlcNAcase/GalNAcase activity ratio found in other

Table 2. Specific Activity of *Sc*HEX toward Various *N*-Acetylhexosaminide Substrates

substrate	specific activity (IU)[a]
*p*NP-GlcNAc	666 ± 11[b]
*p*NP-GalNAc	230 ± 4[b]
$(GlcNAc)_6$	180 ± 25
$(GlcNAc)_5$	146 ± 11
$(GlcNAc)_4$	71 ± 6
$(GlcNAc)_3$	122 ± 12
$(GlcNAc)_2$	126 ± 5

[a]IU = μmol/min of GlcNAc released per milligram of enzyme. [b]IU = μmol/min of *p*NP released per milligram of enzyme. Results are presented as means ± standard deviation (n = 3).

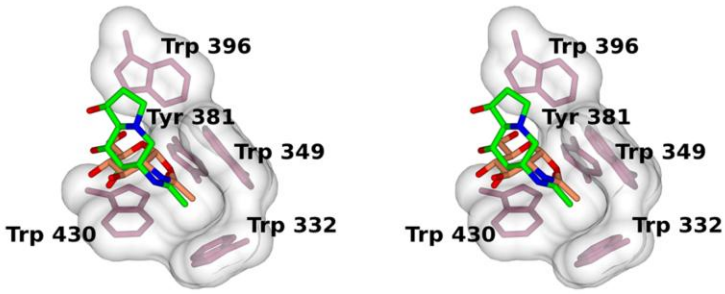

Figure 4. Stereo view of hydrophobic residues in the −1 sugar binding subsite for molecule A of *Sc*HEX complexed with 6-Ac-Cas. The position of NGO is shown when the structure of its complex is superposed on that with 6-Ac-Cas. 6-Ac-Cas is shown with C atoms in green, and NGO is shown in coral. The molecular surface around the hydrophobic residues is shown (calculated by CCP4*mg*).

GH20 enzymes.[19] *Sc*HEX also displayed specific activities ranging from 71 to 180 IU/mg toward chitooligosaccharide substrates (Table 2), confirming that the enzyme most likely acts on smaller chain products of chitin degradation *in vivo*. To further investigate the glycosidase activity, time-course profiles for the hydrolysis of $(GlcNAc)_6$ were determined under conditions described above. Time-course analysis of the *Sc*HEX activity toward $(GlcNAc)_6$ yielded a hydrolysis profile whereby $(GlcNAc)_5$ and GlcNAc are released as primary products at the early stage of the reaction, followed by decreasing concentrations of $(GlcNAc)_4$, $(GlcNAc)_3$, and $(GlcNAc)_2$ (Figure 5). The corresponding increase in GlcNAc, the low accumulation of smaller oligomers such as $(GlcNAc)_2$ at the early onset, and the very similar affinity of *Sc*HEX for all chitooligosaccharides (see below) confirms that the enzyme acts in a processive manner, trimming off GlcNAc units from the nonreducing ends of substrates of varying degrees of polymerization, as previously demonstrated on homologues.[3,5,43] The same cleavage pattern was observed when $(GlcNAc)_{2-5}$ chitooligomers were used as substrates, with the appearance of $n-1$ products at an early stage of the reaction, concomitant with gradual increases in GlcNAc concentrations (not shown).

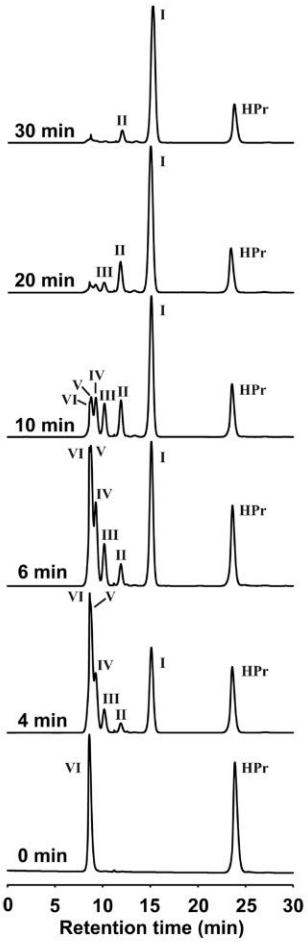

Figure 5. Time-course hydrolysis of $(GlcNAc)_6$ by *Sc*HEX. Samples were analyzed by measuring absorption at 210 nm following an isocratic HPLC separation of products on an Aminex HPX-87H ion exclusion column at 45 °C, as described in Experimental Procedures. Chromatograms are shown for acid-quenched reactions after 0, 4, 6, 10, 20, and 30 min of incubation. Retention times were compared to known chitinooligosaccharide standards: VI, $(GlcNAc)_6$; V, $(GlcNAc)_5$; IV, $(GlcNAc)_4$; III, $(GlcNAc)_3$; II, $(GlcNAc)_2$; I, (GlcNAc); HPr, propionic acid normalization standard.

The *Sc*HEX activity was also tested against longer chain chitins and bulkier substrates, including glycol chitin 80%, glycol chitin 40%, chitosan 24%, chitin crabshell, colloidal chitin, and peptidoglycans from *Bacillus subtilis* and *Streptomyces sp.* After 18 and 24 h of incubation, no significant oligomer was detected in the reaction mixture, except for very low concentrations of GlcNAc (not shown). GlcNAc was not detected in identical assays conducted with the mock supernatant or water as negative controls, confirming that the activity is specific to *Sc*HEX. The bulk of these observations indicate that *Sc*HEX possesses *N*-acetylhexosaminidase activity toward short chain chitin oligomers but not toward long chain chitin or chitosan. This result was expected given the high sequence identity and similar activity observed with other GH20 family members, namely the highly homologous *Sp*HEX.[44] Similar to most other GH20 members characterized, increasing the length and complexity of chitin substrates considerably affects enzyme affinity and catalysis in *Sc*HEX.

Michaelis–Menten Kinetics. *Sc*HEX showed lower specific activity in its purified form than that calculated from the fresh outer-cell growth supernatant immediately after protein expression, most likely due to poor enzyme stability in solution over time. As a result, kinetic parameters were calculated from the 95% pure *Sc*HEX, providing a better portrait of the *in vivo* activity of *Sc*HEX. Considering the high purity of the enzyme in the outer-cell medium and the absence of background activity from the expression organism (as tested from a control *S. lividans* growth assay), this expression system provides a considerable advantage for the industrial production of *Sc*HEX. Indeed, protein purification often cannot be performed in industrial settings due to high costs, setup and productivity issues. The kinetic parameters K_M and k_{cat} were calculated for each chitooligomer under known optimal conditions (see below). Hydrolysis of the substrates showed typical Michaelis–Menten hyperbolic kinetics with substrate concentrations ranging from 0.25 mM to 3 mM (Figure S2). Results show that K_M and k_{cat} parameters are very similar for all substrates, varying from a mere 2- to 3-fold difference in all cases (Table 3). The enzyme displays the lowest affinity toward $(GlcNAc)_2$ ($K_M = 1.97 \pm 0.42$), which correlates with a slightly higher k_{cat} ($k_{cat} = 593 \pm 94$). However, these differences do not translate into higher catalytic efficiency of *Sc*HEX for this substrate and no other significant catalytic efficiency differences were observed for substrate chain lengths ranging from 2 to 6 *N*-acetylglucosamine units $[(GlcNAc)_{2-6}]$. These results demonstrate that substrate affinity is very similar for short

Table 3. Kinetic Parameters for *Sc*HEX

substrate	K_M (mM)	k_{cat} (s^{-1})	k_{cat}/K_M ($mM^{-1}s^{-1}$)
$(GlcNAc)_2$	1.97 ± 0.42	593 ± 94	297 ± 12
$(GlcNAc)_3$	0.76 ± 0.10	330 ± 16	432 ± 25
$(GlcNAc)_4$	0.90 ± 0.15	232 ± 10	258 ± 20
$(GlcNAc)_5$	0.59 ± 0.09	271 ± 1	459 ± 19
$(GlcNAc)_6$	0.98 ± 0.22	409 ± 63	423 ± 63

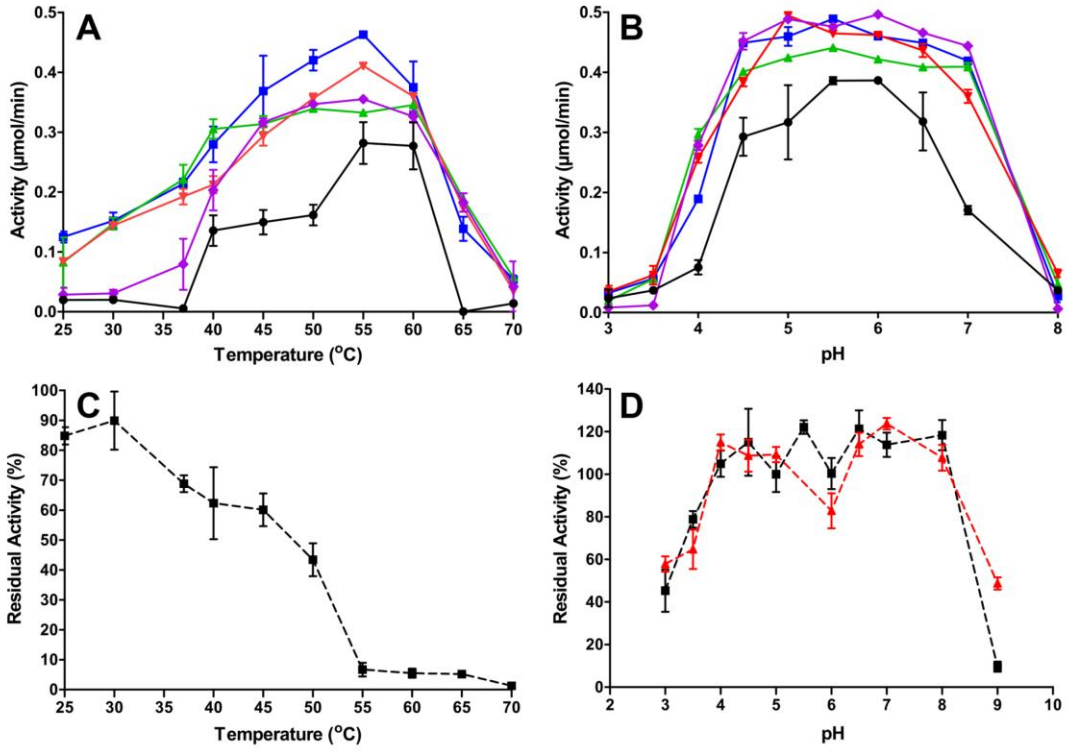

Figure 6. Effect of pH and temperature on *Sc*HEX activity against chitooligosaccharides. (A) Effect of temperature on *Sc*HEX activity. Enzyme activity was tested for $(GlcNAc)_2$ (blue squares), $(GlcNAc)_3$ (green up triangles), $(GlcNAc)_4$ (red down triangles), $(GlcNAc)_5$ (purple diamonds), and $(GlcNAc)_6$ (black circles). (B) Effect of pH on *Sc*HEX activity (same symbols and color code). (C) Residual activity of *Sc*HEX against *p*NP-GlcNAc after a 15-min incubation at various temperatures. (D) Residual activity of *Sc*HEX against *p*NP-GlcNAc after 1 h (black squares) and 3-month (red up triangles) incubation at various pHs. See Experimental Procedures for details.

chitooligomers of varying degrees of polymerization, supporting the observation that *Sc*HEX is an exo-acting glycosidase that cleaves from the nonreducing end of substrates through a processive hydrolytic mechanism, as previously demonstrated on homologues.[3,5,43]

Most GH20 members have been kinetically characterized in the presence of unnatural substrate analogues, such as pNP-GlcNAc, pNP-GalNAc, and/or 4-methylumbelliferyl-β-D-galactopyranosides (4-MUG). Only a restricted set of HEX enzymes has been studied in the presence of natural chitooligomers, including ExoI from *Vibrio furnissii*,[49] *Le*-Hex20A from *Lentinula edodes*,[53] *Vh*Nag from *Vibrio harveyi* 650,[43] and *Stm*Hex from *Stenotrophomonas maltophilia*.[54] The catalytic efficiency of *Sc*HEX compares advantageously with other HEX members, showing very similar k_{cat}/K_M against $(GlcNAc)_{2-6}$ substrates. In fact, *Sc*HEX from crude supernatant is 1700-fold more efficient than pure *Stm*Hex against $(GlcNAc)_6$.[54] Still, even with equal catalytic efficiency, *Sc*HEX remains advantageous from an industrial standpoint due to its chitin degrading ability in the growth supernatant, thus preventing the need for further protein purification.

Enzyme Stability. To provide details on the potential applicability and robustness of *Sc*HEX for the industrial production of GlcNAc, the effect of temperature on activity was determined by monitoring hydrolysis of $(GlcNAc)_{2-6}$ chitooligosaccharides from 25 to 70 °C (Figure 6A). Although *Streptomycetes* are soil-dwelling bacteria that thrive at mesophilic temperatures, *Sc*HEX showed optimal activity at temperatures ranging from 45 to 60 °C with a maximal activity observed at 55 °C for almost all substrates tested. These values are similar to those observed in GH20 members from *Sotalia fluviatilis*,[45] *Streptomyces thermoviolaceus*,[46] *Penicillium oxalicum*,[7] and *Aspergillus oryzae*.[47] Enzyme activity toward $(GlcNAc)_6$ was particularly affected outside the 55−60 °C range (Figure 6A), dropping to near zero at physiological temperatures or lower. The smaller substrates $(GlcNAc)_{2-4}$ were not as affected by drastic temperature drops as $(GlcNAc)_{5-6}$, further lending support to the biological importance of *Sc*HEX in hydrolysis of small chitooligosaccharides in the chitinolytic system of *S. coelicolor* A(3)2.

Thermal stability of *Sc*HEX was also assessed by characterizing enzyme stability after a 15 min incubation at temperatures ranging from 25 to 70 °C prior to reaction initiation (Figure 6C). Despite an optimal activity of 55−60 °C, *Sc*HEX stability at higher temperatures was considerably reduced, dropping dramatically for temperatures higher than that of the optimal growth of its host organism (30 °C). Indeed, while *Sc*HEX retained 43% activity at 50 °C, this efficiency dropped to less than 5−6% when incubated at higher temperatures. This property is similar to NagA from *Pseudomonas fluorescens* JK-0412[5] and β-HEX from *Capsicum annuum*.[48] These results demonstrate the *in vivo* trade-off between enzyme stability and catalytic efficiency, whereby increased stability at lower temperatures is favored over increased enzyme activity. While far from a catalytically perfect enzyme, *Sc*HEX is just good enough to perform its required chitinolytic activity *in vivo*,

dx.doi.org/10.1021/bi401697j | *Biochemistry* 2014, 53, 1789−1800

providing *S. coelicolor* A(3)2 with sufficient enzymatic activity to survive.

The effect of pH on *Sc*HEX activity was also determined by monitoring the hydrolysis of $(GlcNAc)_{2-6}$ chitooligosaccharides from pH 3 to 8 (Figure 6B). *Sc*HEX showed a broad pH tolerance, with optimal activity detected between pH 4.5 and 7. Again, $(GlcNAc)_6$ proved a more stringent substrate by displaying optimal activity between pH 5 and 6.5. Many other GH20 enzymes, such as HEX from *Sotalia fluviatilis*, NagC from *Streptomyces thermoviolaceus*, HEX1 and HEX2 from *Paenibacillus sp.* TS12, and DspB from *Aggregatibacter actinomycetemcomitans*, showed similar optimal activity between pH 5 and 6.[4,39,45,46] Interestingly, ScHEX did not display significant pH-dependent activity variations between chitooligomers of varying degrees of polymerization. This result contrasts with previous observations on β-GlcNAcase and chitodextrinase from *Vibrio furnissii*, two enzymes that showed a shift in pH-activity profiles with the smaller $(GlcNAc)_2$ substrate relative to longer chitin oligomers.[49]

*Sc*HEX also displayed very good residual activity after incubating the enzyme at different pH values for extended periods of time (1 h and 3 months) (Figure 6D). The enzyme maintained almost the same level of activity between pH 4−8 after 1 h or 3 months of incubation in different pH buffer conditions. Additionally, although enzyme activity was significantly affected after 3 months of incubation at 4 °C, *Sc*HEX retained the same residual pH-activity profile as that of the fresh enzyme.

Effect of Carbohydrates on *Sc*HEX Activity. To elucidate the effect of possible activators/inhibitors on catalytic efficiency, *Sc*HEX was preincubated for 15 min in the presence of 3 mM of the following sugars prior to reaction initiation: mannose, fructose, arabinose, glucuronic acid, sucrose, galactose, glucose, xylose, lactose, and GlcNAc. Interestingly, mannose, fructose, glucuronic acid, lactose, and GlcNAc significantly increased enzyme activity by a factor of 33%, 47%, 63%, 28%, and 35%, respectively (Table 4). In contrast, β-*N*-acetylhexosaminidase activity was either unaffected or weakly inhibited by arabinose, sucrose, galactose, glucose, and xylose. The stimulating effect on HEX activity by sugars was also observed in HEX from *Sotalia fluviatilis*, which displayed comparable increases upon incubation with glucuronic acid (65%), fructose (58%), and lactose (70%).[45] While sucrose and galactose do not significantly affect *Sc*HEX activity, both sugars were shown to increase chitinohydrolysis of the *Sotalia fluviatilis* enzyme by 43% and 80%, respectively. Interestingly, preincubation of *Sc*HEX with the reaction product GlcNAc increased enzyme activity by more than 35% relative to control, indicating that product inhibition is not an issue with *Sc*HEX, contrasting with results observed with other GH20 members, namely, *Po*HEX and ExoI from *Penicilium oxalicum* and *Vibrio furnissii*, respectively.[7,49] Overall, the activating effects of fructose and glucuronic acid on *Sc*HEX activity are significant and could be used to enhance the efficiency of the enzyme in GlcNAc production. The exact molecular phenomenon underlying such activation was never investigated in the GH20 family but could result from a potential induced fit and/or conformational selection mechanism triggered by the binding of substrate analogues, thus favoring a catalytically competent enzyme-bound state over the unbound, inactive ground state. This type of ligand binding mechanism was previously characterized on a number of other enzyme systems and has recently attracted considerable attention because both mechanisms may act as a flux and be affected by changes in ligand concentrations.[50]

Table 4. Effect of Carbohydrates on *Sc*HEX Activity

compd	relative activity (%)[a]
control	100
mannose	133 ± 5.3
fructose	147 ± 8.2
arabinose	128 ± 32
glucuronic acid	163 ± 10
sucrose	82 ± 12
galactose	83 ± 12
glucose	104 ± 13
xylose	92 ± 12
lactose	128 ± 14
GlcNAc	135 ± 15

[a]Enzyme assays were carried out with 0.25 mM *p*NP-GlcNAc using *Sc*HEX preincubated for 15 min with 3 mM of each compound. Activities were compared with control, which was performed with pure *Sc*HEX. Results were presented as means ± standard error (n = 3).

CONCLUSION

In the present work, we found that the β-*N*-acetylhexosaminidase from *Streptomyces coelicolor* A3(2) can be produced extracellularly in high yield and with good purity from *S. lividans* cultures. The 3D structure of *Sc*HEX is very similar to that of *Sp*HEX, with which it shares 94% sequence identity. Complexes have been obtained with the inhibitor 6-Ac-Cas and by soaking a catalytic acid/base residue variant of the enzyme, E302Q, with chitobiose. This allowed the capture of the NAG−oxazoline intermediate in the −1 subsite, which binds in a similar manner to the stable inhibitor NAG−thiazoline. The enzyme extract exhibits high chitinolytic activity toward chitooligosaccharides, offering potential for the production of GlcNAc as a chemical precursor. The enzyme demonstrates a wide pH-activity range from 4.5 to 7 and exhibits optimal activity at temperatures up to 55 °C. Kinetic measurements for *Sc*HEX with chitin oligomers showing degrees of polymerization 2−6 have shown k_{cat}/K_M values of a similar order of magnitude. These kinetic parameters are superior or comparable to previously described β-*N*-acetylhexosaminidases, offering an improvement for the industrial application of *Sc*HEX. The release of sequentially shorter chitin oligomeric products from $(GlcNAc)_6$ over time lends support to an exoglycosidase activity, with the enzyme cleaving sugars from the nonreducing end of substrates, as with other GH20 family members. Enzyme activity can be significantly stimulated in the presence of sugars, notably fructose, glucuronic acid, and GlcNAc. Thus, some sugars may be used to increase yield and product inhibition is not an issue. Further work will enable the identification of conditions that can maximize the potential yield of GlcNAc by such an extract in an industrial setting. *Sc*HEX adds to the GH20 repertoire, from a structural and mechanistic standpoint and provides an enabling technology for the high-level bioproduction of monosaccharides.

ASSOCIATED CONTENT

Supporting Information

A sequence alignment of *Sc*HEX with members of the GH20 β-*N*-acetylhexosaminidase family and Michaelis−Menten kinetics profiles for the hydrolysis of $(GlcNAc)_{2-6}$ by *Sc*HEX. This

material is available free of charge via the Internet at http://pubs.acs.org.

Accession Codes

Coordinates and structure factors have been deposited in the Protein Data Bank with accession numbers 4C7D, 4C7F, and 4C7G.

■ AUTHOR INFORMATION

Corresponding Author

*E-mail: nicolas.doucet@iaf.inrs.ca. Fax: (450) 686-5501. Tel.: (450) 687-5010, ext. 4212.

Author Contributions

The manuscript was written through contributions of all authors. All authors have given approval to the final version of the manuscript.

Funding

This work was supported by a Natural Sciences and Engineering Research Council of Canada (NSERC) Discovery grant (RGPIN 402623-2011), an NSERC Engage grant, and a "Fonds de Recherche Québec−Santé" (FRQS) Research Scholar Junior 1 Career Award (to N.D). N.N.T was the recipient of a Ph.D. scholarship from the "Fondation Universitaire Armand-Frappier de l'INRS". W.A.O. is funded by the United Kingdom Biotechnology and Biological Sciences Research Council (Grant BB/K003836/1).

Notes

The authors declare no competing financial interest.

■ ACKNOWLEDGMENTS

The authors thank Julie Payet (INRS) for technical assistance and François Lépine (INRS) for mass spectrometry. Data collection was performed at the Diamond Light Source beamlines IO3 and IO4 (Oxfordshire, UK) and staff are thanked for provision of data collection facilities.

■ ABBREVIATIONS

HEX, *β*-*N*-acetylhexosaminidase; *Sc*HEX, *β*-*N*-acetylhexosaminidase from *Streptomyces coelicolor* A3(2); GlcNAc, *N*-acetylglucosamine; GalNAc, *N*-acetylgalactosamine; GH, glycoside hydrolase; *p*NP, *para*-nitrophenyl

■ REFERENCES

(1) Slamova, K., Bojarova, P., Petraskova, L., and Kren, V. (2010) *β*-*N*-acetylhexosaminidase: what's in a name...? *Biotechnol. Adv. 28*, 682−693.

(2) Gravel, R. A., Clark, J. T. R., Kaback, M. M., Mahuran, D., Sandhoff, K., and Suzuki, K. (1995) in *The metabolic basis of inherited disease* (Scriver, C. R., Beaudet, A. L., Sly, W. S., and Valle, D., Eds.), pp 1807−1839, McGraw-Hill, Inc., New York.

(3) Kerrigan, J. E., Ragunath, C., Kandra, L., Gyemant, G., Liptak, A., Janoosy, L., Kaplan, J. B., and Ramasubbu, N. (2008) Modeling and biochemical analysis of the activity of antibiofilm agent dispersin B. *Acta Biol. Hung. 59*, 439−451.

(4) Manuel, S. G., Ragunath, C., Sait, H. B., Izano, E. A., Kaplan, J. B., and Ramasubbu, N. (2007) Role of active-site residues of dispersin B, a biofilm-releasing *β*-hexosaminidase from a periodontal pathogen, in substrate hydrolysis. *FEBS J. 274*, 5987−5999.

(5) Park, J. K., Kim, W. J., and Park, Y. I. (2010) Purification and characterization of an exo-type *β*-*N*-acetylglucosaminidase from *Pseudomonas fluorescens* JK-0412. *J. Appl. Microbiol. 110*, 277−286.

(6) Mark, B. L., Wasney, G. A., Salo, T. J., Khan, A. R., Cao, Z., Robbins, P. W., James, M. N., and Triggs-Raine, B. L. (1998) Structural and funtional characterization of *Streptomyces plicatus β*-*N*-acetylhexosaminidase by comparative molecular modeling and site-directed mutagenesis. *J. Biol. Chem. 273*, 19618−19624.

(7) Ryslava, H., Kalendova, A., Doubnerova, V., Skocdopol, P., Kumar, V., Kukacka, Z., Pompach, P., Vanek, O., Slamova, K., Bojarova, P., Kulik, N., Ettrich, R., Kren, V., and Bezouska, K. (2011) Enzymatic characterization and molecular modeling of an evolutionarily interesting fungal *β*-*N*-acetylhexosaminidase. *FEBS J. 278*, 2469−2484.

(8) Jiang, Y. L., Yu, W. L., Zhang, J. W., Frolet, C., Guilmi, A. M. D., Zhou, C. Z., Vernet, T., and Chen, Y. (2011) Structural basis for the substrate specificity of a novel *β*-*N*-acetylhexosaminidase StrH protein from *Streptococcus pneumoniae* R6. *J. Biol. Chem. 286*, 43004−43012.

(9) Liu, T., Zhang, H., Liu, F., Chen, L., Shen, X., and Yang, Q. (2011) Active-pocket size differentiating insectile from bacterial chitinolytic *β*-*N*-acetyl-D-hexosaminidases. *Biochem. J. 438*, 467−474.

(10) Mark, B. L., Vocadlo, D. J., Knapp, S., Triggs-Raine, B. L., Withers, S. G., and James, M. N. (2001) Crystallographic evidence for substrate-assisted catalysis in a bacterial *β*-hexosaminidase. *J. Biol. Chem. 276*, 10330−10337.

(11) Williams, S. J., Mark, B. L., Vocadlo, D. J., James, M. N. G., and Withers, S. G. (2002) Aspartate 313 in the *Streptomyces plicatus* hexosaminidase plays a critical role in substrate-assisted catalysis by orienting the 2-acetamido group and stabilizing the transition state. *J. Biol. Chem. 277*, 40055−40065.

(12) Howard, M. B., Ekborg, N. A., Weiner, R. M., and Hutcheson, S. W. (2003) Detection and characterization of chitinases and other chitin-modifying enzymes. *J. Ind. Microbiol. Biotechnol. 30*, 627−635.

(13) Chen, J. K., Shen, C. R., and Liu, C. L. (2010) *N*-Acetylglucosamine: production and applications. *Mar. Drugs 8*, 2493−2516.

(14) Sashiwa, H., Fujishima, S., Yamano, N., Kawasaki, N., Nakayama, A., Muraki, E., Hiraga, K., Oda, K., and Aiba, S. (2002) Production of *N*-acetyl-D-glucosamine from *α*-chitin by crude enzymes from *Aeromonas hydrophila* H2330. *Carbohydr. Res. 337*, 761−763.

(15) Pichyangkura, R., Kudan, S., Kuttiyawang, K., Sukwattanasinitt, M., and Aiba, S. (2002) Quantitative production of 2-acetoamodo-2-D-glucose from crystalline chitin by bacterial Chitinase. *Carbohydr. Res. 337*, 557−559.

(16) Saito, A., Fujii, T., Yoneyama, T., Redenbach, M., Ohno, T., and Watanabe, T. (1999) High-multiplicity of Chitinase genes in *Streptomyces coelicolor* A3(2). *Biosci. Biotechnol. Biochem. 63*, 710−718.

(17) Saito, A., Ishizaka, M., Francisco, P. B. J., Fujii, T., and Miyashita, K. (2000) Transcriptional co-regulation of five Chitinase genes scattered on the *Streptomyces coelicolor* A3(2) chromosome. *Microbiology 146*, 2937−2946.

(18) Bentley, S. D., Chater, K. F., Cerdeño-Tárraga, A. M., Challis, G. L., Thomson, N. R., James, K. D., Harris, D. E., Quail, M. A., Kieser, H., Harper, D. B. A., Brown, S., Chandra, G., Chen, C. W., Collins, M., Cronin, A., Fraser, A., Goble, A., Hidalgo, J., Hornsby, T., Howarth, S., Huang, C. H., Kieser, T., Larke, L., Murphy, L., Oliver, K., O'Neil, S., Rabbinowitsch, E., Rajandream, M. A., Rutherford, K., Rutter, S., Seeger, K., Saunders, D., Sharp, S., Squares, R., Squares, S., Taylor, K., Warren, T., Wietzorrek, A., Woodward, J., Barrell, B. G., Parkhill, J., and Hopwood, D. A. (2002) Complete genome sequence of the model actinomycete *Streptomyces coelicolor* A3(2). *Nature 417*, 141−147.

(19) Horsch, M., Mayer, C., Sennhauser, U., and Rast, D. M. (1997) *β*-*N*-acetylhexosaminidase: a target for the design of antifungal drugs. *Pharmacol. Ther. 76*, 187−218.

(20) Seidl, V. (2008) Chitinases of filamentous fungi: a large group of diverse proteins with multiple physiological functions. *Fungal Biol. Rev. 22*, 36−42.

(21) Saito, A., Shinya, T., Miyamoto, K., Yokoyama, T., Kaku, H., Minami, E., Shibuya, N., Tsujibo, H., and Nagata, Y. E. A. (2007) The *dasABC* gene cluster, adjacent to *dasR*, encodes a novel ABC transporter for the uptake of *N,N*,-diacetylchitobiose in *Streptomyces coelicolor* A3(2). *Appl. Environ. Microbiol. 73*, 3000−3008.

(22) Saito, A., Fujii, T., Shinya, T., Shibuya, N., Ando, A., and Miyashita, K. (2008) The *msiK* gene, encoding the ATP-hydrolysing component of *N,N*9-diacetylchitobiose ABC transporters, is essential

for induction of Chitinase production in *Streptomyces coelicolor* A3(2). *Microbiology 154*, 3358−3365.
(23) Saito, A., Miyashita, K., Biukobic, G., and Schrempf, H. (2001) Characteristics of a *Streptomyces coelicolor* A3(2) extracellular protein targeting chitin and chitosan. *Appl. Environ. Microbiol. 67*, 1268−1273.
(24) Hoell, I. A., Dalhus, B., Heggset, E. B., Aspmo, S. I., and Eijsink, V. G. H. (2006) Crystal structure and enzymatic properties of a bacterial family 19 Chitinase reveal differences from plant enzymes. *FEBS J. 273*, 4889−4900.
(25) Heggset, E. B., Hoell, I. A., Kristoffersen, M., Eijsink, V. G. H., and Vårum, K. M. (2009) Degradation of chitosans with Chitinase G from *Streptomyces coelicolor* A3(2): production of chito-oligosaccharides and insight into subsite specificities. *Biomacromolecules 10*, 892−899.
(26) Caufrier, F., Martinou, A., Dupont, C., and Bouriotis, V. (2003) Carbohydrate esterase family 4 enzymes: substrate specificity. *Carbohydr. Res. 338*, 687−692.
(27) Hurtubise, Y., Shareck, F., Kluepfel, D., and Morosoli, R. (1995) A cellulase/xylanase-negative mutant of *Streptomyces lividans* 1326 defective in cellobiose and xylobiose uptake is mutated in a gene encoding a protein homologous to ATP-binding proteins. *Mol. Microbiol. 17*, 367−377.
(28) Hopwood, D. A., Bibb, M. J., Chater, K. F., Kieser, T., Vruton, C. J., Kieser, H. M., Lydiate, D. J., Smith, C. P., and Ward, J. M. (1985) *Genetic manipulation of Streptomyces—A Laboratory Manual*, The John Innes Foundation, Norwich, U.K.
(29) Ho, S. N., Hunt, H. D., Horton, R. M., Pullen, J. K., and Pease, L. R. (1989) Site-directed mutagenesis by overlap extension using the polymerase chain. *Gene 77*, 51−59.
(30) Winn, M. D., Ballard, C. C., Cowtan, K. D., Dodson, E. J., Emsley, P., Evans, P. R., Keegan, R. M., Krissinel, E. B., Leslie, A. G. W., McCoy, A., McNicholas, S. J., Murshudov, G. N., Pannu, N. S., Potterton, E. A., Powell, H. R., Read, R. J., Vagin, A., and Wilson, K. S. (2011) Overview of the CCP4 suite and current developments. *Acta Crystallogr., Sect. D: Biol. Crystallogr. 67*, 235−242.
(31) McCoy, A. J., Grosse-Kunstleve, R. W., Adams, P. D., Winn, M. D., Storoni, L. C., and Read, R. J. (2007) Phaser crystallographic software. *J. Appl. Crystallogr. 40*, 658−674.
(32) Emsley, P., Lohkamp, B., Scott, W. G., and Cowtan, K. (2010) Features and development of Coot. *Acta Crystallogr., Sect. D: Biol. Crystallogr. 66*, 486−501.
(33) Murshudov, G. N., Vagin, A. A., and Dodson, E. J. (1997) Refinement of macromolecular structures by the maximum-likelihood method. *Acta Crystallogr., Sect. D: Biol. Crystallogr. 53*, 240−255.
(34) Gutternigg, M., Kretschmer-Lubich, D., Paschinger, K., Rendic, D., Hader, J., Geier, P., Ranftl, R., Jantsch, V., Lochnit, G., and Wilson, I. B. (2007) Biosynthesis of truncated N-linked oligosaccharides results from non-orthologous hexosaminidase-mediated mechanisms in nematodes, plants, and insects. *J. Biol. Chem. 282*, 27825−27840.
(35) He, Y., Macauley, M. S., Stubbs, K. A., Vocadlo, D. J., and Davies, G. J. (2010) Visualizing the reaction coordinate of an O-GlcNAc hydrolase. *J. Am. Chem. Soc. 132*, 1807−1809.
(36) http://www.cazy.org/Glycoside-Hydrolases.html. (2013) Glycoside Hydrolase family classification.
(37) Henrissat, B., and Bairoch, A. (1993) New families in the classification of glycosyl hydrolases based on amino acid sequence similarities. *Biochem. J. 293*, 781−788.
(38) Henrissat, B., and Bairoch, A. (1996) Updating the sequence-based classification of glycosyl hydrolases. *Biochem. J. 316*, 695−696.
(39) Sumida, T., Ishii, R., Yanagisawa, T., Yokoyama, S., and Ito, M. (2009) Molecular cloning and crystal structural analysis of a novel *β*-*N*-acetylhexosaminidase from *Paenibacillus* sp. TS12 capable of degrading glycosphingolipids. *J. Mol. Biol. 392*, 87−99.
(40) Intra, J., Pavesi, G., and Horner, D. S. (2008) Phylogenetic analyses suggest multiple changes of substrate specificity within the glycosyl hydrolase 20 family. *BMC Evol. Biol. 8*, 214 DOI: doi:10.1186/1471-2148-8-214.
(41) Jiang, Y. L., Yu, W. L., Zhang, J. W., Frolet, C., Guilmi, A. M. D., Zhou, C. Z., Vernet, T., and Chen, Y. (2011) Structural basis for the substrate specificity of a novel *β*-*N*-acetylhexosaminidase StrH protein from *Streptococcus pneumoniae* R6. *J. Biol. Chem. 286*, 43004−43012.
(42) Prag, G., Papanikolau, Y., Tavlas, G., Vorgias, C. E., Petratos, K., and Oppenheim, A. B. (2000) Structures of chitobiase mutants complexed with the substrate di-*N*-acetyl-D-glucosamine: the catalytic role of the conserved acidic pair, aspartate 539 and glutamate 540. *J. Mol. Biol. 300*, 611−617.
(43) Suginta, W., Chuenark, D., Mizuhara, M., and Fukamizo, T. (2010) Novel *β*-*N*-acetylglucosaminidases from *Vibrio harveyi* 650: cloning, expression, enzymatic properties, and subsite identification. *BMC Biochem. 11*, 40 DOI: doi:10.1186/1471-2091-11-40.
(44) Robbins, P., Overbye, K., Albright, C., Benfield, B., and Pero, J. (1992) Cloning and high-level expression of Chitinase-encoding gene of *Streptomyces plicatus*. *Gene 111*, 69−76.
(45) Gomes, J. E., Souza, D. S. L., Nascimento, R. M., Lima, A. L. M., Melo, J. A. T., Rocha, T. L., Miller, R. N. G., Franco, O. L., Grossi-de-Sa, M. F., and Abreu, L. R. D. (2010) Purification and characterization of a liver-derived *β*-*N*-acetylhexosaminidase from marine mammal *Sotalia fluviatilis*. *Protein J. 29*, 188−194.
(46) Kubota, T., Miyamoto, K., Yasuda, M., Inamori, Y., and Tsujibo, H. (2004) Molecular characterization of an intracellular *β*-*N*-acetylglucosaminidase involved in the chitin degradation system of *Streptomyces thermoviolaceus* OPC-520. *Biosci. Biotechnol. Biochem. 68*, 1306−1314.
(47) Plíhal, O., Sklenár, J., Hofbauerová, K., Novák, P., Man, P., Pompach, P., Kavan, D., Ryslavá, H., Weignerová, L., Charvátová-Pisvejcová, A., Kren, V., and Bezouska, K. (2007) Large propeptides of fungal *β*-*N*-acetylhexosaminidases are novel enzyme regulators that must be intracellularly processed to control activity, dimerization, and secretion into the extracellular environment. *Biochemistry 46*, 2719−2734.
(48) Ghosh, S., Meli, V. S., Kumar, A., Thakur, A., Chakraborty, N., Chakraborty, S., and Datta, A. (2011) The *N*-glycan processing enzymes alpha-mannosidase and beta-D-*N*-acetylhexosaminidase are involved in ripening-associated softening in the non-climacteric fruits of capsicum. *J. Exp. Bot. 62*, 571−582.
(49) Keyhani, N. O., and Roseman, S. (1996) The chitin catabolic cascade in the marine bacterium *Vibrio furnissii:* molecular cloning, isolation, and characterization of a periplasmic *β*-*N*-acetylglucosaminidase. *J. Biol. Chem. 271*, 33425−33432.
(50) Hammes, G. G., Chang, Y. C., and Oas, T. G. (2009) Conformational selection or induced fit: a flux description of reaction mechanism. *Proc. Natl. Acad. Sci. U.S.A. 106*, 13737−13741.
(51) Goujon, M., McWilliam, H., Li, W., Valentin, F., Squizzato, S., Paern, J., and Lopez, R. (2010) A new bioinformatics analysis tools framework at EMBL-EBI. *Nucleic Acids Res. 38*, W695−699.
(52) Potterton, L., McNicholas, S., Krissinel, E., Gruber, J., Cowtan, K., Emsley, P., Murshudov, G. N., Cohen, S., Perrakis, A., and Noble, M. (2011) Developments in the CCP4 molecular-graphics project. *Acta Crystallogr., Sect. D: Biol. Crystallogr. 60*, 2288−2294.
(53) Konno, N., Takahashi, H., Nakajima, M., Takeda, T., and Sakamoto, Y. (2012) Characterization of *β*-*N*-acetylhexosaminidase (LeHex20A), a member of glycoside hydrolase family 20, from *Lentinula edodes* (shiitake mushroom). *AMB Express 2*, 29.
(54) Katta, S., Ankati, S., and Podile, A. R. (2013) Chitooligosaccharides are converted to *N*-acetylglucosamine by *N*-acetyl-*β*-hexosaminidase from *Stenotrophomonas maltophilia*. *FEMS Microbiol. Lett. 348*, 19−25.

Supporting information

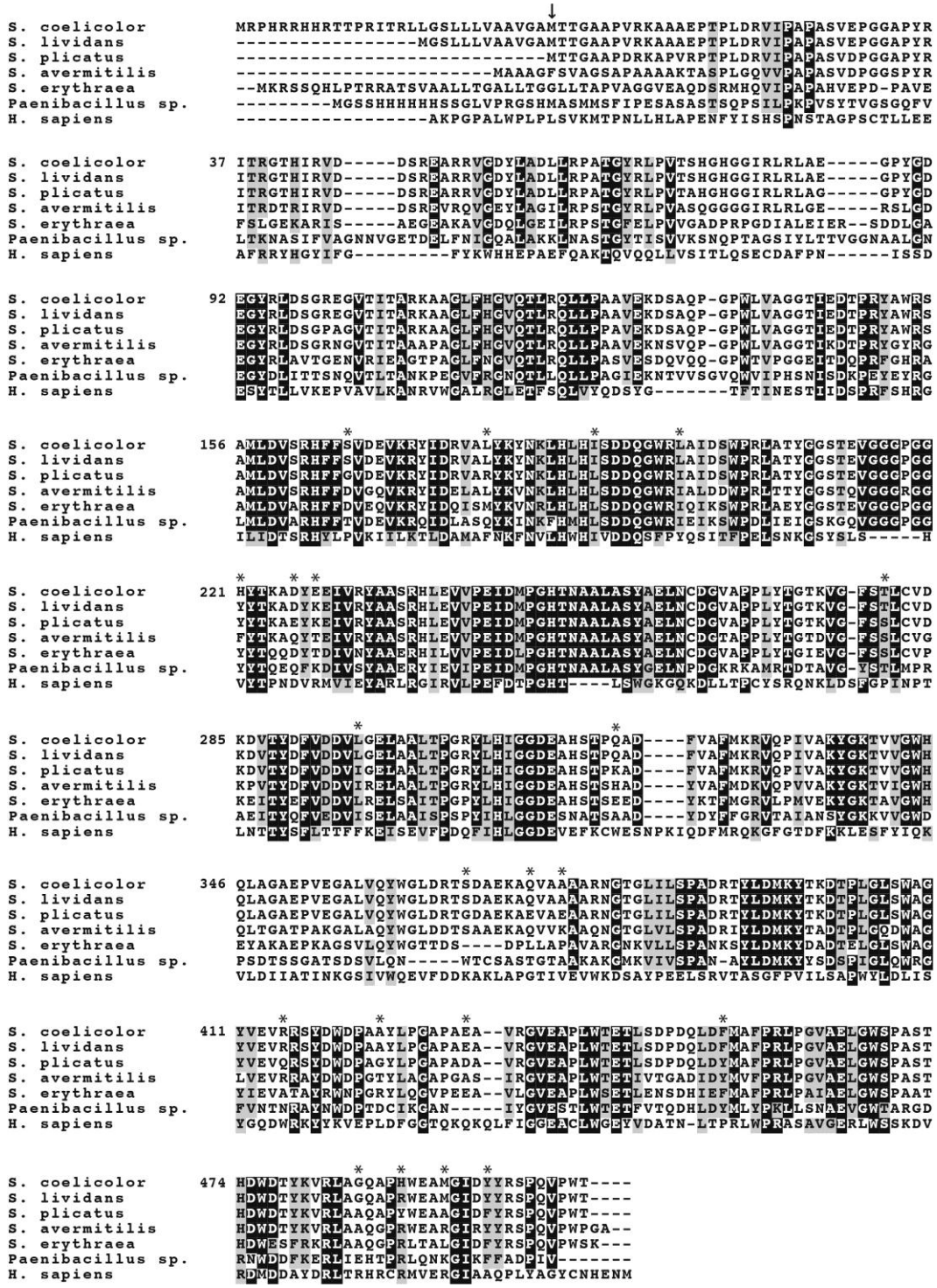

Figure S1. Sequence alignment of *Sc*HEX with members of the GH20 β-*N*-acetylhexosaminidase family. Alignment was performed with GH20 homologues from

Streptomyces coelicolor (NP_627016.1), *Streptomyces lividans* (ZP_05526012.1), *Streptomyces plicatus* (PDB entry 1HP4), *Streptomyces avermitilis* (BAB69153.1), *Saccharopolyspora erythraea* (YP_001106047.1), *Paenibacillus Sp.* (PDB entry 3GH4), and *Homo sapiens* HEXB (PDB entry 1NOU). Residues showing >90% identity (similarity) are highlighed in black (grey). *Sc*HEX is numbered according to PDB entry 4C7D. The arrow identifies the position of the initiating methionine. Alignment was performed with ClustalW2[51] and processed with BoxShade 3.21.

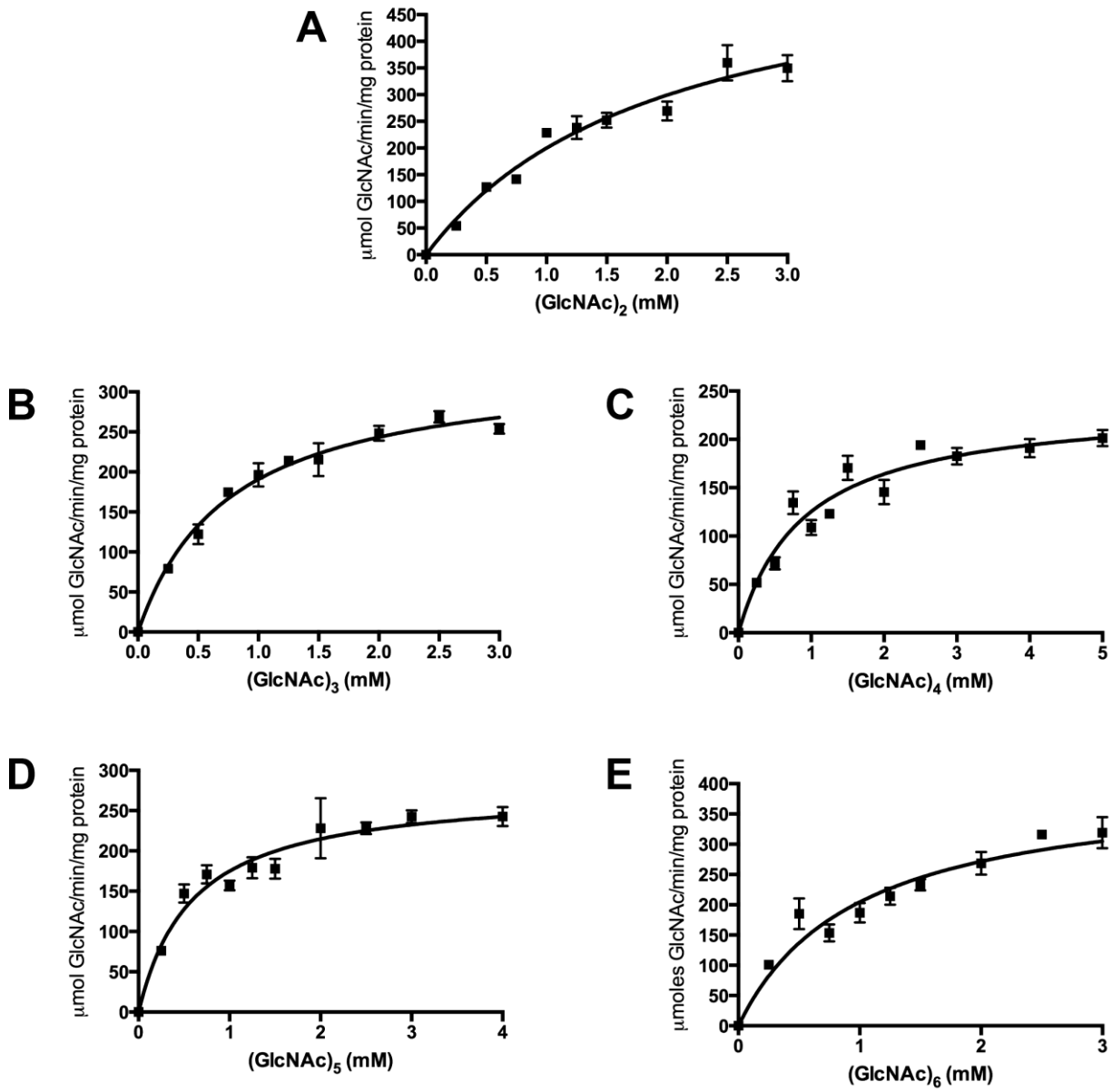

Figure S2. Michaelis-Menten kinetics profiles for the hydrolysis of $(GlcNAc)_{2\text{-}6}$ by *Sc*HEX. A) $(GlcNAc)_2$, B) $(GlcNAc)_3$, C) $(GlcNAc)_4$, D) $(GlcNAc)_5$, E) $(GlcNAc)_6$. See Experimental Procedures for details.

2.3. Presentation of article 2 – "Characterization of chitinase C from *Streptomyces coelicolor* A3(2) and its application in *N*-acetylglucosamine production"

The scientific manuscript entitled "Characterization of chitinase C from *Streptomyces coelicolor* A3(2) and its application in *N*-acetylglucosamine production" was submitted to the journal *Enzyme and Microbial Technology* (impact factor of 2.966 as of April 2015) in March 2015 and is awaiting for review.

2.3.1. Contribution of authors

The results presented in this manuscript were obtained entirely by the student. The manuscript was written by the student and by N. Doucet.

2.3.2. Résumé

La bioconversion enzymatique de la chitine est d'un intérêt considérable pour la production de composés bioactifs naturels tels que les chitooligosaccharides et la *N*-acétyl-D-glucosamine (GlcNAc). Dans la nature, des enzymes clés sont impliquées dans la catalyse de la chitine. L'hydrolyse de ce biopolymère abondant produit des dérivés de monosaccharide glucosidique, qui possède une valeur substantielle pour les domaines médicaux et biotechnologiques. Pour cette étude, la chitinase C (ChiC), qui catalyse la décomposition de la chitine et présente dans la bactérie du sol *Streptomyces coelicolor* A3(2), a été exprimée, purifiée et caractérisée. L'enzyme purifiée s'est révélée être thermoactive, favorisant la conversion de la chitine en chitobiose [$(GlcNAc)_2$] à une température optimale de 55°C. Alors que ChiC peut hydrolyser les chitines cristallines et solubles pour produire le $(GlcNAc)_2$, il a été démontré que l'enzyme présente une activité plus élevée contre la β-chitine que contre α-chitine. À partir du profil de l'hydrolyse de chitine de coquilles de crabes, les résultats ont révélé que ChiC utilise un mécanisme endoprocessif pour la bioconversion de chitooligosaccharides. En utilisant une combinaison de ChiC et de *N*-acétylhexosaminidase de *S. coelicolor* A3(2) (*Sc*HEX) avec la chitine cristalline comme substrat, la réaction a comme produit le GlcNAc avec une pureté supérieure à 95% après 8 heures d'incubation. Ce

rendement représente l'une des bioconversions enzymatiques les plus efficaces caractérisées à ce jour pour la conversion de chitooligosaccharides en GlcNAc, ce qui rend le duo ChiC-*Sc*HEX potentiellement applicable à la production industrielle efficace de cet important composé bioactif.

2.3.3. Article 2

Characterization of chitinase C from *Streptomyces coelicolor* A3(2) and its application in *N*-acetylglucosamine production

Nhung Nguyen-Thi[1,2,3] *& Nicolas Doucet*[1,4,5,#]

[1]INRS-Institut Armand-Frappier, Université du Québec, 531 Boul. des Prairies, Laval, Québec, H7V 1B7, Canada.

[2]Institute of Military Science and Technology, 17 Hoang Sam, Hanoi, Vietnam.

[3]Vietnam Academy of Science and Technology, 18 Hoang Quoc Viet, Hanoi, Vietnam.

[4]PROTEO, the Québec Network for Research on Protein Function, Structure, and Engineering, 1045 Avenue de la Médecine, Université Laval, Québec, Québec, G1V 0A6, Canada.

[5]GRASP, the Groupe de Recherche Axé sur la Structure des Protéines, 3649 Promenade Sir William Osler, McGill University, Montréal, Québec, H3G 0B1, Canada.

Nhung Nguyen-Thi: nhung.nguyenthi@iaf.inrs.ca

Corresponding author: Nicolas Doucet, Email: nicolas.doucet@iaf.inrs.ca; Phone: (450) 687-5010, x4212; Fax: (450) 686-5501

Abstract

The enzymatic bioconversion of chitin is of considerable interest for the natural production of bioactive compounds such as chitooligosaccharides and *N*-acetyl-D-glucosamine (GlcNAc). Key enzymes are involved in the natural processing of chitin, hydrolyzing this abundant biopolymer to yield monosaccharide derivatives of glucose with substantial value to the medicinal and biotechnological fields. In this study, chitinase C (ChiC) from the soil bacterium and chitin decomposer *Streptomyces coelicolor* A3(2) was expressed, purified and characterized. The purified enzyme was found to be thermoactive, converting chitin to chitobiose [$(GlcNAc)_2$] at an optimal temperature of 55°C. While ChiC could hydrolyze both crystalline chitin and soluble chitin to produce $(GlcNAc)_2$, the enzyme exhibited higher activity against β-chitin than α-chitin. Crab shell chitin hydrolysis profiles also revealed that ChiC catalyzes the bioconversion of chitooligosaccharides through an endo-nonprocessive mode of action. When combining ChiC with an *N*-acetylhexosaminidase from *S. coelicolor* A3(2) (*Sc*HEX) in an assay using crystalline chitin as substrate, GlcNAc was generated as final product with an yield 90% after 8h incubation. This chitin hydrolysis yield represents one of the most efficient enzyme bioconversion of chitooligosaccharides to GlcNAc characterized to date, making the ChiC-*Sc*HEX pair a potentially suitable contender for the viable industrial production of this important bioactive compound.

Keywords: *N*-acetylglucosamine, chitinase, chitin, *Streptomyces coelicolor*, chitooligosaccharides.

1. Introduction

Chitin is formed of β(1,4)-linked units of *N*-acetyl-D-glucosamine (GlcNAc), shaping one of the most abundant natural biopolymers on earth after cellulose. The enzymatic bioconversion of chitin is of considerable interest due to its contribution to the carbon and nitrogen cycles of the biosphere, allowing the transformation of biomass to generate bioactive chitooligosaccharides [1-4] and GlcNAc, a monosaccharide derivative of glucose with substantial industrial value in medicinal and biotechnological applications [5-7]. Recently, GlcNAc has been used as a supplement for the treatment of osteoarthritis and inflammatory bowel disease [8, 9]. It has also been used in many treatment trials, namely for cancer, autoimmune reactions, sexual disorders and intestinal diseases [6]. As a result, the industrial bioproduction of GlcNAc with satisfactory yields and purity remains an imperative for profitable commercialization.

Like cellulose, chitin is mostly insoluble in water. Its hydrogen-bonding pattern requires solubilizing agents that induce inter-chain repulsions or disturb intermolecular hydrogen bonding for dissolution. Chitin can be structurally classified into α-chitin—in which the chains of the unit cell are antiparallel—or β-chitin—in which the neighboring chains are aligned in a parallel fashion [10]. Every year, more than 100 billion tons of chitin accumulates in nature, making it an unlimited and still relatively unexploited resource biomaterial for the production of GlcNAc [7, 11-13]. Due to extreme insolubility, the large-scale production of GlcNAc from chitin is still far from optimized. Production currently relies on a chemical hydrolysis method which requires concentrated hydrochloric acid at high temperatures [14, 15]. This process is at the root of many industrial and environmental obstacles, including acidic wastes, low production yields, high energy costs, and product separation issues [6]. In recent years, the environmentally friendly

65 enzymatic processes developed to break down chitin have gained in efficiency and robustness,
66 though yields and issues pertaining to final product purity remain challenging [14, 16-21]. As a
67 result, uncovering new and effective biocatalysts to optimize chitin degradation remains crucial
68 for the efficient enzymatic production of GlcNAc from this insoluble polymer.

69 Chitinases, which hydrolyze the β(1,4) linkages of chitin, are key enzymes in the natural
70 processing of this biomaterial. Based on their hydrolytic function, chitinases are classified into
71 endochitinases (E.C. 3.2.1.14), exochitinases (E.C. 3.2.1.29), and *N*-acetylglucosaminidases
72 (E.C. 3.2.1.30) [22]. The first group randomly cleaves the chitin polymer to yield soluble, low
73 molecular weight oligomers such as chitotetraose and chitopentaose. The second group catalyzes
74 the progressive release of chitobiose from the non-reducing or reducing end of the polymer
75 microfibril. Finally, the third group releases *N*-acetylglucosamine monomers from
76 chitooligomers and chitobiose, which are produced by the endochitinases and exochitinases,
77 respectively. These enzymes are expected to act in concert to generate complete hydrolysis of the
78 polymer [23, 24].

79 *Streptomyces* spp. are soil bacteria and major decomposers of chitin. *Streptomyces*
80 *coelicolor* A3(2) is a Gram-positive bacterium whose genome was fully sequenced in 2002,
81 revealing 13 putative chitinases [25]. A number of *Streptomyces coelicolor* A3(2) chitinase
82 sequences and activities were previously investigated and characterized against 4-methyl-
83 umbelliferyl *N,N',N''*-triacetyl chitotriose, including eight chitinases: ChiA, ChiB, ChiC, ChiD,
84 ChiE, ChiF, ChiG, and ChiH. The transcription mechanism governing the regulation of these
85 genes and the expression levels of each chitinase were thoroughly investigated [26-28].
86 However, the exo- or endo-character of these *Streptomyces* enzymes, the possible occurrence of
87 multiple catalytic mechanisms (processivity) and how each chitinase is involved in chitin

breakdown still remains elusive. Among the abovementioned chitinases, ChiC belongs to family GH18 and contains three domains: a putative substrate-binding domain, a fibronectin type III-like domain, and a catalytic domain similar to many other GH18 chitinases, such as Chi63 from *S. plicatus,* ChiIII from *S. griseus*, ChiC from *S.lividans*, or ChiC from *Serratia marcescens* [29-31]. Although members of this family are evolutionarily diverse, their catalytic domain retains the typical $(\alpha/\beta)_8$ fold. GH18 enzymes catalyze chitin hydrolysis through a double displacement cleavage mechanism, in which the initial configuration of the scissile bond is retained by the newly generated reducing end [32]. GH18 enzymes also retain the conserved catalytic motif DXDXE [33, 34] and hydrolyze chitin through a substrate-assisted mechanism with participation of the adjacent pyranose acetamido group [35]. The GH18 family contains non-processive endo-acting chitinases as well as processive enzymes with exo- or endo-binding modes. To effectively break down crystalline polymers, non-processive endo-acting enzymes need the presence of substrate-binding and substrate-disrupting domains to increase substrate accessibility [36, 37]. Meanwhile, processive chitinases have the ability to attach to their crystalline substrate during hydrolytic reactions, *i.e.* the substrate successively binds to the active site after each cleavage and slides along the cleft for the next turnover to occur. This processive mechanism is thought to be the most effective way to enzymatically breakdown recalcitrant polysaccharides [32, 38-41].

It was reported that the complete degradation of chitin requires the concerted action of chitinases and *N*-acetylhexosaminidases (HEX) [23, 24]. In this mechanism, chitinases degrade chitin into chitooligomers, which are subsequently hydrolyzed by HEX to release GlcNAc [42, 43]. We recently characterized a β-*N*-acetylhexosaminidase from *S. coelicolor* A(3)2 (*Sc*HEX), an enzyme displaying significant hydrolytic activity toward chitooligosaccharides, from which it can yield pure GlcNAc without any byproduct [44]. In the present work, we recombinantely

111 expressed and characterized ChiC from *S. coelicolor* A3(2) (gene accession number
112 2SC6G5.20c) to further clarify the chitinolytic system of this important soil bacterium, in
113 addition to developing and characterizing an efficient enzyme combination using ChiC and
114 *Sc*HEX to help improve the enzymatic breakdown of raw chitin biomass to produce the
115 industrially-relevant GlcNAc compound. We observe that the ChiC-*Sc*HEX pair performs one of
116 the most efficient enzymatic bioconversions of chitooligosaccharides to GlcNAc characterized to
117 date, promising high applicability for raw biomass transformation.
118

119 **2. Materials and Methods**

120

121 *2.1 Reagents*

122 Crab shell α-chitin was purchased from Sigma-Aldrich. β-chitin extracted from squid pens was
123 obtained from Kyowa Oil Company, Japan. Chitooligosaccharides [$(GlcNAc)_n$; n=1-6] were
124 purchased from V-Labs (Covington, LA, USA). Cell wall peptidoglycan from the Gram-positive
125 *Bacillus subtilis* and *Streptomyces* sp. microorganisms were also purchased from Sigma-Aldrich.
126 Glycol chitin-80 and glycol chitin-40 (80% and 40% acetylated, respectively) were prepared as
127 previously described [10]. Chitosan-24 and chitosan-19.2 (24% and 19.2% acetylated,
128 respectively) were obtained from HaloSource (Bothell, WA, USA). For protein expression, the
129 strain *S. lividans* IAF 10-164 [*msiK*$^-$] was employed [45]. This host harbors a mutated *msiK* gene,
130 which encodes for a sugar import ABC transporter essential for the induction of chitinase
131 production in *S. coelicolor* A3(2) [43], thus preventing the possibility of overlapping chitinase
132 activities between the expression host and the cloned enzyme.
133

134 *2.2. Gene expression and protein purification*

135 Strain *S. lividans* 10-164 carrying plasmid pC109-*chiC* (accession number 2SC6G5.20c)
136 was cultivated in 500 mL of M14 medium with Tween 80% (2 ml/L) and 1% xylose (w/v) as the
137 sole carbon source. The culture was incubated at 34°C with agitation (250 rpm). After 72 h of
138 incubation, the supernatant was harvested by filtering through a No.1 Whatman membrane (GE
139 Healthcare) to remove mycelia. The resulting protein mixture was then concentrated by
140 ultrafiltration using a 10-kDa cut-off membrane, generating a final yield of 1070 mg/L. The
141 concentrated solution was dialyzed against 10 mM Tris-HCl buffer, pH 7.6 and then loaded on a
142 Hi-Trap DEAE FF column (GE Healthcare) pre-equilibrated with 10 mM Tris-HCl buffer, pH
143 7.6. ChiC was eluted with a linear gradient of 10 mM Tris-HCl buffer containing 1M NaCl, pH
144 7.6. The protein was eluted at a concentration of 40 mM NaCl. Elution fractions were analyzed
145 by SDS-PAGE and fractions containing ChiC were pooled and concentrated to 4 mg/mL by
146 ultrafiltration. Partially purified enzyme (1 mg) was loaded on size-exclusion Protein-Pak 125
147 (7.8 mm × 30 cm) HPLC columns (Waters Corporation). Elution was performed at a flow rate of
148 0.5 mL/min in isocratic mode with a 0.1 M sodium phosphate buffer, pH 6.0 (25°C). The
149 collected elution fractions (1 mL each) were analyzed by SDS-PAGE to assess purity. Total
150 protein concentration was determined using a Bio-Rad Protein Assay (Bio-Rad). For mock
151 expression of ChiC, the strain *S. lividans* 10-164 containing plasmid pC109 without insert of the
152 c*hiC* gene was cultivated following the same protocol. The culture supernatant after expression
153 was used as a mock control for all enzyme assays.

154

155 *2.3 Substrate specificity*

156 The substrates used in this study are α-chitin from crab shell, β-chitin from squid pens,
157 soluble chitin (glycol chitin-40% and 80%), chitosan (24% and 19.2%), peptidoglycan, and

158 chitooligomers with degrees of polymerization ranging from 2 to 6 units of GlcNAc. Enzyme
159 assays were carried out with 0.5 mg/mL of substrate at 55°C in 50 mM phosphate buffer
160 containing 150 mM NaCl (pH 5). After 10 minutes of reaction, 100 µL aliquots were taken and
161 mixed with 100 µL of 1 M H_2SO_4 to stop the reaction. The end products were analyzed by HPLC
162 by injecting 100 µL of the reaction solution on an Aminex HPX-87H Ion Exclusion Column (7.8
163 mm × 30 cm) (Bio-Rad) heated at 45°C, running in isocratic mode with a mobile phase of 5 mM
164 H_2SO_4 at a flow rate of 0.5 mL/min [46]. Retention times of released products were compared
165 with the retention times of known standards to identify chemical species. Product concentrations
166 were calculated by comparison of peak areas for known concentrations of each standard. Enzyme
167 activity was expressed in IU/mg of protein, where 1 IU is defined as 1 µmole of released
168 $(GlcNAc)_2$ per minute. Control assays were also performed with water and a mock supernatant.
169
170 *2.4 Michaelis-Menten kinetics*
171 Enzyme kinetics assays were performed with crab shell chitin powder as substrate using
172 8 different substrate concentrations ranging from 0.125 to 1.0 mg/mL. The kinetic parameters
173 V_{max} and K_M were determined at optimal temperature and pH in the aforementioned buffer.
174 Enzyme assays were started by the addition of 196 nM ChiC and quenched with 0.5 mM H_2SO_4.
175 Activity was calculated as IU/mg of protein, where 1 IU is defined as 1 µmole of released
176 $(GlcNAc)_2$ per minute. Kinetic parameters were calculated by a non-linear regression fit to the
177 Michaelis-Menten equation using GraphPad Prism 4.
178

179 *2.5 Mode of action*

180 To determine whether ChiC is an exo- or endo-type enzyme acting in a processive or
181 non-processive manner, time-course profiles for the hydrolysis of crab shell chitin and
182 chitohexaose were determined using the same reaction conditions described above. After each
183 time interval, 100 µL aliquots were taken and mixed with 100 µL of 1 M H_2SO_4 prior to HPLC
184 injection. Products were detected at 210 nm, as described above.

185

186 *2.6 Optimal pH, temperature and stability*

187 To determine optimal temperature for ChiC activity, enzyme assays were performed with
188 0.5 mg/mL of crab shell chitin for 10 minutes at various temperatures (25 to 70°C) in 50 mM
189 phosphate buffer containing 150 mM NaCl. The optimal pH for chitin hydrolysis was determined
190 at the optimal temperature in 50 mM citric buffer with 150 mM NaCl (pH 3, 3.5, 4, 4.5), 50
191 mM phosphate buffer with 150 mM NaCl (pH5, 5.5, 6, 6.5, 7), and 50 mM Tris-HCl buffer
192 with 150 mM NaCl (pH 8, 9). The reactions were performed for 10 min and the enzyme activity
193 was calculated as mentioned above. To investigate the effect of pH and temperature on ChiC
194 stability, assays were performed by pre-incubating the enzyme at different temperatures for 1 h
195 and at different pH for 1 h and 5 months. The enzyme assays were then run with crab shell chitin
196 for 10 min. Activities were compared with control, which was performed with pure enzyme kept
197 in water at 4°C.

198 *2.7 Enzymatic production of GlcNAc from crab shell chitin using ChiC and ScHEX from S.*
199 *coelicolor A3(2)*

200 GlcNAc production was carried out by incubating crab shell chitin in 50 mM phosphate
201 buffer containing 150 mM NaCl (pH 5) at 55°C with known concentrations of 10-fold
202 concentrated supernatants of ChiC and *Sc*HEX. To examine the effect of the *Sc*HEX and ChiC
203 combination on GlcNAc production, enzyme assays were performed as follows: 1) both enzymes
204 were added at the beginning of the reaction, or 2) ChiC was first added at the beginning of the
205 reaction and *Sc*HEX was added when $(GlcNAc)_2$ released by ChiC reached saturation. At each
206 time point, 100 µL aliquots of the reaction mixture were taken and analyzed by HPLC, as
207 described above. To investigate the effect of enzyme ratios on GlcNAc production, enzyme
208 assays with crab shell chitin were performed with various concentrations of ChiC and *Sc*HEX for
209 6 hours in the same reaction conditions. GlcNAc production yields were calculated by comparing
210 the amount of GlcNAc released to the maximal theoretical yield, which is equal to the initial
211 substrate concentration considering that 1 mg of chitin could produce a maximum of 1.06 mg of
212 GlcNAc.

$$\text{Yield GlcNAc (\%)} = \frac{\text{GlcNAc released (mg)} \times 100}{\text{Initial chitin concentration (mg)} \times 1.06}$$

213

214 To evaluate efficiency and product purity, the 10-fold concentrated supernatants of ChiC
215 and *Sc*HEX were added to the reaction incubated with crab shell chitin (10 mg/mL) at 55°C, pH
216 5. The time course of the hydrolysis reaction was recorded until the rate of GlcNAc generation
217 remained stable. The efficiency and product purity were evaluated by quantifying GlcNAc
218 production as described above.

219

220 **3. Results and Discussion**

221

222 *3.1 ChiC substrate specificity*

223 Amino acid sequence alignment of ChiC with other GH18 chitinases shows that the
224 enzyme is highly similar to other *Streptomyces* spp. homologues, such as chitinase 63 from *S.*
225 *plicatus* (95% identity), or ChiC from *S. lividans* (94% identity). *Streptomyces* spp. are known
226 for their ability to decompose chitin in nature. However, their substrate specificity towards
227 natural and long chitooligosaccharides was never investigated. Rather, the chitinase activity of
228 these homologues was investigated towards fluorogenic and/or short substrates like 4-
229 methylumbelliferyl *N*,*N*',*N*''-triacetyl chitotriose or chitobiose [4-MU-$(GlcNAc)_3$ or 4-MU-
230 $(GlcNAc)_2$] [30, 47]. The complete genome sequencing of *S. coelicolor* A3(2) revealed a number
231 of putative chitinases, including 6 GH18 chitinases: ChiA, ChiB, ChiC, ChiD, ChiE, ChiH, and 2
232 GH19 chitinases (ChiF, ChiG) [26-28]. The activity of each enzyme in chitin degradation
233 remains uncharacterized, except for ChiG—a chitin binding protein that specifically targets
234 chitin and chitosan [48, 49]. It was also previously shown that the *chiC* gene displays higher
235 expression levels than its counterparts, suggesting that the encoded ChiC enzyme plays a crucial
236 role within the chitinolytic system of *S. coelicolor* [26]. To investigate this activity, we cloned
237 and expressed *chiC* in the *S. lividans* 10-164 host for enzyme characterization. Enzyme members
238 of the GH18 glycoside hydrolase family are diverse in sequence and have been known to
239 degrade peptidoglycan, soluble and insoluble forms of chitin, in addition to chitosan forms with
240 low degrees of acetylation (13%) [28]. As a result, the following compounds were used to
241 investigate the substrate specificity of ChiC: α-chitin from crab shell, β-chitin from squid pens,
242 glycol chitin-40, glycol chitin-80, chitosan-24, chitosan-19.2, peptidoglycan, and chitooligomers
243 with degrees of polymerization ranging from 2 to 6 GlcNAc units [$(GlcNAc)_{2\text{-}6}$]. Our results

244 show that ChiC can break down both kinds of chitin substrates (Table 1). The enzyme
245 hydrolyzed β-chitin more easily than α-chitin, a more tightly packed crystalline substrate
246 structure. However, the similar substrate specificity of ChiC toward α- and β-chitin (1.5-fold
247 difference) contrasts with that of similar enzymes, which typically show much higher activity
248 toward β-chitin than α-chitin (4.6-fold difference or higher) [17, 20, 50]. Because α-chitin is
249 readily available and wildly dispersed in nature relative to β-chitin, this makes ChiC a promising
250 and potentially unique candidate for raw biomass degradation.

251 **Table 1.** Specific activity of ChiC toward various substrates.

Substrate	Specific activity (IU/mg)
Powdered β-chitin	981 ± 43
Crabshell α-chitin	664 ± 86
Glycol chitin 80%	231 ± 2
Glycol chitin 40%	43 ± 8
Chitosan 24%	238 ± 20
Chitosan 19.2%	59 ± 2
Peptidoglycan	n/d
$(GlcNAc)_6$	4120 ± 80
$(GlcNAc)_5$	4072 ± 128
$(GlcNAc)_4$	9215 ± 504
$(GlcNAc)_3$	1379 ± 58
$(GlcNAc)_2$	n/d

252 n/d: not detectable; IU= μmol/min of GlcNAc released per mg of enzyme. Results are presented as means ± standard
253 error (*n*=3).

254 ChiC did not hydrolyze peptidoglycan but could hydrolyze chitosan with degrees of
255 acetylation (DA) of 24% and 19.2%, albeit with lower efficiency (Table 1). GH18 enzymes use a
256 substrate-assisted mechanism that relies on the participation of the *N*-acetyl group of GlcNAc for
257 catalysis [51-53]. In peptidoglycan, the glycan moiety is formed by GlcNAc and *N*-

acetylmuramic acid (MurNAc) cross-linked to peptides. Because this structure resembles that of chitin, some GH18 chitinases with broad substrate specificities have been shown to hydrolyze peptidoglycan [54], which we did not observe with ChiC. ChiC nevertheless degraded chitosan with DA as low as 19.2%, comparable to the *Bacillus* sp. Hu1 chitinase, albeit with lower efficiency than ChiB from *Serratia marcescens.* These two enzymes were shown to hydrolyze chitosan with DA as low as 20% and 13%, respectively [14, 55, 56]. GH18 members have a strong preference for acetylated units due to the direct catalytic involvement of the acetamido-group at subsite -1. Despite the fact that deacetylated chitosan units would make for nonproductive binding [38], chitosan polymer chains displaying relatively low amounts of acetylated units remain decent substrates for these enzymes. ChiC also showed significant activity against chitooligomers with degrees of polymerization ranging from 3 to 6 GlcNAc units [$(GlcNAc)_{3\text{-}6}$]. The active site of GH18 homologues is a long substrate-binding cleft with five or more sub-sites that can accommodate GlcNAc units forming polymer chains [56]. The highest ChiC specific activity was observed with $(GlcNAc)_4$ (9215 ± 504 IU/mg) (Table 1), suggesting that substrate accommodation in the active site of ChiC is optimal for chitooligomers displaying four units of GlcNAc. No activity was observed with $(GlcNAc)_2$, supporting the fact that this dimer is the final product of chitin hydrolysis [57, 58]. Control assays with mock growth supernatants showed no activity toward the tested substrates, ruling out the possibility of a contaminant chitinase activity in the cell extract of the expression host.

To assess the chitin degradation efficiency of ChiC, kinetic parameters K_M (0.4 mg/mL) and V_{max} (1207 IU/mg) were calculated for crab shell chitin under optimal conditions (pH 5, 55°C, see below). The effect of crab shell chitin concentration on ChiC activity was analyzed by hyperbolic regression of the initial velocity with substrate concentrations ranging from 0.125

281 mg/mL to 1.0 mg/mL. The enzyme exhibited high affinity towards chitin, with a corresponding
282 K_M value of 0.4 mg/mL. This demonstrates stronger affinity than that reported for homologous
283 chitinases from *Bacillus* sp. BG-11 (12 mg/mL) [59], or chitinases C1 (1.4 mg/mL) and C3 (0.8
284 mg/mL) from *Vibrio alginolyticus* [60].
285
286 *3.2 Mode of action*
287 Chitin degrading enzymes possess an active-site cleft that fits long-chain polymer
288 substrates, cleaving in a processive or non-processive manner to produce chitobiose as final
289 product. The reaction is non-processive when the enzyme-substrate complex dissociates after
290 each reaction cycle, and processive when a number of attacks can occur as the substrate remains
291 attached to the active site [38, 39, 55]. Non-processive GH18 endo-acting enzymes recognize
292 substrates at random positions within the polymer chain. Some enzymes are incapable of
293 releasing short chitooligomers, generating trimers or tetramers as final products of the reaction
294 [38, 39, 41, 61]. Processive GH18 enzymes can either bind in an endo- or exo-acting fashion.
295 Endo-acting enzymes bind at internal positions within the substrate chain, while exo-acting
296 enzymes bind and remove two sugar units at the end of each substrate polymer chain. For
297 processive exo-acting enzymes, the substrate slides along the binding pocket for the next
298 hydrolysis to occur. Since the accessibility of the enzyme to the crystalline substrate is
299 energetically demanding and recognized as the rate-limiting step of hydrolysis, this processive
300 manner is thought to be important for crystalline biomass conversion [32, 38, 39, 41, 62]. In
301 some cases, processivity may reduce enzyme efficiency and comes at a large cost in terms of
302 enzyme hydrolytic rate [61]. For non-processive enzymes, the presence of carbohydrate-binding

303 modules (CBMs) facilitates substrate binding and disruption, providing means for improving
304 enzymatic degradation of recalcitrant polysaccharides [36, 37, 63].

305 To elucidate the mode of action of ChiC and to decipher whether it acts in a non-
306 processive or processive fashion, hydrolysis profiles of crab shell chitin and chitohexaose
307 [$(GlcNAc)_6$] were investigated. Time-course hydrolysis of crab shell chitin showed that the
308 release of $(GlcNAc)_2$ gradually increases with incubation time (Figure 1A). ChiC converted
309 chitin to predominantly produce $(GlcNAc)_2$, together with small amounts of the GlcNAc
310 monomer as final product. The occurrence of odd-numbered oligomers [$(GlcNAc)_3$ and
311 $(GlcNAc)_5$] in the initial phase of the hydrolysis reaction (Figure 1B) reflects the fact that ChiC
312 acts in a non-processive fashion, as previously discussed for the *Serratia marcescens* chitinase
313 enzymes [38, 41, 55]. Similarly, the initial stage of ChiC hydrolysis toward chitohexaose
314 produces equal amounts of $(GlcNAc)_4$, $(GlcNAc)_3$, and $(GlcNAc)_2$, supporting a non-processive
315 mode of action (Figure 1C).

316 During the early stages of chitin hydrolysis (Figure 1B), the appearance of $(GlcNAc)_6$,
317 $(GlcNAc)_5$, $(GlcNAc)_4$ (hardly detected), and $(GlcNAc)_3$ was observed, suggesting that ChiC is
318 an endo-acting enzyme. In the later stage hydrolysis, the disappearance of $(GlcNAc)_6$,
319 $(GlcNAc)_5$, and $(GlcNAc)_4$ was faster than that of $(GlcNAc)_3$ (not shown). This could be
320 explained by the fact that ChiC showed higher specific activities for $(GlcNAc)_6$, $(GlcNAc)_5$ and
321 $(GlcNAc)_4$ than for $(GlcNAc)_3$ (Table 1). The same cleavage pattern was observed towards
322 insoluble β-chitin and soluble chitins (including glycol-chitin and chitooligomers), confirming
323 the non-processive, endo-acting mechanism of ChiC. With the crystalline polymer, the number
324 of endo-binding sites is much higher than the number of exo-binding sites, making endo-binding
325 a more productive mode of action for hydrolysis [62].

327 *3.3 Optimal temperature, pH and stability*

328 The influence of temperature on ChiC activity was studied by carrying out enzyme assays
329 at different temperatures. The enzyme displayed optimal temperature from 50°C to 65°C, with
330 maximal activity observed at 55°C (Figure 2A). ChiC activity was gradually decreased at
331 temperatures below 50°C, retaining less than 30% activity below 30°C. Similarly, only 25%
332 maximal activity was observed when the reaction temperature reached 70°C. In this regard, ChiC
333 is not so different from other chitinases previously characterized, such as ChiA, ChiB, ChiC
334 from *Serratia marcescens* [31], chitinase from *Bacillus* sp. Hu1 [14], BG-11 from *Bacillus* sp.
335 [59], and Chit62 from *Serratia marcescens* B4A [64], which have all been reported to be active
336 within a similar temperature range. The thermal stability of ChiC was measured by assaying
337 activity with an enzyme solution pre-incubated at temperatures ranging between 20°C and 70°C
338 for 1 h. The enzyme showed good thermal stability below 55°C, retaining more than 75% of its
339 optimal activity. However, stability decreased significantly when incubated at 60°C (48%
340 residual activity) or above, retaining only 11% optimal activity when preincubated at 70°C
341 (Figure 2A). Since ChiC showed optimal working temperature and good thermal stability at
342 55°C, the enzyme may prove useful for prolonged incubation times required in many industrial
343 GlcNAc production settings, although we suspect that enzyme immobilization would
344 considerably improve thermal stability and residual activity, in addition to allowing enzyme
345 recycling.

346 The effect of pH on ChiC activity is shown in Figure 2B. ChiC displayed good activity in
347 the range of pH 4.5 to 6, with maximum activity at pH 5. Similar pH optima were observed for
348 several chitinases, such as the chitinase from *Ralstonia* sp. A-471 [65] and those from

Streptomyces violasceusniger MTCC 3959 [18], *Aeromonas* sp. DYU-too7 [66] and *Aeromonas* sp. GJ-18 [67]. On the other hand, some chitinases show varying optimal pH working conditions, including the chitinases from *Microbispora* sp. V2 (pH 3) [68], *Bacillus* sp. Hu1 (pH 6.5) [14], *Bacillus cereus* (pH 5.8) [69], *Bacillus circulans* No.4.1 (pH 8) [36], and *Bacillus* sp. BG-11 (pH 8.5) [59]. The enzymatic activity of ChiC was remarkably vulnerable to pH variations outside the range of pH 4.5–6, and almost completely abolished at $9 \leq pH \leq 3.5$. This property indicates that ChiC is optimally active for a narrow pH range relative to other chitinases characterized. Indeed, the chitinase from *Streptomyces violasceusniger* MTCC 3959 retained roughly 80% activity between pH 3–10 [18], similar to the behavior of ChiA from *Serratia marcescens* (active between pH 4–11) [31], the chitinase from *Streptomyces erythraus* (active between pH 3–11) [70], or ChiC36 from *Bacillus cereus* 6E1 (active between pH 2.5–8) [69]. The residual activity of ChiC upon prolonged incubation in diverse pH conditions was determined by incubating the enzyme at different pH for 1 h and 5 months at 4°C (Figure 2B). ChiC showed residual pH stability for a broad range of pH values, retaining more than 75% of activity between pH 3.5–9. The residual activity of the enzyme remained ~60% when incubated at pH 3 and pH 10, but was completely lost at pH 2. The enzyme showed similar profiles after a 5-month incubation, but the residual enzyme activity was still considerably affected, retaining 60-80% activity between pH 3.5–9. In line with its optimal pH activity, ChiC showed the highest stability at pH 5.5 and was inactive when incubated at $10 \leq pH \leq 3$ for an extended period of time.

370 *3.4 Enzymatic production of GlcNAc from crab shell chitin using ChiC and ScHEX from* S.
371 coelicolor *A3(2)*

372 We recently solved the three-dimensional structure of a β-*N*-acetylhexosaminidase from
373 *S. coelicolor* A3(2) (*Sc*HEX), a glycosidase that catalyzes the glycosidic linkage hydrolysis of
374 gluco- and galacto-configured *N*-acetyl-β-D-hexosaminides [44]. The enzyme was investigated
375 for its β-*N*-acetylhexosaminidase activity, showing substantial turnover toward
376 chitooligosaccharides of varying degrees of polymerization. The final hydrolytic reaction yielded
377 pure GlcNAc without any byproduct, promising high applicability for the enzymatic production
378 of this highly valued chemical. However, *Sc*HEX was found to be inactive in presence of raw
379 substrates such as crab shell chitin, as β-*N*-acetylhexosaminidases cannot typically recognize
380 complex chitin substrates. From an industrial standpoint, a truly interesting and advantageous
381 enzymatic breakdown of raw chitin biomass would thus minimally require a combination of β-*N*-
382 acetylhexosaminidase and chitinase activities.

383 In the present study, *Sc*HEX was combined with ChiC in an assay with crab shell chitin
384 to investigate their combined efficiency in GlcNAc production. Both enzymes showed optimal
385 activity at 55°C and in the same buffer at pH 5-5.5, which is ideal for their combination in a
386 reaction mixture. The expression of ChiC and *Sc*HEX using the *S. lividans* expression system
387 secreted enzymes with ~95% purity (Figure S1), while the background cell supernatant showed
388 no chitinase or β-*N*-acetylhexosaminidase activity (as tested from a mock *S. lividans* growth
389 assay). As a result, 10-fold concentrated *Sc*HEX and ChiC supernatants were used to investigate
390 GlcNAc production. Furthermore, as we recently reported, the *Sc*HEX supernatant exhibited
391 higher hydrolytic activity than purified *Sc*HEX [44], allowing one to use crude enzyme

392 supernatants without further purification, saving time and reducing costs for the potential
393 industrial production of GlcNAc.

394 To examine the effect of *Sc*HEX on chitin hydrolysis by ChiC, both enzymes were either
395 added to the mixture at the beginning of the reaction, or *Sc*HEX was added when the rate of
396 conversion of chitin to $(GlcNAc)_2$ by ChiC reached saturation. At specific time intervals,
397 aliquots of the reaction mixture were isolated to calculate GlcNAc production yields. The results
398 showed that the concentration of GlcNAc accumulated faster and at higher concentrations when
399 both enzymes were added simultaneously, suggesting that no inhibition occurred, either by
400 *Sc*HEX or by the reaction product (Figure S2). Consequently, both ChiC and *Sc*HEX were added
401 in tandem for further investigation. The concentration ratio of each enzyme in the reaction
402 mixture is an important factor contributing to the synergistic activity of each glycosidase in
403 chitin hydrolysis [20, 71]. To investigate the effect of this ratio in GlcNAc production, enzyme
404 assays with 0.5 mg/mL crab shell chitin were performed with various ratios of concentrated
405 ChiC and *Sc*HEX. The synergy between ChiC and *Sc*HEX revealed that the highest yield in
406 GlcNAc production was obtained for a 50% (w/w) ratio between ChiC and *Sc*HEX (Figure 3A).
407 Using this enzyme ratio, we evaluated the production efficiency and GlcNAc purity using 10-
408 fold concentrated supernatants of ChiC and *Sc*HEX in presence of crab shell chitin. The maximal
409 GlcNAc production was observed after 8 h of incubation with 1 mg/mL of each enzyme, yielding
410 90% pure GlcNAc (Figure 3B). When assessing product purity by HPLC, the main by-product
411 was $(GlcNAc)_2$ (2.2%), while the concentrations of $(GlcNAc)_4$ and $(GlcNAc)_5$ were negligible
412 (below 0.5%) (Figure 4). No other chitooligomer was observed after an 8-h incubation period,
413 indicating substantial purity and significant yield improvements relative to previous studies
414 reporting on the biocatalytic production of GlcNAc (Table 2). Indeed, most reports describe

maximal GlcNAc production yields of 41-85% with incubation periods ranging between 1 to 19 days, demonstrating that the combination of ChiC and ScHEX from *S. coelicolor* A3(2) is an efficient enzymatic mixture for GlcNAc production from a crude chitin substrate.

Table 2. Comparative reaction efficiency in enzymatic GlcNAc production

Enzyme	Organism	α-chitin conc. (mg/mL)	GlcNAc yield (%)	Time consumed	Reference
Crude enzymes	*Penicillium monoverticillium* CFR, *Aspergillus flavus* CFR 10 and *Fusarium oxysporum* CFR	10	78 - 80	48 h	Suresh *et al.* 2012 [1
Crude enzymes	*Paenibacillus illioisensis* KJA-424	2.5	62.2	24 h	Jung *et al.*2007 [72]
Crude enzymes	*Aeromonas sp. GJ-18*	14	83	5 days	Kuk *et al.* 2005[67]
Crude enzymes	*Burkholderia cepacia* TU09,	3.3	85	7 days	Pichyangkura *et al.* 2002
Crude enzymes	*Bacillus licheniformis* SK-1	10	41	6 days	
Crude cellulases	*Trichoderma viride* and *Acremonium cellulolyticus*	10	74	19 days	Sashiwa *et al.* 2003 [2
Crude enzymes	*Aeromonas hydrophylas* H2330	5	77	10 days	Sashiwa *et al.* 2002 [1
Crude enzymes	*Aeromonas* sp. PTCC	10	79	24 h	Jamialahmadi *et al.* 2011
Crude enzymes	*Streptomyces coelicolor* A3(2) ChiC and *Sc*HEX	10	90	8 h	This study

4. Conclusion

In the present work, we found that ChiC from *S. coelicolor* A3(2) can efficiently hydrolyze crystalline α-chitin, β-chitin, and chitooligosaccharides to yield $(GlcNAc)_2$ as final product. The enzyme is an endo-acting, non-processive biocatalyst expressed in high yields and displaying high stability, in addition to showing similar substrate specificity toward α- and β-chitin. Since α-chitin is readily available and wildly dispersed in nature relative to β-chitin, this result favorably contrasts with the majority of other β-chitin-specific chitinases previously characterized. The *S. lividans* expression system we developed is advantageous from an

industrial standpoint due to the possibility of using ChiC obtained straight from the growth supernatant, preventing the need for further protein purification. Combining ChiC with *Sc*HEX in a 50% mixture (w/w) of crude supernatant expression allows the degradation of chitin substrates to yield GlcNAc with significantly higher efficiency and improved product purity relative to previous reports, promising a practical and effective procedure for the enzymatic breakdown of raw chitin biomass.

Competing Interests

The authors declare that they have no conflict of interest.

Acknowledgements

The authors thank François Shareck (INRS) for providing the original pC109-*chiC* construct. This work was supported by a Natural Sciences and Engineering Research Council of Canada (NSERC) Discovery grant (RGPIN 402623-2011) (to N.D.). N.D. holds a FRQS Research Scholar Junior 1 Career Award.

Appendix A. Supplementary data

Supplementary data associated with this article is provided as Appendix A.

450 **Figure Legends**

451

452 **Figure 1.** Time-course hydrolysis of crab shell chitin and chitohexaose by ChiC. A) HPLC
453 chromatogram showing acid-quenched reactions after 0, 10, 15, 20, 30, 60 and 120 minutes of
454 ChiC incubation with crab shell chitin. Enzyme assays were performed with 50 µg/mL ChiC, 5
455 mg/mL crab shell chitin in 50 mM phosphate buffer containing 150 mM NaCl. B) and C)
456 Product formation during ChiC degradation of crab shell chitin (B) and $(GlcNAc)_6$ (C).
457 Reactions were performed with 5 µg/mL ChiC and 5 mg/mL substrate in the same reaction
458 buffer. Retention times were compared to known chitooligosaccharide standards: III, $(GlcNAc)_3$;
459 II, $(GlcNAc)_2$; I, (GlcNAc); HPr, propionic acid normalization standard. The H_2SO_4 peak from
460 the HPLC mobile phase is hidden for clarity (retention time: 6.8 min). Product concentrations
461 were calculated from HPLC chromatograms, as described in Materials and Methods. Legend:
462 Blue diamonds (♦), $(GlcNAc)_6$; Purple stars (*), $(GlcNAc)_5$; Olive green squares (■), $(GlcNAc)_4$;
463 Green triangles (▲), $(GlcNAc)_3$; Red crosses (+), $(GlcNAc)_2$; Orange circles (●), GlcNAc.

464

465 **Figure 2.** Effect of temperature and pH on ChiC activity and stability. A) Effect of temperature
466 on ChiC activity and stability, showing relative activity as a function of temperature (triangles,
467 solid line). Enzyme activity is expressed relative to the optimal activity observed at 55°C.
468 Residual activity is shown after a 1-hour enzyme preincubation at different temperatures
469 (squares, dashed line). Activities are calculated relative to a control enzyme kept at 4°C. B)
470 Effect of pH on ChiC activity and stability. Relative activity is shown as a function of pH
471 (circles, solid line). Enzyme activities are expressed relative to the optimal activity observed at
472 pH 5. Residual activity is shown after enzyme preincubation at various pH (dashed line) for 1

473 hour (black squares) and 5 months (gray triangles). Activities are compared to a control enzyme
474 incubated in water at 4°C. See Materials and Methods for detailed procedures.
475
476 **Figure 3.** Synergistic production of GlcNAc by ChiC and *Sc*HEX. A) Degradation of crystalline
477 α-chitin by combination mixtures of ChiC and *Sc*HEX. The enzymes were mixed in such a way
478 that the total enzyme concentration (w/w) equals 80 µg/mL. The mixture was then added to a 0.5
479 mg/mL chitin solution in optimal conditions for 4 h. B) Production of GlcNAc by a 50% (w/w)
480 ratio of ChiC and *Sc*HEX. The ChiC and *Sc*HEX mixture was incubated with crab shell chitin
481 (10 mg/mL) at 55°C, pH 5 for 24 h. See Materials and Methods for detailed procedures.
482
483 **Figure 4.** HPLC chromatograms of crab shell chitin hydrolysates after an 8-h incubation period
484 with a concentrated supernatant of ChiC-*Sc*HEX mixture (50% w/w). Retention times are
485 compared to known chitooligosaccharide standards: VI, $(GlcNAc)_6$; V, $(GlcNAc)_5$; IV,
486 $(GlcNAc)_4$; III, $(GlcNAc)_3$; II, $(GlcNAc)_2$; I, (GlcNAc); HPr, propionic acid normalization
487 standard; H_2SO_4, sulfuric acid from mobile phase.
488
489

490 **References**

491 [1] Cohen E. Chitin polymerization and degradation as targets for pesticide action. Arch Insect
492 Biochem Physiol. 1993;22:245-61.
493 [2] Oliveira E, El Gueddari, N., Moerschbacher, B., Peter, M., and Franco, T. Growth of
494 phytopathogenic fungi in the presence of partially acetylated chitooligosaccharides.
495 Mycopathologia. 2008;166:163-74.
496 [3] Sakuda S, Isogai, A., Matsumoto, S., and Suzuki, A. Search for microbial insect growth
497 regulators. II. Allosamidin, a novel insect chitinase inhibitor. J Antibiot. 1987;40:296-300.
498 [4] Vinetz JM, Valenzuela, J. G., Specht, C. A., Aravind, L., Langer, R. C., Ribeiro, J. M. C.,
499 and Kaslow, D. C. Chitinases of the avian malaria parasite *Plasmodium gallinaceum*, a class of
500 enzymes necessary for parasite invasion of the mosquito midgut. J Biol Chem. 2000;275:10331-
501 41.
502 [5] Aam BB, Heggset EB, Norberg AL, Sorlie M, Varum KM, Eijsink VG. Production of
503 chitooligosaccharides and their potential applications in medicine. Mar Drugs. 2010;8:1482-517.
504 [6] Chen JK, Shen CR, Liu CL. N-Acetylglucosamine: production and applications. Mar Drugs.
505 2010;8:2493-516.
506 [7] Howard MB, Ekborg NA, Weiner RM, Hutcheson SW. Detection and characterization of
507 chitinases and other chitin-modifying enzymes. J Ind Microbiol Biotechnol. 2003;30:627-35.
508 [8] Talent JM, Gracy RW. Pilot study of oral polymeric *N*-acetyl-D-glucosamine as a potential
509 treatment for patients with osteoarthritis. Clin Ther. 1996;18:1184-90.
510 [9] Salvatore S, Heuschkel R, Tomlin S, Davies SE, Walker-Smith JA, French I, et al. Pilot study
511 of *N*-acetyl glucosamine, a nutritional substrate for glycosaminoglycan synthesis, in paediatric
512 chronic inflammatory bowel disease. Pharmacol Ther. 2000; 14:1567-79.

513 [10] Morley KL, Chauve G, Kazlauskas R, Dupont C, Shareck F, Marchessault RH. Acetyl xylan
514 esterase-catalyzed deacetylation of chitin and chitosan. Carbohydr Polym. 2006;63:310-5.
515 [11] Tharanathan RN, Kittur FS. Chitin-the undisputed biomolecule of great potential. Crit Rev
516 Food Sci Nutr. 2003;43:61-87.
517 [12] Kurita K. Chitin and chitosan: functional biopolymers from marine crustaceans. Mar
518 Biotechnol. 2006;8:203-26.
519 [13] Cohen E. Chitin biochemistry: synthesis, hydrolysis and inhibition. Adv Insect Physiol.
520 2010;38:5-74.
521 [14] Dai DH, Hu WL, Huang GR, Li W. Purification and characterization of a novel
522 extracellular chitinase from thermophilic *Bacillus* sp. Hu1. African J Biotechnol. 2011;10:2476-
523 85.
524 [15] Jeraj N, Kunic B, Lenasi H, Breskvar K. Purification and molecular characterization of
525 chitin deacetylase from *Rhizopus nigricans.* Enzyme Microb Technol. 2006;39:1294-9.
526 [16] Sashiwa H, Fujishima S, Yamano N, Kawasaki N, Nakayama A, Muraki E, et al. Production
527 of *N*-Acetyl-D-glucosamine from α-chitin by crude enzymes from *Aeromonas hydrophila*
528 H2330. Carbohydr Res. 2002;337:761-3.
529 [17] Pichyangkura R, Kudan S, Kuttiyawang K, Sukwattanasinitt M, Aiba S. Quantitative
530 production of 2-Acetoamodo-2-D-glucose from crystalline chitin by bacterial chitinase.
531 Carbohydr Res. 2002;337:557-9.
532 [18] Nagpure A, Gupta RK. Purification and characterization of an extracellular chitinase from
533 antagonistic *Streptomyces violaceusniger.* J Basic Microbiol. 2013;53:429-39.

534 [19] Suresh PV. Biodegradation of shrimp processing bio-waste and concomitant production of
535 chitinase enzyme and *N*-acetyl-D-glucosamine by marine bacteria: production and process
536 optimization. World J Microbiol Biotechnol. 2012;28:2945-62.
537 [20] Sashiwa H, Fujishima S, Yamano N, Kawasaki N, Nakayama A, Muraki E, et al. Enzymatic
538 production of *N*-acetyl-D-glucosamine from chitin. Degradation study of *N*-
539 acetylchitooligosaccharide and the effect of mixing of crude enzymes. Carbohydr Polym.
540 2003;51:391-5.
541 [21] Jamialahmadi K, Behravan J, Fathi Najafi M, Tabatabai Yazdi M, Shahverdi AR, Faramarzi
542 MA. Enzymatic production of *N*-Acetyl-D-Glucosamine from chitin using crude enzyme
543 preparation of *Aeromonas* sp. PTCC1691. Biotechnology. 2011;10:292-7.
544 [22] Cohen-Kupiec R, Chet I. The molecular biology of chitin digestion. Curr Opin Biotechnol.
545 1998;9:270-7.
546 [23] Horsch M, Mayer C, Sennhauser U, Rast DM. β-*N*-acetylhexosaminidase: a target for the
547 design of antifungal drugs. Pharmacol Ther. 1997;76:187-218.
548 [24] Seidl V. Chitinases of filamentous fungi: a large group of diverse proteins with multiple
549 physiological functions. Fungal Biol Rev. 2008;22:36-42.
550 [25] Bentley SD, Chater KF, Cerdeno-Tarraga AM, Challis GL, Thomson NR, James KD, et al.
551 Complete genome sequence of the model actinomycete *Streptomyces coelicolor* A3(2). Nature.
552 2002;417:141-7.
553 [26] Saito A, Ishizaka M, Francisco PB, Jr., Fujii T, Miyashita K. Transcriptional co-regulation
554 of five chitinase genes scattered on the *Streptomyces coelicolor* A3(2) chromosome.
555 Microbiology. 2000;146:2937-46.

[27] Redenbach M, Kieser, H. M., Denapaite, D., Eichner, A., Cullum, J., Kinashi, H. & Hopwood, D. A. A set of ordered cosmids and a detailed genetic and physical map for the 8 Mb *Streptomyces coelicolor* A3(2) chromosome. Mol Microbiol. 1996;21:77-96.

[28] Saito A, Fujii T, Yoneyama T, Redenbach M, Ohno T, Watanabe T, et al. High-multiplicity of chitinase genes in *Streptomyces coelicolor* A3(2). Biosci Biotechnol Biochem. 1999;63:710-8.

[29] Robbins PW, Overbye K, Albright C, Benfield B, Pero J. Cloning and high-level expression of chitinase-encoding gene of Streptomyces plicatus. Gene. 1992;111:69-76.

[30] Fujii T, Miyashita K. Multiple domain structure in a chitinase gene (chiC) of Streptomyces lividans. J Gen Microbiol. 1993;139:677-86.

[31] Suzuki K, Sugawara N, Suzuki M, Uchiyama T, Katouno F, Nikaidou N, et al. Chitinases A, B, and C1 of *Serratia marcescens* 2170 produced by recombinant *Escherichia coli*: enzymatic properties and synergism on chitin degradation. Biosci Biotechnol Biochem. 2002;66:1075-83.

[32] Davies G, Henrissat B. Structures and mechanisms of glycosyl hydrolases. Structure. 1995;3:853-9.

[33] Andersen OA, Dixon MJ, Eggleston IM, van Aalten DM. Natural product family 18 chitinase inhibitors. Nat Prod Rep. 2005;22:563-79.

[34] Hoell IA, Klemsdal SS, Vaaje-Kolstad G, Horn SJ, Eijsink VG. Overexpression and characterization of a novel chitinase from *Trichoderma atroviride* strain P1. Biochim Biophys Acta. 2005;1748:180-90.

[35] Tronsmo A, Harman GE. Detection and quantification of *N*-acetyl-beta-D-glucosaminidase, chitobiosidase, and endochitinase in solutions and on gels. Anal Biochem. 1993;208:74-9.

577 [36] Watanabe T, Ito Y, Yamada T, Hashimoto M, Sekine S, Tanaka H. The roles of the C-
578 terminal domain and type III domains of chitinase A1 from *Bacillus circulans* WL-12 in chitin
579 degradation. J Bacteriol. 1994;176:4465-72.
580 [37] Suzuki K, Taiyoji M, Sugawara N, Nikaidou N, Henrissat B, Watanabe T. The third
581 chitinase gene (chiC) of *Serratia marcescens* 2170 and the relationship of its product to other
582 bacterial chitinases. Biochem J. 1999;343:587-96.
583 [38] Horn SJ, Sorbotten A, Synstad B, Sikorski P, Sorlie M, Varum KM, et al. Endo/exo
584 mechanism and processivity of family 18 chitinases produced by *Serratia marcescens*. FEBS J.
585 2006;273:491-503.
586 [39] Hult EL, Katouno F, Uchiyama T, Watanabe T, Sugiyama J. Molecular directionality in
587 crystalline beta-chitin: hydrolysis by chitinases A and B from *Serratia marcescens*. Biochem J.
588 2005;388:851-6.
589 [40] von Ossowski I, Stahlberg J, Koivula A, Piens K, Becker D, Boer H, et al. Engineering the
590 exo-loop of *Trichoderma reesei cellobiohydrolase*, Cel7A. A comparison with *Phanerochaete*
591 *chrysosporium* Cel7D. J Mol Biol. 2003;333:817-29.
592 [41] Sikorski P, Sorbotten A, Horn SJ, Eijsink VG, Varum KM. *Serratia marcescens* chitinases
593 with tunnel-shaped substrate-binding grooves show endo activity and different degrees of
594 processivity during enzymatic hydrolysis of chitosan. Biochemistry. 2006;45:9566-74.
595 [42] Saito A, Shinya T, Miyamoto K, Yokoyama T, Kaku H, Minami E, et al. The *dasABC* gene
596 cluster, adjacent to *dasR*, encodes a novel ABC transporter for the uptake of *N*,*N*,-
597 diacetylchitobiose in *Streptomyces coelicolor* A3(2). Appl Environ Microbiol. 2007;73:3000-8.
598 [43] Saito A, Fujii T, Shinya T, Shibuya N, Ando A, Miyashita K. The *msiK* gene, encoding the
599 ATP-hydrolysing component of *N*,*N*'-diacetylchitobiose ABC transporters, is essential for

induction of chitinase production in *Streptomyces coelicolor* A3(2). Microbiology. 2008;154:3358-65.

[44] Thi NN, Offen WA, Shareck F, Davies GJ, Doucet N. Structure and activity of the *Streptomyces coelicolor* A3(2) beta-*N*-acetylhexosaminidase provides further insight into GH20 family catalysis and inhibition. Biochemistry. 2014;53:1789-800.

[45] Hurtubise Y, Shareck F, Kluepfel D, Morosoli R. A cellulase/xylanase-negative mutant of *Streptomyces lividans* 1326 defective in cellobiose and xylobiose uptake is mutated in a gene encoding a protein homologous to ATP-binding proteins. Mol Microbiol. 1995;17:367-77.

[46] Gutierrez-Roman MI, Dunn MF, Tinoco-Valencia R, Holguin-Melendez F, Huerta-Palacios G, Guillen-Navarro K. Potentiation of the synergistic activities of chitinases ChiA, ChiB and ChiC from Serratia marcescens CFFSUR-B2 by chitobiase (Chb) and chitin binding protein (CBP). World J Microbiol Biotechnol. 2014;30:33-42.

[47] Robbins PW, Albright C, Benfield B. Cloning and expression of a Streptomyces plicatus chitinase (chitinase-63) in Escherichia coli. J Biol Chem. 1988;263:443-7.

[48] Saito A, Miyashita K, Biukovic G, Schrempf H. Characteristics of a *Streptomyces coelicolor* A3(2) extracellular protein targeting chitin and chitosan. Appl Environ Microbiol. 2001;67:1268-73.

[49] Hoell IA, Dalhus B, Heggset EB, Aspmo SI, Eijsink VGH. Crystal structure and enzymatic properties of a bacterial family 19 chitinase reveal differences from plant enzymes. FEBS J. 2006;273:4889-900.

[50] Sashiwa H, Fujishima S, Yamano N, Kawasaki N, Nakayama A, Muraki E, et al. Production of *N*-acetyl-D-glucosamine from beta-chitin by enzymatic hydrolysis. Chem Lett. 2001:308-9.

622 [51] Tews I, Perrakis A, Oppenheim A, Dauter Z, Wilson KS, Vorgias CE. Bacterial chitobiose
623 structure provides insights into catalytic mechanism and the basic of Tay-Sachs disease. Nat
624 Struct Biol. 1996;3.
625 [52] Mark BL, Vocadlo, D. J., Knapp, S., Triggs-Raine, B. L., Withers, S. G., James, M. N.
626 Crystallographic evidence for substrate-assisted catalysis in a bacterial beta-hexosaminidase. J
627 Biol Chem Commun (Camb). 2001;276:10330-7.
628 [53] Williams S. J. MBL, Vocadlo D. J., James M. N. G., and Withers S. G. Aspartate 313 in the
629 *Streptomyces plicatus* hexosaminidase plays a critical role in substrate-assisted catalysis by
630 orienting the 2-acetamido group and stabilizing the transition state. J Biol Chem.
631 2002;277:40055-65.
632 [54] Bokma E, van Koningsveld GA, Jeronimus-Stratingh M, Beintema JJ. Hevamine, a
633 chitinase from the rubber tree *Hevea brasiliensis*, cleaves peptidoglycan between the C-1 of *N*-
634 acetylglucosamine and C-4 of *N*-acetylmuramic acid and therefore is not a lysozyme. FEBS
635 Lett.411:161-3.
636 [55] Sørbotten A, Horn SJ, Eijsink VG, Varum KM. Degradation of chitosans with chitinase B
637 from *Serratia marcescens*: Production of chito-oligosaccharides and insight into enzyme
638 processivity. FEBS J. 2005;272:538-49.
639 [56] Zakariassen H, Aam BB, Horn SJ, Varum KM, Sorlie M, Eijsink VG. Aromatic residues in
640 the catalytic center of chitinase A from *Serratia marcescens* affect processivity, enzyme activity,
641 and biomass converting efficiency. J Biol Chem. 2009;284:10610-7.
642 [57] van Aalten DM, Komander D, Synstad B, Gaseidnes S, Peter MG, Eijsink VG. Structural
643 insights into the catalytic mechanism of a family 18 exo-chitinase. Proc Natl Acad Sci USA.
644 2001;98: 8979-84.

645 [58] van Aalten DM, Synstad B, Brurberg MB, Hough E, Riise BW, Eijsink VG, et al. Structure
646 of a two-domain chitotriosidase from *Serratia marcescens* at 1.9-angstrom resolution. Proc Natl
647 Acad Sci USA. 2000;97:5842-7.
648 [59] Bhushan B. Production and characterization of a thermostable chitinase from a new
649 alkalophilic *Bacillus* sp. BG-11. J Appl Microbiol. 2000;88:800-8.
650 [60] Ohishi K, Yamagishi, M., Ohta, T. Purification and properties of two chitinases from *Vibrio*
651 *alginolyticus* H-8. J Ferment Bioengin. 1996;82:598-600.
652 [61] Horn SJ, Sikorski P, Cederkvist JB, Vaaje-Kolstad G, Sørlie M, Synstad B, et al. Costs and
653 benefits of processivity in enzymatic degradation of recalcitrant polysaccharides. Proc Natl Acad
654 Sci USA. 2006;103:18089-94.
655 [62] Norberg AL, Dybvik AI, Zakariassen H, Mormann M, Peter-Katalinic J, Eijsink VG, et al.
656 Substrate positioning in chitinase A, a processive chito-biohydrolase from *Serratia marcescens*.
657 FEBS Lett. 2011;585:2339-44.
658 [63] Vaaje-Kolstad G, Horn SJ, Van Aalten DMF, Synstad B, Eijsink VG. The non-catalytic
659 chitin-binding protein CBP21 from *Serratia marcescens* is essential for chitin degradation. J Biol
660 Chem. 2005;280:28492-7.
661 [64] Babashpour S, Aminzadeh S, Farrokhi N, Karkhane A, Haghbeen K. Characterization of a
662 chitinase (Chit62) from *Serratia marcescens* B4A and its efficacy as a bioshield against plant
663 fungal pathogens. Biochem Genet. 2012;50:722-35.
664 [65] Mitsuhiro U, Yukiko K, Aji S, Masami N, Kazutaka M. Purification and characterization of
665 chitinase B from moderately thermophilic bacterium *Ralstonia* sp. A-471. Biosci Biotechnol
666 Biochem. 2005;69:842-4.

667 [66] Lien TS, Yu ST, Wu ST, Too JR. Induction and purification of a thermophilic chitinase
668 produced by *Aeromonas* sp. DYU-Too7 using glucosamine. Biotechnol Bioproc Eng.
669 2007;12:610-7.
670 [67] Kuk JH, Jung WJ, Jo GH, Kim YC, Kim KY, Park RD. Production of *N*-acetyl-beta-D-
671 glucosamine from chitin by *Aeromonas* sp. GJ-18 crude enzyme. Appl Microbiol Biotechnol.
672 2005;68:384-9.
673 [68] Nawani NN, Kapadnis BP, Das AD, Rao AS, Mahajan SK. Purification and characterization
674 of a thermophilic and acidophilic chitinase from *Microbispora* sp. V2. J Appl Microbiol.
675 2002;93:965-75.
676 [69] Wang SY, Moyne AL, Thottappilly G, Wu SJ, Locy RD, Singh NK. Purification and
677 characterization of a *Bacillus cereus* exochitinase. Enzyme Microb Technol. 2001;28:492-8.
678 [70] Hara S, Yamamura Y, Fujii Y, Mega T, Ikenaka T. Purification and characterization of
679 chitinase produced by *Streptomyces erythraeus*. J Biochem. 1989; 105:484-9.
680 [71] Sukwattanasinitt M, Zhu H, Sashiwa H, Aiba S. Utilization of commercial non-chitinase
681 enzymes from fungi for preparation of 2-acetamido-2-deoxy-D-glucose from b-chitin. Carbohydr
682 Res. 2002;337:133-7.
683 [72] Jung WJ, Souleimanov A, Park RD, Smith DL. Enzymatic production of *N*-acetyl
684 chitooligosaccharides by crude enzyme derived from *Paenibacillus illioisensis* KJA-424.
685 Carbohydr Polym. 2007;67:256-9.

Figure 1

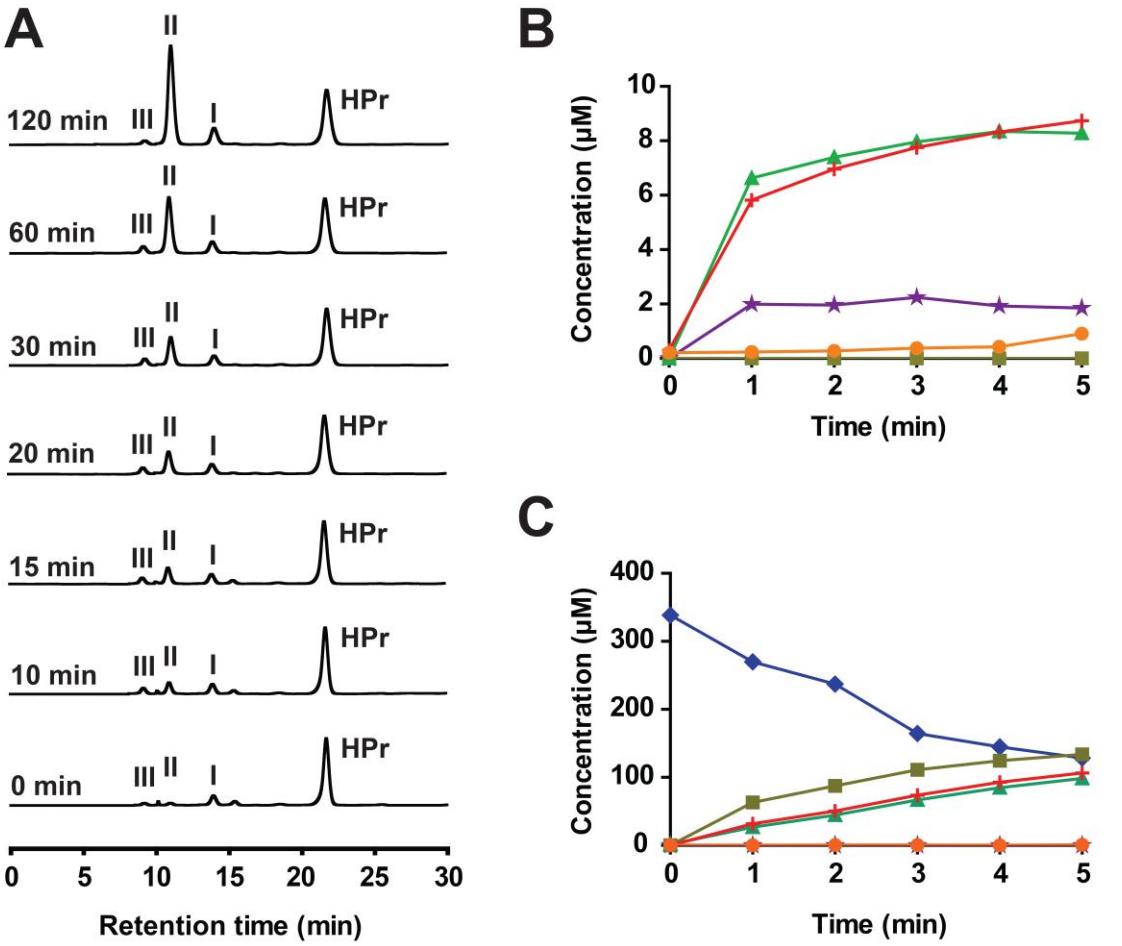

Figure 2

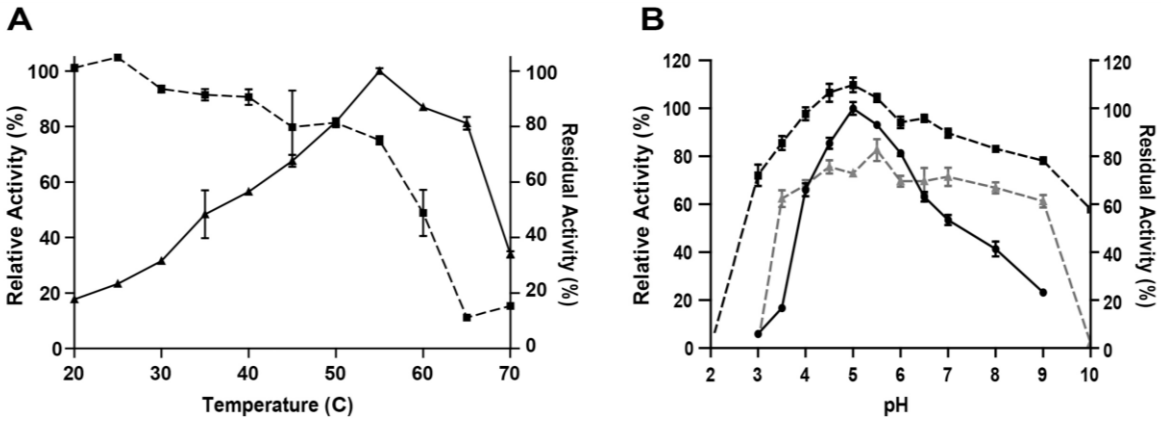

Figure 3

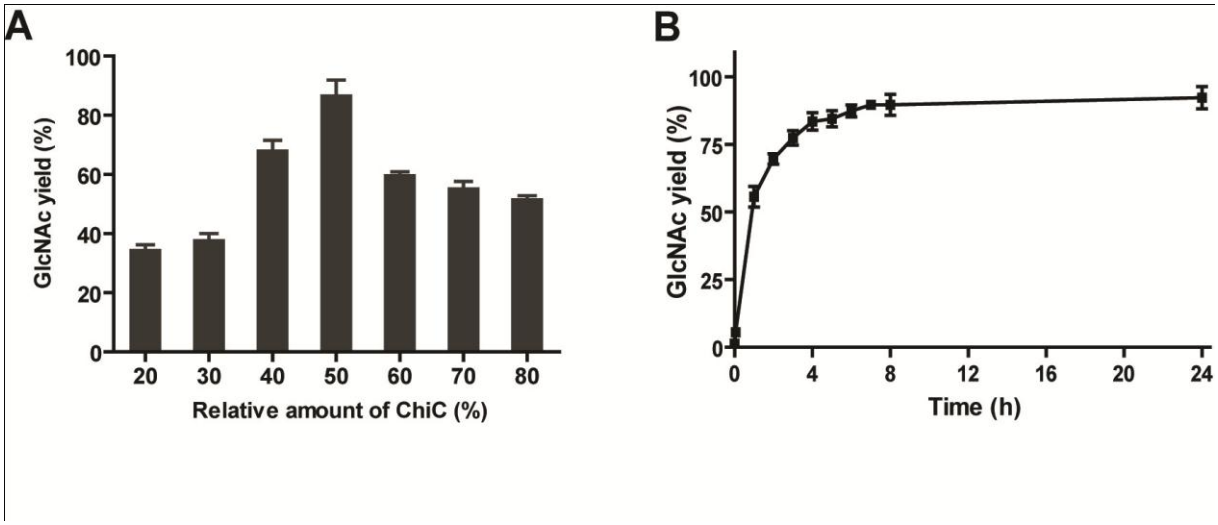

Figure 4

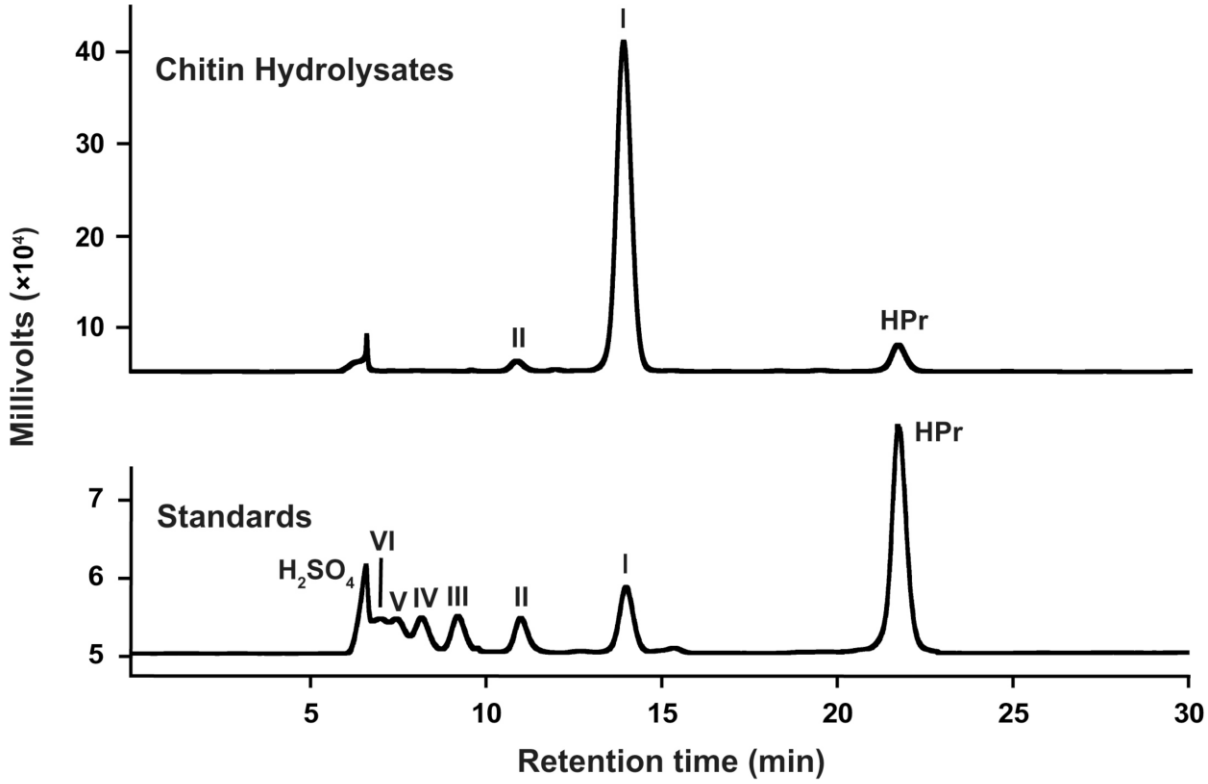

Appendix A - Supporting Information for:

Characterization of chitinase C from *Streptomyces coelicolor* A3(2) and its application in *N*-acetylglucosamine production

Nhung Nguyen-Thi[1,2,3] *& Nicolas Doucet*[1,4,5,#]

[1]INRS-Institut Armand-Frappier, Université du Québec, 531 Boul. des Prairies, Laval, Québec, H7V 1B7, Canada.

[2]Institute of Military Science and Technology, 17 Hoang Sam, Hanoi, Vietnam.

[3]Vietnam Academy of Science and Technology, 18 Hoang Quoc Viet, Hanoi, Vietnam.

[4]PROTEO, the Québec Network for Research on Protein Function, Structure, and Engineering, 1045 Avenue de la Médecine, Université Laval, Québec, Québec, G1V 0A6, Canada.

[5]GRASP, the Groupe de Recherche Axé sur la Structure des Protéines, 3649 Promenade Sir William Osler, McGill University, Montréal, Québec, H3G 0B1, Canada.

Address correspondence to Nicolas Doucet: nicolas.doucet@iaf.inrs.ca

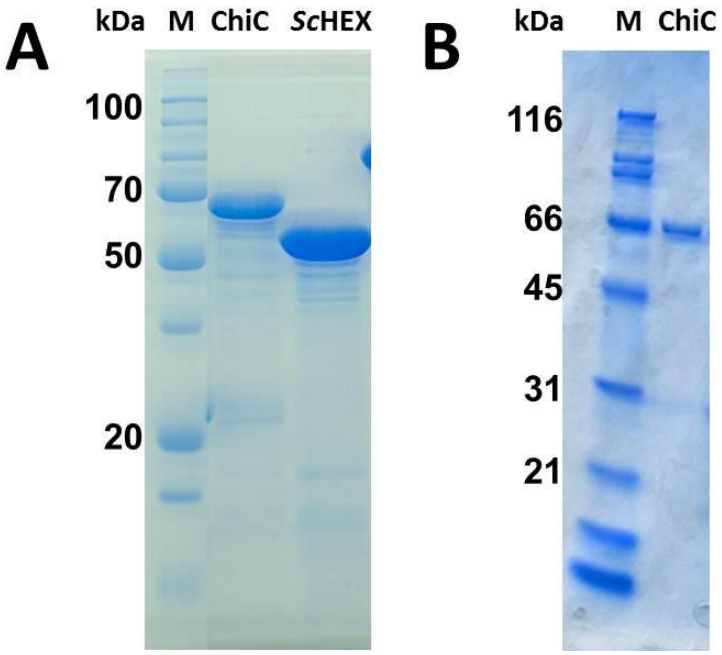

Figure S1. Expression and purification of ChiC. A) SDS-PAGE of supernatant of ChiC and *Sc*HEX from *S. coelicolor A3(2)*. M, Bio-Rad All-blue molecular weight standard; ChiC, ChiC supernatant; ScHEX, ScHEX supernatant; B, SDS-PAGE of ChiC after purification. M, Bio-Rad Low Range molecular weight standard; ChiC, ChiC purified to homogeneity after size exclusion chromatography.

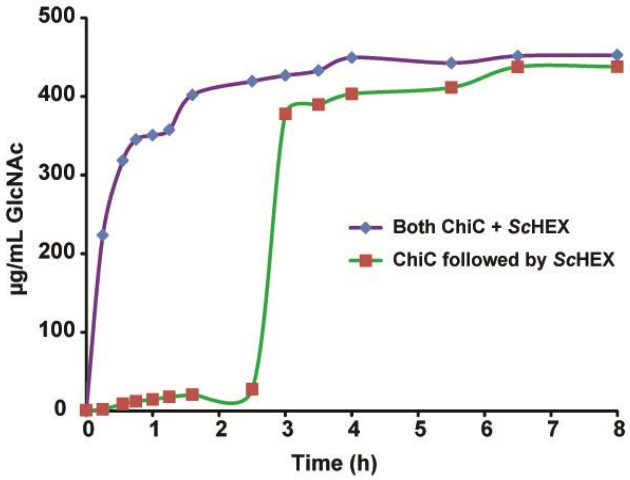

Figure S2. Effect of *Sc*HEX on chitin hydrolysis by ChiC. The ChiC and *Sc*HEX (each 10 µg/mL) were incubated with crab shell chitin (0.5 mg/mL) at 55°C, pH 5 for 8 h. Blue diamond, solid purple line, both enzymes were added at the beginning of the reaction; Red square, green solid line, ChiC was first added at the beginning of the reaction and *Sc*HEX was added after 2.5 hours when $(GlcNAc)_2$ released by ChiC reached saturation.

2.4. Discussion

To this day, the development of an environmentally friendly method for fast and large-scale production of bioactive compounds such as chitooligosaccharides and GlcNAc remains an urgent need for the industry. For the industrial production of GlcNAc, many environmentally friendly enzymatic processes have been developed and gained a certain efficiency, however, with low product purity and productivity (*2*). For instance, crude enzymes derived from *Aeromonas hydrophila* H2330 can produce GlcNAc from chitin with a yield of up to 77% in 10 days (*48*). This process yielded almost pure GlcNAc with high yield but with low productivity. Another enzymatic process for raw chitin hydrolysis produces large amounts of GlcNAc (up to 78 g/L/h) with no environmental release, thus ensuring economic and environmental viability of the technique (*9*). However, the final product was often GlcNAc contaminated with $(GlcNAc)_2$ and various oligomers whose elimination is essential and requires energy and costly steps. From an application standpoint, ChiC and *Sc*HEX is a truly advantageous enzymatic mixture for obtaining high GlcNAc yields with extremely high purity and low costs owing to the use of crude enzymes without purification steps. ChiC itself can be applied in the production of chitoologomers, which are bioactive compounds that have high value in medicine, cosmetic and other applications (*206*). Moreover, enzymatic hydrolysis of chitin sometimes requires a chemical or physical pre-treatment step to disrupt the resistant structure and to increase substrate accessibility (*17, 206, 207*). In the case of ChiC and *Sc*HEX, the substrate for the hydrolysis of the mixture was raw chitin, which was not pretreated, to form colloidal chitin, proving the robustness of the enzymes in the hydrolysis. Furthermore, for industrial applications, a large amount of pure enzymes is required. ChiC and *Sc*HEX were produced with a high yield and purity, thereby, meeting the requirements.

Besides, for an effective conversion of long saccharides, it is known that the processivity of catalytic enzymes taking part in the process is crucial. However, in some cases, processivity may reduce enzyme efficiency and comes at a large cost in terms of enzyme speed (*29, 110*). Therefore, developing a comprehensive kinetic description as well as a mechanism of chitinolytic enzymes is important to our understanding of processivity in biomass conversion, which could provide the means for the design of enhanced enzyme

mixtures for biomass conversion. In fact, information obtained from processivity of chitinase research can be useful and can be applied to secondary generation of bioethanol, a biodegradable and nonpolluting fuel that can replace exhaustible fossil resources (*12*). So far, many enzymes have been investigated for their good activity toward long polymers displaying a processive mode of action. Only a few nonprocessive enzymes were found and showed good activity in polysaccharide bioconversion. From the results shown in the two articles presented in this chapter, ChiC and *Sc*HEX have been shown as a highly active complex for chitin degradation. ChiC demonstrates nonprocessive properties and is an effective enzyme. These results supplement the lack of information regarding nonprocessive family 18 chitinases. It has been suggested that processivity is necessary and beneficial for interacting with insoluble substrates. Nevertheless, towards soluble polymers, nonprocessivity is better regarding enzyme speed (*13, 29*). Concerning the nonprocessive ChiC, the enzyme displays a significant activity towards insoluble chitin, suggesting that processivity is not likely the most essential mechanism for degrading insoluble substrates. In contrast, *Sc*HEX, an excellent enzyme for chitooligosaccharides, presents some properties that are hallmarks for processivity, which could be advantageous to its significant activity towards the soluble oligomers. Previous studies suggest that processive enzymes show a greater number of aromatic residues interacting with polymeric substrates than that of nonprocesssive enzymes (*13, 29, 71, 110*). The complex structures of *Sc*HEX with ligands reveal an active site with multiple subsites packed with four Trp (Trp332, Trp349, Trp396, Trp430), providing a tightly hydrophobic environment for holding the long substrate. The *Sc*HEX active site also contains two conserved residues, Val 287 and Trp437, which have been shown to play an essential role for the binding of long and linear chained substrates in other GH20 homologs (*133*). Compared to other bacterial chitinolytic HEXs (such as SpHex from *S. plicatus* or SmCHB from *S. marcescens* (*119, 125*)), *Sc*HEX reveals the same deep substrate-binding pocket. This deep active site architecture of *Sc*HEX is also suitable for holding polysaccharide chains and is important for keeping the enzyme attached to the substrate once bound. Collectively, from these features of ChiC and *Sc*HEX, it seems that processivity is neither the most effective way for insoluble substrate degradation nor an obstacle to enzyme speed when acting on soluble oligomers.

For further clarification, some other useful information could be obtained to provide more insight for investigating biomass degradation. The significant points presented below are about the importance of synergistic interactions, substrate-binding domain in chitin degradation and the contribution of enzyme flexibility for efficiently degrading the polymer.

2.4.1. Synergistic interactions and importance of the substrate-binding domain

In the enzymatic conversion of biomass polysaccharides, the efficiency of the conversion partially depends on the ability of GH enzymes to access the recalcitrant substrate, to disrupt the polymer packing and, importantly, to direct a single polymer chain into the catalytic site (*12*). This is so challenging that, in most cases, a single enzyme cannot take into account all of the issues of the process. As a result, a complex of enzymes accomplishes this and acts in a synergistic manner for full conversion. They also need exo- and/or endo-mode(s) of action and processive (multiple attack) and/or non-processive mechanism(s) to simultaneously or consecutively carry out the breakdown (*12, 13*). Understanding how enzymes accomplish this could provide information for the design of enhanced enzyme complexes for biomass conversion. So far, one typical example of an efficient GH mixture in chitin degradation that was thoroughly investigated was the chitinolytic system from *Serratia marcescens*. The system includes one lytic polysaccharide monooxygenase (a CBP) that increases enzyme accessibility to the substrate, two processive enzymes ChiA and ChiB, one nonprocessive ChiC, and a GH20 HEX that cleaves chitobiose to completely convert chitin into its monomers (*13, 207*). The synergistic action to produce monomers could be observed with the combination of three chitinases, or with only ChiB and ChiC, however, with very low yields and high concentrations of dimers and trimers as byproducts. The efficiency clearly increased in the presence of the CBP although the existence of oligomer products was still so obvious. Indeed, the combination containing 25 µM of all five *S. marcescens* proteins gave the highest final yield (about 350 µM of GlcNAc corresponding to 0.77 % of productivity) from the hydrolysis of 10 mg/L colloidal chitin after 8h of reaction (*207*). In our study, the synergistic effect was obtained with only two enzymes – the nonprocessive ChiC and *Sc*HEX – with a much higher efficiency. In fact, with 32 µM of the two enzymes, with the same substrate concentration and reaction time, the productivity obtained from the mixture was 90%. It is a huge difference, demonstrating a significantly high effect of the synergistic

interaction between the *S. coelicolor* A3(2) ChiC and *Sc*HEX. As shown in our articles, ChiC displays an endo nonprocessive mode of action to hydrolyze chitin, releasing oligomers, and *Sc*HEX is an exo-acting enzyme that has no activity on chitin and just cleaves the oligomers products formed from the chitin hydrolysis by ChiC. The release of chitooligosaccharides from chitin hydrolysis by ChiC provides the most favorable substrates for *Sc*HEX, continuing cleavages to form GlcNAc as final product. This indicates that the two enzymes undergo harmonious activities for synergistic action for full conversion. Figure 2.1 presents the proposed mechanism of the synergistic action of ChiC and ScHEX.

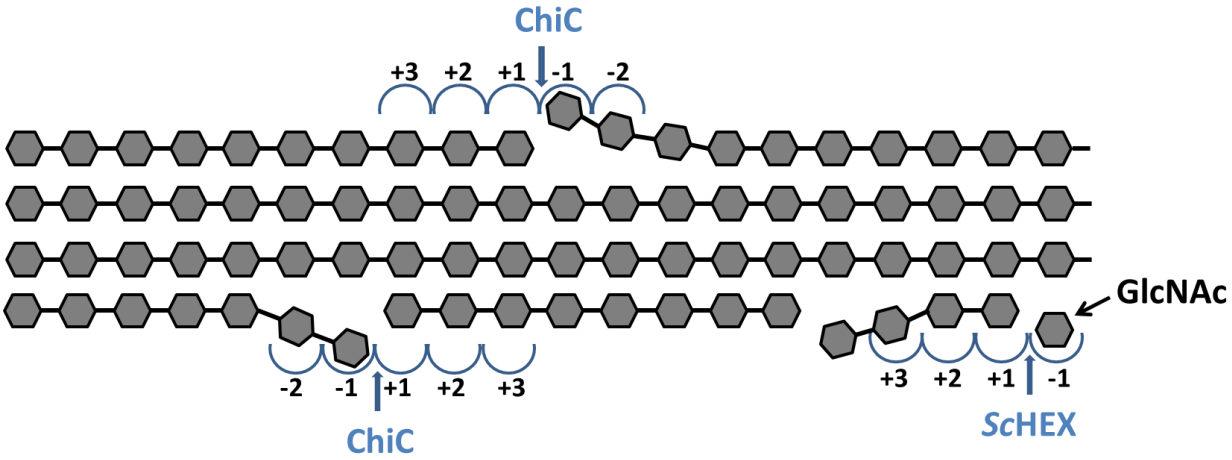

Figure 2.1. Proposed mechanism of synergistic action of ChiC and *Sc*HEX in chitin degradation. Positive and negative numbers shown as glycon and aglycon subsites of the active site of the enzymes. Arrows represent the sites where the cleavages occur. Each hexagon represents a single unit (GlcNAc) of the chitin polymer.

In the reaction mixture, there is no enzyme like CBP to disrupt the polymer packing. Thus, it is postulated that ChiC has a very good ability to access the recalcitrant substrate and to disrupt the polymer packing. From the amino acid sequence alignment, it has been shown that ChiC has one chitin-binding domain (ChtB), one fibronectin type III-like domain and one catalytic domain (*107*). From our results, ChiC shows a nonprocessive but does not show a processive mechanism, which is supposed to be the most effective way in enzymatic degradation of recalcitrant polysaccharides (*71, 74, 108, 109, 208*). In fact, to effectively breakdown crystalline polymers, non-processive endo-acting enzymes need the presence of substrate-binding domains and/or substrate-disrupting domains to increase substrate accessibility (*12, 104, 111*). In particular, non-processive cellulases might be more efficient

than processive ones if they are offered a sufficiently disrupted substrate or if they can act in concert with a carbohydrate-binding protein (CBP) or domain (CBD) (*12*). It seems that this is also the case of ChiC and it could be suggested that the ChtB domain and maybe also the fibronectin type III-like domain excellently perform these roles, which would explain the good activity of ChiC towards the polymer.

2.4.2. Enzyme flexibility plays an important role for efficiently degrading the recalcitrant polymer

In the degradation of recalcitrant polysaccharides, many systems require the synergistic action of processive and nonprocessive GHs, whereas the processive enzymes undergo multiple attacks on the single polymer chain when binding, meanwhile the nonprocessive enzymes provide new sites for productive attachment of the processive enzymes (*13*). These accomplished activities hence enhance the rate of degradation. However, in this study, we showed that efficient hydrolysis of long insoluble substrates can be obtained without the presence of processive enzymes. It has been known that processive enzymes bind individual chains in long tunnels or deep clefts, which are important for processive enzymes to remain attached to the substrate when bound. Since accessibility of the enzyme to the insoluble substrate is energetically demanding and is considered as the rate-limiting step in hydrolysis, this processive manner is thought to be the most effective one for crystalline biomass conversion (*71, 74, 108-110*). In contrast, nonprocessive enzymes show shallower active sites which do not support processivity. Therefore, nonprocessive enzymes may possess other features which contribute to enzyme efficiency beyond the role of the extra domains as discussed in section 2.4.1. In fact, the shallower active site could accommodate not only one single chain but also a crystalline pack of polymer chains. Besides, the enzymes may perform more than one cleavage per enzyme-substrate association primarily. With respect to crystalline polymers, the number of endo-binding sites are much more than the number of exo-binding sites, making the endo-nonprocessive mode a beneficial mode in hydrolysis (*110*). One more property of nonprocessive enzymes is that their CBM modules may help the enzymes loosely associate with the substrates, which allows for the enzymes to be more flexible in their association (*209, 210*). From the crystal structure of the catalytic domain of the nonprocessive chitinase ChiC2 from *S. marcescens*, it has been suggested that

the enzyme is flexible in order to be more adapted to binding to a crystalline surface than to a soluble single chain. ChiC2 also shows fewer aromatic residues that could contribute to the loose association with the substrate. The authors suggested that these features provide dynamic and flexible ability to the nonprocessive enzymes in binding to recalcitrant polymers. The ChiC2 structural data also emphasized the unusual flexibility of the catalytic residue Glu141, a feature currently only observed in one other nonprocessive endochitinase, which is the *Lactococcus lactis ssp. lactis* chitinase (*211*). Furthermore, MD simulation work on ChiC2 also demonstrated the role of the flexibility of the catalytic domain, primarily near the site of hydrolysis, for nonprocessivity. Since *S. coelicolor* ChiC is also nonprocessive and homologous with *S. marcescens* ChiC2, although the crystal structure of *S. coelicolor* ChiC has not been resolved, it may be assumed that the flexibility of *S. coelicolor* ChiC and also the presence of the ChtB domain in its structure could promote enzyme activity towards long and insoluble chitin. This flexibility feature of the nonprocessive enzyme may support what was previously suggested, that differences in processivity likely result from structural and dynamic variations (*13*).

Full and highly effective degradation of chitin, as mentioned above, requires a concerted action of ChiC and *Sc*HEX, and also flexibility of ChiC when working in a nonprocessive mode. Indeed, flexibility of enzymes in the mixture has also been clearly observed in crystal structures of *Sc*HEX in the native form or in complexes with 6-Ac-Cas (6-acetamido-6-deoxy-castanospermine) and in structures of mutant E302Q soaked with $(GlcNAc)_2$. As shown in the results and Figure 1C and Figure 3 of Article 2, the loop 3 of *Sc*HEX molecule B has two different conformations, A and B, in apo form. In molecule A of the native form, this loop has conformation A. The orientation of the loop, especially the side chain of the catalytic residues Asp301 and Glu302, changes apparently into conformation B when the enzymes were bound to the inhibitor or the substrate. Indeed, residues Asp301 and Glu302 rotated about 90^o and 180^o after binding the ligands, respectively. These new orientations result in the creation of new hydrogen bonds between the catalysts and the ligands in the active site, assuming the function of the new hydrogen bond network in stabilizing the residues Asp301 and Glu302 in binding with the ligands. This conformational flexibility of *Sc*HEX could support the "open-close" mechanism, which was proposed for *Of*HEX1 from *Ostrinia furnacalis (133).* When in apo form, *Sc*HEX is in an "open" state with

wide space in the active site (the measured distance from Glu302 to Trp396 is 13.8 Å). Upon binding of $(GlcNAc)_2$, the protein is captured in an oxazoline intermediate form and turns into a "closed" state via the rotation of the catalytic residues and also the loop (at this time, the equivalent distance between Gln302 and Trp396 is 6.4 Å) (Figure 2.2). New bonds between the ligand and Asp301, Tyr381, Asp313 and Tyr393 have been formed, as shown in Figure 3 and scheme 2 of Article 2. The new hydrogen bond network formed owing to the conformational changes is necessary for catalytic efficiency (*133*). Therefore, this crystallographic evidence suggests that conformational flexibility of the active site of *Sc*HEX plays an important role in ligand binding or catalysis. In short, it could be postulated that the flexibility of ChiC and *Sc*HEX is an important factor contributing to the effective catalysis of the enzymes in the polymer conversion.

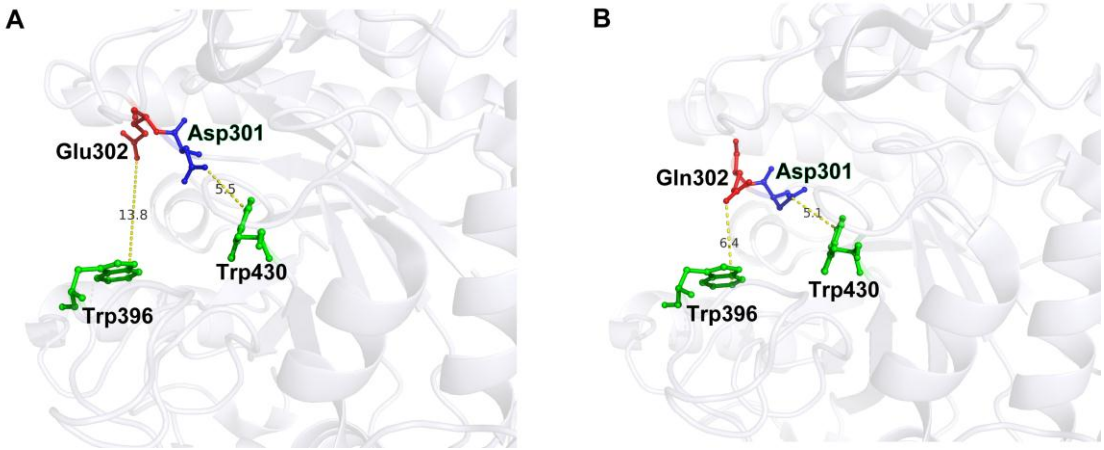

Figure 2.2. Conformational flexibility in *Sc*HEX. A, The wide space of active site of *Sc*HEX in apo form. B, The narrower active site of *Sc*HEX-E302Q in $(GlcNAc)_2$-bound form. The distances were measured from OD2 of Asp301 to CH2 of Trp430; and from OE2 of Glu302/Gln302 to CH2 of Trp396. This figure was drawn with PyMOL using PDB structures 4C7D, and 4C7G.

In general, the obtained results contribute to our understanding of the activity and mechanism of the chitinolytic enzymes from *S. coelicolor* A3(2) and provide insights on the high potential as a good system in crude chitin conversion. The results show that enzyme processivity, synergic activities, role of the carbon-binding domain and enzyme flexibility are important factors and contribute to efficiency of biomass conversion. The results also bring good information for enzymatic depolymerization of other structural polysaccharides, like

cellulose or xylan, that can be useful for biofuel production or in other industrial fields. Due to the presence of chitin in the cell wall of fungi, these enzymes might also be applied as biocontrol agents against fungal pathogens.

CHAPTER 3. THE STRUCTURE-FUNCTION-FLEXIBILITY RELATIONSHIP OF XYLANASE B

3.1. Context of chapter 3

Protein molecules are naturally dynamic and their conformational changes are evidently related to stages or actions in catalysis: binding to substrates, relocating catalytic groups, liberating products, etc. (*192*). Understanding the link between structure, function and motional properties in enzymes effectively provides a better understanding of the catalytic reactions and offer new means to control, improve or inhibit their molecular function.

*Sc*HEX and ChiC from *S. coelicolor* A3(2), with their high activity toward chitooligomers and crystalline chitins, reveal one of the most crude enzyme mixtures for degrading crystalline chitin to produce pure GlcNAc. From enzymatic profiles and crystal structures, it has been shown that enzyme flexibility is important for catalytic activities and enzyme efficiency. Consequently, we were interested in investigating the dynamic property of the enzymes in polysaccharide degradation. For that purpose, NMR methods have revealed one of the most advanced methods in studying protein motion at the molecular level. However, ChiC and *Sc*HEX are two large proteins with 535 and 609 residues, respectively, that are not suitable for NMR experiments. In an NMR spectrum, each peak contains information about only a single interatomic interaction between atoms in a residue. Because the tumbling time of the protein in solution (or rotational correlation time – τ_c) is related to protein size, therefore, large proteins give larger τ_c values, resulting in peak broadening and reducing the ratio of signal/noise. Large proteins have more atoms, generating more peaks in the spectrum, which could increase peak overlap or produce a poorly dispersed spectrum (*212*). As a result, ChiC and *Sc*HEX could not be used for the dynamic study. Instead, XlnB2 from *S. lividans* is ideal for NMR experiments and was chosen for this purpose.

In fact, XlnB2 could be a good alternative to ChiC and *Sc*HEX in studying dynamics in polysaccharide conversions. First, XlnB2 is a GH11 protein with a suitable size for NMR experiments with a molecular weight of 22 kDa containing 191 residues. XlnB2 was expressed in *S. lividans* 10-164, a cellulose- and xylanase-negative mutant. XlnB2 is a monomer that is already expressed with high yields in minimal medium, which makes it well adapted to isotopic labeling and heteronuclear 2D and 3D NMR spectroscopy experiments.

Thermostability assays showed that the enzyme is stable at room temperature for days (*156*), making it perfectly adaptable to the long NMR relaxation experiments required by this study.

Secondly, XlnB2, ChiC and *Sc*HEX are the key enzymes taking part in the bioconversion of polysaccharides of biomass and they show several related properties. Both chitin and xylan contain β-1,4-glycosidic bonds linking GlcNAc and xylose units, respectively. Chitinolytic enzymes and xylanases that catalyze this hydrolytic reaction belong to different GH families. Because they share the same ability to cleave the β-1,4-glycosidic bonds of polymers with long saccharide chains, the enzymes utilize a general acid/base catalytic mechanism and may share a similar active site architecture with multiple subsites to fit polysaccharide chains. In fact, ChiC, *Sc*HEX and XlnB2 adopt the same retaining mechanism that converts their substrates to generate products with the same anomeric configuration. Therefore, we hoped that studying xylan bioconversion could bring some useful information for biomass degradation in general. Furthermore, many xylanase GH11 enzymes have been used as models for biomass conversion as well as for protein dynamic investigations. A lot of evidence from X-ray structures, molecular dynamics or NMR has shown dynamic motions in other GH11 xylanase homologs. However, all the data just gave a "snapshot" picture but could not give full information on enzyme dynamics during catalysis. Therefore, XlnB2 was chosen for dynamic investigations by NMR that could bring further insight into biomass conversion.

Structural analysis has shown that GH11 xylanases are highly homologous at the structure and sequence levels. However, GH11 members show a wide variation in enzyme specificity, such as optimal pH and temperature, thermostability, or substrate specificity (*11*). So far, only a few structural or sequence differences have been found to account for these variations in their properties. Since proteins are far from being static assemblies, they are inherently dynamic and the dynamics play an important role in biological functions (*161*). Dynamics in certain families seem to be conserved among structural and functional homologs catalyzing similar enzymatic reactions (*197*, *198*). In many other cases, proteins are dynamic in evolution: evolutionary changes in protein sequence and structure are often closely related to local or global protein flexibility (*199*). Other evidence suggests that structurally conserved proteins may not share the same dynamic properties and dynamics are encoded from the primary sequence (*200*). Due to the different behavior of dynamics relating sequences and

structures among families, acquiring an understanding on the structure/function/dynamic relationship is necessary for engineering improved biocatalysts. In particular, investigation on protein dynamic motion is more important to get a full live picture of protein action in substrate binding, catalysis, or product release. Despite methodological advances in recent years, the relationship between the internal motions of proteins and their catalytic properties remains to be well elucidated. Conflicting data have been reported regarding the effects of ligand binding on protein motions on catalytic timescales that can be investigated by NMR relaxation studies. Concerning GH11 xylanases, the dynamic property has not been well characterized. There is poor information on flexibility of some representatives of GH11, which were chosen for studies as models of glycoside hydrolases (*153, 162-166*). To date, based on MD, crystal structure and mutagenesis evidence, it was suggested that the GH11 protein adopts an open-closed movement during the whole catalytic cycle, which follows three conformations: B-binding conformation (ligand binds to the active site) →C-closed conformation (the thumb closed to the active site and the reaction may occur) → L-loose-conformation (the reaction products diffuse away) → B (binding) (*11, 163*). There is also another hypothesis suggesting that the thumb motion plays an essential role in the open-closed movement (*163, 164, 166, 169, 170*). However, in some other investigations, it was proven that xylanase is highly ordered (*213*) and that the thumb does not undergo any movement even in the presence of ligand (*214-216*). This apparent conflict is due to the limitations of the methods used; therefore more consistent data are required to go beyond these results in order to provide more insight for the full catalytic process. Moreover, all evidence for GH11 dynamic property obtained from mutagenesis and crystal structure provides no information about time scale and just can give limited information on dynamic due to packed and rigid crystal structure, which is not natural existence of protein in solution (*11*).

In this study we used NMR spectroscopy to probe the flexibility of XlnB2 in the apo form and upon binding of short and long xylooligomers. To study internal dynamics and to investigate their importance in XlnB2 catalysis, NMR experiments were carried out using the *S. lividans* WT XlnB2 and XlnB2-E87A enzymes. XlnB2-E87A is an inactive variant that is mutated at the catalytic residue Glu87. NMR relaxation dispersion experiments ^{15}N-CPMG were performed on ^{15}N isotopically-enriched XlnB2 and XlnB2-E87A (in apo and ligand-bound forms) to probe motions occurring on the timescale of catalysis. ^{1}H, ^{13}C, and ^{15}N

resonances were assigned using HNCACB, CBCA(CO)NH, HNCO, and HN(CA)CO experiments. To decipher the active site residues and/or residues involved in substrate discrimination and binding, two-dimensional ^{1}H-^{15}N HSQC titration experiments on WT XlnB2 and on XlnB-E87A with substrates were also performed. Finally, X-ray crystallography was employed to determine the molecular structure of XlnB2. Our results illuminate the atomic-scale dynamics of XlnB2 on the time-scale of catalysis, providing more information for polysaccharide conversion

3.2. Presentation of article 3 – "Conformational exchange experienced by free and ligand-bound xylanase B2 from *Streptomyces lividans* 66"

3.2.1. Contribution of authors

The work presented in this manuscript was conceived, and designed by the student under the direction of N. Doucet. The protein was prepared and purified by the student. The NMR data were obtained at the QANUC NMR facility (McGill University) and IRIC - University de Montréal, and then processed and analyzed by the student and by D. Gagné. The manuscript was written by the student, D. Gagné, and N. Doucet. This manuscript will be submitted for publication shortly.

3.2.2. Résumé

Les xylanases catalysent l'hydrolyse du xylane, une ressource de carbone et d'énergie très abondante possédant des ramifications commerciales importantes. Des efforts continus ont été consacrés à l'amélioration catalytique de ces enzymes, mais le succès demeure limité en raison de la mauvaise compréhension de leurs propriétés moléculaires. Des récentes études ont suggéré que la flexibilité atomique pourrait contrôler l'activité catalytique de certains membres de la famille des xylanases GH11 via une boucle près du site actif (la boucle « thumb loop ») et de ses mouvements conservés. Des études cristallographiques et des simulations de dynamique moléculaire ont suggéré que certains membres de la famille comptent potentiellement sur un mécanisme de type « ouvert-fermé » pour remplir leur fonction catalytique. Malheureusement, ces méthodes s'appuient sur des preuves structurelles

statiques, ou encore fournissent des informations dynamiques à des échelles de temps beaucoup plus rapides que la réaction catalytique. Dans cette étude, nous avons utilisé une combinaison de dispersion de relaxation ^{15}N-CPMG, de mutagenèse dirigée et d'expériences de titrage RMN pour analyser les mouvements moléculaires de l'ordre de la microseconde à la milliseconde subis par la xylanase B2 (XlnB2) et son mutant catalytique E87A chez l'organisme du sol *Streptomyces lividans* 66. Dans sa forme libre, les résidus démontrant de l'échange conformationnel sont essentiellement regroupés dans les doigts et dans les régions de la paume composant la fente catalytique. Un modèle de réseau anisotrope (ANM) suggère que le pouce et les doigts des boucles avoisinantes initient un mouvement dans la direction opposée lors de la liaison des ligands, permettant à l'enzyme d'ouvrir et de fermer son site de liaison. Ce mouvement nécessite la contribution de Thr120, un résidu situé à la base de la boucle « thumb loop » et qui agit comme une charnière. Ces résultats fournissent une preuve expérimentale directe pour valider le mécanisme « ouvert-fermé » précédemment postulé, en plus d'offrir de nouvelles perspectives sur le mécanisme catalytique des xylanases de la famille GH11.

3.2.3. Article 3

Conformational exchange experienced by free and ligand-bound xylanase B2 from S*treptomyces lividans 66*

Nhung Nguyen-Thi [1,2,3], Donald Gagne[1], Jean-François Couture[4,5,6] & Nicolas Doucet[1,5,6]*

[1]INRS-Institut Armand-Frappier, Université du Québec, 531 Boul. des Prairies, Laval, Québec, H7V 1B7, Canada.

[2]Institute of Military Science and Technology, 17 Hoang Sam, Hanoi, Vietnam.

[3]Vietnam Academy of Science and Technology, 18 Hoang Quoc Viet, Hanoi, Vietnam.

[4]Ottawa Institute of Systems Biology, Department of Biochemistry, Microbiology and Immunology, University of Ottawa, 451 Smyth Road, Ottawa, Ontario, K1H 8M5, Canada.

[5]PROTEO, the Québec Network for Research on Protein Function, Structure, and Engineering, 1045 Avenue de la Médecine, Université Laval, Québec, Québec, G1V 0A6, Canada.

[6]GRASP, the Groupe de Recherche Axé sur la Structure des Protéines, 3649 Promenade Sir William Osler, McGill University, Montréal, Québec, H3G 0B1, Canada.

*Corresponding author: nicolas.doucet@iaf.inrs.ca

Abstract

Xylanases catalyze the hydrolysis of xylan, a very abundant carbon and energy resource with important commercial ramifications. Continuous efforts have been devoted to the catalytic improvement of these enzymes, but success has been limited due to poor understanding of their molecular properties. Recent reports have suggested that atomic flexibility could regulate the catalytic activity of GH11 xylanase family members, namely through a conserved active-site loop motion. Crystallographic studies and molecular dynamics simulations have suggested that some family members potentially rely on an open-closed active-site lid mechanism to perform their catalytic function. Unfortunately, these methods rely on static structural evidence or provide dynamic information on timescales that order of magnitude faster than the catalytic reaction. In this study, we used a combination of ^{15}N-CPMG relaxation dispersion, site-directed mutagenesis, and NMR titration experiments to investigate the microsecond-to-millisecond motions experienced by xylanase B2 (XlnB2) and its catalytically impaired mutant (E87A) from the soil organism *Streptomyces lividans 66*. In the free form, residues presenting conformational exchange are essentially clustered in the fingers and palm regions of the catalytic cleft. Anisotropic Network Model (ANM) calculations suggest that the thumb-loop and fingers initiate a movement in the opposite direction upon ligand binding, allowing the enzyme to open and close its binding cleft. This motion requires the contribution of Thr120, a residue located at the base of the thumb-loop, which acts as a hinge. These results provide direct experimental evidence to validate the previously postulated open-closed mechanism and offer new insights on the catalytic mechanism of GH11 xylanases.

Introduction

Plant cellulosic polysaccharides account for more than 50% of all plant biomass, therefore constituting the most abundant organic carbon resource on the planet (*1, 2*). Cellulosic biomass is considered an inexhaustible energy source for enzymatic hydrolysis in a number of renewable energy domains, including fuel production, food preparation, paper industry, and medical treatment. However, these enzymatic hydrolysis processes, which could have an important positive impact on the environment, suffer from high production costs and the recalcitrant nature of the polysaccharide substrates (*1-3*). For those reasons, finding and developing improved enzymes that can overcome these limitations is an important area of protein engineering aimed at industrial biocatalysis. Moreover, the principles that govern the enzymatic breakdown of these polymers remain elusive, and promising fundamental and industrial biotechnological breakthroughs could be achieved from a greater understanding of their natural molecular breakdown. Therefore, continuous efforts have been devoted to gain further insights into the molecular function of plant cellulosic enzymes.

Xylanases are involved in the degradation of heteroxylan (hemicellulose), one of the major components of plant biomass. They are glycoside hydrolases that cleave internal β-1,4-xylosidic bonds in heteroxylan, which constitutes a linear chain of β-D-xylopyranoses, variously substituted with arabinose, galactose, glucuronic acid, and other groups. These enzymes are critical for heteroxylan degradation to release fermentable sugar and platform molecules, which can be used in numerous applications, such as biofuel production or in the pulp and paper industry. The ability of enzymes to be folded and active under specific, unnatural and/or extreme conditions, such as high temperatures, pressure, or alkali environments, is a considerable economic restriction for these processes (*1*). For example, the bleaching of paper pulp in crucial

yet unavoidable alkali pH ranges requires the utilization of biocatalysts to reduce the production of lasting and toxic organochlorine compounds (*4*). Based on amino acid sequence similarity and hydrophobic cluster analysis, the Carbohydrate-Active Enzyme Database (CAZy, http://cazy.org/) classifies xylanases into six families: GH5, GH8, GH10, GH11, GH30, and GH43. Among them, the GH11 family has been thoroughly characterized and is considered a true xylanase family because of high substrate specificity (*1, 5, 6*). Several GH11 members have been structurally and functionally characterized as β-glycosidase models (*7-17*). The typical characteristic of the GH11 architecture is the overall conserved structure of the β-jelly roll domain, which shows a closed right-handed architecture, and an active site cleft covered by a 'thumb-loop'. Despite high structural homology, GH11 family members display important biophysical variability, including an optimal catalytic pH that varies between 1 and 9, and distinctive thermostability (*1*). Interestingly, few sequence and structure differences have been found to account for these variations. As such, improving the catalytic efficiency of these enzymes is of high commercial value, but also requires an understanding of the structural and mechanistic details responsible for their diverse properties (*9*).

Evidence from crystal structures and molecular dynamic (MD) simulations on several GH11 xylanases (*7, 17-21*) have proposed the existence of a thumb-loop motion, which may play a major role in substrate binding, product release, and/or catalysis (*17, 19, 21-23*). While these studies provide information on protein flexibility, they do not offer details on the potential motions occurring during the catalytic reaction of the enzyme, *i.e.* on the microsecond-to-millisecond (μs-ms) timescale (*24*). Indeed, crystal structure investigation provides access to limited snapshots of possible xylanase conformations, while MD simulations explore motions on a much faster timescale (ns), which is far from the timescale of the catalytic reaction (ms).

In this study, we characterized the motional behavior of the 21-kDa GH11 family member xylanase B2 (XlnB2) from *Streptomyces lividans 66* in its free and bound forms. In the culture medium of *Streptomyces lividans 66*, two forms of XlnB are secreted, namely XlnB1 and XlnB2. XlnB1 is composed of two discrete structural and functional units, an N-terminal catalytic domain and a C-terminal xylan binding domain, whereas XlnB2 contains the catalytic domain only. Both forms have the same specific activity on xylan (*25*). The enzyme retains endo-activity toward xylan, in which XlnB yields a large amount of oligoxylosides, with a degree of polymerization ranging from one to eight units of xylose. Kinetic parameters include a K_m (V_{max}) of 3.71 mg/mL (1.96 mmol/mg), with a calculated k_{cat} of 1020 s^{-1} on a typical substrate (*26*). The present work describes the NMR assignments, titration, and ^{15}N-CPMG relaxation dispersion experiments on the apo and ligand-bound XlnB2 and its catalytically impaired XlnB2-E87A variant. Our results show that the enzyme can adopt at least two conformational states, similar to the open-closed mechanism initially proposed by Muilu *et al*. (*18*). In the free form, residues experiencing motions are clustered in the fingers region. Upon ligand binding, motions are triggered in the surrounding area of the active cleft, a coordinated shift that involves the fingers and the thumb-loop. Vibrational motions calculated using the Anisotropic Network Model (ANM) suggest that the fingers and thumb-loop motions move in opposite directions to close the active cleft. Finally, the mobility of the thumb-loop appears to be articulated by Thr120, which acts as a hinge.

Experimental procedures

Cloning, mutagenesis and protein purification

Cloning of the gene encoding XlnB2 was performed as previously described(*27*) and variant XlnB2-E87A was generated by site-directed mutagenesis using standard procedures. The sequence encoding for the XlnB2-E87A variant without its signal sequence was amplified from vector pIAF935, which contained *xlnB2* as template using the following DNA primers: 5'-CCGGTACCGACACGGTCGTCACGA-3' (forward primer, with the *Kpn*I site underlined), and 5'-CCGAGCTCTCACCCGCCGACGTTGATGCT-3' (reverse primer, with the *Sac*I site underlined). The point mutation E87A was introduced by overlap extension PCR(*28*), using the following DNA primers: 5'-CCGCTCGTCGCGTACTACATCGTCG-3' (forward), and 5'-CGACGATGTAGTACGCGACGAGCGG-3' (reverse). The 593bp *Kpn*I-*Sac*I-digested PCR product containing the E87A mutation was cloned into the same restriction sites in plasmid pC109 (NEB, Ipswich, MA USA), which carries a thiostrepton resistance marker. The resulting construct was subsequently transformed into *Streptomyces lividans 66* (American Type Culture Collection, Manassas, VA, USA) 10-164 protoplasts and plated on R5 medium without antibiotic for 16h at 34°C, at which point agar plates were flooded with thiostrepton solution and further incubated 3–4 days at 34°C. The resulting plasmid was isolated and positive clones were confirmed by DNA sequencing.

XlnB2 and XlnB2-E87A were enriched by cultivation of the transformed *S. lividans* strains in M14 media supplemented with $(^{15}NH_4)_2SO_4$ (Sigma-Aldrich, St-Louis, MO USA) and 1% xylose (w/v) as the sole nitrogen and carbon sources. For multi-dimensional NMR experiments, the xylose was replaced by ^{13}C-glucose (w/v) (Sigma-Aldrich, St-Louis, MO USA).

It is known that glucose represses the secretion of extra-cellulosic enzymes in *Streptomyces lividans(26)*. However, the production of the targeted enzymes with ^{13}C-glucose was shown sufficient for NMR experiments. After 72 hours of incubation, proteins were harvested with final yields of 63 mg/L and 36 mg/mL of ^{13}C/^{15}N-labeled XlnB2 and XlnB2-E87A, respectively. The proteins were concentrated by ultrafiltration and dialyzed against 10 mM citric buffer at pH 4.5 prior to loading on a CM FF column (GE Healthcare, Baie d'Urfé, QC Canada) pre-equilibrated with 20 mM citrate buffer, pH 4.5. The enzymes were eluted with a linear gradient of 20 mM citrate buffer, pH 4.5 containing 1 M NaCl. Fractions containing XlnB2 or XlnB2-E87A were collected, dialyzed in water, and lyophylized. Mass spectrometry was also employed to confirm sequence identity and integrity. Protein concentration was determined by UV-Vis spectroscopy using a predicted extinction coefficient value of $\varepsilon_{280} = 63830\ M^{-1}\ cm^{-1}$ (ExPASy ProtParam).

Resonance Assignments

NMR samples were prepared by resolubilizing lyophilized, uniformly ^{15}N or ^{15}N/^{13}C-labeled proteins in 20 mM MES (pH 6.5), 20 mM NaCl, 0.01% NaN_3 and 10% ^2H_2O. All NMR experiments were recorded at 298 K on samples containing 0.6-0.8 mM protein in 5 mm Shigemi NMR tubes. NMR experiments were carried out on 600 and 800 MHz Innova NMR spectrometers (Agilent, Santa Clara CA USA) equipped with triple-resonance cold probes and pulsed field gradients. For backbone assignments of XlnB2, a series of ^{1}H, ^{15}N 2D (HSQC) and ^{1}H, ^{13}C, ^{15}N 3D (HNCACB, HNCO, HN(CA)CO, CBCA(CO)NH, NOESY) experiments were performed. All spectrums were processed with NMRPipe(*29*) and analyzed with NMRView 8 (Merck and Co., Whitehouse Station, NJ USA). The backbone assignments of XlnB2-E87A was achieved by overlapping the ^{1}H-^{15}N-HSQC spectrum with the corresponding assigned spectrum

of XlnB2. Peaks showing chemical shift variations were confirmed using 3D assignment experiments.

NMR Titration Experiments

All NMR titration experiments were performed in 20 mM MES (pH 6.5), 20 mM NaCl and 0.01% NaN_3. Concentrations of 657 µM (661 µM) of ^{15}N-labeled XlnB2 (XlnB2-E87A) were used for the titration of unlabeled xylobiose (xylopentaose). ^{1}H-^{15}N-HSQC experiments were collected at 800 MHz with 256 and 8192 points in the t_1 and t_2 dimensions, respectively. ^{1}H-^{15}N-HSQC spectra of XlnB2 were acquired by gradually increasing the ligand:enzyme molar ratios to 0.3, 1.2, 3, 6, 12, 20, 30, 40, 60, 80, and 100. Similarly, ^{1}H-^{15}N-HSQC spectra of XlnB2-E87A were collected with increasing ligand:enzyme molar ratios of 0.3, 1.2, 3, 6, 12, 20, 30, 60, 80, 90 and 100. Chemical shift variations (Δδ) were calculated using the equation described by Grzesiuk *et al.*(*30*): $\Delta\delta\ (ppm) = ((\Delta\delta_{HN}^2 + \Delta\delta_N^2/25)/2)^{1/2}$. The dissociation constant (K_d) was determined for each residue showing Δδ ≥ 0.05 ppm and averaged, as previously described(*31*). The K_d corresponds to the intercept on the x-axis (ligand concentration) at 50% the total variation of Δδ.

Relaxation Dispersion Experiments (µs-ms Motions)

Backbone amide ^{15}N-CPMG relaxation dispersion experiments were recorded at 25°C for XlnB2 (657 µM) and XlnB2-E87A (661 µM) in the apo and saturated-bound forms with B_0 fields of 14.1 T (600 MHz) and 18.77 T (800 MHz). The constant time delay τ_{cp} was set to 20 ms and interleaved two-dimensional spectra were collected in a constant time manner with τ_{cp} CPMG repetition delays of 0.625, 0.714 (×2), 1.0, 1.25, 1.67, 2.0, 2.50 (×2), 3.33, 5.0, and 10

ms. Global residue fits and model analyses were performed by fitting 600- and 800-MHz CPMG dispersion data to the single quantum CPMG equation (*32*) using GraphPad Prism 5.

Results

NMR assignments and spectrum comparison

The ^{1}H-^{15}N-HSQC (Heteronuclear Single Quantum Coherence) spectra of XlnB2 and XlnB2-E87A show well-dispersed resonances, indicating well-folded proteins (Figure 1A). We used a combination of 2D [HNCO] and 3D [HNCACB, CBCA(CO)NH, HN(CA)CO] NMR experiments to sequentially assign the ^{1}H, ^{13}C, and ^{15}N backbone resonances of XlnB2 and XlnB2-E87A. Peak assignments were confirmed with a ^{15}N-NOESY. A total of 171 (175) ^{1}H-^{15}N peaks were assigned for XlnB2 (XlnB2-E87A), corresponding to 92% (94%) of non-proline residues. Most of the unassigned residues were located on finger loops, suggesting that these residues experience line broadening. For XlnB2-E87A, we assigned four additional peaks, corresponding to residues Asn46, Ser70, Asp110 and Glu177. In both enzymes, the NH cross peaks from arginine residues and the indole NH cross peaks from the tryptophan side chains were not assigned.

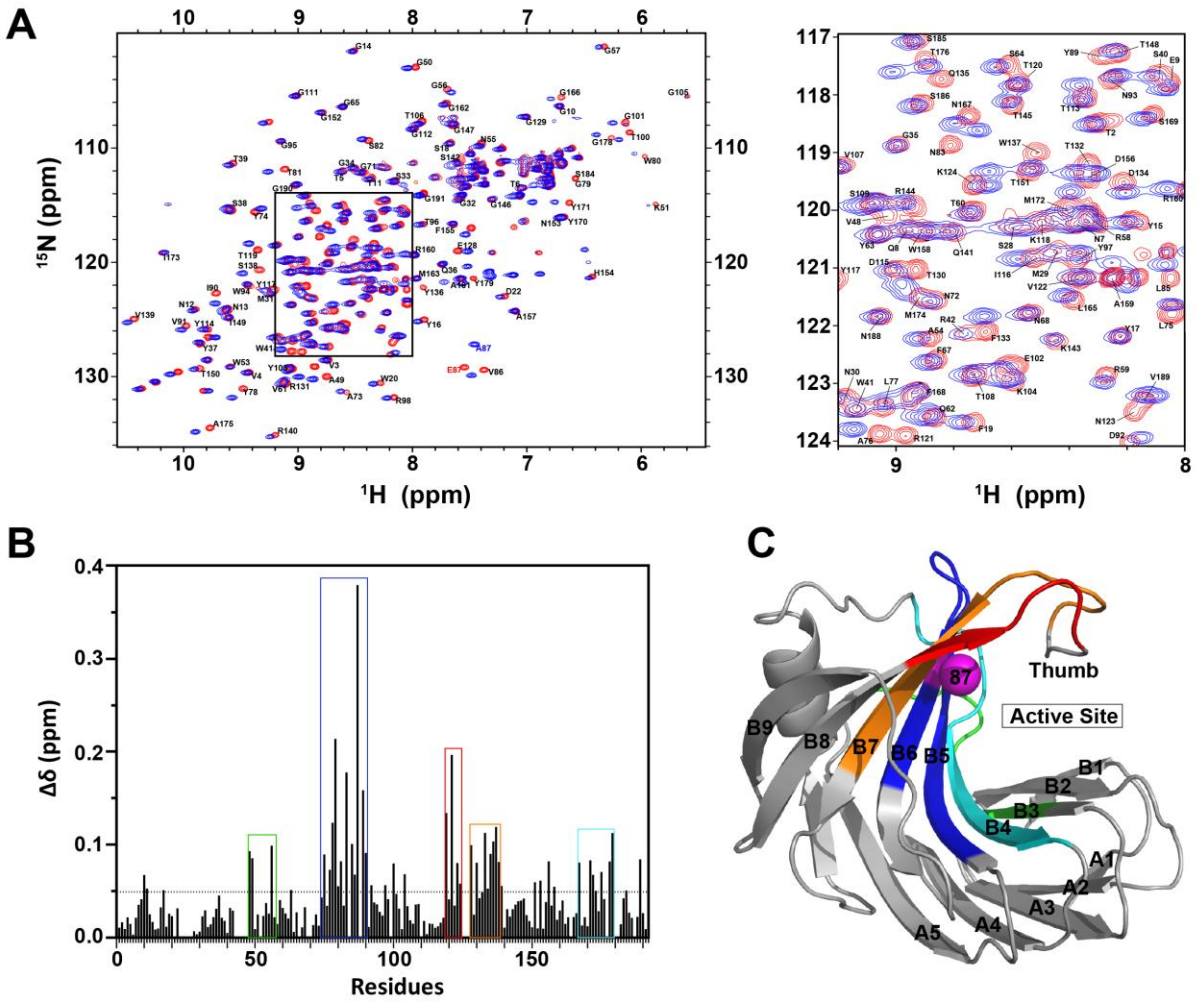

Figure 1. Chemical shift changes in XlnB2 and XlnB2-E87A. (A) Overlapped ^{1}H-^{15}N HSQC spectra of XlnB2 (red) and XlnB2-E87A (blue). A close-up view of the central spectral region is shown on the top right. Amino acids are identified by the single letter code followed by sequential residue numbers. (B) Bar-graph representing chemical shift variations between XlnB2 and its E87A variant. A dotted line indicates the significant chemical shift variations. Residue clusters presenting the most significant changes are color-identified and reported on the (C) three-dimensional structure of XlnB2.

Residues affected by the mutation can be identified by quantifying the chemical shift variations ($\Delta\delta$) between XlnB2 and its variant. An overlay of the two ^{1}H-^{15}N-HSQC spectra showed $\Delta\delta$ for each residue (Figure 1A). All residues with a $\Delta\delta > 0.05$ ppm are considered significant (Figure 1B). As expected, Glu87 ($\Delta\delta = 0.37$ ppm) and the surrounding residues of the B5 and B6 β-strands showed the most significant chemical shift variations (blue box, Figures 1B-C). Important chemical shift differences were also observed for residues of the B3, B4 and B7 β-strands (and associated loops), as well as in the thumb-loop (red and orange boxes, Figures 1B-C).

Effect of the mutation on binding kinetics

Chemical shift perturbations upon ligand binding can provide valuable information on the expected binding site(s), as well as on the kinetics of binding. We used this technique to characterize and compare the binding of XlnB2 and its variant. XlnB is an endo-xylanase, which hydrolyzes xylan into oligoxylosides with lengths ranging from one to eight xylose units (*26*). Among these products, xylotriose is the smallest substrate of the endo-cleavage, which then releases xylose and xylobiose. We investigated the binding affinity of xylose, xylobiose, and xylotriose on XlnB2 and variant E87A by ligand titration using chemical shift variations in the ^{1}H-^{15}N-HSQC spectra upon increasing ligand concentration, until saturation. All residues with a $\Delta\delta > 0.05$ ppm were considered significantly affected by the presence of the ligand and are highlighted on the 3D structure of XlnB2 (Figures 2A-B). A total of 3 residues (Gln8, Gly10 and Tyr17) and 11 residues (Gly10, Thr11, Phe19, Trp20, Gly79, Glu128, Thr130, Lys143, Leu165, Tyr171 and Ile173) displayed important chemical shift perturbations ($\Delta\delta > 0.1$ ppm) upon binding to xylobiose in XlnB2 and its E87A variant, respectively (Figure 2D). Despite a weak-binding affinity ($K_d \approx 8$ mM), both proteins showed similar K_d values in presence of xylobiose

(Table 1), suggesting that the mutation did not affect binding extensively. Although the number of residues with a $\Delta\delta > 0.1$ ppm is larger for XlnB2-E87A, most residues affected by the presence of the ligand are near the active-site cleft. Previous studies suggested that the active site of GH11 family members could accommodate linear xylan made of 5-6 units. The catalytic cleft of the GH11 family is approximately 30-35 Å, whereas a xylose moiety is ~ 6 Å long between the O_1 to O_4 atoms (*1*). Based on these observations, we titrated XlnB2-E87A with a xylopentaose, containing 5 xylose units (Figure S1). The mutation of the acid/base glutamate residue E87 to an alanine blocks the first step of the reaction and prevents the distortion of the substrate conformation (*33*). The titration experiment with xylopentaose thus provides information on the conformational transition of long ligands in xylanase-ligand interaction (Figure 2C). A total of 10 residues (Gly10, Tyr17, Trp20, Ala73, Thr120, Phe133, Tyr136, Tyr171, Ile173 and Tyr179) showed $\Delta\delta > 0.1$ ppm in the enzyme variant (Figure 2D). As previously observed with xylobiose, the most significantly affected residues are located near the active site, with a very low ligand affinity ($K_d \approx 8$ mM) (Table 1).

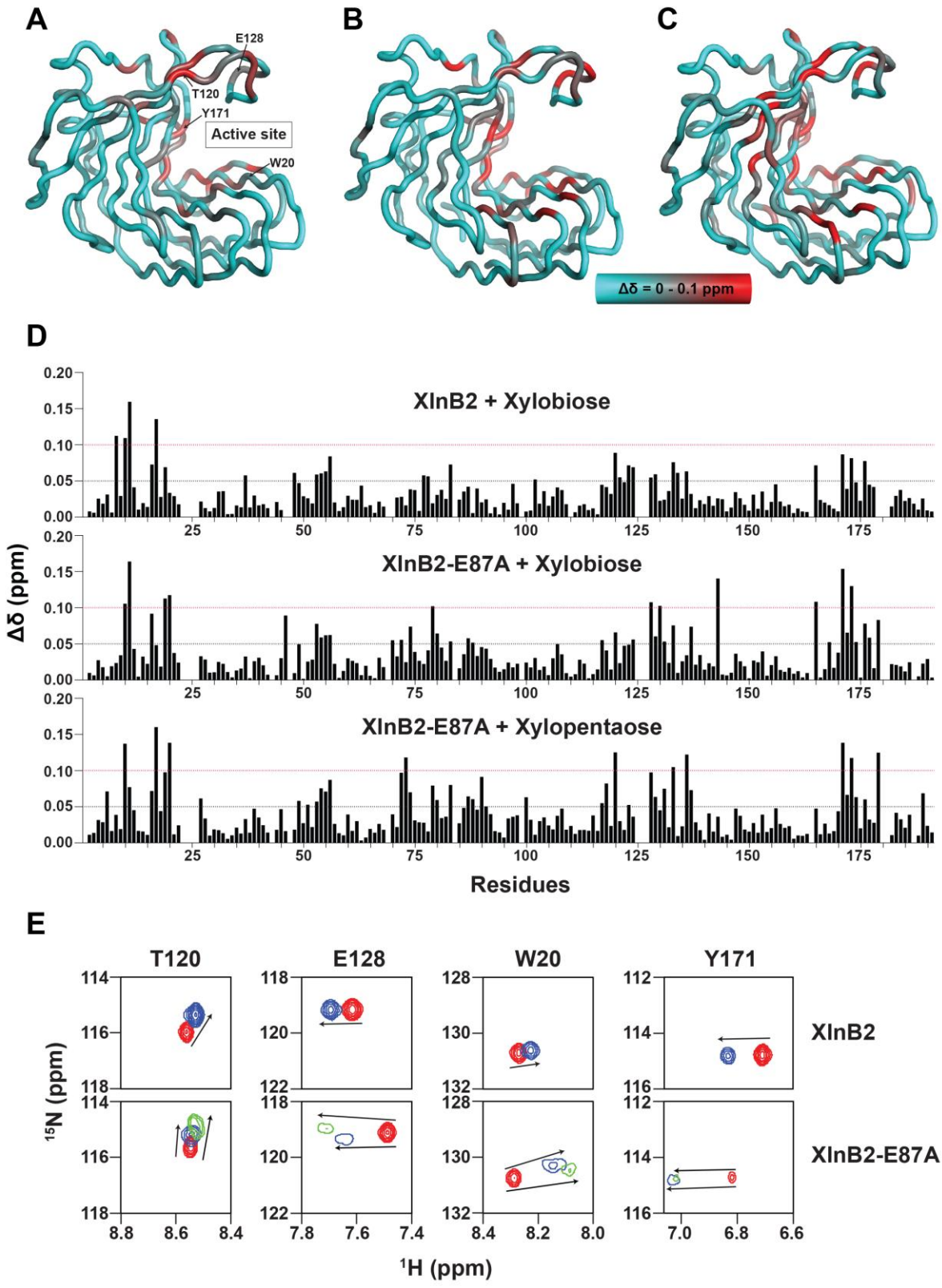
A
B
C
E128
T120
Y171
Active site
W20
Δδ = 0 - 0.1 ppm
D
XlnB2 + Xylobiose
XlnB2-E87A + Xylobiose
XlnB2-E87A + Xylopentaose
Δδ (ppm)
Residues
E
T120
E128
W20
Y171
XlnB2
XlnB2-E87A
15N (ppm)
1H (ppm)

Figure 2. ^{1}H-^{15}N chemical shift variations of XlnB2 and XlnB2-E87A upon binding to ligands. Structural mapping of chemical shift variations (Δδ) observed for (A) XlnB2 induced by xylobiose; (B) XlnB2-E87A induced by xylobiose; and (C) XlnB2-E87A induced by xylopentaose. The Δδ was calculated between free and ligand-saturated enzymes as described by the equation $\Delta\delta(ppm) = ((\Delta\delta_{HN}^2 + \Delta\delta_N^2/25)/2)^{1/2}$ and reported on the three-dimensional structure of XlnB2 using a cyan-to-red color scale with a 0.0-0.1 ppm range. The location of the active site and key residues is reported on the 3D structure in (A). (D) Bar graph representation of the chemical shift variations observed for XlnB2 and XlnB2-E87A upon binding to xylobiose and xylopentaose. Significant (Δδ > 0.05 ppm) and important (Δδ > 0.1 ppm) chemical shift changes are represented on the graph by black and red dotted lines, respectively. (E) ^{1}H-^{15}N chemical shift kinetics for residues Trp20, Thr120, Glu128, and Tyr171 in XlnB2 and XlnB2-E87A. The ^{1}H-^{15}N peak position of the free enzyme is shown in red. The ^{1}H-^{15}N peak position upon binding to saturation with xylobiose (xylopentaose) is shown in blue (green). NMR spectra were processed using Sparky (*34*). All images were prepared with PyMOL and graphs were produced with GraphPad Prism.

Table 1. Ligand affinities (K_d) for XlnB2 and its E87A variant upon binding to xylobiose and xylopentaose. K_d values were measured by NMR titration, as previously described (*31*). N/A = Not available

	K_d (mM) Xylobiose	K_d (mM) Xylopentaose
XlnB2[a]	7.07	N/A
XlnB2-E87A[a]	8.71	7.93

[a]Binding affinity average for residues Trp20, Thr120, Glu128, Thr130, Tyr171.

Although the mutation did not extensively disturb the conformational transition step upon binding to xylobiose, Glu128 and Thr130 showed significant Δδ in the E87A variant (Figures 2B-C). Interestingly, these two non-conserved residues of the thumb-loop (Figure S2) were also significantly affected by the mutation (Figure 1). Recent studies showed that the direction of the ^{1}H, ^{15}N chemical shifts could provide valuable information on the nature of the binding (*35*). We investigated this possibility in XlnB2 and discovered that the ^{1}H, ^{15}N chemical shift direction for Glu128 was identical between XlnB2 and its variant upon binding to xylobiose (Figure 2E). Furthermore, the direction and intensity of the movement was also similar upon binding to both ligands, suggesting that the length of the ligand did not affect the magnetic environment or direction of the thumb-loop movement. Upon binding to XlnB2 and XlnB2-E87A, we also observed important chemical shift variations for Thr120 (Figure 2D), a residue that links the thumb-loop with the main enzyme scaffold. It was previously suggested that Thr120 could operate as a hinge for the thumb-loop (*21*). Much like with Glu128, Thr120 showed coordinated chemical shift changes upon binding to xylobiose and xylopentaose (Figure 2E), further suggesting that the movement and orientation of the thumb loop is the same in XlnB2 and its E87A variant. Two other residues, Trp20 and Tyr171, located on opposite sides of the active site, were also highly affected upon binding. These conserved residues play an important role in substrate binding in GH11 members (Table 1; Figure S2) (*1, 36, 37*). Our results demonstrate similar behavior, showing similar K_d values (Table 1) upon ligand binding, and coordinated chemical shift responses (Figure 3E).

Motions of the thumb-loop and fingers

It was previously demonstrated that protein flexibility could be involved in the catalytic events in many enzyme systems (*38*). Previous studies on endo-1,4-xylanase from *Hypocrea*

jacorina, a GH11 family member, showed that the width of the active-site cleft is reduced from 6.7 to 4.8 Å upon binding of 2,3-epoxypropyl-β-D-xyloside (*1*). In order to characterize the potential bending movement in XlnB2, we performed ^{15}N-CPMG (Carr-Purcell-Meiboom-Gill) relaxation dispersion on the apo and bound forms of XlnB2 and its catalytically impaired mutant (XlnB2-E87A). This NMR technique is particularly well suited to identify residues experiencing motions on the µs-ms timescale, overlapping with the rate of catalysis in most enzyme systems (including xylanases) (*39*).

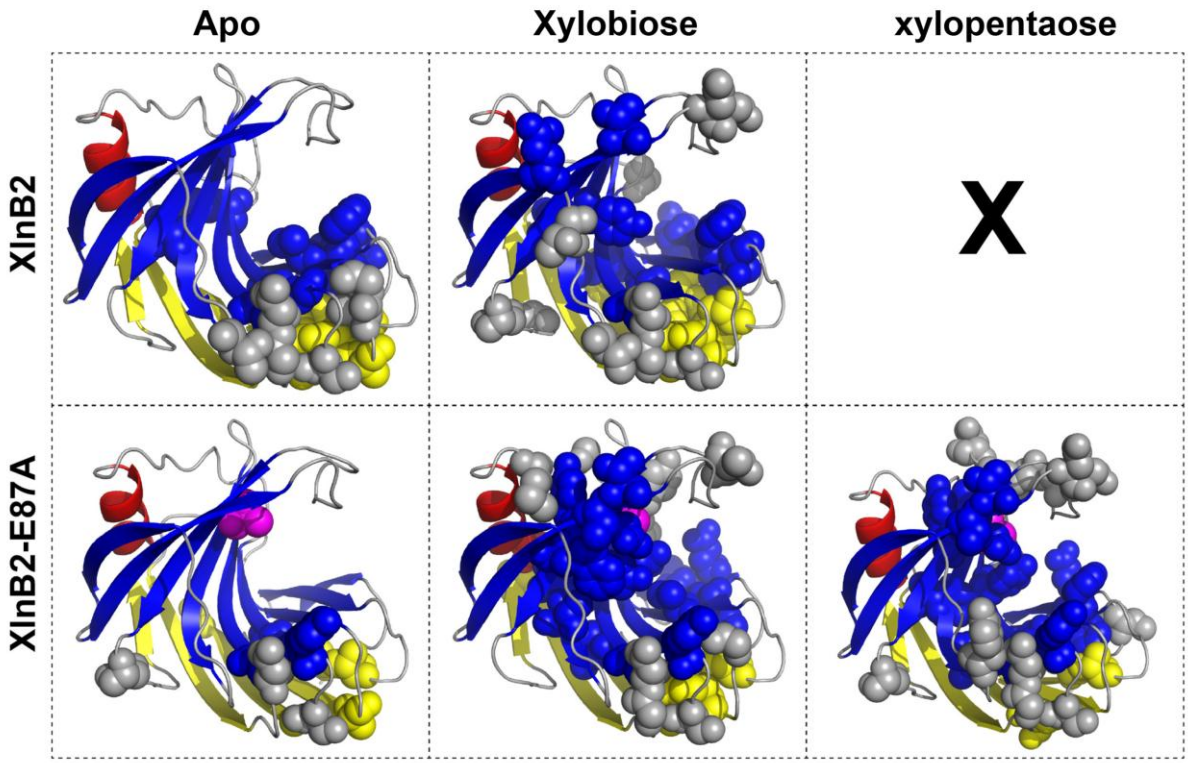

Figure 3. Residues experiencing microsecond-to-millisecond (µs-ms) conformational exchange in free and bound forms of XlnB2 and XlnB2-E87A. Overview of the µs-ms atomic motions mapped on the 3D structure XlnB2 and its catalytically-impaired E87A variant. Residues with a $R_{ex} > 1.8$ s^{-1} are represented by colored spheres. The color refers to the region of the protein: β-sheet A (yellow), β-sheet B (blue), helix (red) and loops (gray). All images were prepared with PyMOL and graphics were produced with GraphPad Prism.

All residues displaying R_2 ($1/\tau_{CP}$) > 1.8 s^{-1} experienced significant conformational exchange and are shown on the structure of XlnB2 and its E87A variant (Figure 3). In the free form (Figure 3, first column), a total of 22 (12) residues showed atomic motions in XlnB2 (XlnB2-E87A). In the WT enzyme, dynamic residues are clustered in the fingers. While the profile remains similar in both proteins, the global rate of conformational exchange (k_{ex}) is higher in the mutant, with a difference more visible in the palm near the fingers (k_{ex} = 1220 ± 392 s^{-1} for XlnB2 *vs* k_{ex} = 2794 ± 399 s^{-1} for XlnB2-E87A). The increased global k_{ex} in the mutant might be the consequence of reduced protein stability. Upon binding to xylobiose (Figure 3, middle column), a total of 29 (32) residues showed conformational exchange in XlnB2 (XlnB2-E87A), while 33 residues had a R_2 ($1/\tau_{CP}$) > 1.8 s^{-1} with XlnB2-E87A in the presence of saturating concentration of xylopentaose (Figure 3, right column). When reported on the 3D structure, dynamic residues in presence of ligand are visible in the surrounding area facing the active cleft. Millisecond motions also extend to the thumb-loop and Thr120 region, which are involved in the conformational transition step upon binding. Furthermore, the k_{ex} of Thr120 (646 ± 69 s^{-1}) upon binding to xylopentaose coincides with the k_{ex} of the residues on the thumb-loop (536 ± 82 s^{-1}), which supports the hypothesis that their movement is coordinated. It is also worth mentioning that two residues of the fingers, Ser182 and Gly183, experience conformational exchange in free and bound forms (Figure 4). Because their k_{ex} > 3000 s^{-1} is well above the expected rate of catalysis of the reaction in XlnB2 (k_{cat} = 1020 s^{-1}) (*26*), that their motions are observed in free and bound states, and that none of these residues showed significant chemical shift changes upon binding to ligands, their motion most likely does not play a direct role in binding or catalysis in XlnB2. Nonetheless, their movement could be important for folding, stability or another unknown enzyme function.

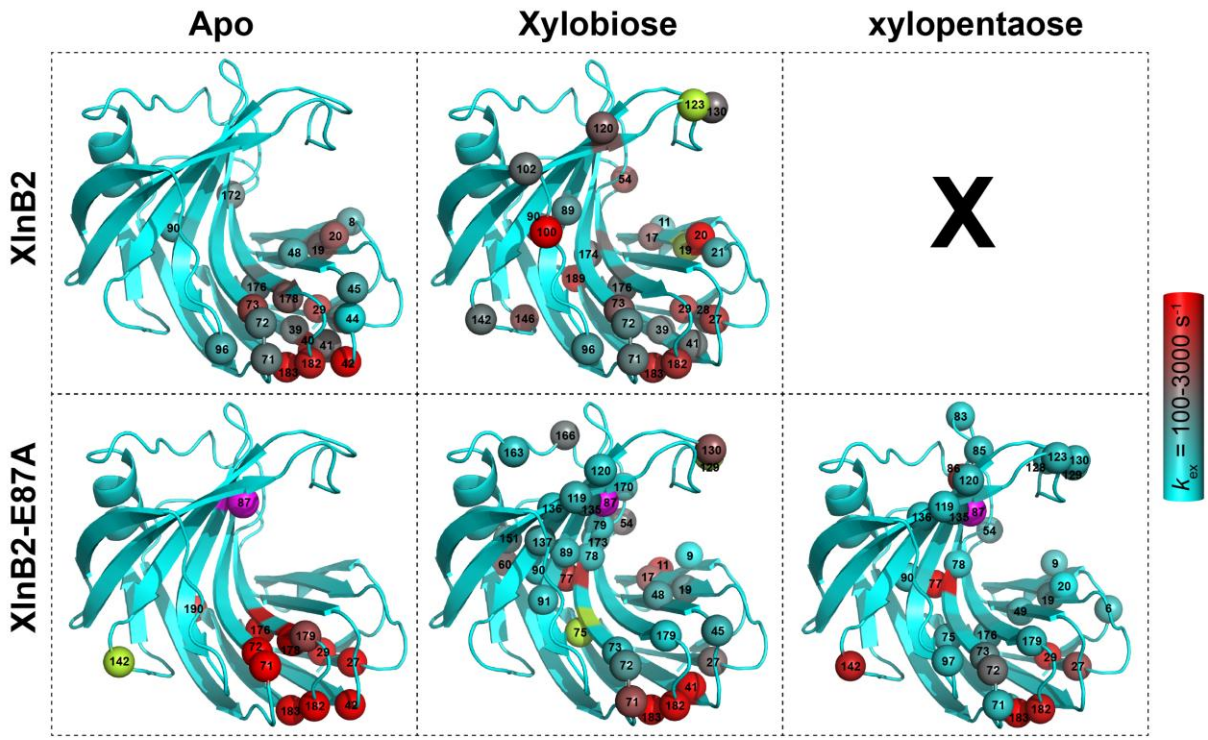

Figure 4. Residues experiencing microsecond-to-millisecond (μs-ms) conformational exchange in the free and bound forms of XlnB2 and XlnB2-E87A. Conformational exchange was probed using ^{15}N-CPMG relaxation dispersion for XlnB2 and its catalytically impaired variant E87A in the free and xylobiose-saturated (or xylopentaose-saturated) bound forms. Residues with a $\Delta R_2\,(1/\tau_{cp}) > 1.8\ s^{-1}$ are reported as spheres on the 3D structure of the enzyme. The color-graded scale represents the rate of conformational exchange (k_{ex}), calculated using the single quantum CPMG equation. Residues with a $\Delta R_2\,(1/\tau_{cp}) > 1.8\ s^{-1}$ for which a k_{ex} could not be extracted are colored in lime. The mutation site (E87A) is represented by a magenta-colored sphere. All images were prepared with PyMOL and graphics were produced with GraphPad Prism.

Anisotropic Network Model (ANM)

To offer a model describing the motions observed by NMR relaxation, we performed a simple anisotropic network modeling using the ANM web server application (http://anm.csb.pitt.edu), which can predict global motions of macromolecules (*40*). The predicted model confirms experimental motions observed on the millisecond timescale and suggests that the enzyme operates by a twisting mechanism to close the active-site cleft (Figure 5). This open-closed twist describes the simultaneous movement of the thumb-loop and fingers in opposite directions. According to this model, the thumb-loop and fingers would move back to their original position to initiate a new catalytic cycle once the reaction is completed. Further analyses are required to verify whether this motion is involved in substrate positioning and/or product release in XlnB2.

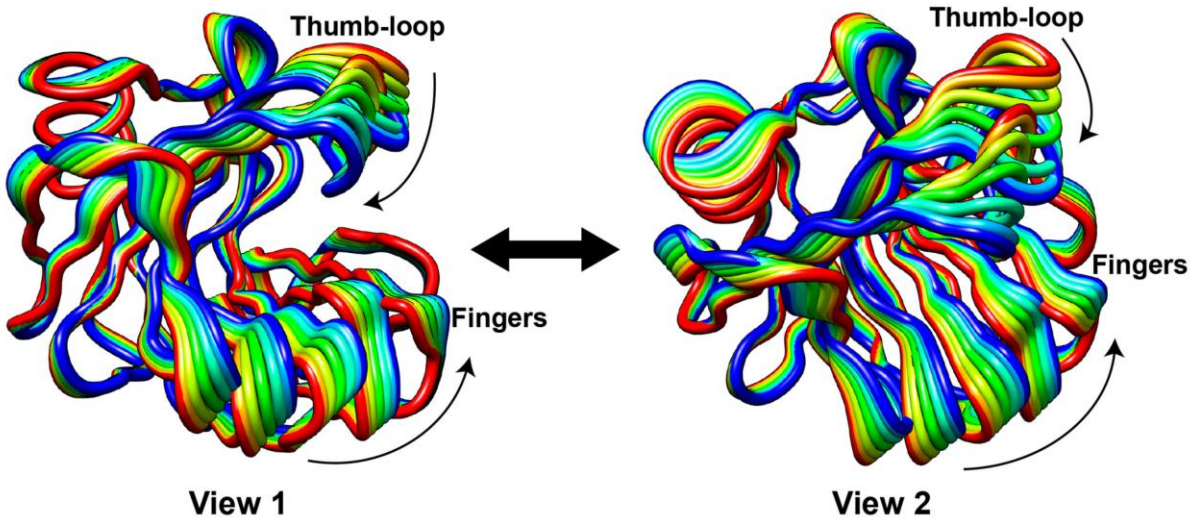

Figure 5. Proposed active-site dynamic model for XlnB2 from *Streptomyces lividans 66*. The vibrational motions were calculated using the Anisotropic Network Model (ANM) server (http://anm.csb.pitt.edu). Each color-graded ribbon represents a position as a function of time (from red to blue). Images were prepared with UCSF Chimera.

Discussion

Protein engineering involves the modification of an enzyme to impart a new or improved function. While the theoretical principles of protein engineering remain quite simple, important challenges still remain with respect to the targeting of relevant functional residues and the importance of predicting the functional role of flexibility events in enzyme activity. The field of protein dynamics is progressing fast, with real advances favored by the development of new NMR spectroscopy methodologies, in addition to constant improvements in bio-computational capabilities. These methods provide scientists with the ability to precisely measure atomic motions of proteins on a broad range of timescales, allowing one to picture motional events that could be liked to substrate binding and/or product release, either directly or indirectly involved in the catalytic step of the reaction (*41*). By gaining information on the atomic motions occurring during binding or catalysis, we hoped to bring forth significant evidence to demonstrate the importance of flexibility events in the design of improved xylanases, further facilitating the modification of their molecular properties.

Previous studies in GH11 family enzymes have illustrated the existence of fast ns-timescale motions in some xylanase members. In the present work, we showed that XlnB2 from *S. lividans* 66 also experiences conformational exchange around the active site on the catalytically relevant ms timescale. According to these results, the enzyme could adopt at least two conformational states, supporting the open-closed mechanism previously postulated (*18*). Our results corroborate the fact that the enzyme adopts an open conformation in its free form, where the thumb-loop remains rigid on the catalytic timescale. The presence of millisecond motions in the fingers and palm (near the fingers)—which are triggered upon substrate binding—might help the enzyme to bind to different substrate sizes. Our results also support the fact that

the active-site cleft closes upon binding, which involves the coordinated movement of the thumb-loop and fingers. This motion may also require the proper positioning of key residues of the thumb-loop to increase the binding and/or catalytic efficiency. The length of the substrate did not play a significant role in this motion, as evidenced by similar rates of conformational exchange observed in presence and absence of ligand. Interestingly, the movement of the thumb-loop requires the contribution of the hinge residue Thr120, located between the loop and the enzyme core. Despite not being directly involved in catalysis, mutagenesis studies confirmed the role of this residue in thumb-loop function, its mutation leading to reduced activity(*21*). Asp134 links the thumb-loop with the enzyme scaffold (Figure S3), but we could not observe any motion and/or significant chemical shift changes at this position. Previous studies performed on the GH11 xylanase from *Thermobacillus xylanilyticus* showed that its deletion leads to reduced catalytic activity, even though the reduction was much smaller ($k_{cat}/K_m \approx$ 15-fold) than for the replacement of Thr120 (*21*). Nevertheless, these results validate the critical importance of catalytic timescale motions linking Thr120 and the thumb-loop to control the open-closed mechanism of XlnB2, further improving our understanding of the catalytic reaction in GH11 xylanase family members.

References

1. Paes, G., Berrin, J. G., and Beaugrand, J. (2012) GH11 xylanases: Structure/function/properties relationships and applications, *Biotechnol Adv 30*, 564-592.
2. Uffen, R. L. (1997) Xylan degradation: a glimpse at microbial diversity, *J Ind Microbiol Biotechnol 19*, 1-6.

3. Bastawde, K. B. (1992) Xylan structure, microbial xylanases, and their mode of action, *World J Microbiol Biotechnol 8*, 353-368.

4. Viikari, L., Kantelinen, A., Sundquist, J., and Linko, M. . (1994) Xylanases in bleaching: From an idea to the industry, *FEMS Microbiol Rev 13*, 335-350.

5. Gilkes, N. R., Henrissat, B., Kilburn, D. G., Miller, R. C. Jr & Warren, R. A. J. (1991) Domains in microbial beta-1, 4-glycanases: sequence conservation, function, and enzyme families, *Microbiol Rev 55*, 303-315.

6. Henrissat, B., Davies, G. (1997) Structural and sequence-based classification of glycoside hydrolases, *Curr Opin Struct Biol 7*, 637-644.

7. Campbell R.L., R. D. R., Wakarchuk W.W., To R., Sung W., Yaguchi M. (1993) A comparison of the structures of the 20 kDa xylanases from *Trichoderma harzianum* and *Bacillus circulans*. In: Suominen P, Reinikainen T, eds. Proceedings of the second TRICEL symposium on Trichoderma reesei cellulases and other hydrolases., *Helsinki, Finland: Foundation for Biotechnical and Industrial Fermentation Research*, 63-72.

8. Torronen, A., Harkki, A., and Rouvinen, J. (1994) Three-dimensional structure of endo-1,4-beta-xylanase II from *Trichoderma reesei*: two conformational states in the active site, *EMBO J 13*, 2493-2501.

9. Torronen, A., and Rouvinen, J. (1995) Structural comparison of two major endo-1,4-xylanases from Trichoderma reesei, *Biochemistry 34*, 847-856.

10. McIntosh, L. P., Hand, G., Johnson, P. E., Joshi, M. D., Korner, M., Plesniak, L. A., Ziser, L., Wakarchuk, W. W., and Withers, S. G. (1996) The pKa of the general acid/base carboxyl group of a glycosidase cycles during catalysis: a 13C-NMR study of *Bacillus circulans* xylanase, *Biochemistry 35*, 9958-9966.

11. Connelly, G. P., and McIntosh, L. P. (1998) Characterization of a buried neutral histidine in Bacillus circulans xylanase: internal dynamics and interaction with a bound water molecule, *Biochemistry 37*, 1810-1818.

12. Plesniak, L. A., Connelly, G. P., Wakarchuk, W. W., and McIntosh, L. P. (1996) Characterization of a buried neutral histidine residue in *Bacillus circulans* xylanase: NMR assignments, pH titration, and hydrogen exchange, *Protein Sci 5*, 2319-2328.

13. Wakarchuk WW, C. R., Sung WL, Davoodi J, Yaguchi M. (1994a) Mutational and crystallographic analysis of the active site residues of the *Bacillus circulans* xylanase, *Protein Sci 3*, 467-475.

14. WakarchukWW, S., Campbell RL, CunninghamA,Watson DC, Yaguchi M. (1994b.) Thermostabilization of the *Bacillus subtilis* xylanase by the introduction of disulfide bonds, *Protein Eng 7*, 1379-1386.

15. Lawson, S. L., Wakarchuk, W. W., and Withers, S. G. (1997) Positioning the acid/base catalyst in a glycosidase: studies with *Bacillus circulans* xylanase, *Biochemistry 36*, 2257-2265.

16. Torronen, A., and Rouvinen, J. (1997) Structural and functional properties of low molecular weight endo-1,4-beta-xylanases, *J Biotechnol 57*, 137-149.

17. Vieira, D. S., Degreve, L., and Ward, R. J. (2009) Characterization of temperature dependent and substrate-binding cleft movements in *Bacillus circulans* family 11 xylanase: a molecular dynamics investigation, *Biochimica et biophysica acta 1790*, 1301-1306.

18. Muilu, J., Torronen, A., Perakyla, M., and Rouvinen, J. (1998) Functional conformational changes of endo-1,4-xylanase II from *Trichoderma reesei*: a molecular dynamics study, *Proteins 31*, 434-444.

19. Pollet, A., Vandermarliere, E., Lammertyn, J., Strelkov, S. V., Delcour, J. A., and Courtin, C. M. (2009) Crystallographic and activity-based evidence for thumb flexibility and its relevance in glycoside hydrolase family 11 xylanases, *Proteins 77*, 395-403.

20. Havukainen, R., Torronen, A., Laitinen, T., and Rouvinen, J. (1996) Covalent binding of three epoxyalkyl xylosides to the active site of endo-1,4-xylanase II from *Trichoderma reesei*, *Biochemistry 35*, 9617-9624.

21. Paes, G., Tran, V., Takahashi, M., Boukari, I., and O'Donohue, M. J. (2007) New insights into the role of the thumb-like loop in GH-11 xylanases, *Protein engineering, design & selection : PEDS 20*, 15-23.

22. Cervera, T. M., Andre-Leroux, G., Lafond, M., Georis, J., Juge, N., and Berrin, J. G. (2009) Molecular determinants of substrate and inhibitor specificities of the *Penicillium griseofulvum* family 11 xylanases, *Biochimica et biophysica acta 1794*, 438-445.

23. Murakami, M. T., Arni, R. K., Vieira, D. S., Degreve, L., Ruller, R., and Ward, R. J. (2005) Correlation of temperature induced conformation change with optimum catalytic activity in the recombinant G/11 xylanase A from *Bacillus subtilis* strain 168 (1A1), *FEBS letters 579*, 6505-6510.

24. Loria, J. P., Berlow, R. B., and Watt, E. D. (2008) Characterization of enzyme motions by solution NMR relaxation dispersion, *Acc Chem Res 41*, 214-221.

25. Hurtubise, Y., Shareck, F., Kluepfel, D., Morosoli, R. . (1995) A cellulase/xylanase-negative mutant of *Streptomyces lividans* 1326 defective in cellobiose and xylobiose uptake is mutated in a gene encoding a protein homologous to ATP-binding proteins, *Mol microbiol 17*, 367-377.

26. Kluepfel, D., Vats-Mehta, S., Aumont, F., Shareck, F., Morosoli, R. . (1990) Purification and characterization of a new xylanase (xylanase B) produced by *Streptomyces lividans* 66, *Biochem J 267*, 45-50.

27. Gauthier, C., Li, H., and Morosoli, R. (2005) Increase in xylanase production by *Streptomyces lividans* through simultaneous use of the Sec- and Tat-dependent protein export systems, *App Env Microbio 71*, 3085-3092.

28. Ho, S. N., Hunt, H. D., Horton, R. M., Pullen, J. K., and Pease, L. R. (1989) Site-directed mutagenesis by overlap extension using the polymerase chain reaction, *Gene 77*, 51-59.

29. Delaglio, F., Grzesiek, S., Vuister, G. W., Zhu, G., Pfeifer, J., and Bax, A. (1995) NMRPipe: a multidimensional spectral processing system based on UNIX pipes, *J Biomol NMR 6*, 277-293.

30. Grzesiek, S., Stahl, S. J., Wingfield, P. T., and Bax, A. (1996) The CD4 determinant for downregulation by HIV-1 Nef directly binds to Nef. Mapping of the Nef binding surface by NMR, *Biochemistry 35*, 10256-10261.

31. Mittermaier, A., and Meneses, E. (2013) Analyzing protein-ligand interactions by dynamic NMR spectroscopy, *Protein-Ligand Interactions: Methods in Molecular Biology 1008*, 243-266.

32. Carver, J. P., and Richards, R. E. (1972) A general two-site solution for the chemical exchange produced dependence of T_2 upon the Carr-Purcell pulse separation, *J. Magn. Reson. 6*, 89-105.

33. Vandermarliere, E., Bourgois, T.M., Rombouts, S., Van, C. S., Volckaert, G., Strelkov, S.V., Delcour, J.A., Rabijns A., and Courtin C.M. (2008) Crystallographic analysis shows substrate binding at the −3 to +1 active-site subsites and at the surface of glycoside hydrolase family 11 endo-1,4-β-xylanases, *Biochem J 410*, 71-79.

34. Goddard, T. D., and Kneller, D. G. (2008) Sparky, version 3, *University of California San Francisco (CA)*.

35. Axe, J. M., and Boehr, D. D. (2013) Long-range interactions in the alpha subunit of tryptophan synthase help to coordinate ligand binding, catalysis, and substrate channeling, *J Mol Biol 425*, 1527-1545.

36. Wakarchuk, W. W., Campbell, R.L., Sung, W.L., Davoodi, J, Yaguchi, M. (1994a) Mutational and crystallographic analysis of the active site residues of the *Bacillus circulans* xylanase, *Protein Sci 3*, 467-475.

37. Ludwiczek, M. L., D'Angelo, I., Yalloway, G. N., Brockerman, J. A., Okon, M., Nielsen, J. E., Strynadka, N. C., Withers, S. G., and McIntosh, L. P. (2013) Strategies for modulating the pH-dependent activity of a family 11 glycoside hydrolase, *Biochemistry 52*, 3138-3156.

38. Gutteridge, A., and Thornton, J. (2004) Conformational change in substrate binding, catalysis and product release: an open and shut case?, *FEBS letters 567*, 67-73.

39. Loria, J. P., Rance, M., and Palmer, A. G., 3rd. (1999) A relaxation-compensated Carr-Purcell-Meiboom-Gill sequence for characterizing chemical exchange by NMR spectroscopy, *J Am Chem Soc 121*, 2331-2332.

40. Eyal, E., Lum, G., and Bahar, I. (2015) The Anisotropic Network Model web server at 2015 (ANM 2.0), *Bioinformatics*.

41. Doucet, N., and Pelletier, J. N. (2009) Gaining insight into enzyme function through correlations with protein motions, In *Protein Engineering Handbook* (Lutz, S., and Bornscheuer, U. T., Eds.) 1st ed., pp 187-211, Wiley-VCH, Weinheim.

Supporting information

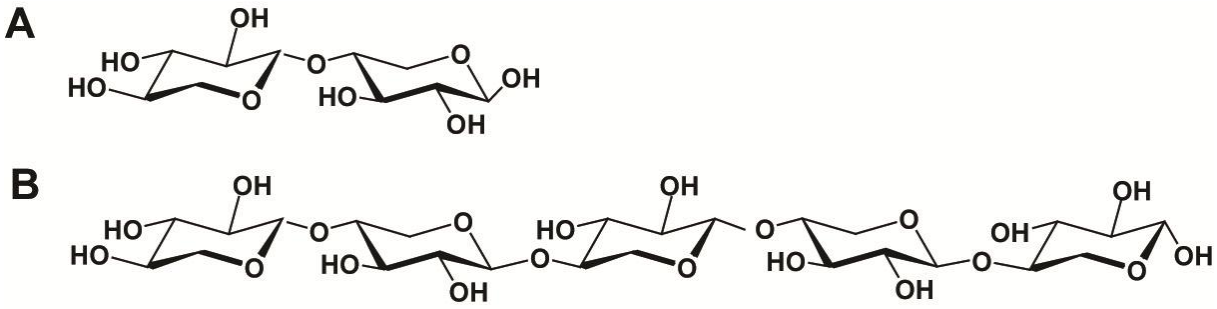

Figure S1. Chemical structures of the xylan molecules. (A) Xylobiose; (B) Xylopentaose.

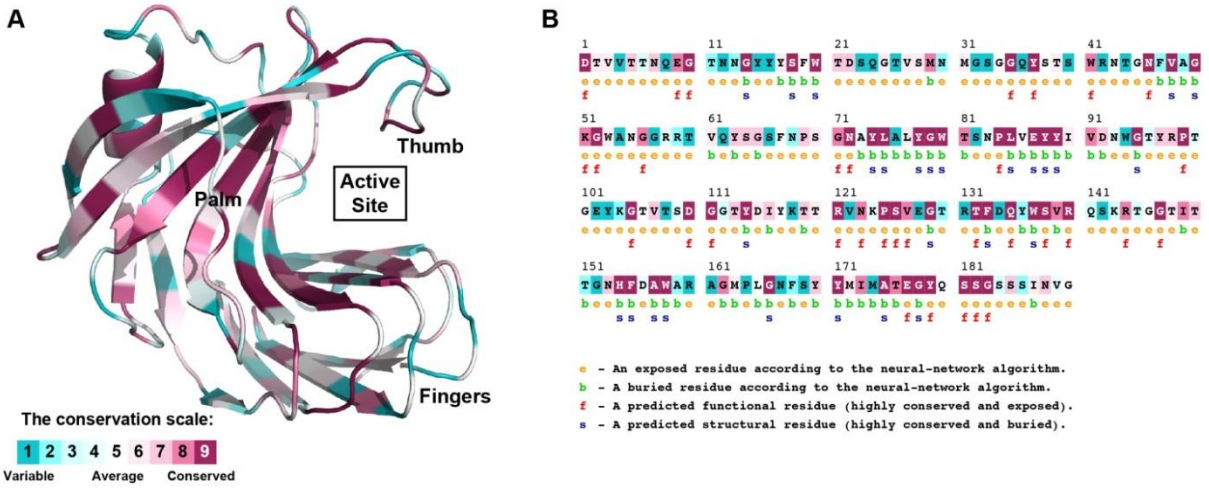

Figure S2. Evolutionary conservation of amino acid positions among GH11 family members. (A) Color-graded conservation score for residues of XlnB2. Color ramping is reported on the tridimensional structure of XlnB2; and (B) on its amino acid sequence. The structure was generated using the ConSurf server and PyMOL.

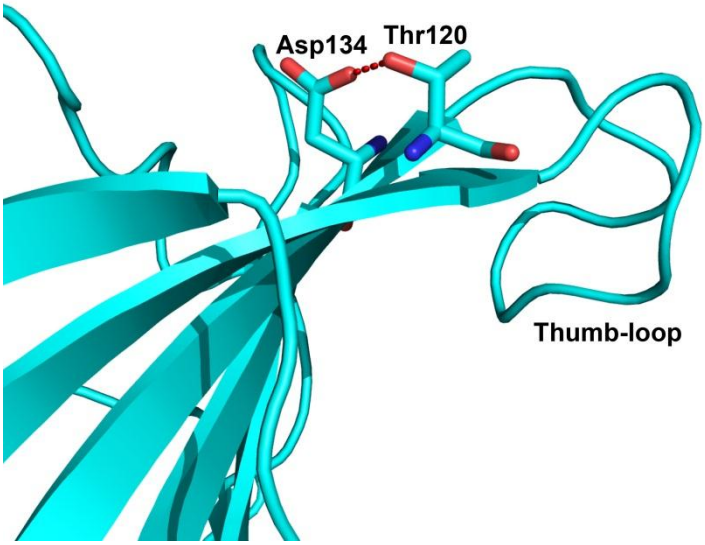

Figure S3. Molecular interactions between Thr120 and Asp134. Residues Thr120 and Asp134 are represented in sticks on the 3D structure of XlnB2. Carbon, nitrogen and oxygen atoms are colored in cyan, blue and red, respectively. The red dotted line identifies hydrogen bonding between the two residue side chains. The image was prepared using PyMOL.

3.3. Discussion

Our ^{15}N-CPMG results on the apo form of the WT XlnB2 and its mutant display the concerted motions on the fingers but do not show any movement on the thumb loop. The presence of ligands promotes additional motions on the opposite side of the fingers and on the thumb loop, which might change the active site capacity to undergo a loose conformation during catalysis. From all the results, it is possible to assume that the protein follows the open-closed propensity in the catalytic cycle, with consecutive different conformational states as hypothesized previously. In the apo form, the enzyme is in relaxing state or open conformation, ready for substrate binding. When substrate binds, it may proceed in concerted clamping motions in the active site and the thumb loop to form closed conformation for catalytic reaction. Once the product is synthesized, the protein loses its closed conformation to return to its relaxing state as in the apo form, opening the protein for the product to diffuse away.

Recently, the mechanism of ligand binding coupled to conformational changes has been described as two limiting cases: the "induced fit" and the "conformational selection" mechanism. In both cases, it is postulated that all protein conformations pre-exist in solution. In the induced fit mechanism, the ligand binds to the predominant free conformation followed by a conformational change in the protein to give the preferred ligand-bound conformation. Meanwhile in the "conformational selection" mechanism, the ligand selects the most favorable conformation that is present only in small amounts, eventually undergoing a population shift of conformations, redistributing the conformational states. In this mechanism, the binding interaction does not 'induce' a conformational change, therefore, in many cases, enzymes at every step select their proper conformation optimized for substrate binding, chemical reaction, and product release (*194-196*). In the case of XlnB2, ligand binding changes the protein dynamic landscape. This means that the binding does convert the protein into a form that resembles the substrate-bound form, which may be essential for catalysis. Besides, in all forms, population for each cluster calculated from experiencing conformational exchange residues is 80-99%. It would appear that substrate binding induces a conversion of protein conformation, meaning that XlnB2 may adopt an "induced fit mechanism".

Our ^{15}N-CPMG results have also shown that some conserved residues in the active site of XlnB2 did not experience conformational exchange, particularly the catalytic residues E87 and E177. In some other GH11 homologs, it was postulated that their active sites exhibit conformational change due to structural movement of catalytic residues, such as in xylanase XYNII from *Trichoderma reesei* (*217*) or E78Q-BCX from *Bacillus circulans* (*165*). This conformational exchange is thought to be necessary for both substrate binding and for the dissociation of the resulting non-covalent complex. In XlnB2-WT, no chemical exchange was observed on the nucleophile residue E87 (the other catalytic residue E177 was not assigned). In XlnB2-E87A, the acide/base residue E177 did not show any relaxation dispersion either. However, the mutated residue A87, the highly conserved residue Y78, and the residue T120 displayed dispersion. In fact, residue T120 was proposed to be flexible to play a role as a linker of the thumb loop (*167*). Many other conserved residues who play a role in substrate binding and adjacent residues showed relaxation perturbation, such as W20, N72, I90, T119, T176, and Y179. These observations suggest that despite the rigid catalytic residues, other conserved functional residues that are dynamic on the µs-ms time scale may play critical roles in the positioning and/or structural dynamics of catalytically relevant amino acid residues, building a dynamic amino acid network, and providing flexibility to the active site for executing binding and catalysis. This supports the concept that active-site residues are involved directly in chemical catalysis change networks depending protein is in ligand-free resting state or actively turning over substrate/products (*218*). In fact, these residues pave along the long active cleft of XlnB2, providing a favourable environment for penetrating of the polysaccharide, then holding and pushing simultaneously for sliding of the polymer in the catalytic reaction.

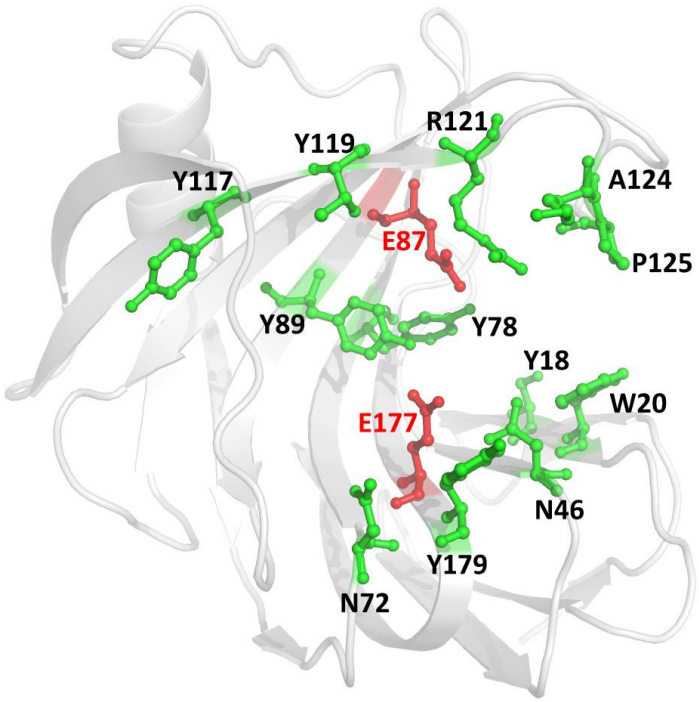

Figure 3.1. Conserved active-site residues (represented as sticks and spheres) mapped on the crystal structure of XlnB2. The catalytic residues are colored in red. Figure generated using PyMOL.

In biomass degradation, one of the most important properties playing a role in the conversion of polysaccharides is processivity. It has been suggested that several properties affecting the processivity are derived from the type of active site involved (deep and tunnel for processive, but wide pocket for nonprocessive) and the flexibility of the active site of the enzyme (*13*). With the proposed processive mechanism, the enzyme keeps binding to the polymer when product is expulsed, then, the lid closes on the enzyme. It has been suggested that the unbound subsites and other factors, such as loop movement, help to push the enzyme moving along the chain or the chain sliding along the active site for the ensuing cleavage to occur (*74*). In the case of XlnB2, the thumb loop together with the palm structurally creates an active site. It was clearly observed in the CPMG experiments that the thumb loop moves upon the binding of the substrate on the catalytic timescale. By anisotropic network modeling (ANM), it is proposed that the direction of movement of the fingers and the thumb is upward/downward for opening/closing the active cleft. Therefore, it may be assumed that the movement of the thumb and fingers provides the driving force for the enzyme or the chain to keep moving after each cleavage occurs in the processive mechanism.

In short, the results of this work confirm the importance of local and global motions in ligand binding and catalysis. The thumb loop flexibility assisting substrate binding and catalysis could provide a clue or a starting point for enzyme mutagenesis to improve its flexibility, hence, enhancing enzyme activity. Indeed, GH11 engineering has brought much information relating their structure and flexibility for enhancement of thermostability as well as enzyme activity. For example, the rigidity of the α-helix can contribute to thermostabilty even though this may reduce catalytic activity (*163*). Also, in particular GH11 members, the length and flexibility of the thumb loop play an important role in enzyme thermostability and enzyme activity (*167, 168*). Thus, the comprehensive knowledge obtained on the motional characterization of XlnB2 could be a meaningful contribution to designing improved catalysts.

CHAPTER 4. CONCLUSIONS AND PERSPECTIVES

4.1. Conclusions

Chitin and xylan show great potential as sustainable energy resources for enzymatic conversion of biomass into bioactive compounds, which can be widely used in a number of areas such as bioethanol production, food or non-food industry, medicine, and cosmetics. However, despite a number of studies reporting on the prospect and feasibility of bioconversion of these polysaccharides, limited processes are applied in industry due to the recalcitrance of the biopolymer. Because of the high industrial demand for environmentally friendly and cost-effective biomass conversion technologies, finding microbial organisms and secreted robust enzymes which can effectively convert the insoluble polymers as well as understanding the enzymatic systems working could bring essential knowledge to be applied later in the industry. Also, because of the highly complex nature of biomass, the functional diversity of enzymes as well as their natural flexibility, efficient use of enzymes requires a molecular insight on the structure-function-flexibility relationship of their catalytic mechanism to improve their efficiency.

In the context of valuable molecule manufacturing, our work has revealed a promising strategy of using an enzyme complex in the first place for GlcNAc production from abundant sources of chitin. *Sc*HEX and ChiC from *S. coelicolor* A3(2), with high activity toward chitooligomers and crude crystalline chitins, were successfully expressed and characterized. The combination of supernatants of *Sc*HEX and ChiC in an assay with raw chitin allowed for the production of GlcNAc as a final product with a yield of 90% after 8h of incubation, leading to an efficient way for the industrial production of pure GlcNAc. Moreover, the secretion of ChiC and *Sc*HEX with high yields and high purity (after overexpression by the *S. lividans* 10-164 expression system), requiring no further purification steps, allows the enzymes to meet the requirements for effectiveness and inexpensiveness of biocatalysts in green chemistry. Therefore, the enzyme system developed in this work should be advantageous for industrial applications.

Making use of an unlimited and renewable resource like chitin in enzymatic conversion of biomass for producing valuable molecules is an economic and environmentally friendly strategy that could replace chemical synthesis. Due to the recalcitrant nature of chitin, it is meaningful to find effective enzymes for bioconversion of the biomass. However, in

order to maximize the use of enzymes for such applications, it is necessary to study the fundamental mechanisms that govern biomass breakdown. We have shown that the synergistic action of ChiC – a chitinase that can depolymerize the long and insoluble substrates, and *Sc*HEX – a robust enzyme that can significantly and irreversibly transform chitooligomers into monomers, is essential for the full degradation of chitin. Moreover, by HPLC, we have observed that ChiC acts as an endo non-processive enzyme, which could be an efficient mode in terms of enzyme speed when acting on long-chain substrates. The additional CBM in ChiC could be a factor that could help disrupt the stack and recalcitrance of chitin, assisting ChiC in substrate binding and catalysis. These observations should be useful for choosing an appropriate enzyme system for biomass degradation. Our work also pointed out that *Sc*HEX is an exo-acting enzyme that excellently cleaves chitooligomers from the reducing end. Crystal structures of the native *Sc*HEX and mutant *Sc*HEX-E314Q have been resolved in order to understand the catalytic mechanism of the chitooligosaccharide hydrolysis, which is the substrate-assisted mechanism. The crystallographic results obtained with the fluctuation of loop 3 of *Sc*HEX also emphasized the importance of enzyme dynamics in catalysis. Moreover, enzyme flexibility is also suggested to be significant for ChiC efficiency when acting in a non-processive mode.

Finally, to further elucidate the importance of enzyme flexibility, considerable achievements have been reached with respect to the internal dynamics of protein during catalysis. NMR experiments carried out with XlnB2 and XlnB2-E87A illuminated the atomic scale dynamics of the xylanase. In the apo form, flexibility of the fingers clearly occurs on the time scale of catalysis. In the presence of ligands, the finger motions are retained while emerging dynamics on the thumb loop and the area surrounding the active cleft appear, suggesting a global clamping movement on the catalytic time frame. Data support the open-closed movement hypothesis of the active site and the thumb during ligand binding and catalysis. This information could be beneficial to enzyme engineering in bio-refining applications.

In general, this work not only demonstrates one the most efficient enzymatic systems for the bioconversion of abundant chitin but also broadens our knowledge about biomass degradation. Acting on biopolymers, a synergistic action of several enzymes is required. Besides, processivity is important for the enzymes hydrolyzing insoluble substrates but non-

processivity is more effective in terms of enzyme speed. Additionally, enzyme flexibility is one of the central factors that could play an important role in substrate binding and catalysis and could also help to promote activity of the enzymes degrading polysaccharides. The results obtained indicate the relationship between structure, function and enzyme flexibility of the GH enzymes in biomass degradation.

4.2. Perspectives

The common goal of every enzyme study is to find and improve biocatalysts for wide human demands. The idea that we may be able to modify an enzyme to modulate its enzymatic function is fascinating. Enzyme engineering for enzymatic processes is designed not only based on the available properties of enzymes but it is also designed to fit process' specifications. For that purpose, the properties of effective, stable, selective and productive catalysts working under specific conditions are required to minimize costs and lead to feasible applications (*219*). Generally, kinetic, structural and other mechanistic data are sufficient for enzyme characterization. However, to fit the manufacturing process, other information and also enzyme engineering, such as third generation biocatalysts, are often required. Key approaches for engineering this new generation of biocatalysts are based on directed evolution, sequence analysis, gene synthesis, bioinformatic tools, and computer modeling (*219*). These approaches could be employed to develop our obtained results for feasible and applicable use in GlcNAc production or other platform molecule manufacturing.

Results obtained for ChiC and *Sc*HEX showed that using this mixture of enzymes, GlcNAc could be produced with final yield of 9.5 g/L in 8 hours. The yield is rather high compared to other systems reported previously. However, the total amount of enzyme used was 2 mg/L, which is high. Even though ChiC and *Sc*HEX are secreted with high yields, in order to use them in an application, it is necessary to enhance enzyme activity to reduce the total amount of enzymes used. The fact that both enzymes have optimal working conditions at 55^{o}C but are not stable for a long time at this temperature could be one of the reasons which limited the enzyme activity. Therefore, it is also necessary to improve enzyme thermostability. Nevertheless, such a high temperature can be another concern regarding the application of this enzyme system at a large-scale production. In fact, if the reactions have to

occur at 55^{o}C, this high temperature may cause many disadvantages including high cost and wasted energy. As a result, it could be more beneficial for large-scale applications, if the enzyme activity can reach its maximum at a lower temperature. For those purposes, identification of key residues or regions for enzyme activity or stability which can be obtained from literature, sequence alignment and also from known structural data should be acquired. From resolved crystal structures of *Sc*HEX together with data from its homologs, it has been shown that Asp301, Glu302, Trp332, Trp349, Trp396, Trp430, Val 287 and Trp437 are crucial residues for binding to long substrates and also for processivity, which is proven to be beneficial for enzyme acting on soluble chitinolytic substrates. The loop 3 from residue 299 to residue 308 of *Sc*HEX – a special motif which displays fluctuation in ligand binding, could be an important factor affecting enzyme activity. These residues and this loop could be the targets for a semi-rational mutation approach in order to make a library of variants, which could help identify and design significant, desired candidates with better activity and thermostability. Besides, enzyme immobilization and product purification and separation methods should be studied to find an overall solution for obtaining pure GlcNAc.

Furthermore, crystal structures of ChiC in its native form and in complex with long ligands should be obtained to determine some structural hallmarks for the non-processive mechanism and also important residues and structural motifs in substrate binding and catalytic mechanisms. The resolvable structures could elucidate the important factors associated with the carbohydrate-binding domain of ChiC, which play a role in the disruption of the insoluble substrate. The obtainable results could also give more information about the role of enzyme flexibility in the context of a non-processive mechanism.

Additionally, as part of the last objective, the crystal structure of XlnB2-WT was resolved, showing the highly conserved β-jelly roll domain, which presents a closed right-handed architecture. The result provides exact information on the position of each amino acid in the scaffold that is excellently assistant and supplemental to NMR results. However, no information about the exact residues that bind to or interact with ligands/substrates was obtained. Therefore, structures of XlnB2-WT and XlnB2-E87A in complexes with short and long ligands are required to clarify the interaction between the enzymes and the ligands/substrates, hence, to elucidate the catalytic mechanism of the enzymes. The study should confirm the description of the expected active site and ligand binding site that were

predicted by NMR data in Article 3. The study might also help to supplement the lack of information about the aglycon subsites of GH11 xylanases that is important for understanding the catalytic mechanism of the enzymes in branched xylan or heteroxylan degradation.

Results from Article 3 demonstrate the motion of the thumb loop when bound to xylobiose/xylopentaose. These substrates are comprised of two/five units of xylose that are linear but not branched substrates of xylanases. In fact, the natural substrate for xylanase is heteroxylan consisting of a repeating β-1,4-linked xylose backbone branched with acetyl, arabinofuranosyl, and 4-O-methyl glucuronyl groups. Heteroxylan, when bound in the active site of xylanase, may cover more than 5 subsites, which is the number of subsites formed from the binding with xylopentaose. Therefore, a CPMG for XlnB2-E87A bound with oat xylan could be a good experiment to uncover the dynamic property of the enzyme upon the binding of naturally long substrates. Even though the enzyme could not saturately bind to xylan in the solution due to the substrate's high molecular weight, the experiment with unsaturated binding might give useful information to answer the above question. Finally, uncovering protein flexibility coupled with previous reported studies may provide more information to understand the functional diversity of GH11 xylanases showing their structural conservation.

REFERENCES

1. Clark, J. H., Luque, R., and Matharu, A. S. (2012) Green chemistry, biofuels, and biorefinery, *Annu Rev Chem Biomol Eng 3*, 183-207.
2. Chen, J. K., Shen, C. R., and Liu, C. L. (2010) *N*-Acetylglucosamine: Production and applications, *Mar. Drugs 8*, 2493-2516.
3. Alves, N. M., and Mano, J. F. (2008) Chitosan derivatives obtained by chemical modifications for biomedical and environmental applications, *Int J Biol Macromol 43*, 401-414.
4. Merino, S. T., and Cherry, J. (2007) Progress and challenges in enzyme development for biomass utilization, *Adv Biochem Eng Biotechnol 108*, 95-120.
5. Creamer, P. (2000) Osteoarthritis pain and its treatment, *Curr Opin Rheumatol 12*, 450-455.
6. Tamaia, Y., Miyatakea, K., Okamotoa, Y., Takamorib, Y., Sakamotob, K., and Minamia, S. (2003) Enhanced healing of cartilaginous injuries by *N*-acetyl-D-glucosamine and glucuronic acid, *Carbohyd Polym 54*, 251-262.
7. Burtan, A. F., and Freeman, H. J. (1993) *N*-Acetyl glucosamine as a gastroprotective agent, *WO Patent NO. 9323055*.
8. Salvatore, S., Heuschkel, R., Tomlin, S., Davies, S. E., Edwards, S., Walker-Smith, J. A., French, I., and Murch, S. H. (2000) A pilot study of N-acetyl glucosamine, a nutritional substrate for glycosaminoglycan synthesis, in paediatric chronic inflammatory bowel disease, *Aliment Pharmacol Ther 14*, 1567-1579.
9. Louise, C. A., Pedro, A., and Charles, A. H. (1999) Process for producing *N*-acetyl-D-glucosamine, *US Patent NO. 5998173*.
10. Dodd, D., and Cann, I. K. (2009) Enzymatic deconstruction of xylan for biofuel production, *Glob Change Biol Bioenergy 1*, 2-17.
11. Paes, G., Berrin, J. G., and Beaugrand, J. (2012) GH11 xylanases: Structure/function/properties relationships and applications, *Biotechnol Adv 30*, 564-592.
12. Eijsink, V. G., Vaaje-Kolstad, G., Vårum, K.M., and Horn, S.J. (2008) Towards new enzymes for biofuels: lessons from chitinase research, *Trends Biotechnol. 26*, 228-235.
13. Payne, C. M., Baban, J., Horn, S. J., Backe, P. H., Arvai, A. S., Dalhus, B., Bjoras, M., Eijsink, V. G., Sorlie, M., Beckham, G. T., and Vaaje-Kolstad, G. (2012) Hallmarks of processivity in glycoside hydrolases from crystallographic and computational studies of the *Serratia marcescens* chitinases, *J Biol Chem 287*, 36322-36330.
14. Gallezot, P. (2012) Conversion of biomass to selected chemical products, *Chem Soc Rev 41*, 1538-1558.

15. Spellman, F. (2012) Forest-Based Biomass Energy: Concepts and Applications, p 229, CRC Press.

16. Zakariassen, H., Aam, B. B., Horn, S. J., Varum, K. M., Sorlie, M., and Eijsink, V. G. (2009) Aromatic residues in the catalytic center of chitinase A from *Serratia marcescens* affect processivity, enzyme activity, and biomass converting efficiency, *J Biol Chem 284*, 10610-10617.

17. Cohen, E. (2010) Chitin biochemistry: synthesis, hydrolysis and inhibition, *Adv Insect Physiol 38*, 5-74.

18. Tharanathan, R. N., and Kittur, F. S. (2003) Chitin--the undisputed biomolecule of great potential, *Crit Rev Food Sci Nutr 43*, 61-87.

19. Howard, M. B., Ekborg, N.A., Weiner, R.M., Hutcheson, S.W. (2003) Detection and characterization of chitinases and other chitin-modifying enzymes, *J Ind Microbiol Biotechnol 30*, 627-635.

20. Kurita, K. (2006) Chitin and chitosan: Functional biopolymers from marine *Crustaceans*, *Mar Biotechnol 8*, 203-226.

21. Jang, M. K., Kong, B. G., Jeong, Y. I., Lee, C. H. and Nah, J. W. (2004) Physicochemical characterization of α-chitin, β-chitin, and γ-chitin separated from natural resources, *J Polym Sci 42*, 3423-3432.

22. Morley, K. L., Chauve, G., Kazlauskas, R., Dupont, C., Shareck, F., Marchessault, R.H. (2006) Acetyl xylan esterase-catalyzed deacetylation of chitin and chitosan, *Carbohydr Polym 63*, 310-315.

23. Imai, T., Watanabe, T., Yui, T., and Sugiyama, J. (2003) The directionality of chitin biosynthesis: a revisit, *Biochem J 374*, 755-760.

24. Cohen-Kupiec, R., Chet, I. (1998) The molecular biology of chitin digestion, *Curr Opin Biotechnol 9*, 270-277.

25. Synowiecki, J., and Al-Khateeb, N. A. (2003) Production, properties, and some new applications of chitin and its derivatives, *Crit Rev Food Sci Nutr 43*, 145-171.

26. Liu, D., Wei, Y., Yao, P. & Jiang, L. (2006) Determination of the degree of acetylation of chitosan by UV spectrophotometry using dual standards, *Carbohydr Res 341*, 382-385.

27. Gooday, G. W., Zhu, W. Y., O'Donnell, R. (1992) What are the roles of chitinases in the growing fungus?, *FEMS Microbiol Lett 100*, 387-392.

28. Beckham, G. T. C., M. F. (2011) Examination of the alpha-chitin structure and decrystallization thermodynamics at the nanoscale, *J Phys Chem B 115*, 4516-4522.

29. Horn, S. J., Sikorski, P., Cederkvist, J.B., Vaaje-Kolstad, G.,Sørlie, M., Synstad, B., Vriend, G., Vårum, K. M., and Eijsin, V.G.H. (2006) Costs and benefits of processivity in enzymatic degradation of recalcitrant polysaccharides, *PNAS 103*, 18089-18094.

30. Fushinobu, S. (2014) Metalloproteins: A new face for biomass breakdown, *Nat Chem Biol 10*, 88-89.

31. Vaaje-Kolstad, G., Westereng, B., Horn, S. J., Liu, Z., Zhai, H., Sorlie, M., and Eijsink, V. G. (2010) An oxidative enzyme boosting the enzymatic conversion of recalcitrant polysaccharides, *Science 330*, 219-222.

32. Sahai, A. S., Manocha, M.S. (1993) Chitinases of fungi and plant: their involvement in morphogenesis and host-parasite interaction, *FEMS Microbiol Rev 11*, 317-338.

33. Horsch, M., Mayer, C., Sennhauser, U., Rast, D.M. (1997) β-*N*-acetylhexosaminidase: a target for the design of antifungal drugs, *Pharmacol Ther 76*, 187-218.

34. Duo-Chuan, L. (2006) Review of fungal chitinases, *Mycopathologia 161*, 345-360.

35. Seidl, V. (2008) Chitinases of filamentous fungi: a large group of diverse proteins with multiple physiological functions, *Fungal Biol Rev 22*, 36-42.

36. Rast, D. M., Baumgartner, D., Mayer, C., and Hollenstein, G. O. (2003) Cell wall-associated enzymes in fungi, *Phytochemistry 64*, 339-366.

37. Rast, D. M., Horsch, M., Furter, R., Gooday, G. W. (1991) A complex chitinolytic system in exponentially growing mycelium of *Mucor rouxii:* properties and function, *J Gen Microbiol 137*, 2797-2810.

38. Slamova, K., Bojarova, P., Petraskova, L., Kren, V. (2010) β-*N*-acetylhexosaminidase: what's in a name...?, *Biotechnol Adv 28*, 682-693.

39. Lunetta, J. M., Johnson, S. M., Pappagianis, D. (2010) Molecular cloning, characterization and expression analysis of two β-*N*-acetylhexosaminidase homologs of *Coccidioides posadasii*, *Med Mycol 48*, 744-756.

40. Mandel, M. A., Galgiani, J. N., Kroken, S., Orbach, M. J. . (2006) *Coccidioides posadasii* contain single chitin synthase genes corresponding to classes I to VII, *Fungal Genet Biol 43*, 775-788.

41. Cole, G. T., Hung, C. Y. (2001) The parasitic cell wall of *Coccidiodes immitis*, *Med Mycol 39*, 31-40.

42. Okada, T., Ishiyama, S., Sezutsu, H., Usami, A., Tamura, T., Mita, K., Fujiyama, K., Seki, T. (2007) Molecular cloning and expression of two novel β-*N*-acetylglucosaminidases from silkworm *Bombyx mori*, *Biosci Biotechnol Biochem 71*, 1626-1635.

43. Aumiller, J. J., Hollister, J. R., Javis, D. L. (2006) Molecular cloning and functional characterization of β-*N*-acetylglucosaminidase genes from Sf9 cells, *Protein Expr Purif 47*, 571-590.

44. Danishefsky, I., Steiner, H., Bella, A., Jr., and Friedlander, A. (1969) Investigations on the chemistry of heparin. VI. Position of the sulfate ester groups, *J Biol Chem 244*, 1741-1745.

45. Bhavanandan, V. P., and Meyer, K. (1966) Mucopolysaccharides: *N*-acetylglucosamine- and galactose-6-sulfates from keratosulfate, *Science 151*, 1404-1405.

46. Dai, D. H., Hu, W.L., Huang, G.R., and Li, W. (2011) Purification and characterization of a novel extracellular chitinase from thermophilic *Bacillus* sp. Hu1, *African J. Biotechnol 10*, 2476-2485.

47. Natasa, J., Barbara, K, Helena, L, Katja, B. (2006) Purification and molecular characterization of chitin deacetylase from *Rhizopus nigricans.*, *Enzyme Microb Technol 39*, 1294-1299.

48. Sashiwa, H., Fujishima, S., Yamano, N., Kawasaki, N., Nakayama, A., Muraki, E., Hiraga, K., Oda, K., Aiba, S. . (2002) Production of *N*-Acetyl-D-glucosamine from α-chitin by crude enzymes from *Aeromonas hydrophila* H2330, *Carbohydr Res 337*, 761-763.

49. Pichyangkura, R., Kudan, S., Kuttiyawang, K., Sukwattanasinitt, M., Aiba, S. . (2002) Quantitative production of 2-Acetoamodo-2-D-glucose from crystalline chitin by bacterial chitinase., *Carbohydr Res 337*, 557-559.

50. Nagpure, A., and Gupta, R. K. (2013) Purification and characterization of an extracellular chitinase from antagonistic *Streptomyces violaceusniger*, *J Basic Microbiol 53* 429-439.

51. Suresh, P. V. (2012) Biodegradation of shrimp processing bio-waste and concomitant production of chitinase enzyme and *N*-acetyl-D-glucosamine by marine bacteria: production and process optimization, *World J Microbiol Biotechnol 28*, 2945-2962.

52. Sashiwa, H., Fujishimaa, S., Yamanoa, N., Kawasakia, N., Nakayamaa, A., Murakia, E., Sukwattanasinittb, M., Pichyangkurac, Aibaa, S. (2003) Enzymatic production of *N*-acetyl-D-glucosamine from chitin. Degradation study of *N*-acetylchitooligosaccharide and the effect of mixing of crude enzymes, *Carbohydr Pol 51*, 391-395.

53. Jamialahmadi, K., Behravan, J., Fathi, N.M., Tabatabai, Y.M., Shahverdi, A.R., and Faramarzi, M. A. (2011) Enzymatic production of *N*-Acetyl-D-Glucosamine from chitin using crude enzyme preparation of *Aeromonas* sp. PTCC1691, *Biotechnology 10*, 292-297.

54. Sashiwa, H. F., S.; Yamano, N.; Kawasaki, N.; Nakayama, A.; Muraki, E.; Aiba, S. (2001a) Production of *N*-acetyl-D-glucosamine from β−chitin by enzymatic hydrolysis, *Chem Lett*, 308-309.

55. Chern, L. L., Stackebrandt, E., Lee, S. F., Lee, F. L., Chen, J. K., and Fu, H. M. (2004) Chitinibacter tainanensis gen. nov., sp. nov., a chitin-degrading aerobe from soil in Taiwan, *Int J Syst Evol Microbiol 54*, 1387-1391.

56. Rifaat, H. M., Nagieb, Z. A., and Ahmed, Y. M. . (2006) Production of xylanases by *Streptomyces* species and their bleaching efect on rice straw pulp, *App Eco Environ Resear 4*, 151-160.

57. Petterson, R. C. (1984) The chemical composition of wood. - In: The chemistry of Solid Wood, Wowell, R. M. (Ed.), Advanced in Chemistry Series, 207, *American Chemical Society Washington, D. C*, 57-126.

58. http://en.wikipedia.org/wiki/Xylan. (2010).

59. Pollet, A., Delcour, J. A., and Courtin, C. M. (2010) Structural determinants of the substrate specificities of xylanases from different glycoside hydrolase families, *Crit Rev Biotechnol 30*, 176-191.

60. Taylor, E. J., Gloster, T. M., Turkenburg, J. P., Vincent, F., Brzozowski, A. M., Dupont, C., Shareck, F., Centeno, M. S., Prates, J. A., Puchart, V., Ferreira, L. M., Fontes, C. M., Biely, P., and Davies, G. J. (2006) Structure and activity of two metal ion-dependent acetylxylan esterases involved in plant cell wall degradation reveals a close similarity to peptidoglycan deacetylases, *J Biol Chem 281*, 10968-10975.

61. Uffen, R. L. (1997) Xylan degradation: a glimpse at microbial diversity, *J Ind Microbiol Biotechnol 19*, 1-6.

62. He, L., Bickerstaff, G. F., Paterson, A. and Buswell, J. A. (1993) Purification and partial characterisation of two xylanases that differ in hydrolysis of soluble and insoluble xylan fractions, *Enzyme Microb Technol 15*, 13-18.

63. Zhang, J., Siika-Aho, M., Puranen, T., Tang, M., Tenkanen, M., and Viikari, L. (2011.) Thermostable recombinant xylanases from *Nonomuraea lexuosa* and *Hermoascus aurantiacus* show distinct properties in the hydrolysis of xylans and pretreated wheat straw, *Biotechnol Biofuels 4*.

64. Brzezinski, R., Dery, C. V., and Beaulieu, C. (1999) Thermostable xylanase DNA, protein and methods in use, *USA patent 5871730*.

65. http://www.cazy.org/Glycoside-Hydrolases.html.

66. Davies, G. J., Gloster, T. M., Henrissat, B. (2005) Recent structural insights into the expanding world of carbohydrate-active enzymes, *Curr Opin Struct Biol 15*, 637-645.

67. Cantarel, B. L., Coutinho, P.M., Rancurel, C., Bernard, T., Lombard, V., Henrissat, B. (2009) The carbohydrate-active enzymes database (Cazy): an expert resource for glycogenomic, *Nucleic Acids Res. 37*, D233-D238.

68. Zhao, Y., Park, R. D., and Muzzarelli, R. A. A. (2010) Chitin deacetylases: Properties and applications, *Mar Drugs 8*, 24-46.

69. Sørlie, M., Zakariassen, H., Norberg, A. L. & Eijsink, V. G. H. (2012) Processivity and substrate-binding in family 18 chitinases, *Biocatal Biotransform 30* 353-365.

70. Davies, G. J., Planas, A., and Rovira, C. (2012) Conformational analyses of the reaction coordinate of glycosidases, *Acc Chem Res 45*, 308-316.

71. Horn, S. J., Sorbotten, A., Synstad, B., Sikorski, P., Sorlie, M., Varum, K. M., and Eijsink, V. G. (2006) Endo/exo mechanism and processivity of family 18 chitinases produced by *Serratia marcescens*, *The FEBS journal 273*, 491-503.

72. Zhou, W., Irwin, D. C., Escovar-Kousen, J., and Wilson, D. B. (2004) Kinetic studies of *Thermobifida fusca* Cel9A active site mutant enzymes, *Biochemistry 43*, 9655-9663.

73. Koivula, A., Kinnari, T., Harjunpaa, V., Ruohonen, L., Teleman, A., Drakenberg, T., Rouvinen, J., Jones, T. A., and Teeri, T. T. (1998) Tryptophan 272: an essential

determinant of crystalline cellulose degradation by *Trichoderma reesei* cellobiohydrolase Cel6A, *FEBS Lett 429*, 341-346.

74. Davies, G., and Henrissat, B. (1995) Structures and mechanisms of glycosyl hydrolases, *Structure 3*, 853-859.

75. Mark, B. L., Vocadlo, D. J., Knapp, S., Triggs-Raine, B. L., Withers, S. G., James, M. N. . (2001) Crystallographic evidence for substrate-assisted catalysis in a bacterial β-hexosaminidase, *J Biol Chem Commun (Camb) 276*, 10330-10337.

76. Williams, S. J., Mark, B. L., Vocadlo, D. J., James, M. N. G., and Withers, S. G. (2002) Aspartate 313 in the *Streptomyces plicatus* hexosaminidase plays a critical role in substrate-assisted catalysis by orienting the 2-acetamido group and stabilizing the transition state, *J Biol Chem 277*, 40055-40065.

77. Hiromi, K. (1970) Interpretation of dependency of rate parameters on the degree of polymerization of substrate in enzyme-catalyzed reactions. Evaluation of subsite affinities of exo-enzyme, *Biochem Biophys Res Commun 40*, 1-6.

78. Hiromi, K., Nitta, Y., Numata, C., and Ono, S. (1973) Subsite affinities of glucoamylase: examination of the validity of the subsite theory, *Biochim Biophys Acta 302*, 362-375.

79. Thoma, J. A., and Allen, J. D. (1976) Subsite mapping of enzymes: collecting and processing experimental data--a case study of an amylase-malto-oligosaccharide system, *Carbohydr Res 48*, 105-124.

80. Allen, J. D. (1980) Subsite mapping on enzymes: application to polysaccharide depolymerases, *Methods Enzymol 64*, 248-277.

81. Davies, G. J., Wilson, K. S., and Henrissat, B. (1997) Nomenclature for sugar-binding subsites in glycosyl hydrolases, *Biochem J 321 (Pt 2)*, 557-559.

82. Saito, A., Shinya, T., Miyamoto, K., Yokoyama, T., Kaku, H., Minami, E., Shibuya, N., Tsujibo, H., Nagata, Y. (2007) The *dasABC* Gene Cluster, Adjacent to *dasR*, Encodes a Novel ABC Transporter for the Uptake of *N,N*,-Diacetylchitobiose in *Streptomyces coelicolor* A3(2), *Appl Environ Microbiol 73*, 3000-3008.

83. Saito, A., Fujii, T., Shinya, T., Shibuya, N., Ando, A., and Miyashita, K. (2008) The *msiK* gene, encoding the ATP-hydrolysing component of *N,N*9-diacetylchitobiose ABC transporters, is essential for induction of chitinase production in *Streptomyces coelicolor* A3(2), *Microbiology 154*, 3358-3365.

84. Bhattacharya, D., Nagpure, A., and Gupta, R. K. (2007) Bacterial chitinases: properties and potential, *Crit Rev Biotechnol 27*, 21-28.

85. Dahiya, N., Tewari, R., Hoondal, G. S. (2006) Biotechnological aspects of chitinolytic enzymes: a review *App Microbiol Biotechnol 71*, 773-782.

86. Henrissat, B., and Bairoch, A. (1993) New families in the classification of glycosyl hydrolases based on amino acid sequence similarities, *Biochem J 293 (Pt 3)*, 781-788.

87. Henrissat, B., and Bairoch, A. (1996) Updating the sequence-based classification of glycosyl hydrolases, *Biochem J 316 (Pt 2)*, 695-696.

88. Hart, P. J., Pfluger, H. D., Monzingo, A. F., Hollis, T., and Robertus, J. D. (1995) The refined crystal structure of an endochitinase from *Hordeum vulgare* L. seeds at 1.8 A resolution, *J Mol Biol 248*, 402-413.

89. Monzingo, A. F., Marcotte, E. M., Hart, P. J., and Robertus, J. D. (1996) Chitinases, chitosanases, and lysozymes can be divided into procaryotic and eucaryotic families sharing a conserved core, *Nat Struct Biol 3*, 133-140.

90. Robertus, J. D., Monzingo, A. F., Marcotte, E. M., and Hart, P. J. (1998) Structural analysis shows five glycohydrolase families diverged from a common ancestor, *J Exp Zool 282*, 127-132.

91. Fukamizo, T. (2000) Chitinolytic enzymes: catalysis, substrate binding, and their application, *Curr Prot Pept Sci 1*, 105-124.

92. Tronsmo, A., and Harman, G. E. (1993) Detection and quantification of *N*-acetyl-beta-D-glucosaminidase, chitobiosidase, and endochitinase in solutions and on gels, *Anal Biochem 208*, 74-79.

93. Keyhani, N. O., and Roseman, S. (1996) The chitin catabolic cascade in the marine bacterium *Vibrio furnissii:* Molecular cloning, isolation, and characterization of a periplasmic β-*N*-acetylglucosaminidase, *J Biol Chem 271*, 33425-33432.

94. Tsuijibo, H., Kondo, N., Tanaka, K., Baba, N., Inamori, Y. (1999) Molecular analysis of the gene encoding a novel transglycosylative enzyme from *Alteromonas* sp. strain O-7 and its physiological role in the chitinolytic system, *J Bacteriol 181*, 5461-5466.

95. Kerrigan, J. E., Ragunath, C., Kandra, L., Gyemant, G., Liptak, A., Janoosy, L., Kaplan, J.B. , and Ramasubbu, N. (2008) Modeling and biochemical analysis of the activity of antibiofilm agent Dispersin B, *Acta Biologica Hungarica 59*, 439-451.

96. Itoh, Y., Wang, X., Hinnebusch, B. J., Preston, III J. F. , and Romeo, T. (2005) Depolymerization of -1,6-*N*-Acetyl-D-glucosamine disrupts the integrity of diverse bacterial biofilms, *J Bacteriol 187*, 382-387.

97. Kaplan, J. B., Ragunath, C., Ramasubbu, N., Fine, D. H. (2003) Detachment of *Actinobacillus actinomycetemcomitans* biofilm cells by an endogenous β-hexosaminidase activity, *J Bacteriol 185*, 4693-4698.

98. Huang, Q.-S., Xie, X-L., Liang, G., Gong, F., Wang, Y., Wei, X-Q., Wang, Q., Ji, Z-J., and Chen, Q-X. (2012) The GH18 family of chitinases: Their domain architectures functions and evolutions, *Glycobiology 22* 23-34.

99. Mitsuhiro, U., Yukiko, K., Aji, S., Masami, N., Kazutaka, M. (2005) Purification and characterization of chitinase B from moderately thermophilic bacterium *Ralstonia* sp. A-471, *Biosci Biotechnol Biochem 69*, 842-844.

100. Wang, S. Y., Moyne, A.L,, Thottappilly, G., Wu, S.J., Locy, R.D., Singh, N.K. (2001) Purification and characterization of a *Bacillus cereus* exochitinase, *Enzyme Microb Technol 28*, 492-498.

101. Kuk, J. H., Jung, W. J., Jo, G. H., Kim, Y. C., Kim, K. Y., Park, R. D. (2005) Production of *N*-acetyl-beta-D-glucosamine from chitin by *Aeromonas* sp. GJ-18 crude enzyme, *Appl Microbiol Biotechnol 68*, 384-389.

102. Suzuki, K., Sugawara, N., Suzuki, M., Uchiyama, T., Katouno, F., Nikaidou, N., Watanabe, T. (2002) Chitinases A, B, and C1 of *Serratia marcescens* 2170 produced by recombinant *Escherichia coli*: enzymatic properties and synergism on chitin degradation, *Biosci Biotechnol Biochem 66*, 1075-1083.

103. Nawani, N. N., Kapadnis, B.P., Das, A.D., Rao, A.S., Mahajan, S.K. (2002) Purification and characterization of a thermophilic and acidophilic chitinase from *Microbispora* sp. V2., *J Appl Microbiol 93*, 965-975.

104. Watanabe, T., Ito, Y., Yamada, T., Hashimoto, M., Sekine, S., and Tanaka, H. (1994) The roles of the C-terminal domain and type III domains of chitinase A1 from *Bacillus circulans* WL-12 in chitin degradation, *J Bacteriol 176*, 4465-4472.

105. Bhushan, B. (2000) Production and characterization of a thermostable chitinase from a new alkalophilic *Bacillus* sp. BG-11, *J Appl Microbiol 88*, 800-808.

106. Babashpour, S., Aminzadeh, S., Farrokhi, N., Karkhane, A., and Haghbeen, K. (2012) Characterization of a chitinase (Chit62) from *Serratia marcescens* B4A and its efficacy as a bioshield against plant fungal pathogens, *Biochem Genet 50*, 722-735.

107. Saito, A., Fujii, T., Yoneyama, T., Redenbach, M., Ohno, T., Watanabe, T., and Miyashita, K. (1999) High-multiplicity of chitinase genes in *Streptomyces coelicolor* A3(2), *Biosci Biotechnol Biochem 63*, 710-718.

108. Hult, E. L., Katouno, F., Uchiyama, T., Watanabe, T., and Sugiyama, J. (2005) Molecular directionality in crystalline beta-chitin: hydrolysis by chitinases A and B from *Serratia marcescens*, *Biochem J 388 (Pt 3)*, 851-856.

109. Sikorski, P., Sorbotten, A., Horn, S. J., Eijsink, V. G., and Varum, K. M. (2006) *Serratia marcescens* chitinases with tunnel-shaped substrate-binding grooves show endo activity and different degrees of processivity during enzymatic hydrolysis of chitosan, *Biochemistry 45*, 9566-9574.

110. Norberg, A. L., Dybvik, A. I., Zakariassen, H., Mormann, M., Peter-Katalinic, J., Eijsink, V. G., and Sorlie, M. (2011) Substrate positioning in chitinase A, a processive chito-biohydrolase from *Serratia marcescens*, *FEBS Lett 585*, 2339-2344.

111. Suzuki, K., Taiyoji, M., Sugawara, N., Nikaidou, N., Henrissat, B., Watanabe, T. (1999) The third chitinase gene (chiC) of *Serratia marcescens* 2170 and the relationship of its product to other bacterial chitinases, *Biochem J 343 Pt 3*, 587-596.

112. Arakane, Y., Zhu, Q., Matsumiya, M., Muthukrishnan, S., and Kramer, K. J. (2003) Properties of catalytic, linker and chitin-binding domains of insect chitinase, *Insect Biochem Mol Biol 33*, 631-648.

113. Andersen, O. A., Dixon, M. J., Eggleston, I. M., and van Aalten, D. M. (2005) Natural product family 18 chitinase inhibitors, *Nat Prod Rep 22*, 563-579.

114. Hoell, I. A., Klemsdal, S. S., Vaaje-Kolstad, G., Horn, S. J., and Eijsink, V. G. (2005) Overexpression and characterization of a novel chitinase from *Trichoderma atroviride* strain P1, *Biochim Biophys Acta 1748*, 180-190.

115. Brameld, K. A., Shrader, W. D., Imperiali, B., and Goddard, W. A., 3rd. (1998) Substrate assistance in the mechanism of family 18 chitinases: theoretical studies of potential intermediates and inhibitors, *J Mol Biol 280*, 913-923.

116. Zakariassen, H., Aam, B.B., Horn, S.J., Vårum, K.M., Sørlie, M., and Eijsink, V.G. (2009) Aromatic residues in the catalytic center of chitinase A from *Serratia marcescens* affect processivity, enzyme activity, and biomass converting efficiency, *J Biol Chem 284*, 10610-10617.

117. Sumida, T., Ishii, R, Yanagisawa, T, Yokoyama, S, Ito, M. . (2009) Molecular cloning and crystal structural analysis of a novel β-*N*-acetylhexosaminidase from *Paenibacillus* sp. TS12 capable of degrading glycosphingolipids, *J Mol Biol 392*.

118. Gomes, J. E., Souza, D. S. L., Nascimento, R. M. , Lima, A. L. M., Melo, J. A. T., Rocha, T. L., Miller, R. N. G. , Franco, O. L. , Grossi-de-Sa, M. F. , Abreu, L. R. D. . (2010) Purification and characterization of a liver-derived β-*N*-Acetylhexosaminidase from marine mammal *Sotalia fluviatilis*, *Protein J 29*, 188-194.

119. Mark, B. L., Wasney, G. A., Salo, T. J., Khan, A. R., Cao, Z., Robbins, P. W., James, M. N., and Triggs-Raine, B. L. (1998) Structural and funtional characterization of *Streptomyces plicatus* β-*N*-Acetylhexosaminidase by comparative molecular modeling and site-directed mutagenesis, *J Biol Chem 273*, 19618-19624.

120. Reyes, F., Calatayud, J., Vazquez, C., Martinez, M. J. (1989) β–*N*-Acetylglucosaminidase from *Aspergillus nidulans* which degrades chitin oligomers during autolysis, *FEMS Microbiol Lett 65*.

121. Eriquez, L. A., and Pisano, M. A. (1979) Purification and characterization of an extracellular β-*N*-acetylhexosaminidase from *Paecilomyces persicinus*, *J Bacteriol 137*, 620-626.

122. Geimba, M. P., Riffel, A., and Brandelli, A. (1998) Purification and characterization of β-*N*-acetylhexosaminidase from the phytopathogenic fungus *Bipolaris sorokiniana*, *J Appl Microbiol 85*, 708-714.

123. Koga, K., Iwamoto, Y., Sakamoto, H., Hatano, K., Sano, M., and Kato, I. (1991) Purification and characterization of β-*N*-acetylhexosaminidase from *Trichoderma harzianum*, *Agric Biol Chem 55*, 2817-2823.

124. Jones, C. S., Kosman, D.J. (1980) Purification, properties, kinetics, and mechanism of β-*N*-acetylglucosaminidase from *Aspergillus niger*, *J Biol Chem 255*, 11861-11869.

125. Tews, I., Perrakis, A., Oppenheim, A., Dauter, Z., Wilson, K. S., Vorgias, C. E. (1996) Bacterial chitobiose structure provides insights into catalytic mechanism and the basic of Tay-Sachs disease, *Nat Struct Biol 3*, 638-648.

126. Manuel, S. G., R. C., Sait, B. R. H., Era, A. Izano, Kaplan, J. B. , and Ramasubbu, N. (2007) Role of active-site residues of dispersin B, a biofilm-releasing β-hexosaminidase from a periodontal pathogen, in substrate hydrolysis, *The FEBS journal 274*, 5987-5999.

127. Park, J. K., Kim, W.J. and Park, Y.I. . (2010) Purification and characterization of an exo-type β-*N*-acetylglucosaminidase from *Pseudomonas fluorescens* JK-0412, *J Appl Microbiol 110*, 277-286.

128. Ryslava, H., Kalendova, A., Doubnerova, V., Skocdopol, P., Kumar, V., Kukacka, Z., Pompach, P., Vanek, O., Slamova, K., Bojarova, P., Kulik, N., Ettrich, R., Kren, V., Bezouska, K. (2011) Enzymatic characterization and molecular modeling of an evolutionarily interesting fungal β-*N*-acetylhexosaminidase, *The FEBS journal 278*, 2469-2484.

129. Jiang, Y. L., Yu, W. L., Zhang, J. W., Frolet, C., Guilmi, A. M. D., Zhou, C. Z., Vernet, T., and Chen, Y. (2011) Structural basis for the substrate specificity of a novel β-*N*-Acetylhexosaminidase StrH protein from *Streptococcus pneumoniae* R6, *J Biol Chem 286*, 43004-43012.

130. Ramasubbu, N., Thomas, L.M., Ragunath, C, Kaplan, J.B. (2005) Structural analysis of Dispersin B, a biofilm-releasing from the periodontopathogen *Actinobacillus actinomycetemcomitans*, *J Mol Biol 349*, 475-486.

131. Mark, B. L., Mahuran, D.J., Cherney, M.M., Zhao, D., Knapp, S., James, M.N.G. (2003) Crystal structure of human β-hexosaminidase B: Understanding the molecular basis of Sandhoff and Tay-Sachs disease, *J Mol Biol 327*, 1093-1109.

132. Fekete, A., Borbas, A., Gyemant, G., Kandra, L., Fazekas, E., Ramasubbu, N., Antus, S. (2011) Synthesis of β-(1-6)-linked *N*-acetyl-D-glucosamine oligosaccharide substrates and their hydrolysis by Dispersin B, *Carbohydr Res 346*, 1445-1453.

133. Liu, T., Zhang, H., Liu, F., Wu, Q., Shen, X., and Yang, Q. (2011) Structural determinants of an insect β-*N*-Acetyl-D-hexosaminidase specialized as a chitinolytic enzyme, *J Biol Chem 286*, 4049-4058.

134. Gutternigg, M., Kretschmer-Lubich, D., Paschinger, K., Rendic, D., Hader, J., Geier, P., Ranftl, R., Jantsch, V., Lochnit, G., and Wilson, I. B. (2007) Biosynthesis of truncated N-linked oligosaccharides results from non-orthologous hexosaminidase-mediated mechanisms in nematodes, plants, and insects, *J Biol Chem 282*, 27825-27840.

135. Geisler, C., Aumiller, J. J., and Jarvis, D. L. (2008) A fused lobes gene encodes the processing β-*N*-acetylglucosaminidase in Sf9 cells, *J Biol Chem 283*, 11330-11339.

136. Husakova, L., Riva, S., Casali, M., Nicotra, S., Kuzma, M., Hunkova, Z., and Kren, V. (2001) Enzymatic glycosylation using 6-*O*-acylated sugar donors and acceptors: β-*N*-acetylhexosaminidase-catalysed synthesis of 6-*O*,*N*,*N*'-triacetylchitobiose and 6'-*O*,*N*,*N*'-triacetylchitobiose, *Carbohydr Res 331*, 143-148.

137. Fialova, P., Namdjou, D. J., Ettrich, R., Prikrylova, W., Rauvolfova, J., Krenek, K., Kuzma, M., Elling, L., Bezouska, K., and Kren, V. (2005) Combined application of galactose oxidase and β-*N*-acetylhexosaminidase in the synthesis of complex immunoactive *N*-acetyl-D-galactosaminides, *Adv Synth Catal 347*, 997-1006.

138. Ogata, M., Zeng, X. X., Usui, T., Uzawa, H. (2007) Substrate specificity of *N*-acetylhexosaminidase from *Aspergillus oryzae* to artificial glycosyl acceptors having various substituents at the reducing ends, *Carbohydr Res 342*, 23-30.

139. Fialova, P., Weignerova, L., Rauvolfova, Prikrylova, V., Pisvejcova, A., Ettrich, R., Kuzma, M., Sedmera, P., Kren, V. (2004) Hydrolytic and transglycosylation reactions of N-acyl modified substrates catalysed by β-*N*-acetylhexosaminidases, *Tetrahedron 60*.

140. Saito, A., Miyashita, K., Biukovic, G., and Schrempf, H. (2001) Characteristics of a *Streptomyces coelicolor* A3(2) extracellular protein targeting chitin and chitosan, *Appl Environ Microbiol 67*, 1268-1273.

141. Schrempf, H. (2001) *Recognition and degradation of chitin by streptomycetes*, Vol. 79, 2002/01/31 ed., Antonie Van Leeuwenhoek.

142. Saito, A., Ishizaka, M., Francisco, P. B., Jr., Fujii, T., and Miyashita, K. (2000) Transcriptional co-regulation of five chitinase genes scattered on the *Streptomyces coelicolor* A3(2) chromosome, *Microbiology 146 (Pt 11)*, 2937-2946.

143. Joshi, M. D., Sidhu, G., Pot, I., Brayer, G. D., Withers, S. G., and McIntosh, L. P. (2000) Hydrogen bonding and catalysis: a novel explanation for how a single amino acid substitution can change the pH optimum of a glycosidase, *J Mol Biol 299*, 255-279.

144. Joshi, M. D., Sidhu, G., Nielsen, J. E., Brayer, G. D., Withers, S. G., and McIntosh, L. P. (2001) Dissecting the electrostatic interactions and pH-dependent activity of a family 11 glycosidase, *Biochemistry 40*, 10115-10139.

145. Sapag, A., Wouters, J., Lambert, C., de Ioannes, P., Eyzaguirre, J., and Depiereux, E. (2002) The endoxylanases from family 11: computer analysis of protein sequences reveals important structural and phylogenetic relationships, *J Biotechnol 95*, 109-131.

146. Torronen, A., and Rouvinen, J. (1995) Structural comparison of two major endo-1,4-xylanases from *Trichoderma reesei*, *Biochemistry 34*, 847-856.

147. Krengel, U., and Dijkstra, B. W. (1996) Three-dimensional structure of Endo-1,4-beta-xylanase I from *Aspergillus niger*: molecular basis for its low pH optimum, *J Mol Biol 263*, 70-78.

148. Fushinobu, S., Ito, K., Konno, M., Wakagi, T., and Matsuzawa, H. (1998) Crystallographic and mutational analyses of an extremely acidophilic and acid-stable xylanase: biased distribution of acidic residues and importance of Asp37 for catalysis at low pH, *Protein Eng 11*, 1121-1128.

149. Hakulinen, N., Turunen, O., Janis, J., Leisola, M., and Rouvinen, J. (2003) Three-dimensional structures of thermophilic beta-1,4-xylanases from *Chaetomium thermophilum* and *Nonomuraea flexuosa*. Comparison of twelve xylanases in relation to their thermal stability, *Eur J Biochem 270*, 1399-1412.

150. Sakka, K., Kojima, Y, Kondo, T, Karita, S, Shimada, K, Ohmiya, K. (1994) Purification and characterization of xylanase A from *Clostridium stercorarium* F-9 and a recombinant *Escherichia coli*, *Biosci Biotechnol Biochem 58*, 1496-1499.

151. Fernandez-Espinar, M. T., Piñaga, F, Sanz, P, Ramon, D, Vallés, S. (1993) Purification and characterization of a neutral endoxylanase from *Aspergillus nidulans*, *FEMS Microbiol Lett 113*, 223-228.

152. Kumar, P. R., Eswaramoorthy, S., Vithayathil, P.J., Viswamitra, M.A. . (2000) The tertiary structure at 1.59 Å resolution and the proposed amino acid sequence of a family-11 xylanase from the thermophilic fungus *Paecilomyces varioti* Bainier, *J Mol Biol 295*, 581-593.

153. Murakami, M. T., Arni, R. K., Vieira, D. S., Degreve, L., Ruller, R., and Ward, R. J. (2005) Correlation of temperature induced conformation change with optimum catalytic activity in the recombinant G/11 xylanase A from *Bacillus subtilis* strain 168 (1A1), *FEBS Lett 579*, 6505-6510.

154. Irwin, D., Jung, E. D., and Wilson, D. B. (1994) Characterization and sequence of a *Thermomonospora fusca* xylanase, *Appl Environ Microbiol 60*, 763-770.

155. Kluepfel, D., Daigneault, N., Morosoli, R., Shareck, F. (1992) Purification of a new xylanase (xylanase C) produced by *Streptomyces lividans*, *Appl Microbiol Biotechnol 36*, 626-631.

156. Kluepfel, D., Vats-Mehta, S., Aumont, F., Shareck, F., Morosoli, R. . (1990) Purification and characterization of a new xylanase (xylanase B) produced by *Streptomyces lividans* 66, *Biochem J 267*, 45-50.

157. Biely, P., Vrsanska, M., Tenkanan, M., Kluepfel, D. (1997) Endo-β-1,4-xylanase families: differences in catalytic properties., *J Biotechnol 57*, 151-166.

158. Vardakou, M., Dumon, C., Murray, J. W., Christakopoulos, P., Weiner, D. P., Juge, N., Lewis, R. J., Gilbert, H. J., and Flint, J. E. (2008) Understanding the structural basis for substrate and inhibitor recognition in eukaryotic GH11 xylanases, *J Mol Biol 375*, 1293-1305.

159. Katapodis, P., Vrsanska, M., Kekos, D., Nerinckx, W., Biely, P., Claeyssens, M., Macris, B. J., and Christakopoulos, P. (2003) Biochemical and catalytic properties of an endoxylanase purified from the culture filtrate of *Sporotrichum thermophile*, *Carbohydr Res 338*, 1881-1890.

160. Gruber, K., Klintschar, G., Hayn, M., Schlacher, A., Steiner, W., and Kratky, C. (1998) Thermophilic xylanase from *Thermomyces lanuginosus*: high-resolution X-ray structure and modeling studies, *Biochemistry 37*, 13475-13485.

161. Henzler-Wildman, K., and Kern, D. (2007) Dynamic personalities of proteins, *Nature 450*, 964-972.

162. Connelly, G. P., and McIntosh, L. P. (1998) Characterization of a buried neutral histidine in Bacillus circulans xylanase: internal dynamics and interaction with a bound water molecule, *Biochemistry 37*, 1810-1818.

163. Muilu, J., Torronen, A., Perakyla, M., and Rouvinen, J. (1998) Functional conformational changes of endo-1,4-xylanase II from *Trichoderma reesei*: a molecular dynamics study, *Proteins 31*, 434-444.

164. Havukainen, R., Torronen, A., Laitinen, T., and Rouvinen, J. (1996) Covalent binding of three epoxyalkyl xylosides to the active site of endo-1,4-xylanase II from *Trichoderma reesei*, *Biochemistry 35*, 9617-9624.

165. Ludwiczek, M. L., Heller, M., Kantner, T., and McIntosh, L. P. (2007) A secondary xylan-binding site enhances the catalytic activity of a single-domain family 11 glycoside hydrolase, *J Mol Biol 373*, 337-354.

166. Vieira, D. S., Degreve, L., and Ward, R. J. (2009) Characterization of temperature dependent and substrate-binding cleft movements in *Bacillus circulans* family 11 xylanase: a molecular dynamics investigation, *Biochim Biophys Acta 1790*, 1301-1306.

167. Paës, G., Takahashi, M., Tran, V., Boukari, I., O'Donohue, M.J. (2007) New insights into the role of the thumb-like loop in GH-11 xylanases, *Protein Eng Des Sel 20*, 15-23.

168. Cervera, T. M., André-Leroux, G., Lafond, M., Georis, J., Juge, N., Berrin, J.G. (2009) Molecular determinants of substrate and inhibitor specificities of the *Penicillium griseofulvum* family 11 xylanases, *Biochim Biophys Acta 1794*, 438-445.

169. Pollet, A., Vandermarliere, E., Lammertyn, J., Strelkov, S.V., Delcour, J.A., Courtin, C.M. (2009) Crystallographic and activity-based evidence for thumb flexibility and its relevance in glycoside hydrolase family 11 xylanases, *Proteins 77*, 395-403.

170. Campbell, R. L., Rose, D.R., Wakarchuk, W.W., To R., Sung, W., Yaguchi, M. (1993) A comparison of the structures of the 20 kDa xylanases from *Trichoderma harzianum* and *Bacillus circulans*. In: Suominen P, Reinikainen T, eds. Proceedings of the second TRICEL symposium on *Trichoderma reesei* cellulases and other hydrolases, *Helsinki, Finland: Foundation for Biotechnical and Industrial Fermentation Research*, 63-72.

171. Fenwick, R. B., van den Bedem, H., Fraser, J. S., and Wright, P. E. (2014) Integrated description of protein dynamics from room-temperature X-ray crystallography and NMR, *Proc Natl Acad Sci U S A 111*, E445-454.

172. Bastawde, K. B. (1992) Xylan structure, microbial xylanases, and their mode of action, *World J Microbiol Biotechnol 8*, 353-368.

173. Verjans, P., Dornez, E., Delcour, J.A., Courtin ,C.M. (2010) Selectivity forwater-unextractable arabinoxylan and inhibition sensitivity govern the strong bread improving potential of an acidophilic GH11 *Aureobasidium pullulans* xylanase, *Food Chem 123*, 331-337.

174. Goesaert, H., Brijs, K., Veraverbeke, W.S., Courtin, C.M., Gebruers, K., Delcour, J.A. (2005) Wheat flour constituents: how they impact bread quality, and how to impact their functionality, *Trends Food Sci Technol 16*, 12-30.

175. Frederix, S. A., Courtin, C. M., and Delcour, J. A. (2003) Impact of xylanases with different substrate selectivity on gluten-starch separation of wheat flour, *J Agric Food Chem 51*, 7338-7345.

176. Olfa, E., Mondher, M., Issam, S., Ferid, L., Nejib, M.M. (2007) Induction, properties and application of xylanase activity from *Sclerotinia sclerotiorum* S2 fungus, *J Food Biochem 31*, 96-107.

177. Beg, Q. K., Kapoor, M., Mahajan, L., Hoondal, G.S. (2001) Microbial xylanases and their industrial applications: a review, *Appl Microbiol Biotechnol 56*, 326-338.

178. Kumar, R., Singh, S., and Singh, O. V. (2008) Bioconversion of lignocellulosic biomass: biochemical and molecular perspectives, *J Ind Microbiol Biotechnol 35*, 377-391.

179. Morosoli, R., Bertrand, J. L., Mondou, F., Shareck, F., and Kluepfel, D. (1986) Purification and properties of a xylanase from *Streptomyces lividans*, *Biochem J 239*, 587-592.

180. Vats-Mehta, S., Bouvrette, P., Shareck, F., Morosoli, R., and Kluepfel, D. (1990) Cloning of a second xylanase-encoding gene of *Streptomyces lividans* 66, *Gene 86*, 119-122.

181. Gauthier, C., Li, H., and Morosoli, R. (2005) Increase in xylanase production by *Streptomyces lividans* through simultaneous use of the Sec- and Tat-dependent protein export systems, *App Env Microbio 71*, 3085-3092.

182. Chater, K. F., Sandor, B.S., Lee, K.J., Palmer, T., & Schrempf, H. (2010) The complexextracellular biologyof Streptomyces, *FEMS Microbiol Rev 34*, 171-198.

183. http://www.ncbi.nlm.nih.gov/Taxonomy/Browser/wwwtax.cgi?mode=Info&id=1916&lvl=3&lin=f&keep=1&srchmode=1&unlock.

184. Saito, A., Fujii, T., and Miyashita, K. (2003) Distribution and evolution of chitinase genes in *Streptomyces* species: involvement of gene-duplication and domain-deletion, *Antonie Van Leeuwenhoek 84*, 7-15.

185. Bentley, S. D., Chater, K. F., Cerdeno-Tarraga, A. M., Challis, G. L., Thomson, N. R., James, K. D., Harris, D. E., Quail, M. A., Kieser, H., Harper, D., Bateman, A., Brown, S., Chandra, G., Chen, C. W., Collins, M., Cronin, A., Fraser, A., Goble, A., Hidalgo, J., Hornsby, T., Howarth, S., Huang, C. H., Kieser, T., Larke, L., Murphy, L., Oliver, K., O'Neil, S., Rabbinowitsch, E., Rajandream, M. A., Rutherford, K., Rutter, S., Seeger, K., Saunders, D., Sharp, S., Squares, R., Squares, S., Taylor, K., Warren, T., Wietzorrek, A., Woodward, J., Barrell, B. G., Parkhill, J., and Hopwood, D. A. (2002) Complete genome sequence of the model actinomycete *Streptomyces coelicolor* A3(2), *Nature 417*, 141-147.

186. Fukamizo, T., and Brzezinski, R. (1997) Chitosanase from *Streptomyces* sp. strain N174: a comparative review of its structure and function, *Biochem Cell Biol 75*, 687-696.

187. Tanabe, T., Morinaga, K., Fukamizo, T., and Mitsutomi, M. (2003) Novel chitosanase from *Streptomyces griseus* HUT 6037 with transglycosylation activity, *Biosci Biotechnol Biochem 67*, 354-364.

188. Whitford, D. (2004) *Protein structure and function*, John Wiley & Sons, Ltd.

189. Lodish, H., Berk, A., Zipursky, S. L., Matsudaira, P., Baltimore, D., and Darnell, J. (2004) *Molecular Cell Biology, 5th edition*, W. H. Freeman, New York.

190. Chouard, T. (2011) Structural biology: Breaking the protein rules, *Nature 471*, 151-153.

191. Ackers, G. K., Doyle, M. L., Myers, D., and Daugherty, M. A. (1992) Molecular code for cooperativity in hemoglobin, *Science 255*, 54-63.

192. Gutteridge, A., and Thornton, J. (2004) Conformational change in substrate binding, catalysis and product release: an open and shut case?, *FEBS Lett 567*, 67-73.

193. Koshland, D. E. (1958) Application of a theory of enzyme specificity to protein synthesis., *Proc Natl Acad Sci USA 44*, 98–104.

194. Hammes, G. G., Chang, Y. C., and Oas, T. G. (2009) Conformational selection or induced fit: a flux description of reaction mechanism, *Proc Natl Acad Sci USA 106*, 13737-13741.

195. Boehr, D. D., Nussinov, R., and Wright, P. E. (2009) The role of dynamic conformational ensembles in biomolecular recognition, *Nat Chem Biol 5*, 789-796.

196. Ma, B., and Nussinov, R. (2010) Enzyme dynamics point to stepwise conformational selection in catalysis, *Curr Opin Chem Biol 14*, 652-659.

197. Gagne, D., Charest, L-A. ,Morin, S., Kovrigin, E.L., Doucet, N. (2012) Conservation of flexible residue clusters among structural and functional enzyme homologues, *J Biol Chem 287*, 44289-44300.

198. Gagne, D., and Doucet, N. (2013) Structural and functional importance of local and global conformational fluctuations in the RNase A superfamily, *The FEBS journal 280*, 5596-5607.

199. Marsh, J. A., and Teichmann, S. A. (2013) Parallel dynamics and evolution: Protein conformational fluctuations and assembly reflect evolutionary changes in sequence and structure, *Bioessays 35*, DOI 10.1002/bies.201300134.

200. Fang, J., Nevin, P., Kairys, V., Venclovas, C., Engen, J.R., Beuning, P.J. (2014) Conformational analysis of processivity clamps in solution demonstrates that tertiary structure does not correlate with protein dynamics, *Structure 22*, 1-10.

201. Baldwin, A. J., & Kay, L.E. (2009) NMR spectroscopy brings invisible protein states into focus, *Nat Chem Biol 5*, 808-815.

202. Loria, J. P., Rance, M., Palmer III, A. G. (1999) A relaxation compensated Carr-Purcell-Meiboom-Gill sequence for characterizing chemical exchange by NMR spectroscopy, *J. Am. Chem. Soc. 121*, 2331-2332.

203. Vogeli, B., Kazemi, S., Guntert, P., and Riek, R. (2012) Spatial elucidation of motion in proteins by ensemble-based structure calculation using exact NOEs, *Nat Struct Mol Biol 19*, 1053-1057.

204. Sekhar, A., and Kay, L. E. (2013) NMR paves the way for atomic level descriptions of sparsely populated, transiently formed biomolecular conformers, *Proc Natl Acad Sci USA 110*, 12867-12874.

205. Palmer, A. G., 3rd. (2004) NMR characterization of the dynamics of biomacromolecules, *Chem Rev 104*, 3623-3640.

206. Aam, B. B., Heggset, E. B., Norberg, A.L., Sørlie, M., Vårum, K.M., Eijsink, V. G. H. (2010) Production of chitooligosaccharides and their potential applications in medicine, *Mar Drugs 8*, 1482-1517.

207. Gutierrez-Roman, M. I., Dunn, M. F., Tinoco-Valencia, R., Holguin-Melendez, F., Huerta-Palacios, G., and Guillen-Navarro, K. (2014) Potentiation of the synergistic activities of chitinases ChiA, ChiB and ChiC from *Serratia marcescens* CFFSUR-B2 by chitobiase (Chb) and chitin binding protein (CBP), *World J Microbiol Biotechnol 30*, 33-42.

208. von Ossowski, I., Stahlberg, J., Koivula, A., Piens, K., Becker, D., Boer, H., Harle, R., Harris, M., Divne, C., Mahdi, S., Zhao, Y., Driguez, H., Claeyssens, M., Sinnott, M. L., and Teeri, T. T. (2003) Engineering the exo-loop of *Trichoderma reesei cellobiohydrolase*, Cel7A. A comparison with *Phanerochaete chrysosporium* Cel7D, *J Mol Biol 333*, 817-829.

209. Murphy, L., Cruys-Bagger, N., Damgaard, H. D., Baumann, M. J., Olsen, S. N., Borch, K., Lassen, S. F., Sweeney, M., Tatsumi, H., and Westh, P. (2012) Origin of initial burst in activity for *Trichoderma reesei* endo-glucanases hydrolyzing insoluble cellulose, *J Biol Chem 287*, 1252-1260.

210. Nimlos, M. R., Beckham, G. T., Matthews, J. F., Bu, L., Himmel, M. E., and Crowley, M. F. (2012) Binding preferences, surface attachment, diffusivity, and orientation of a family 1 carbohydrate-binding module on cellulose, *J Biol Chem 287*, 20603-20612.

211. Vaaje-Kolstad, G., Bunaes, A. C., Mathiesen, G., and Eijsink, V. G. (2009) The chitinolytic system of *Lactococcus lactis* ssp. lactis comprises a nonprocessive chitinase and a chitin-binding protein that promotes the degradation of alpha- and beta-chitin, *The FEBS journal 276*, 2402-2415.

212. Cavanagh, J., Fairbrother, W.J., Palmer, A.G., Rance, M., Skelton, N.J. (2007) *Protein NMR spectroscopy: Principles and practice.*, Elsevier Academic.

213. Connelly, G. P., Withers, S.G., and McIntosh, L.P. (2000) Analysis of the dynamic properties of *Bacillus circulans* xylanase upon formation of a covalent glycosyl-enzyme intermediate, *Protein Sci 9*, 512-524.

214. Wakarchuk, W. W., Campbell, R.L., Sung, W.L., Davoodi, J, Yaguchi, M. (1994a) Mutational and crystallographic analysis of the active site residues of the *Bacillus circulans* xylanase, *Protein Sci 3*, 467-475.

215. Sidhu, G., Withers, S.G., Nguyen, N.T., McIntosh, L.P., Ziser, L., Brayer, G.D. (1999) Sugar ring distorsion in the glycosyl-enzyme intermediate of a family G/11 xylanase, *Biochemistry 38*, 5346-5354.

216. Vandermarliere, E., Bourgois, T.M., Rombouts, S., Van, C. S., Volckaert, G., Strelkov, S.V., Delcour, J.A., Rabijns A., and Courtin C.M. (2008) Crystallographic analysis shows substrate binding at the −3 to +1 active-site subsites and at the surface of glycoside hydrolase family 11 endo-1,4-β-xylanases, *Biochem J 410*, 71-79.

217. Torronen, A., Harkki, A., and Rouvinen, J. (1994) Three-dimensional structure of endo-1,4-beta-xylanase II from *Trichoderma reesei*: two conformational states in the active site, *EMBO J 13*, 2493-2501.

218. Axe, J. M., Yezdimer, E. M., O'Rourke, K. F., Kerstetter, N. E., You, W., Chang, C. E., and Boehr, D. D. (2014) Amino acid networks in a (beta/alpha)(8) barrel enzyme change during catalytic turnover, *J Am Chem Soc 136*, 6818-6821.

219. Bornscheuer, U. T., Huisman, G. W., Kazlauskas, R. J., Lutz, S., Moore, J. C., and Robins, K. (2012) Engineering the third wave of biocatalysis, *Nature 485*, 185-194.